Title
Aspects of Supersymmetric Surface Defects

Author
Haouzi, Nathan

Publication Date
2018

Peer reviewed|Thesis/dissertation

Aspects of Supersymmetric Surface Defects

by

Nathan Haouzi

A dissertation submitted in partial satisfaction of the

requirements for the degree of

Doctor of Philosophy

in

Physics

in the

Graduate Division

of the

University of California, Berkeley

Committee in charge:

Professor Mina Aganagic, Chair
Professor Ori J. Ganor
Professor Nicolai Reshetikhin

Summer 2018

Aspects of Supersymmetric Surface Defects

Abstract

Aspects of Supersymmetric Surface Defects

by

Nathan Haouzi

Doctor of Philosophy in Physics

University of California, Berkeley

Professor Mina Aganagic, Chair

Starting from type IIB string theory on an ADE singularity, the $\mathcal{N} = (2, 0)$ little string arises when one takes the string coupling g_s to 0. We compactify the little string on the cylinder with punctures, which we fully characterize, for any simple Lie algebra $\mathfrak{g}$. Geometrically, these punctures are codimension two defects that are D5 branes wrapping 2-cycles of the singularity. Equivalently, the defects are specified by a certain set of weights of ${}^L\mathfrak{g}$, the Langlands dual of $\mathfrak{g}$. As a first application of our formalism, we show that at low energies, the defects have a description as a $\mathfrak{g}$-type quiver gauge theory. We compute its partition function, and prove that it is equal to a conformal block of $\mathfrak{g}$-type q-deformed Toda theory on the cylinder, in the Coulomb gas formalism. After taking the string scale limit $m_s \to \infty$, the little string becomes a $(2, 0)$ superconformal field theory (SCFT). As a second application, we study how this limit affects the codimension two defects of the SCFT: we show that the Coulomb branch of a given defect flows to a nilpotent orbit of $\mathfrak{g}$, and that all nilpotent orbits of $\mathfrak{g}$ arise in this way. We give a physical realization of the Bala–Carter labels that classify nilpotent orbits of simple Lie algebras, and we interpret our results in the context of $\mathfrak{g}$-type Toda. Finally, after compactifying our setup on a torus T^2, we make contact with the description of surface defects of 4d $\mathcal{N} = 4$ Super Yang-Mills theory due to Gukov and Witten [1].

To my family.

Contents

List of Figures

Acknowledgments

This thesis could not have been written without the guidance of my advisor, Mina Aganagic. I would like to thank her for teaching me that the most important part of doing research in String Theory is to first and foremost ask good questions. Her depth of knowledge and enthusiasm communicating original ideas have made my years at UC Berkeley some of the most intellectually stimulating in my life. I also owe a great debt of gratitude to my collaborators: I thank Shamil Shakirov and Can Kozçaz, for teaching me everything I know about instanton counting, and Christian Schmid, for sharing with me his extensive knowledge of nilpotent orbits. I feel lucky to have had the opportunity to work with these amazing scientists. My sincere gratitude also goes to the members of my doctoral committee, Ori Ganor and Nicolai Reshetikhin.

I would furthermore like to thank Amihay Hanany, Jacques Distler, Cumrun Vafa, and Peter Koroteev, for providing feedback on some of the ideas presented in this thesis. I cannot forget my instructors and mentors from my time as an undergraduate at MIT: among them, I would especially like to thank Allan Adams, Eric Hudson, Barton Zwiebach and Hong Liu, for encouraging me to pursue a degree in Physics.

I would like to thank my parents Annick and Philippe, my sister Alice, and my grandparents, for their incessant love and support throughout my life. Finally, I would like to thank my friends from Poinca, my friends at No6, Nico, Manuel, Bago, Janvier, Tomas, Tinder, and Santiago. I thank Devyn for being patient with me while I was writing this thesis. I am deeply grateful to you all.

Chapter 1

Introduction

String theory has led to remarkable insights into quantum field theories in various dimensions and many areas of mathematics. Recently, a prolific array of conjectures about properties of gauge theories was obtained from studying the 6d $(2,0)$ superconformal field theory, whose existence is implied by string and M-theory. The 6d theory seems poised to play an important role in mathematics as well, see e.g. [3, 4, 5, 6, 7]. An important example, as well as a main motivation for this thesis, is a conjectured relation between a 4d $\mathcal{N}=2$ theory whose origin is the 6d $(2,0)$ SCFT compactified on a punctured Riemann surface $\mathcal{C}$, and a 2d conformal field theory on the surface, of Toda type, with $\mathcal{W}(\mathfrak{g})$-algebra symmetry. In particular, the partition function of the 4d theory is predicted to equal the conformal block of the 2d theory; this is known as the Alday-Gaiotto-Tachikawa (AGT) correspondence [8]. The conjecture was proven when $\mathfrak{g}=A_1$ in [9, 10]. The generalization of the correspondence to other groups was studied in many papers, see for example [11, 12, 13], and [14] for a recent review. For pure gauge theories of ADE type, the relation between the gauge theory partition function and the norm of a Whittaker vector of the $\mathcal{W}$-algebra was proven not long ago in [15].

However, an obstacle to extending the correspondence to groups other than A_1 is that compactification of the 6d $(2,0)$ SCFT on a Riemann surface does not in general lead to a theory with a Lagrangian description: without it, the partition function of the theory is not computable either, so there is nothing to compare to the Toda conformal block. Another obstacle is that, for $\mathfrak{g}\neq A_1$, the general Toda conformal blocks are known only if they admit a free field representation. One of the main motivations for this thesis is an attempt at a proof and generalization of the correspondence. We therefore find it worthwhile to study a deformation of the SCFT, called the $(2,0)$ little string theory. The little string setup enables one to state a precise and more general version of the AGT relation, and then prove it.

To truly appreciate why the $(2,0)$ SCFT is hard to work with directly, we begin with a review of its main features. We then proceed to introduce the $(2,0)$ little string, which will be the main actor in this work.

1.1 6d $\mathcal{N} = (2, 0)$ Superconformal Field Theories

In the landscape of quantum field theories, six-dimensional SCFTs hold a privileged place: six is the highest number of dimensions where a conformal field theory with supersymmetry can exist [16]. Those SCFTs are truly exotic in many regards: in Physics, the theories with $(1, 0)$ and $(2, 0)$ supersymmetry, for instance, have no description in terms of an action functional.

To truly appreciate this point, let us be more explicit about the field content of such theories. First recall that a theory is said to have $\mathcal{N} = (n_l, n_r)$ supersymmetry when it has n_l chiral and n_r antichiral supersymmetries. The R-symmetry group of such a theory is $Sp(n_l) \times Sp(n_r)$. In six dimensions, a theory with a minimal amount of supersymmetry is then denoted as being a $\mathcal{N} = (1, 0)$ theory; it has 8 supercharges and a R-symmetry of $Sp(1) \equiv SU(2)$. The massless content of such a theory is as follows:

A vector multiplet contains a gauge field and a right-handed Weyl spinor field. Note that there is no scalar present, so in particular one cannot speak of the Coulomb branch of a $(1, 0)$ theory.

A hypermultiplet contains four real scalars ϕ_i and a left-handed Weyl spinor. Accordingly, giving a vev to the ϕ_i fields describes the Higgs branch of the theory.

Additionally, we find a tensor multiplet, which contains a self-dual two-form $B_{[\mu\nu]}$, a single real scalar ϕ, and one left-handed Majorana spinor. Giving a vev to this scalar ϕ then parameterizes a tensor branch of the theory.

Our main focus in this thesis will be on six-dimensional theories that have a higher amount supersymmetry and no gravity. The only two candidates are $\mathcal{N} = (1, 1)$ and $\mathcal{N} = (2, 0)$ theories. Let us first look at what the field content of the former theory looks like. The only multiplet is a vector multiplet, which is made up of a $\mathcal{N} = (1, 0)$ vector multiplet and hypermultiplet. Therefore, the $(1, 1)$ multiplet contains in the bosonic sector one vector field A_μ and four real scalar fields ϕ_i, for a total of 4+4=8 degrees of freedom. The fermionic sector contains one Dirac spinor, that is to say one Weyl left-handed spinor and one Weyl-handed right spinor, for a total of 4+4=8 degrees of freedom, as it should be. The R-symmetry is $Sp(1) \times Sp(1) \equiv SO(4)$. Each spinor is a doublet under one of the two $Sp(1)$ groups, and the scalars transform under the $SO(4)$ symmetry. It is not hard to write an action functional for this theory:

$$S = \int d^6x \, \frac{1}{g_{6d}^2} \, F^a_{\mu\nu} F^{a\mu\nu} + \dots \, , \tag{1.1.1}$$

where the dots stand for terms including the fermions to make the action supersymmetric. The greek indices are spacetime indices, while the a index labels the generators of the Lie algebra of the gauge group G. The theory is simply the maximally supersymmetric Yang-Mills in six dimensions, which is IR free; note that the coupling has dimension $[g_{6d}^2] = (\text{length})^2$, which means the theory is non-renormalizable.

Let us repeat this exercise for a $\mathcal{N} = (2, 0)$ theory, and we will see why this case is much more interesting. The basic multiplet is no longer a vector multiplet, but a tensor multiplet, made up of a $\mathcal{N} = (1, 0)$ tensor multiplet and hypermultiplet. The bosonic sector

now comprises a self-dual two-form field $B_{[\mu\nu]}$ and five real scalar fields ϕ_i, for a total of 3+5=8 degrees of freedom. The fermionic sector contains two left Weyl spinors, again giving 8 degrees of freedom. The R-symmetry is $Sp(2) \equiv SO(5)$. The group $Sp(2)$ acts non-trivially on the fermions, while $SO(5)$ rotates the scalars. The presence of the tensor $B_{[\mu\nu]}$ is surprising, because it suggests that some of the degrees of freedom of the $(2,0)$ theory are described by strings instead of the usual particles we find in quantum field theories. The strings couple to the tensor fields via the interaction:

$$q_i \int B^i_{\mu\nu}\, d\sigma^{\mu\nu} + \dots \ , \tag{1.1.2}$$

where q_i is a charge, $d\sigma^{\mu\nu}$ is the surface element on the worldsheet, and once again the dots stand for fermionic terms required by supersymmetry. No scale can be present in a conformal theory, so in particular, the tension of these strings has to vanish at the superconformal point. For this reason, we say that the $(2,0)$ theories contain so-called tensionless strings.

We can attempt to write an action functional for the theory; a natural guess is

$$S = \int d^6x\, \frac{1}{g^2_{6d}}\, F^a_{\mu\nu\rho} F^{a\mu\nu\rho} + \dots \ , \tag{1.1.3}$$

where $F_{\mu\nu\rho} = \partial_{[\mu} B_{\nu\rho]}$. Note that this time, the coupling g^2_{6d} is dimensionless. The self-duality of the tensor implies that $F_{\mu\nu\rho} = \frac{1}{6}\epsilon^{\sigma\lambda\tau}_{\mu\nu\rho} F_{\sigma\lambda\tau}$. But then we obtain $F^a_{\mu\nu\rho} F^{a\mu\nu\rho} = 0$, so the action we wrote down does not make sense. It turns out to be possible to write a sensible action for a free field $(2,0)$ theory, in which case a necessary condition for the tensor self-duality condition to be satisfied is to set $g^2_{6d} = 1$. However, an interacting theory action functional cannot be written down. Another way to phrase this is that the field strength of a gauge field can be written as $F^a_{\mu\nu} = \partial_{[\mu} A^a_{\nu]} + f^a_{bc} A^b_\mu A^c_\nu$, where f^a_{bc} is a structure constant, but no similar expression seems to exist for the tensor field strength: one could guess that $F^a_{\mu\nu\rho} = \partial_{[\mu} B^a_{\nu\rho]} + \dots$, but nobody knows how one could fill the dots.

The $(2,0)$ theories have a beautiful classification, based on the following observation: First note that the self-duality of the tensor imposes $(q^e_i, q^m_i) = (q_i, q_i)$ for the dyonic charge or the string that couples to it. One can show that Dirac quantization implies $\overrightarrow{q} \cdot \overrightarrow{q}' \in \mathbb{Z}$, while anomaly cancellation of the string worldsheet [17] imposes $\vec{q} \cdot \vec{q} = 2$. Therefore, one can identify the string charges with the roots of a simply-laced Lie algebra (recall that a root α of such an algebra satisfies $|\alpha|^2 = 2$). That is to say, the $(2,0)$ theories have an ADE classification.

By now, it should be apparent that analyzing the $(2,0)$ SCFT directly is excessively hard, due to the lack of a good definition of the theory. We therefore turn our attention to a certain "mass deformation" of the SCFT, the so-called $(2,0)$ little string theory, which in many regards will be easier to study.

1.2 6d $\mathcal{N} = (2, 0)$ Little Strings

String dynamics become particularly rich near impurities. Perhaps the most notable example is the local excitations felt by open strings that end on D-branes. In this case, the states localized on a D-brane couple to the bulk, since open strings ending on a brane can combine into a closed string that is allowed to leave the brane. One typically decouples the D-brane physics from the bulk by keeping the string coupling g_s constant and taking a low energy limit $E/m_s \to 0$, where m_s is the string mass, related to the fundamental string tension by $T = m_s^2$ (we neglect 2π factors here and in the rest of this thesis). Then, if one obtains an interacting theory in the limit, it will be a local quantum field theory; this is exactly what happens in the case of D-branes, where at low energies, the theory becomes a non-abelian gauge theory.

Does the situation differ at all if the spacetime impurities are NS5 branes instead of D-branes? It turns out that surprisingly, the dynamics of NS5 branes can be decoupled from the bulk physics without the need to take the low energy limit $m_s \to \infty$. Instead, bulk physics is decoupled from the branes by considering a different limit: one takes the string coupling $g_s \to 0$, while keeping E/m_s fixed. The resulting theory on the NS5 branes is called little string theory[1]. It is not a local quantum field theory, but instead an honest (noncritical) theory of strings in six dimensions. Indeed, it exhibits T-duality upon compactification, and has a Hagedorn spectrum at high energies for the density of states. Gravity is decoupled from the onset, since we took $g_s \to 0$, and the only parameter left is m_s. Note that had we considered this limit for D-branes, we would have ended up with a free theory, since g_s is a coupling for both open and closed strings.

Suppose we have k parallel and overlapping NS5 branes in type II string theory, and we send $g_s \to 0$. The branes break half of the supersymmetry and 16 supercharges survive. If one considers type IIA, the surviving six-dimensional supersymmetry on the branes is $(2, 0)$ (while it is $(1, 1)$ in type IIB). We call the resulting theory a $(2, 0)$ little string of type A_{k-1}. Different constructions of the theory exist after making use of various dualities. For instance, the duality between type IIA and M-theory implies that the $(2, 0)$ A_{k-1} little string can be obtained from considering k M5 branes with a transverse circle of radius R, when $R \to 0$ and $M_P \to \infty$ so that we can keep $M_P^3 R = m_s^2$ constant. Using orientifold planes, we can also engineer D_k theories in the same fashion.

The setup we will be most interested in produces more general theories than presented so far, and can be obtained by yet another duality: recall that k NS5 branes with a transverse circle in type IIA is T-dual to an A_{k-1} surface singularity with a circle that only affects the bulk physics (and therefore decouples in the $g_s \to 0$ limit relevant to us) in type IIB. we therefore compactify type IIB string theory on a surface X, which is a hyperkähler manifold, obtained by resolving a $\mathbb{C}^2/\Gamma$ singularity, with Γ a given discrete subgroup of $SU(2)$. This has

[1]Little strings were originally discovered in [18, 19, 20]. For a self-contained review of the theory's basic features, see [21]. Recently, there has been a renewed interest in its study, in a variety of contexts [22, 23, 24, 25, 26, 27, 28, 29, 30, 31, 32, 33].

the advantage of not only producing the A_{k-1} little string theory, but also D_k and E_k theories, since discrete subgroups of $SU(2)$ have an ADE classification, by the McKay correspondence; see the appendix A for details on this.

After we take the limit $m_s \to \infty$ in the little string, no parameter survives (apart from the discrete parameter k that labels the theory) and we recover the $(2,0)$ SCFT of section 1.1. One could ask how the tensionless strings of the SCFT come about in the different setups we described. In the type IIA picture, we can consider D2 branes stretching between different fivebranes. The separation between the NS5 branes corresponds to giving a vev to the scalars of the tensor multiplets, thereby probing the tensor branch of the theory. The ends of the D2 branes are strings on the fivebranes. At the superconformal point, the NS5 branes are put on top of each other. The D2 brane ends therefore become tensionless strings of the $(2,0)$ SCFT of type A_{k-1}. In the M-theory picture, we instead consider putting the k M5 branes on top of each other, and an analogous effect happens to the "M-strings" [34], which are the ends of M2 branes stretching between the fivebranes. Also note that in this picture, the $SO(5)$ R-symmetry of the SCFT is easily visible as a rotation in the directions perpendicular to the stack of fivebranes. Finally, in the IIB setup, the strings are D3 branes wrapping compact 2-cycles (these are topologically 2-spheres) that blow up the ADE singularity; when the 2-cycles shrink to zero size, the strings become tensionless.

Finally, we discuss the moduli space of the $(2,0)$ little string, which is

$$\mathcal{M} = (\mathbb{R}^4 \times S^1)^n / W \ . \tag{1.2.4}$$

In the above, n is the rank and W the Weyl group of $\mathfrak{g}$. In our type IIB setup, the scalar fields parameterizing $\mathcal{M}$ come from the moduli of the metric on the resolved singularity X; they are encoded in the periods of a triplet of self-dual two-forms $\omega_{I,J,K}$ and the NS and RR B-fields, along the 2-cycles S_a generating $H_2(X,\mathbb{Z})$. Their natural normalizations are

$$\int_{S_a} m_s^4\, \omega_{I,J,K}/g_s, \qquad \int_{S_a} m_s^2\, B_{NS}/g_s, \qquad \int_{S_a} m_s^2\, B_{RR}. \tag{1.2.5}$$

A power of g_s accompanies NS sector fields but not the RR sector ones, since this is how they enter the low energy action of the IIB string. The canonical mass dimension of scalars in a two-form theory is two. In taking g_s to zero, we tune the moduli of IIB so that the above combinations are kept fixed. The compact directions in $\mathcal{M}$ come from periods of the RR B-field and have radius m_s^2. In the low energy limit, when we send m_s to infinity, the moduli space becomes simply $(\mathbb{R}^5)^n/W$, since periodicity of the scalars coming from B_{RR} becomes infinite. The periodicity of scalars coming from B_{NS} would have been m_s^2/g_s; it is lost at the outset since g_s is taken to zero.

The perturbative string theory description is good away from the singularity at the origin of the moduli space $\mathcal{M}$. We are taking g_s to zero, in addition, so from IIB string perspective, the theory is under excellent control.

1.3 Outline of the Thesis

The thesis is organized as follows:

In Chapter 2, we start with type IIB string theory on a resolved singularity X, take the limit $g_s \to 0$, and compactify the resulting $(2,0)$ little string theory on a Riemann surface $\mathcal{C}$, which we will take to be the cylinder. D5 branes are introduced as points on $\mathcal{C}$. They are codimension 2 defects of the $(2,0)$ little string. We give a geometric description of the defects, for $\mathfrak{g}$ a simple Lie algebra, and give the 5d $\mathcal{N}=1$ quiver gauge theory that describes them at low energies. The defects will turn out to have an elegant group theoretical interpretation, in terms of certain (co)weights of $\mathfrak{g}$. These coweights carry the charge of D5 branes, and will be divided in two categories: polarized and unpolarized. This Chapter is based on [27, 35, 36].

In Chapter 3, we compute the 5d supersymmetric partition function of the little string on $\mathcal{C} \times \mathbb{R}^4$, with $\mathbb{R}^4$ regulated by Ω-background, using techniques of [37, 38, 39, 40, 41, 42]. we show that the partition function equals the q-deformed conformal block of $\mathfrak{g}$-type Toda CFT on $\mathcal{C}$. The q-deformed vertex operator insertions are in one to one correspondence with the defect D5 branes. The q-deformed conformal blocks have a $\mathcal{W}_{q,t}(\mathfrak{g})$ algebra symmetry developed by Frenkel and Reshetikhin [43]. They are written as integrals over positions of screening currents, with an integrand that is a correlator in a free theory. We show that, computing the integrals by residues, one recovers the partition function of the little string. The numbers of screening charge integrals are related to the values of the Coulomb moduli. In establishing the correspondence between Toda CFT and the $(2,0)$ theory, the central role is played by strings, obtained by wrapping D3 branes on compact 2-cycles in X, and at points on $\mathcal{C}$. The D3 branes are finite tension excitations – they are vortices on the Higgs branch of little string theory on $\mathcal{C}$. The theory on D3 branes, derived by a perturbative IIB computation, is a 3d $\mathfrak{g}$-type quiver gauge theory compactified on an S^1, which in presence of defect D5 branes has $\mathcal{N}=2$ supersymmetry. The 3d theory turns out to have a manifest relation to Toda CFT: its partition function, expressed as an integral over Coulomb moduli, is identical to the q-Toda CFT conformal block – D3 branes are the screening charges. Interpreting the partition function instead in terms of the Higgs branch of the 3d gauge theory, it equals the 5d partition function, at integer values of Coulomb moduli. The physics at play is the gauge/vortex duality which originates from two different, yet equivalent ways to describe vortices: from the perspective of the theory on the D3 branes, or from the perspective of the bulk theory with fluxes. In the latter description, the vortex flux is responsible for shifting the Coulomb moduli by integer values in Ω-background. This results in a *triality* of relations between three different classes of theories: a 5d theory on D5 branes, a 3d theory on D3 branes, and q-deformed Toda. Lastly, we make contact with the representation theory of quantum affine algebras $U_q(\hat{\mathfrak{g}})$. This Chapter is based on [44, 45, 27, 36].

In Chapter 4, we take the string mass m_s to infinity in the little string to obtain the $(2,0)$ CFT on $\mathcal{C}$. We show that the Coulomb branch of the 5d quiver gauge theory on D5 branes flows to a nilpotent orbit of $\mathfrak{g}$ in the limit. The fact that codimension 2 defects of a $(2,0)$ CFT are characterized by nilpotent orbits was analyzed by different means in

[46, 47, 48, 49, 50, 51, 52, 53]. In our setup, we show that the coweight data of the D5 branes encodes the Bala–Carter labels of the nilpotent orbits. Furthermore, we analyze the relation of our defects to parabolic subalgebras of $\mathfrak{g}$. Finally, we point out a surprising relation between the D5 brane quivers of the little string and the so-called weighted Dynkin diagrams of $\mathfrak{g}$. This Chapter is based on [54, 35, 36].

In Chapter 5, we first review how Gukov and Witten analyze surface defects of 4d $\mathcal{N} = 4$ SYM from a gauge theory perspective. This is done by studying the singular behavior of the gauge and Higgs fields in SYM near the defect [1, 55]. We provide the origin of these defects using the $(2, 0)$ little string on $\mathcal{C}$, compactified on an additional torus T^2. At energies below the Kaluza–Klein scale of compactification and the string scale, the little string becomes the 4d $\mathcal{N} = 4$ SYM theory. The defects come from D5 branes wrapping the T^2, or equivalently, from D3 branes at points on T^2. In particular, the S-duality of 4d SYM theory with defects is realized in little string theory as T-duality on the torus; the case without defects was studied already some time ago in [56]. In the CFT limit, the resolution [57, 58, 59] of the (singular) Coulomb branch of the theory on the D3 branes is in fact described by the cotangent bundle $T^*(G/\mathcal{P})$, where $\mathcal{P}$ is a parabolic subgroup of the gauge group G. This space already appeared in [1] as an alternate way to describe surface defects. It comes about as a moduli space of solutions to Hitchin's equations. By compactifying our setup on an additional circle, and using T-duality to relate D5 branes to monopoles on $\mathbb{R} \times T^2$, studied in [41, 42], we show that the Seiberg–Witten curve of the brane defects reduces in the CFT limit to the spectral curve of the Hitchin integrable system. The occurrence of the space $T^*(G/\mathcal{P})$ therefore has a geometric interpretation. Indeed, a given set of D5 branes wrapping 2-cycles of X will determine a unique parabolic subalgebra of $\mathfrak{g}$ at low energies. This Chapter is based on [54].

In Chapter 6, we study the Toda side of the $m_s \to \infty$ limit. There, the q-deformation disappears and one recovers ordinary Toda CFT, with $\mathcal{W}(\mathfrak{g})$ algebra symmetry. In particular, the codimension-two defects of the 6d $(2, 0)$ CFT are expected to be classified from the perspective of the 2d Toda theory. This can be done by studying the Seiberg-Witten curve of the quiver gauge theory on the D5 branes. At the root of the Higgs branch, and in the m_s to infinity limit, the curve develops poles at the puncture locations. The residues at each pole obey relations which describe the level 1 null states of the Toda CFT. We argue that this characterization of defects as null states of the CFT naturally gives the same parabolic subalgebra classification obtained in chapter 4. This chapter is based on [54, 35].

In Chapter 7, we give other realizations of the little string defects, at finite m_s. Most notably, when $\mathfrak{g} = A_n$ or D_n, we engineer a T-dual setup for the defects using a web of branes in type IIB [2]. We point out that the coweight formalism generalizes Hanany–Witten transitions, and we engineer both polarized and unpolarized weights. This Chapter is based on [54, 35].

In chapter 8, we provide a plethora of examples to illustrate the results of the thesis. This Chapter is based on [54, 36].

Finally, in Chapter 9, we conclude and briefly describe various ideas that would be worth pursuing in the future.

Chapter 2

Surface Defects as D5 branes in Little String Theory

As explained in the previous chapter, we start with type IIB string theory compactified on a resolved ADE singularity X, and send $g_s \to 0$ to obtain $(2,0)$ little strings. We further compactify the little string theory on a Riemann surface $\mathcal{C}$; in this thesis, the Riemann surface will be the cylinder $\mathcal{C} = \mathbb{R} \times S^1(\hat{R})$. Note that $X \times \mathcal{C}$ is a solution of the type IIB string theory, since the cylinder has a flat metric. We now introduce defects in the setup.

2.1 ADE-type Defects

We would like to introduce codimension two defects in the little string theory, which are at points on $\mathcal{C}$ and fill the remaining 4 directions. In the little string limit, type IIB string theory essentially has a unique candidate for such an object: these are D5 branes that wrap *non-compact* 2-cycles in X, are points on $\mathcal{C}$, and fill the rest of the spacetime[1].

We choose a class $[S^*]$ in the coweight lattice[2] $\Lambda_*^\vee$ of $\mathfrak{g}$. Each coweight then specifies the charge of a D5 brane wrapping some non-compact 2-cycle of X. We can expand a given set of coweights, identified here with a non-compact homology class $[S^*]$, in terms of fundamental coweights:

$$[S^*] = -\sum_{a=1}^{n} m_a \, w_a^\vee \quad \in \Lambda_*^\vee \,, \tag{2.1.1}$$

with m_a non-negative integers and $n = \text{rank}(\mathfrak{g})$. The $w_a^\vee$ are the n fundamental coweights of $\mathfrak{g}$. Each fundamental coweight is conveniently written with Dynkin labels as a vector of size n,

[1] String-like defects in 6d SCFTs were given an analogous description in [60], replacing D5 with D3 branes. This leads to degenerate vertex operators of $\mathcal{W}_{q,t}(\mathfrak{g})$ algebra; see for instance [31].

[2] In this section, $\mathfrak{g}$ is simply-laced, so the coweight lattice (respectively coroot lattice) is the same as the weight lattice (respectively root lattice). However, we will consider non simply-laced defects next, where the distinction will matter, so we write this section in a language appropriate to any simple Lie algebra.

with a 1 in the a-th entry and 0 everywhere else. For instance, $w_2^\vee = [\ 0,\ \ 1,\ \ 0,\ \ 0, \ldots,\ \ 0]$. In what follows, all coweights will be written in this fundamental coweight basis.

Though in principle a very generic assortment of D5 branes can be studied in this setup (with the only requirement that the branes preserve the same supersymmetry), a beautiful structure will emerge when one imposes a "conformality" constraint on the coweights. In brane language, we want to impose that the total flux due to the D5 branes vanishes at infinity. We therefore need to add some D5 branes wrapping a compact homology class $[S]$ in the coroot lattice of $\mathfrak{g}$; we have the following expansion in terms of simple positive coroots:

$$[S] = \sum_{a=1}^{n} d_a\, \alpha_a^\vee \quad \in\ \Lambda^\vee\ , \tag{2.1.2}$$

with d_a non-negative integers. The vanishing flux condition takes the form:

$$[S + S^*] = 0\,. \tag{2.1.3}$$

Now, if $S + S^*$ vanishes in homology, then $\#(S_a \cap (S + S^*))$ also vanishes, for all $a = 1, \ldots, n$, and $[S_a]$ the homology class corresponding to the simple root α_a. After a little algebra, and making use of the fact that

$$S_a \cap S_b^* = \delta_{ab} \tag{2.1.4}$$

in homology, we can rewrite (2.1.3) as

$$\sum_{b=1}^{n} C_{ab}\, d_b = m_a\ , \tag{2.1.5}$$

with $C_{ab} \equiv \langle \alpha_a, \alpha_b^\vee \rangle$ the Cartan matrix of $\mathfrak{g}$. In 4d $\mathcal{N} = 2$ language, equation (2.1.5) is nothing but a vanishing beta function condition, which justifies why we dubbed this constraint a "conformality" condition.

A single D5 brane will brake half of the supersymmetry, leaving only 8 supercharges; since we will ultimately be considering a collection of many D5 branes, it is important that they preserve the same supersymmetry. To this end, it is not enough to choose the class of S^*, and we must choose the actual cycles inside it. D5 branes wrapping different components of S_* preserve the same supersymmetry if their central charges are aligned. These, in turn, are determined by the periods of the triplet of self-dual two forms $\vec{\omega} = (\omega_I, \omega_J, \omega_k)$ on the non-compact cycles S_a^*. Supersymmetry is preserved if they determine a collection of vectors, $\int_{S_b^*} \vec{\omega}$, which point in the same direction for all b, corresponding to all the central charges being aligned. Then, all the non-compact D5 branes preserve the same half of supersymmetries of the $(2, 0)$ theory. Up to a rotation under which $\vec{\omega}$ is a vector, we can choose

$$\int_{S_a^*} \omega_I > 0, \qquad \int_{S_a^*} \omega_{J,K} = 0.$$

Next, we pick a metric on X by picking periods of $\omega_{I,J,K}$ through the compact cycles S_a. The choice we make will affect the supersymmetry that D5 branes wrapping compact 2-cycles

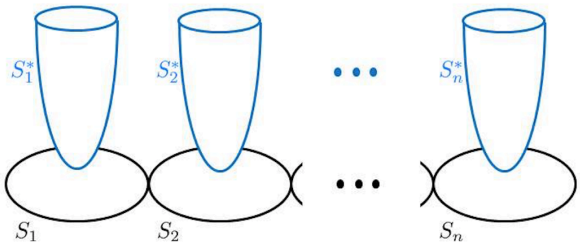

Figure 2.1: The vanishing cycles of A_n singularity S_a (in black) and the dual non-compact cycles S_a^* (in blue). S_a^* is constructed as the fiber of the cotangent bundle T^*S_a over a generic point on S_a.

preserve. It does not affect the non-compact D5 branes, which extend to infinity in X, as it only affects the data of X near the singularity. We will begin by setting

$$\int_{S_a} \omega_{J,K} = 0, \ \int_{S_a} B_{NS} = 0, \tag{2.1.6}$$

for all a's and letting

$$\tau_a = \int_{S_a} (m_s^2 \, \omega_I / g_s + i \, B_{RR}) \tag{2.1.7}$$

be arbitrary complex numbers with $\mathrm{Re}(\tau_a) > 0$. Recall that X has a sphere's worth of choices of complex structure. In the complex structure in which ω_I is a $(1,1)$ form, and having chosen (2.1.6), (2.1.7), both $[S_b^*]$ and $[S_a]$ have holomorphic 2-cycles representatives, and the D5 branes wrapping both the compact and the non-compact 2-cycles preserve the same supersymmetry. The fact that all the D5 branes preserve the same supersymmetry is important, as it leads to a quiver gauge theory description at low energies, with the quiver diagram based on the Dynkin diagram of $\mathfrak{g}$. Note that relaxing (2.1.6) to generic values corresponds to turning triplets of Fayet-Iliopolous parameters.

We will now determine the low energy description of the compactified $(2,0)$ little string with defects. For generic τ's, at energies below the string scale, the entire system can be described in terms of a 5d $\mathcal{N} = 1$ gauge theory which originates from the D5 branes. In the rest of this thesis, we call this gauge theory T^{5d}.

At long distances, if τ's are not zero, the bulk theory is a theory of abelian self-dual 2-forms. The 2-forms are non-dynamical from the perspective of the compactified theory, since they propagate in all six dimensions. At the same time, τ's determine the inverse gauge couplings of the D5 brane gauge theory. As long as they are non-zero, the theory on the D5 branes has a gauge theory description at low energies[3]. Thus, for non-zero τ and below the

[3]The $1/g_{YM}^2$ in five dimensions has units of mass. The τ is the dimensionless combination $\tau \sim 1/(g_{YM}^2 m_s)$.

string scale, the dynamics of the $(2,0)$ little string theory on $\mathcal{C}$ with defects can be described by the gauge theory *on* the D5 branes.

String theory allows us to determine the gauge theory on the branes: it was in fact worked out in [61]. It is an ADE quiver gauge theory, with gauge group

$$\prod_{a=1}^{n} U(d_a), \tag{2.1.8}$$

and I_{ab} hypermultiplets in the bifundamental $(d_a, \overline{d_b})$ representation for each pair of nodes a and b. The theory has $\mathcal{N}=2$ supersymmetry in four dimensions, since D5 branes break half the supersymmetry of IIB on X. The rank d_a of the gauge group associated to the a-th node of the quiver is the number of D5 branes wrapping the 2-cycle S_a. The hypermultiplets come from the intersections of cycles S_a with S_b. This follows from a computation we can do locally, near an intersection point. A non-zero intersection number I_{ab} of S_a with S_b, for distinct a and b, means that they intersect transversally at I_{ab} points. At a transversal intersection of 2 holomorphic 2-cycles in a 4-manifold, there are 4 directions in which open strings with endpoints on the branes have DN boundary conditions, leading to a massless bifundamental hypermultiplet. The $U(1)$ gauge groups of the D5 branes wrapping cycles are actually massive, by Green-Schwarz mechanism [61], so the gauge groups are $SU(d_a)$ not $U(d_a)$. Correspondingly, the Coulomb moduli associated with the $U(1)$ centers are parameters of the theory, not moduli. Nevertheless, the effects of these $U(1)$'s remain: for example, due to stringy effects [62], the partition function is that of a $U(d_a)$ theory. For this reason, we will write the gauge group with $U(1)$ factors included, trusting the reader can keep in mind the subtle point (the issue of the $U(1)$'s was discussed in [63, 64], from a related perspective.) The D5 branes on S^* do not contribute to the gauge group, since the cycle is non-compact, but they do contribute matter fields: The intersections of non-compact cycles with compact cycles lead to additional fundamental matter hypermultiplets. Since S_a^* correspond to fundamental weights w_a, they do not intersect S_b for $b \neq a$, see equation (2.1.4). Thus, with S^* as in (2.1.1), there are m_a fundamental hypermultiplets on the a'th node. In section 8, we will work out examples of 5d quiver gauge theories that describe the corresponding little string theory on a cylinder with one arbitrary puncture[4].

While the theory has the super-Poincare invariance of a 4d $\mathcal{N}=2$ theory, it is a 5d $\mathcal{N}=1$ theory compactified on a circle of radius R. Recall that D5 branes are points on $\mathcal{C} = \mathbb{R} \times S^1(\hat{R})$, and we are keeping m_s finite. The zero modes of strings that wind around $S^1(\hat{R})$ lead to a Kaluza-Klein tower of states on the T-dual circle of radius

$$R = \frac{1}{m_s^2 \hat{R}}. \tag{2.1.9}$$

The gauge theory description is applicable for energies $E/m_s \ll 1$, and the theory is weakly coupled for $E/m_s \ll \tau$. When we study the partition function, $\exp(-\tau)$ will be the instanton expansion parameter, and we will want this to be less than 1, so we only need $\mathrm{Re}(\tau) > 0$.

[4]Note that when one takes the limit $m_s \to \infty$, and only then, conformal invariance of the theory is recovered, and one can equivalently think of the cylinder as a sphere with two full punctures.

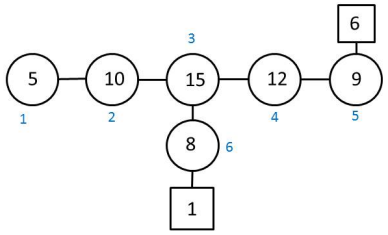

Figure 2.2: Example of a 5d gauge theory describing the E_6 little string on the cylinder with a full puncture defect. The numbers in the nodes denote the ranks of the unitary gauge groups, while the numbers outside the nodes simply label the nodes of the Dynkin diagram.

The resulting tower of states affects the low energy physics [65]. For example, the supersymmetric partition function of the theory depends on R, as we will review in section 3.1. Another way to see this it to do T-duality on the circle. This relates D5 branes which are points on $S^1(\hat{R})$ to D6 branes wrapping $S^1(R)$. In the D6 brane description, the fact that the low energy theory is a five dimensional theory on a circle of radius R is manifest.

The moduli of the $(2,0)$ theory in six dimensions become parameters in five dimensions, and they determine the couplings of the D5 brane gauge theory. The dictionary from geometry to gauge theory data is as follows: The complex combinations of the moduli which we called $\tau_a = \int_{S_a}(\frac{m_s^2}{g_s}\,\omega_I + iB_{RR})$ are the gauge couplings of the effective gauge theory on the D5 branes. The triplets of $\mathcal{N}=2$ Fayet-Iliopolous parameters, one for each node of the quiver, come from the remaining 6d moduli, $\int_{S_a} m_s^2\,\omega_{J,K}/g_s$ and $\int_{S_a} B_{NS}/g_s$. The only other parameters in the theory are the masses of the fundamental hypermultiplets. These come from the positions of the non-compact D5 branes on $\mathcal{C}$: the non-compactness of the cycles in X renders these non-dynamical as well. Finally, since the $U(1)$ centers of the gauge group are not dynamical, the Coulomb moduli associated with them are parameters of the theory as well.

2.2 $BCFG$-type Defects

Let $\mathfrak{g}'$ be a simply-laced Lie algebra. We call $\mathfrak{g}$ a subalgebra of $\mathfrak{g}'$ invariant under the outer automorphism group action of $\mathfrak{g}'$. It is well known that such outer automorphisms of $\mathfrak{g}'$ are in one-to-one correspondence with the automorphisms of the Dynkin diagram of $\mathfrak{g}'$. The resulting subalgebras $\mathfrak{g}$ are called non simply-laced. Let A be an outer automorphism group of $\mathfrak{g}'$. Then either $A=\mathbb{Z}_2$ or $A=\mathbb{Z}_3$, where the precise group action is shown in Figure 2.3 below:

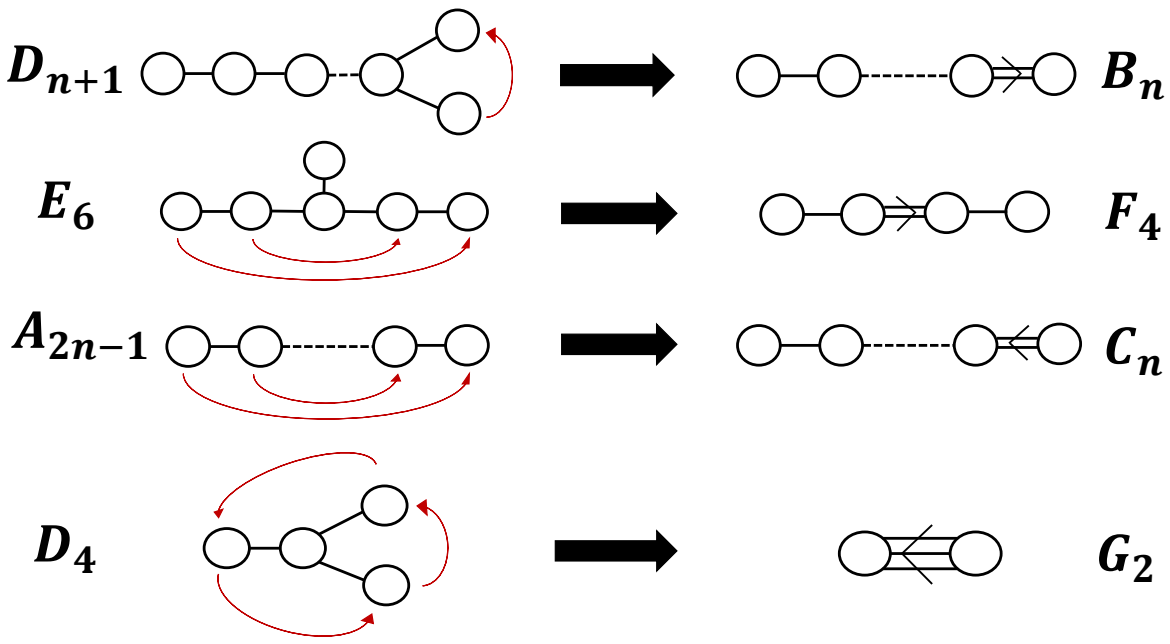

Figure 2.3: The action of the outer automorphism group A on the simply-laced Lie algebras. In the case of D_4, the outer automorphism can be either $\mathbb{Z}_2$ (resulting in B_3) or $\mathbb{Z}_3$ (resulting in G_2).

It should then be clear how one can engineer non-simply laced theories in the little string context [56]. Namely, consider the following nontrivial fibration of X over $\mathbb{C}^2 \times \mathcal{C}$: as one goes around the origin of one of the complex planes $\mathbb{C}$ wrapped by the D5 branes, we require that X goes back to itself, up to the action of the group A. This action will permute some of the compact two-cycles, according to Figure 2.3, and there is a corresponding action on the root lattice of $\mathfrak{g}'$. Let $a \in A$. If the set of simple roots of $\mathfrak{g}'$ is denoted Δ, then the simple roots of $\mathfrak{g}$ are grouped into two sets:

$$\Delta_l = \{\alpha \ \ / \alpha \in \Delta, \ \alpha = a(\alpha)\} \tag{2.2.10}$$

is the set of roots of $\mathfrak{g}'$ invariant under the action of A. They are called the long roots of $\mathfrak{g}$, and we set them to have length squared 2. The remaining simple roots of $\mathfrak{g}$ are constructed as follows:

$$\text{If } A = \mathbb{Z}_2, \ \ \Delta_s = \{\frac{1}{2}(\alpha + a(\alpha)) \qquad / \alpha \in \Delta, \ \alpha \neq a(\alpha)\} \tag{2.2.11}$$

$$\text{If } A = \mathbb{Z}_3, \ \ \Delta_s = \{\frac{1}{3}\left(\alpha + a(\alpha) + a^2(\alpha)\right) \quad / \alpha \in \Delta, \ \alpha \neq a(\alpha)\} \tag{2.2.12}$$

They are called the short roots of $\mathfrak{g}$, and have length squared $2/r$, with r the lacing number of $\mathfrak{g}$ ($r = 2$ if $A = \mathbb{Z}_2$ and $r = 3$ if $A = \mathbb{Z}_3$).

Denoting the Cartan-Killing form by $\langle \cdot, \cdot \rangle$, note we have assumed that the length squared $\langle \alpha_a, \alpha_a \rangle$ of the simple root α_a in $\mathfrak{g}'$ is equal to 2. The simple coroots of $\mathfrak{g}$ are defined by $\alpha_a^\vee = 2\alpha_a / \langle \alpha_a, \alpha_a \rangle$, and recall that the Cartan matrix of $\mathfrak{g}$ is defined as $C_{ab} = \langle \alpha_a, \alpha_b^\vee \rangle$.

Not all D5 brane configurations we described in the previous section 2.1 represent defects in the nontrivial fibration of X over $\mathbb{C}^2 \times \mathcal{C}$; only the D5 branes that wrap 2-cycles left invariant under A-action are allowed. This implies the following for the quiver theory T^{5d} on the D5 branes: starting with a simply-laced quiver theory, the ranks of the flavor and gauge groups which lie in a given orbit of A must be equal. A non simply-laced defect is then well-defined.

A fundamental coweight $w_a^\vee$ of $\mathfrak{g}$ is in fact a sum of fundamental weights of $\mathfrak{g}'$, all belonging in the same A orbit. Therefore, fundamental coweights are appropriate to label the D5 branes wrapping non-compact 2-cycles of the fibered geometry. They are defined by $\langle w_a^\vee, \alpha_b \rangle = \delta_{ab}$, with α_b a simple root of $\mathfrak{g}$, and $a, b = 1, \ldots, \text{rank}(\mathfrak{g})$. Furthermore, the simple coroots are the adequate objects to label the D5 branes wrapping compact 2-cycles of the geometry. Note the fundamental coweights of $\mathfrak{g}$ are the fundamental weights of ${}^L\mathfrak{g}$, and the simple coroots of $\mathfrak{g}$ are the simple roots of ${}^L\mathfrak{g}$. We can therefore equally well label the D5 brane defects using the fundamental weights and simple roots of ${}^L\mathfrak{g}$ if we wish to do so, but we will refrain from doing so in most of this work.

2.3 Defects as a Set of Coweights

It turns out to be very fruitful to study the theory on the Higgs branch, where the gauge group $\prod_{a=1}^n U(d_a)$ is broken to its $U(1)$ centers, one for each node. We force the theory onto the Higgs branch by turning on the remaining moduli of the $(2,0)$ theory $\int_{S_a} \omega_{J,K}, \int_{S_a} B_{NS}$ (see [66] for a detailed analysis from gauge theory perspective); these are the FI parameters in the D5 brane gauge theory (2.1.6). The deformation is normalizable, affecting only the geometry of X near the singularity.

On the Higgs branch, the compact and non-compact D5 branes must recombine: the deformation changes the supersymmetries preserved by the compact D5 branes (it changes their central charges via (2.1.6)), but not the supersymmetries preserved by the non-compact ones (these can be detected at infinity in X). As a consequence, the branes on S in (2.1.2) and on S^* in (2.1.1) are no longer mutually supersymmetric. Correspondingly, we reshuffle the branes and arrange them in a configuration wrapping a set of non-compact cycles S_i^*; their homology classes ω_i now live in the coweight lattice $\Lambda_*^\vee$:

$$\omega_i = [S_i^*] \qquad \in \Lambda_*^\vee. \tag{2.3.13}$$

Therefore, we end up with a set of coweights ω_i, all taken in fundamental representations

of ${}^L\mathfrak{g}$. They can be decomposed as:

$$\omega_i = -w_a^\vee + \sum_{b=1}^{n} h_{ib}\, \alpha_b^\vee , \tag{2.3.14}$$

where $-w_a^\vee$ is the negative of the a-th fundamental coweight, h_{ib} are non-negative integers, and $\alpha_b^\vee$ is a positive simple coroot. Geometrically, the above decomposition of ω_i has the interpretation of having different D5 branes bind together. For the branes to bind, the positions of compact branes must coincide with the position of at least one of the non-compact D5 branes on $\mathcal{C}$. The positions of non-compact D5 branes are mass parameters of the quiver gauge theory, the positions of compact D5 branes on $\mathcal{C}$ are Coulomb moduli; when a Coulomb modulus coincides with one of the masses, the corresponding fundamental hypermultiplet becomes massless and can get expectation values. This, in turn, describes the D5 branes binding (see [67] for a similar example), and allows supersymmetry to be preserved in presence of non-zero FI terms. We denote the set of coweights ω_i as:

$$\mathcal{W}_{\mathcal{S}} = \{\omega_i\} \ . \tag{2.3.15}$$

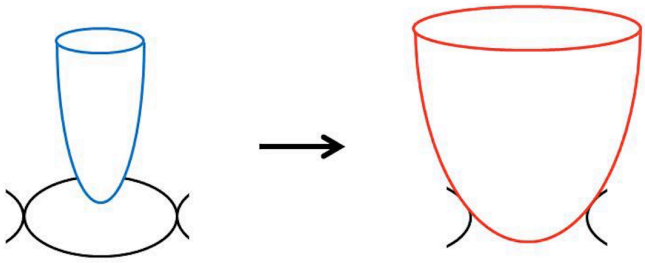

Figure 2.4: D5 branes in classes $\alpha_a^\vee$ and $-w_a^\vee$ bind to a brane in class $-w_a^\vee + \alpha_a^\vee$.

Then, the number of coweights ω_i's is the total rank of the flavor group of T^{5d}: $\sum_{a=1}^{n} m_a$. One can easily show that the constraint (2.1.3) is equvalent to:

$$\sum_{\omega_i \in \mathcal{W}_{\mathcal{S}}} \omega_i = 0 \ , \tag{2.3.16}$$

which is also equivalent to (2.1.5).

In what follows, we will limit our analysis to sets of size:

$$1 \leq |\mathcal{W}_{\mathcal{S}}| \leq n+1 \ ,$$

since the most generic defect of the $\mathfrak{g}$-type little string can always be described by at most $n+1$ coweights satisfying equation 2.3.16.

Example 2.3.1. *Let $\mathcal{W}_S$ be the following set of weights of D_4:*

$$\begin{aligned}
\omega_1 &= [\ \ 1, \ \ 0, \ \ 0, \ \ 0] = -w_1 + 2\alpha_1 + 2\alpha_2 + \alpha_3 + \alpha_4, \\
\omega_2 &= [-1, \ \ 1, \ \ 0, \ \ 0] = -w_1 + \alpha_1 + 2\alpha_2 + \alpha_3 + \alpha_4, \\
\omega_3 &= [\ \ 0, -1, \ \ 1, \ \ 1] = -w_1 + \alpha_1 + \alpha_2 + \alpha_3 + \alpha_4, \\
\omega_4 &= [\ \ 0, \ \ 0, -1, \ \ 0] = -w_3, \\
\omega_5 &= [\ \ 0, \ \ 0, \ \ 0, -1] = -w_4.
\end{aligned}$$

Note that these weights add up to zero. Written as above, these weights define a 5d quiver gauge theory, shown below in Figure 2.5.

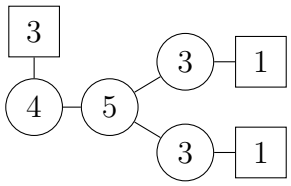

Figure 2.5: Example of a 5d gauge theory describing the D_4 little string with on the cylinder with a full puncture defect. The full puncture is determined by the set of weights $\mathcal{W}_\mathcal{S}$.

All in all, by choosing distinct sets of coweights $\mathcal{W}_\mathcal{S}$, we get an explicit realization of all the defects of the little string satisfying (2.1.5). However, it would be nice to have a finer classification of the defects. It turns out that there is an elegant answer to this problem, which we now present.

2.4 Polarized and Unpolarized Defects

D5 brane defects are divided into two groups, as follows: Pick a coweight ω of $\mathfrak{g}$ in a representation of ${}^L\mathfrak{g}$ generated by (minus) some fundamental coweight $-w_a^\vee$ for some a. If ω is in the Weyl group orbit of $-w_a^\vee$, and if all coweights of $\mathcal{W}_\mathcal{S}$ satisfy this condition, we call the resulting defect *polarized*[5].

If a defect is not polarized, we call it *unpolarized*. The unpolarized defects of the little string theory fall into one of the two following categories:

- The set $\mathcal{W}_\mathcal{S}$ only contains the zero coweight $\omega = [\ \ 0, \ \ 0, \ldots, \ \ 0]$ (with multiplicity one or possibly more).
- The set $\mathcal{W}_\mathcal{S}$ contains a nonzero coweight ω in a representation of ${}^L\mathfrak{g}$ generated by (minus) some fundamental coweight $-w_a^\vee$, but ω itself is not in the Weyl orbit of the coweight $-w_a^\vee$.

[5]The terminology will be explained in Section 4.2, and is directly related to the definition of the parabolic subalgebras of $\mathfrak{g}$.

To fully characterize such an unpolarized defect, it is necessary and sufficient to also specify the representation ω belongs in[6].

Example 2.4.1. – *Consider the following set of coweights of G_2:*

$$\mathcal{W}_{\mathcal{S}} = \{\omega_1 = [\ \ 0,\ \ 1],\ \ \omega_2 = [\ \ 0, -1]\}\ ,$$

written here in the fundamental coweights basis. One can check at once that both coweights satisfy the condition to make $\mathcal{W}_{\mathcal{S}}$ a polarized defect.

– Consider now the following set with a single coweight of F_4:

$$\mathcal{W}_{\mathcal{S}} = \{\omega = [\ \ 0,\ \ 0,\ \ 0,\ \ 0]_1\}\ .$$

This is an unploarized defect of the F_4 little string theory. Note that the null coweight is present in all four of the fundamental representations of F_4, and each one of these designates a distinct defect, so we added an extra label to specify which null coweight we are considering. In the present case, $[\ \ 0,\ \ 0,\ \ 0,\ \ 0]_1$ means that $\omega = -w_1^\vee + \#$ simple positive coroots, with $\#$ a positive integer.

– As a final example, consider the following set of (co)weights of D_5:

$$\mathcal{W}_{\mathcal{S}} = \{\omega_1 = [\ \ 1,\ \ 0,\ \ 0,\ \ 0,\ \ 0],\ \ \omega_2 = [-1,\ \ 0,\ \ 0,\ \ 0,\ \ 0]_3\}\ ,$$

The weight ω_1 belongs in the Weyl group orbit of $-w_1$, and we take it in (minus) the first fundamental representation of D_5; it is a good candidate to make up a polarized defect. However, the weight ω_2 is taken in (minus) the third fundamental representation: $\omega_2 = -w_3 + \#$ simple positive roots (hence the extra label "3"), while it is obviously in the Weyl group orbit of $-w_1$. The set $\mathcal{W}_{\mathcal{S}}$ therefore contains at least one weight (that is, ω_2) which satisfies the unpolarized condition, and we call the resulting defect as a whole unpolarized.

Then, given a set of coweights $\mathcal{W}_{\mathcal{S}}$ defining a polarized defect, the dimension of the Coulomb branch of T^{5d} can be computed in two different ways:

$$\sum_{a=1}^{n} d_a = \sum_{\langle e_\gamma, \omega_i\rangle < 0} |\langle e_\gamma, \omega_i\rangle|\ , \tag{2.4.17}$$

where the integers d_a on the left-hand side are the ranks[7] of the unitary gauge groups in the quiver T^{5d}. The sum on the right-hand side runs over all positive roots e_γ of $\mathfrak{g}$, and the coweights ω_i summed over must satisfy $\langle e_\gamma, \omega_i\rangle < 0$. The fact that the Coulomb branch

[6]The only unpolarized cases where one does not need to provide this additional data are the so-called simple punctures of B_2, B_3, C_2, D_4 and D_5 theories: these defects are uniquely specified by the zero coweight, which belongs in only one of the fundamental representations of ${}^L\mathfrak{g}$.

[7]In fact, a $U(1)$ in each of the n gauge groups is technically frozen, so one should really subtract n to this sum to get the number of normalizable Coulomb moduli. We will keep this subtlety in mind but it will have no incidence on our results.

dimension of the quiver theory T^{5d} is equal to the left sum is obvious, and the equality with the right sum side follows from rewriting the positive simple roots that occur in terms of positive roots.

If $\mathcal{W}_{\mathcal{S}}$ defines an unpolarized defect, the left-hand side of (2.4.17) is still a valid way to evaluate its Coulomb branch dimension, but the right-hand side is no longer applicable. We will have more to say about these defects after explaining the physics of triality in the next chapter.

We want to stress that many distinct sets $\mathcal{W}_{\mathcal{S}}$ often result in one and the same quiver gauge theory T^{5d}; the quivers are simply not a good definition of a defect. Crucial information is contained in the set $\mathcal{W}_{\mathcal{S}}$ that is absent from T^{5d}: namely, the coweights tell us which 2-cycles are wrapped by the D5 branes, and this data is crucial to characterizes a defect.

Finally, note that even though we will focus in this thesis on a single arbitrary puncture on $\mathcal{C}$, the formalism we introduced is automatically suited to study an arbitrary number of defects. Indeed, simply choose a set of coweights $\mathcal{W}_{\mathcal{S}}$, as done before. If there are k subsets of coweights which add up to zero in $\mathcal{W}_{\mathcal{S}}$, then the resulting quiver gauge theory describes k "elementary" punctures on $\mathcal{C}$. This just follows from linearity of equation (2.1.5). For some examples of composite defects, see below in Figure 2.6.

Thought the above argument is true at finite string mass m_s, the linearity of defects is lost in the CFT limit. Indeed, notable counterexamples arise for instance when describing a few of the defects of the E_7 and E_8 little string; for specific details, refer to the appendix B.

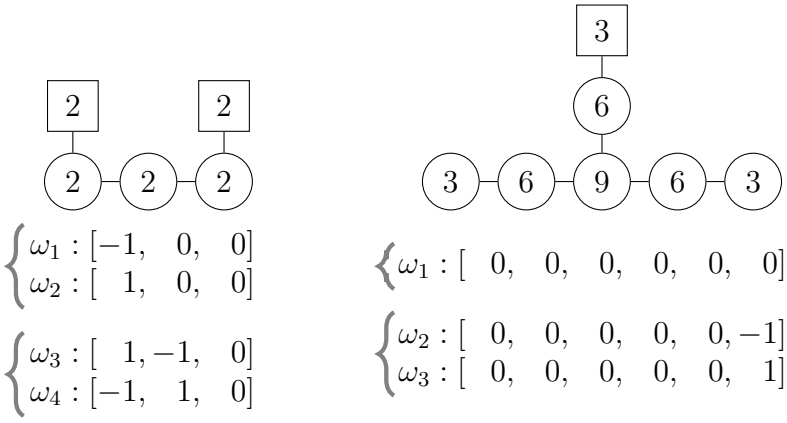

Figure 2.6: Left: two "minimal" punctures of A_3. The two punctures indicate that there are two subsets of weights in $\mathcal{W}_{\mathcal{S}}$ that add up to zero. Note that the second set of weights, made up of $[1, -1, 0]$ and $[-1, 1, 0]$, can be turned into the first set by applying a Weyl reflection about the first simple root of A_3. Right: two E_6 punctures. the first of these is the so-called minimal puncture, denoted by the zero weight in the 6-th fundamental representation, and is unpolarized. The second puncture is polarized.

Chapter 3

$\mathfrak{g}$-type Triality

In this chapter, we show that the instanton partition function of the 5d $\mathfrak{g}$ quiver gauge theory on $\mathbb{C}^2 \times S^1$ with $\mathcal{N} = 1$ supersymmetry is equal to the partition function of its vortices (which are themselves codimension 2, so a 3d theory) at the point of its moduli space where the Coulomb branch meets the Higgs branch. Furthermore, the 3d vortex partition function is nothing but the integral representation of the q-deformed $\mathfrak{g}$-type Toda conformal blocks with $\mathcal{W}_{q,t}(\mathfrak{g})$ algebra.

3.1 5d Gauge Theory Partition Function

We now compute the supersymmetric partition function of the $(2, 0)$ little string theory on $\mathcal{C} \times \mathbb{C}^2$ with a collection of defects at points of $\mathcal{C}$. As we argued above, this is the partition function of a 5d quiver theory on a circle with twisted boundary conditions, $Z_{5d}\left(S^1 \times \mathbb{C}^2\right)$ [37, 68]. When $\mathfrak{g} = ADE$, as we go around the circle S^1, we rotate different $\mathbb{C}$'s by different angles, ϵ_1 and ϵ_2:

$$z_1 \mapsto e^{i\epsilon_1} z_1 \equiv q\, z_1, \qquad z_2 \mapsto e^{i\epsilon_2} z_2 \equiv t^{-1}\, z_2. \tag{3.1.1}$$

The partition function for such ADE-type quiver gauge theories compactified on a circle was computed in [69], lifting the 4d computation from [70]. For the simply laced quivers, all nodes in the quiver designate simple roots that are on an equal footing. However, if the quiver is given by a non simply-laced Lie algebra $\mathfrak{g}$, the nodes label either short or long roots of $\mathfrak{g}$. In [71], the partition function for quivers that are not of finite-type Dynkin diagrams is computed by using equivariant localization. Such quivers are called fractional, and quivers of non-simply laced type fall into this category. An integer r_a is assigned to each node a to distinguish its relative length squared from the other nodes'. In particular, the partition function will reduce to the simply-laced case when all r_a's are equal to one. It was argued that the action of only one of the rotation generators is modified to account for the contribution of a given node a:

$$z_1 \mapsto e^{ir_a\epsilon_1} z_1 \equiv q^{r_a}\, z_1, \qquad z_2 \mapsto e^{i\epsilon_2} z_2 \equiv t^{-1}\, z_2. \tag{3.1.2}$$

The partition function is an index

$$Z_{5d}\left(S^1 \times \mathbb{C}^2\right) = \mathrm{tr}\,(-1)^F\, g \ \ ,$$

where $g = q^{r_a(S_1 - S_R)} t^{-S_2+S_R}$; S_1 and S_2 are the generators of the two rotations around the complex planes in $\mathbb{C}^2$ defined above. F is the fermion number. Finally, S_R is the generator of the $U(1)_R \subset SU(2)_R$ charge of the R-symmetry[1]. We twist by this R-symmetry to preserve supersymmetry.

This index can be computed using equivariant integration, and written as a sum over fixed point contributions on the instanton moduli space labeled by Young diagrams:

$$Z_{5d} = r_{5d} \sum_{\{\mu\}} I_{5d,\{\mu\}}(q,t;a,m,\tau). \tag{3.1.3}$$

The normalization factor r_{5d} contains the tree level and the one loop contributions to the partition function. We have used the following shorthand notation for Young diagrams to express the fixed points:

$$\{\mu\} = \{\mu^a_{I,i}\}_{a=1,\ldots n;\ I=1,\ldots d_a;\ i=1,\ldots,\infty}, \tag{3.1.4}$$

where the number of nodes in the quiver is given by n. The rank of the gauge groups is d_a. Although only finitely many rows of the Young diagrams are non-zero, we let i to run to infinity keeping in mind after a finite value of i, $\mu^a_{I,i}$'s vanish. Sometimes we prefer to suppress one or both subscripts to avoid cumbersome notation and hope that our notation will be clear from the context. The gauge theory partition function will depend on more parameters than just q and t; as we reviewed in Section 2.1, there are gauge couplings τ's, which come from certain moduli of the $(2,0)$ theory in six dimensions; there are also fundamental hypermultiplets masses, which originate from the positions of non-compact D5 branes on $\mathcal{C}$, and Coulomb moduli, which are the positions of the compact D5 branes on $\mathcal{C}$.

In [71], it is shown that the contributions for different multiplets at the node a depend also on the integer r_a. For our purposes, we assign the integer $r_a = 1, 2$, or 3 at every gauge node a in the quiver. The fixed point contributions $I_{5d,\{\mu\}}$ generically have the following form:

$$I_{5d,\{\mu\}} = \ e^{\tau\cdot\mu} \ \cdot \prod_{a=1}^{n} z^{5d}_{V_a,\vec{\mu}^a}\ z^{5d}_{H_a,\vec{\mu}^a}\ z^{5d}_{CS,\vec{\mu}^a} \ \cdot \prod_{a,b=1}^{n} z^{5d}_{H_{ab},\vec{\mu}^a,\vec{\mu}^b}, \tag{3.1.5}$$

where $z^{5d}_{V_a,\vec{\mu}^a}$ and $z^{5d}_{H_a,\vec{\mu}^a}$ are the contributions of the vector and hypermultiplets for node a at fixed points labeled by representations $\{\vec{\mu}^a\}$, respectively. $z_{CS,\vec{\mu}^a}$ stands for the topological Chern-Simons factors. We also have bifundamental matter multiplets charged under two distinct nodes, say a and b, and we label them with $z^{5d}_{H_{ab},\vec{\mu}^a,\vec{\mu}^b}$. We assume that $z^{5d}_{H_{ab},\vec{\mu}^a,\vec{\mu}^b}$ is 1 if there is no bifundamental hypermultiplet between nodes a and b.

[1]When considering type IIB string theory on the surface X, recall that an $SO(5)_R$ R-symmetry is preserved. The D5 branes will only preserve an $SU(2)_R$ subgroup of this R-symmetry, and only a $U(1)_R$ subset is relevant here.

Similar to the simply-laced quivers, the fixed point contributions for all multiplets are written in terms of the same function which is usually referred to as Nekrasov function. However, for the fractional quivers, the Nekrasov functions are modified according to the change in equivariant parameters at different nodes: $(q,t) \mapsto (q^{r_a}, t)$. The most general of Nekrasov function we will need is given by

$$N_{\mu^a\mu^b}(Q;q^{r_{ab}}) = \prod_{i,j=1}^{\infty} \frac{\left(Qq^{r_a\mu_i^a - r_b\mu_j^b}t^{j-i+1};q^{r_{ab}}\right)_\infty}{\left(Qq^{r_a\mu_i^a - r_b\mu_j^b}t^{j-i};q^{r_{ab}}\right)_\infty} \frac{\left(Qt^{j-i};q^{r_{ab}}\right)_\infty}{\left(Qt^{j-i+1};q^{r_{ab}}\right)_\infty}. \tag{3.1.6}$$

where r_{ab} is a positive integer divisor of r_a and r_b for now, and $(x;q)_\infty = \prod_{i=0}^{\infty}(1-x\,q^i)$ is the q-Pochhammer symbol[2]. Let us summarize the contributions from the different multiplets. At each node a, we have a $U(d_a)$ gauge group. The vector multiplets contribute at a fixed point:

$$z^{5d}_{V_a,\vec{\mu}^a} = \prod_{1\le I,J\le d_a} [N_{\mu_I^a\mu_J^a}(e_{a,I}/e_{a,J};q^{r_a})]^{-1}. \tag{3.1.7}$$

Here, $e_{a,I} = \exp(R\,\mathfrak{a}_{a,I})$ encode the d_a exponentiated Coulomb branch parameters of the $U(d_a)$ gauge group at the node a. At each node a, we can also couple m_a hypermultiplets charged in fundamental representation of the $U(d_a)$ gauge group with masses β_a's. They contribute to the partition function:

$$z^{5d}_{H_a,\vec{\mu}^a} = \prod_{1\le\alpha\le m_a}\prod_{1\le I\le d_a} N_{\emptyset\mu_I^a}(v_a^2\,f_{a,\alpha}/e_{a,I};q^{r_a}). \tag{3.1.8}$$

The exponentiated masses of the hypermultiplets are encoded in $f_{a,\alpha} = \exp(R\,\beta_{a,\alpha})$, where α takes m_a values, and $v_a \equiv \sqrt{q^{r_a}/t}$. Note that $\sum_{a=1}^n m_a = |\mathcal{W}_{\mathcal{S}}|$. For every pair of nodes a,b connected by an edge in the Dynkin diagram, we get a bifundamental hypermultiplet. Its contribution to the partition function is:

$$z^{5d}_{H_{ab},\vec{\mu}^a,\vec{\mu}^b} = \prod_{1\le I\le d_a}\prod_{1\le J\le d_b} [N_{\mu_I^a\mu_J^b}(e_{a,I}/e_{b,J};q^{r_{ab}})]^{\Delta_{ab}}. \tag{3.1.9}$$

where Δ is a matrix whose entries Δ_{ab} are equal to either 1 or 0, depending on whether the a'th and the b'th nodes are connected or not. There is an important subtlety arising for fractional quivers: the bifundamental matter can be coupled to gauge nodes corresponding to different length roots. For those multiplets, we have $r_{ab} = \gcd(r_a, r_b)$, the greatest common divisor of r_a and r_b.

[2]We suppress the explict dependence on r_a and r_b to avoid clutter in our notation, and refer only to r_{ab} since they determine the type of the q-Pochhammer symbol. Moreover, we keep r_{ab} generic for now; r_{ab} will be specialized when we introduce the bifundamental contributions.

In a 5d theory, we can turn on a Chern-Simons term of k_a^{CS} units, and its contribution to node a reads

$$z^{5d}_{CS,\vec{\mu}^a} = \prod_{1\leq I\leq d_a} \left(T_{\mu_I^a}\right)^{k_a^{CS}} \tag{3.1.10}$$

Here, T_μ is defined as $T_\mu = (-1)^{|\mu|} q^{\|\mu\|^2/2} t^{-\|\mu^t\|^2/2}$. The 5d $\mathcal{N}=1$ Chern-Simons terms can be determined by conformal invariance; with the rest of the partition function as written, k_a^{CS} on the a-the node is the difference between the ranks of the gauge group on that node and the following node(s). The gauge couplings keep track of the total instanton charge, via the combination

$$\tau \cdot \mu = \sum_{a=1}^{n} \sum_{I=1}^{d_a} \tau_a \, |\mu_I^a|. \tag{3.1.11}$$

3.2 3d Gauge Theory

On the Higgs branch of the little string theory, the bulk theory is abelianized, and the D5 branes are all non-compact. At the same time, there is a new class of branes that plays an important role: these are D3 branes which are at points on $\mathcal{C}$ and which wrap compact 2-cycles in X^3. The D3 branes survive the little string limit, for the same reason D5 branes did: their tensions remain finite.

D3 Branes are Vortices

The D3 branes realize vortices in the D5 brane gauge theory. Vortices are codimension two solutions of gauge theories on the Higgs branch, where the vortex charge is the magnetic flux in two directions traverse to the vortex. A generic collection of vortices in 5d $\mathcal{N}=1$ gauge theories are BPS if the 5d FI parameters are aligned. At each node, the triplet of FI terms transform as a vector under the $SU(2)_R$ symmetry rotations. The orientation of this vector determines the supersymmetry preserved by the vortex. In our setting, the 5d FI parameters are the moduli of the little string in (2.1.6). The background we consider has $\int_{S_a} m_s^2 \omega_J / g_s > 0$ as the only non-zero FI terms in (2.1.6). The vortices are in fact the supersymmetric vacua of the theory on the D3 branes. Due to non-zero 3d FI terms (recall that $\mathrm{Re}(\tau_a) > 0$) in a supersymmetric vacuum, the chiral multiplets from the D3-D5 strings need to get expectation values. This describes D3 branes ending on the D5 branes. As is well known, this turns on magnetic flux on the D5 brane, transverse to the D3 branes [2], consistent with the vortex interpretation.

[3]The D3 branes wrapping non-compact 2-cycles are also important; they are codimension 4 defects of the little string; see for instance [31].

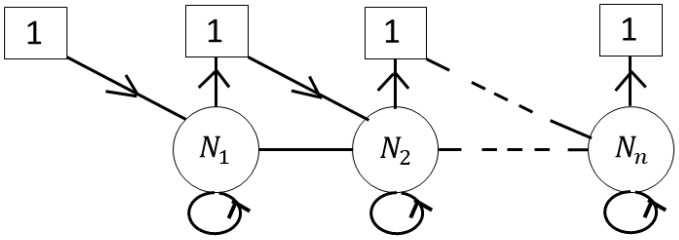

Figure 3.1: D3 brane quiver for a full puncture of the A_n little string.

The Higgs branch of the theory on the D3 branes is the moduli space of vortices. We have thus derived, from string theory, the description of the moduli spaces of vortices in a large class of $\mathfrak{g}$-type $\mathcal{N} = 2$ quiver theories. As far as we are aware, the result is novel, except in some special cases[4].

3d Gauge Theory Partition Function

Again, we can wrap D3 branes on compact or non-compact two cycles on X. The ones on compact cycles are dynamical, whereas the branes on non-compact cycles are not. The quiver gauge theory living on the branes was again constructed by Douglas and Moore, and we will call it G^{3d}. It is a 3d theory with $\mathcal{N} = 4$ supersymmetry[5]. In the $\mathcal{N} = 2$ language, each vector multiplet has an adjoint chiral multiplet. There is also a cubic superpotential. Let N_a be the number of D3 branes wrapping the a-th compact two cycle belonging to the second homology isomorphic to the coroot lattice of $\mathfrak{g}$. Then we have a quiver theory of $\mathfrak{g}$ type with unitary gauge nodes, $U(N_a)$. We obtain bifundamental matter hypermultiplets by quantizing strings stretched between adjacent nodes in the associated Dynkin diagram, described by the previously defined matrix Δ_{ab}.

In addition to the D3 branes, we have D5 branes wrapping cycles in X. As previously mentioned, on the Higgs branch, the D5 branes wrap non-compact two cycles which are described by a collection of coweights $\mathcal{W}_S$. We need to quantize the strings strechted

[4]In mathematical literature, the moduli space of vortices is called the moduli space of quasi-maps; see for example [72], where the quiver in Figure 3.1 appeared before, precisely for this purpose.

[5]Similar to the D5 branes, the D3 branes too feel the stringy effects due to the presence of the transverse circle in $\mathcal{C}$ and the tower of states resulting from it. Therefore, the theory is really three-dimensional at low energies.

between D3 and D5 branes too, which give rise to chiral and anti-chiral multiplets of $\mathcal{N}=2$ supersymmetry at the intersection points of compact cycles wrapped by D3 branes and non-compact cycles with D5 branes. The presence of D5 branes break half of the supersymmetry and we end up with a 3d theory of $\mathcal{N}=2$ supersymmetry.

From the D5 brane point of view, the D3 branes realize vortices. Their charge gives the magnetic flux in the remaining directions transverse to D3 branes. For an arbitrary collection of vortices to be BPS, the FI parameters which are the moduli of little string need to be aligned at each node of the 5d quiver theory. This requirement is satisfied with our choice of parameters (see [27] for details). The chiral multiplets coming from D3-D5 strings get expectation values due to non-zero 3d FI parameters in the supersymmetric vacua.

We can subject the 3d theory to Ω-background as well to compute the partition function on the vortices using localization [73, 74, 75, 76]. Note that we are probing the 5d theory on its Higgs branch; in other words, it is the theory living on the D5 branes wrapping non-compact two cycles. The equivariant action that we used to compute the 5d partition function can be used for the 3d one too. We choose the D3 brane to extend in the plane rotated by the parameter q, and to be transverse to the plane rotated by t. The partition function is again given as an index:

$$Z_{3d}(S^1\times\mathbb{C}) = \mathrm{tr}\,(-1)^F\, g\ , \tag{3.2.12}$$

where $g = q^{r_a(S_1-S_R)}t^{-S_2+S_R}$ consists of rotations $S_{1,2}$ acting on the different planes, and S_R are the R-symmetry rotations. We placed the D3 branes such that S_2 acts on the transverse plane to the branes, and is therefore an R-symmetry generator from the 3d theory perspective. The theory can have at most $U(1)_R$ symmetry, so $S_R - S_2$ is a global symmetry. Localization allows us to write the 3d partition function as a sum over Young diagram just as in the case of the 5d theory. This form will be crucial to see the connection between T^{5d} and G^{3d}. However, there also exists an integral representation of the 3d partition function. The two representations of the partition functions are ultimately related by picking up integration contours and computing the integral via residues. The partition function can be computed as an integral of the Coulomb branch in 3d,

$$Z_{3d} = \int dx\, I_{3d}(x)\ , \tag{3.2.13}$$

where the integrand $I_{3d}(x)$ can easily be read off from the quiver description of the theory. It is given by the product of individual contributions coming from vector multiplets and different types of matter multiplets coupled to the gauge groups on the nodes. Generically, it has the following form,

$$I_{3d}(x) = r_{3d}\prod_{a=1}^{n} z^{3d}_{V_a}(x_a)\, z^{3d}_{H_a}(x_a,f)\prod_{a<b} z^{3d}_{H_{ab}}(x_a,x_b). \tag{3.2.14}$$

r_{3d} is again a normalization factor whose precise form is not important for our purposes. The contributions of each type of multiplet is known, and we collect them here for completeness.

The $\mathcal{N}=4$ vector multiplet for a unitary gauge group $U(N_a)$ is given by

$$z^{3d}_{V_a}(x_a) = e^{\sum_{I=1}^{N_a} \tau_a x_{a,I}} \prod_{1\leq I\neq J\leq N_a} \frac{(e^{x_{a,I}-x_{a,J}};q^{r_a})_\infty}{(t\, e^{x_{a,I}-x_{a,J}};q^{r_a})_\infty}, \tag{3.2.15}$$

where as before, $r_a \equiv r\,\langle \alpha_a, \alpha_a^\vee\rangle/2$ for each node a, with r be the highest number of arrows linking two adjacent nodes in the Dynkin diagram of $\mathfrak{g}$ (and $\langle \alpha_a, \alpha_a^\vee\rangle = 2$ for long roots, in our normalization). The numerator consist of contribution coming from the gauge bosons, and the denominator takes into account the adjoint chiral multiplets within the vector multiplet. The bifundamental hypermultiplets give a similar contribution to the 5d case,

$$z^{3d}_{H_{ab}}(x_a,x_b) = \prod_{1\leq I\leq N_a}\prod_{1\leq J\leq N_b}\left[\frac{(v_{ab}t\, e^{x_{a,I}-x_{b,J}};q^{r_{ab}})_\infty}{(v_{ab}\, e^{x_{a,I}-x_{b,J}};q^{r_{ab}})_\infty}\right]^{\Delta_{ab}}, \tag{3.2.16}$$

where again Δ describes how the nodes are connected to each other. r_{ab} is the greatest common divisor of r_a and r_b for neighboring nodes a and b. The factor v_{ab} is a modified refined factor for non simply-laced Lie algebras: $v_{ab} = \sqrt{q_{ab}/t}$ with $q_{ab} = q^{r_a}$ if both nodes a and b correspond to long roots; otherwise, $v_{ab} = v = \sqrt{q/t}$. Chiral multiplets in the fundamental representation of the a-th gauge group, with S_R R-charge $-r/2$ (not to be confused with the lacing number of $\mathfrak{g}$), contribute $\prod_{1\leq I\leq N_a}(v_a^r\, f_{a,i}e^{-x_{a,I}};q^{r_a})_\infty^{-1}$ to the partition function, while anti-chiral multiplets contribute $\prod_{1\leq I\leq N_a}(v_a^r\, f_{a,i}e^{-x_{a,I}};q^{r_a})_\infty$, with $f_{a,i}$ the associated flavor.

The integral runs over all the Coulomb branch moduli of the n gauge groups in the quiver. To perform this integral, one needs to select a vacuum and pick a contour. We will not attempt to give a precise contour prescription in this thesis, but we conjecture what they should be based on the input from the 5d theory.

3.3 $\mathfrak{g}$-type Toda and its q-deformation

We now review a last important piece of physics that is needed to establish a triality, the Toda conformal field theory on the Riemann surface $\mathcal{C}$. The partition function of the gauge theory on D3 branes presented above is in fact equal to a certain canonical "q-deformation" of the Toda CFT conformal block on $\mathcal{C}$. This CFT has a vertex algebra symmetry called $\mathcal{W}_{q,t}(\mathfrak{g})$ symmetry, and was first described in [77]. Let us remind the reader of the various objects that enter in Toda theory, for $\mathfrak{g}$ a simple Lie algebra.

Free Field Toda CFT

Let $\mathfrak{g}$ be a simple Lie algebra. $\mathfrak{g}$-type Toda field theory can be written in terms of $n = \mathrm{r}k(\mathfrak{g})$ free bosons in two dimensions; there is a background charge contribution, and an exponential potential that couples the bosons to that charge:

$$S_{Toda} = \int dzd\bar{z}\,\sqrt{g}\; g^{z\bar{z}}[\langle \partial_z\varphi, \partial_{\bar{z}}\varphi\rangle + \langle \rho,\varphi\rangle\, QR + \sum_{a=1}^{n} e^{\langle \alpha_a^\vee,\varphi\rangle/b}]. \tag{3.3.17}$$

The bosonic field φ is a vector in the n-dimensional coweight space, whose modes obey a Heisenberg algebra. ρ is the Weyl vector of $\mathfrak{g}$, the bracket $\langle \cdot, \cdot \rangle$ is the Cartan-Killing form on the Cartan subalgebra of $\mathfrak{g}$, and $Q = b + 1/b$ is the background charge. As before, $\alpha_a^\vee$ label the simple positive coroots of $\mathfrak{g}$.

The Toda CFT has a $\mathcal{W}(\mathfrak{g})$ algebra symmetry (see [78] for a review). When $\mathfrak{g} = \mathrm{su}(2)$, the CFT is called Liouville theory, with Virasoro symmetry. The $\mathcal{W}(\mathfrak{g})$ symmetry of Toda is generated by the spin 2 Virasoro stress energy tensor, and additional higher spin currents.

The free field formalism of the Toda CFT was first introduced in [79]. It was then studied in our context in [80, 81, 82, 83, 84]. We label the primary vertex operators of the $\mathcal{W}(\mathfrak{g})$ algebra by an n-dimensional vector of momenta β, and given by:

$$V_\beta^\vee(z) = e^{\langle \beta, \varphi(z) \rangle}. \tag{3.3.18}$$

The conformal blocks of the Toda CFT in free field formalism take the following form:

$$\langle V_{\beta_1}^\vee(z_1) \dots V_{\beta_k}^\vee(z_k) \prod_{a=1}^{n} (Q_a^\vee)^{N_a} \rangle_{free} \,. \tag{3.3.19}$$

In the above, we have defined the screening charges

$$Q_a^\vee \equiv \oint dx \, S_a^\vee(x) \,.$$

These n charges are integrals over the n screening current operators $S_a^\vee(x)$:

$$S_a^\vee(z) = e^{\langle \alpha_a^\vee, \phi(z) \rangle / b} \,. \tag{3.3.20}$$

The $\mathcal{W}(\mathfrak{g})$ algebra can then be defined as a complete set of currents that will commute with the screening charges. For a derivation of the conformal block expression (3.3.19), we refer the reader to [85].

Momentum conservation imposes the following constraint:

$$\sum_{i=1}^{k} \beta_i + \sum_{a=1}^{n} N_a \alpha_a^\vee / b = 2Q. \tag{3.3.21}$$

The last term comes from the background charge on a sphere, induced by the curvature term in (3.3.17). Thus, the above constraint tells us that one of the momenta, say β_∞, corresponding to a vertex operator insertion at $z = \infty$, is fixed in terms of the momenta β_i of the other vertex operators, and the number of screening charges N_a.

The correlators of the theory can be computed by Wick contractions, and the conformal block (3.3.19) takes the form of an integral over the positions x of the N_a screening currents:

$$Z_{Toda} = \int dx \; I_{Toda}(x) \,. \tag{3.3.22}$$

The integrand $I_{Toda}(x,z)$ is a product over various two-point functions:

$$I_{Toda}(x,z) = \prod_{a=1}^{n} I_a^{Toda}(x_a) \cdot I_{a,V}(x_a,z) \cdot \prod_{a<b} I_{ab}^{Toda}(x_a,x_b) \tag{3.3.23}$$

The two-point functions of screening currents with themselves at a given node of the Dynkin diagram of $\mathfrak{g}$ give:

$$I_a^{Toda} = \prod_{1\le I\neq J\le N_a} \langle S_a^\vee(x_{a,I}) S_a^\vee(x_{a,J})\rangle_{free}. \tag{3.3.24}$$

These are the vector multiplet contributions at node a. The two-point functions of screening currents between two distinct nodes a and b is in turn given by:

$$I_{ab}^{Toda} = \prod_{1\le I\le N_a} \prod_{1\le J\le N_b} \langle S_a^\vee(x_{a,I}) S_b^\vee(x_{b,J})\rangle_{free}. \tag{3.3.25}$$

These are the bifundamental hypermultiplet contributions. Finally, the two-point functions of screening currents at a given node with all the vertex operators.

$$I_{a,V}^{Toda} = \prod_{i=1}^{k} \prod_{1\le I\le N_a} \langle S_a^\vee(x_{a,I}) V_{\beta_i}^\vee(z_i)\rangle_{free}, \tag{3.3.26}$$

will correspond to chiral matter contributions. The two-point functions are readily evaluated to be:

$$\langle S_a^\vee(x) S_b^\vee(x')\rangle_{free} = (x-x')^{b^2\langle \alpha_a^\vee, \alpha_b^\vee\rangle} \tag{3.3.27}$$

$$\langle S_a^\vee(x) V_\beta^\vee(z)\rangle_{free} = (x-z)^{-\langle \alpha_a^\vee, \beta\rangle} \tag{3.3.28}$$

After q-deformation, the above conformal block has an interpretation as a 3d partition function.

q-deformed Toda CFT

In [77], a deformation of the $\mathcal{W}(\mathfrak{g})$ algebra was given by deforming the screening currents. Starting with the definition of the quantum number

$$[n]_q = \frac{q^n - q^{-n}}{q - q^{-1}}\ , \tag{3.3.29}$$

and the incidence matrix $I_{ab} = 2\,\delta_{ab} - C_{ab}$, one defines the (q,t)-deformed Cartan matrix, $C_{ab}(q,t) = (q^{r_a}t^{-1} + q^{-r_a}t)\ \delta_{ab} - [I_{ab}]_q$. The number r_a is defined as before: $r_a \equiv r\,\langle \alpha_a, \alpha_a^\vee\rangle/2$, with r the lacing number of $\mathfrak{g}$.

If the Lie algebra $\mathfrak{g}$ is non-simply laced, its Cartan matrix C_{ab} is not symmetric. Then, we first need to introduce the matrix $B_{ab}(q,t)$, which is the symmetrization of $C_{ab}(q,t)$. It is obtained as follows; the symmetrized Cartan matrix is then given by:

$$B_{ab} = r_a\, C_{ab}\ .$$

Its (q,t)-deformation is simply:

$$B_{ab}(q,t) = [r_a]_q \, C_{ab}(q,t) \; .$$

We are now able to construct a q-deformed Heisenberg algebra, generated by n simple root generators α_a, and satisfying:

$$[\alpha_a[k], \alpha_b[m]] = \frac{1}{k}(q^{\frac{k}{2}} - q^{-\frac{k}{2}})(t^{\frac{k}{2}} - t^{-\frac{k}{2}}) B_{ab}(q^{\frac{k}{2}}, t^{\frac{k}{2}}) \delta_{k,-m} \; . \tag{3.3.30}$$

The Fock space representation of the Heisenberg algebra is given by acting on a vacuum state $|\lambda\rangle$ with "simple root" generators:

$$\begin{aligned} &\alpha_a[0]|\lambda\rangle = \langle \lambda, \alpha_a \rangle |\lambda\rangle \\ &\alpha_a[k]|\lambda\rangle = 0 \, , \qquad\qquad \text{for } k > 0. \end{aligned} \tag{3.3.31}$$

From these generators, one can define the (magnetic) screening charge operators:

$$S_a^\vee(x) = x^{-\alpha_a[0]/r_a} \; : \exp\Big(\sum_{k \neq 0} \frac{\alpha_a[k]}{q^{\frac{k\, r_a}{2}} - q^{-\frac{k\, r_a}{2}}} \, e^{kx} \Big) : \; . \tag{3.3.32}$$

The $\mathcal{W}_{q,t}(\mathfrak{g})$ algebra is then defined as a set of the operators commuting with the screening charges[6]. Next, one introduces "fundamental weight" generators $w_a[m]$, through the commutation relation:

$$[\alpha_a[k], w_b[m]] = \frac{1}{k}(q^{\frac{k\, r_a}{2}} - q^{-\frac{k\, r_a}{2}})(t^{\frac{k}{2}} - t^{-\frac{k}{2}}) \, \delta_{ab} \, \delta_{k,-m} \, , \tag{3.3.33}$$

such that

$$\alpha_a[k] = \sum_{b=1}^{n} C_{ab}(q^k, t^k) w_b[k] \; . \tag{3.3.34}$$

Correspondingly, we define (magnetic) degenerate vertex operators:

$$V_a^\vee(x) = x^{w_a[0]/r_a} \; : \exp\Big(- \sum_{k \neq 0} \frac{w_a[k]}{q^{\frac{k\, r_a}{2}} - q^{-\frac{k\, r_a}{2}}} \, e^{kx} \Big) : \; . \tag{3.3.35}$$

Using the notation $\langle \ldots \rangle$ for a vacuum expectation value, and making use of the theta function definition $\theta_{q^{r_a}}(x) = (x \, ; \, q^{r_a})_\infty \, (q^{r_a}/x \, ; \, q^{r_a})_\infty$, we obtain the following two-point functions:

For a given node a,

$$\langle S_a^\vee(x) \, S_a^\vee(x') \rangle_{free} = \frac{(e^{x-x'}; q^{r_a})_\infty}{(t \, e^{x-x'}; q^{r_a})_\infty} \, \frac{(e^{x'-x}; q^{r_a})_\infty}{(t \, e^{x'-x}; q^{r_a})_\infty} \, \frac{\theta_{q^{r_a}}(t \, e^{x-x'})}{\theta_{q^{r_a}}(e^{x-x'})} \; . \tag{3.3.36}$$

[6]One can also define a set of "electric" screenings [77], in the parameter t instead of q, but they will not be needed here.

When a and b are distinct nodes connected by a link,

$$\langle S_a^\vee(x)\, S_b^\vee(x')\rangle_{free} = \frac{(t\, v_{ab}\, e^{x-x'}; q^{r_{ab}})_\infty}{(v_{ab}\, e^{x-x'}; q^{r_{ab}})_\infty}\ . \tag{3.3.37}$$

The two-point of a screening with a "fundamental" vector operator is given by:

$$\langle S_a^\vee(x)\, V_b^\vee(x')\rangle_{free} = \frac{(t\, v_a\, e^{x'-x}; q^{r_a})_\infty}{(v_a\, e^{x'-x}; q^{r_a})_\infty}\ . \tag{3.3.38}$$

In the above, we have $v_a \equiv \sqrt{q^{r_a}/t}$ and $v_{ab} \equiv \sqrt{q^{r_{ab}}/t}$. Recall that if either node a or node b denotes a short root, then $r_{ab} = 1$, while both nodes denote long roots, then $r_{ab} = r$.

The vertex operators that are relevant to us are not exactly the operators $V_a(x')$ introduced above in (3.3.35). Rather, each vertex operator, labeled as $V_{\omega_i}(x_i)$, is a normal ordered product of rescaled "fundamental coweight" operators,

$$W_a(x) =: \exp\Big(\sum_{k\neq 0} \frac{w_a[k]}{(q^{\frac{k\,r_a}{2}} - q^{-\frac{k\,r_a}{2}})(t^{\frac{k}{2}} - t^{-\frac{k}{2}})}\, e^{kx}\Big) :\ , \tag{3.3.39}$$

and rescaled "simple coroot" operators,

$$E_a(x) =: \exp\Big(\sum_{k\neq 0} \frac{\alpha_a[k]}{(q^{\frac{k\,r_a}{2}} - q^{-\frac{k\,r_a}{2}})(t^{\frac{k}{2}} - t^{-\frac{k}{2}})}\, e^{kx}\Big) :\ , \tag{3.3.40}$$

where we dropped the zero mode contributions in the above definitions, since we will not need them in what follows. The fundamental vertex operators ${W_a}^{\pm 1}(f\, v_a^r\, x)$ have two point functions with the screening currents $S_a^\vee(x')$ that are equal to the contributions of either chiral or anti-chiral multiplets of R-charge $-r/2$ as described in Section 3.2.

We now consider a set $\mathcal{W}_S$ of coweights ω_i in the coweight space of $\mathfrak{g}$, taken in fundamental representations of ${}^L\mathfrak{g}$ and satisfying $\sum_{i=1}^{|\mathcal{W}_S|} \omega_i = 0$; to this set $\mathcal{W}_S$, we associate a primary vertex operator:

$$: \prod_{i=1}^{|\mathcal{W}_S|} V_{\omega_i}(x_i) :\ , \tag{3.3.41}$$

where each $V_{\omega_i}(x_i)$ is constructed out of the fundamental coweight and simple coroot vertex operators.

To fully specify the conformal block, we also need to make a choice of contour in (3.3.22). In particular, it is worth noting that for a given theory, the number of contours generically increases after q-deformation, when $\mathfrak{g} \neq A_n$. This is because the number of contours in the undeformed case is equal to the number of solutions to certain hypergeometric equations satisfied by the conformal blocks, while the number of countours in the q-deformed theory is instead the number of solutions to q-hypergeometric equations, which is generically bigger. Giving a prescription for the integration contours when $\mathfrak{g} \neq A_n$ is an open problem in matrix models, and we will not address this question here.

Recovering the undeformed theory is straightforward: we let $q = \exp(R\epsilon_1)$, $t = \exp(-R\epsilon_2)$, and take the R to zero limit. In this limit, q and t tend to 1. The individual $V_{\omega_i}(x_i)$ do not have a good conformal limit, but the products in (3.3.41) do:

$$: \prod_{i=1}^{|\mathcal{W}_S|} V_{\omega_i}(x_i) : \qquad \to \qquad V_\beta^\vee(z).$$

The momentum β carried by $V_\beta^\vee(z)$ is:

$$\beta = \sum_{i=1}^{|\mathcal{W}_S|} \beta_i \, \omega_i \ . \tag{3.3.42}$$

Then, we set the argument of the vertex operators to be:

$$e^{x_i} = z \, q^{-\beta_i} \ . \tag{3.3.43}$$

Then the two-point function

$$\langle S_a^\vee(x) \ : \prod_{i=1}^{|\mathcal{W}_S|} V_{\omega_i}(x_i) : \rangle_{free} \tag{3.3.44}$$

becomes the undeformed two-point (3.3.28) of the vertex operator with the a-th screening current: $(1 - e^x/z)^{-\langle \alpha_a^\vee, \beta \rangle}$, with$\beta$ defined above. In this way, one is able to realize the insertion of any number of primary vertex operators, and have complete control over how the insertion scales in the undeformed limit. Any collection of primary vertex operators with either arbitrary or (partially) degenerate momenta can be analyzed in this way.

3.4 Proof of Triality

In this section, we give the proof of triality. The proof can be divided into two parts: the first part consists of showing that the 5d theory partition function reduces to the 3d partition function of vortices once we tune the Coulomb branch parameters such that we probe the point on the moduli space where the Coulomb branch meets the Higgs branch. The second part is to show that the integral representation of the 3d partition function is nothing but the Coulomb gas representation of the conformal blocks in q-deformed Toda theory.

Gauge/Vortex Duality

The relationship between the 5d $\mathcal{N} = 1$ gauge theory T^{5d}, and the 3d $\mathcal{N} = 2$ gauge theory G^{3d}, is called gauge/vortex duality. The duality comes from two different, yet equivalent descriptions of vortices in the theory: one from the perspective of 5d theory with vortices, and the other from the perspective of the 3d theory on the vortex. The fact that the theory

on vortices captures aspects of dynamics of the "parent" gauge theory was noticed early on in [86] at the level of BPS spectra. Turning on Ω-background $t$ransverse to the vortex, the correspondence becomes more extensive [87, 88]: it is a gauge/vortex duality [89].

The 2d Ω-background transverse to the vortex (with parameter ϵ_2) is necessary. It ensures that the super-Poincare symmetries preserved by the 5d and the 3d theories are the same, since the Ω-background is a form of compactification [90, 91, 92] and breaks half the supersymmetry: after turning it on, both theories are 3d $\mathcal{N} = 2$ theories on a circle. The duality should hold at the level of F-type terms – the Kahler potentials are not protected, and we don't claim to specify them. The duality is the little string analogue [89] of large N dualities in topological string [93, 94, 95, 96]. The D3 brane gauge theory lives in the Higgs phase of the bulk theory. From the bulk perspective, the theory starts out on the Higgs branch, but ends up pushed onto the Coulomb branch due to the vortex flux. In the Higgs phase, the Coulomb moduli are frozen to points where the hypermultiplets can get expectation values. Turning on N units of vortex flux in a $U(1)$ gauge group shifts the corresponding Coulomb modulus a to $a + N\epsilon_2$, where ϵ_2 is the parameter of the Ω in background rotating the complex plane transverse to the vortex. This is a consequence [89] of how Ω-background deforms the Lagrangian of the 5d theory [40, 97]. Once we have a pair of dual theories, one expects that their partition functions in the full Ω-background, depending on $\epsilon_{1,2}$, agree as well. We now show this explicitly.

3d-5d Partition functions

For the first part of the proof, the integral representation of the 3d partition function is not very useful. Instead, we would like to explicitly perform the integrals. Once the appropriate contour is chosen, the contributing poles turn out to be labeled by Young diagrams. Therefore, the 3d partition function can also be expressed as a sum over Young diagrams:

$$Z_{3d} = \int dx\, I_{3d}(x) = \sum_{\{\mu\}} \mathrm{res}_{\{\mu\}}\, I_{3d}(x). \tag{3.4.45}$$

The summand can be easily computed after normalizing it by the residue of the pole at $\{\varnothing\}$:

$$\mathrm{res}_{\{\mu\}} I_{3d}(x)/\mathrm{res}_{\{\varnothing\}} I_{3d}(x) = I_{3d}(x_{\{\mu\}})/I_{3d}(x_{\{\varnothing\}}), \tag{3.4.46}$$

where $x_{\{\mu\}}$ denote μ dependent substitution for the Coulomb branch parameters:

$$\{e^{x_\mu}\} = \{e_{a,I}\, q^{\mu^a_{I,i}} t^{\rho_i}\, v^{\#_a} q^{\#'_a}\}. \tag{3.4.47}$$

The equivalence of the partition functions of G^{3d} and T^{5d} is observed when we move to the special point on the moduli space of the 5d theory where its Coulomb branch meets its

Higgs branch. To this end, we tune the Coulomb branch parameters to equate some of the masses of the hypermultiplets:

$$e_{a,I} = f_i\, t^{N_{a,I}} v^{\#_{a,i,I}} q^{\#'_{a,i,I}}. \tag{3.4.48}$$

Here, $N_{a,I}$ are positive integers that can be interpreted as integer units of vortex flux, which we turn on. Effectively, then, one can get off the root of the Higgs branch, but only to probe the Coulomb branch of T^{5d} on an integer-valued lattice.

This identification results in the truncation of Young diagrams. Let us assume that one of the representations, say μ, labeling the generalized Nekrasov factor $N_{\mu\nu}(Q; q^{r_{\mu\nu}})$, has at most N rows. If we set $Q = q^{r_\nu} t^{-(M+1)}$, one can then show that the Nekrasov factor vanishes unless the length of ν is bounded by $N + M$, i.e. $\ell(\nu) \leq N + M$. Furthermore, we make use of the identity below, which following from the properties of the q-Pochhammer symbol:

$$N_{\mu\nu}(Q; q) = \prod_{a=0}^{r_{\mu\nu}-1} N_{\mu\nu}(q^a Q; q^{r_{\mu\nu}}) \tag{3.4.49}$$

We previously mentioned that the fixed points of the equivariant action used in computing 5d instantons are labeled by Young diagrams, and these Young diagrams are allowed to be of any size. At this point of the moduli space, it is not hard to show that the non-zero contributions to the partition function come from Young diagrams which have less than or equal to N_a rows, otherwise their contribution vanish. We can find a truncation pattern, and easily deduce that each Young diagram is limited in length by an integer. This truncation behavior can be checked directly by studying the generalized Nekrasov factors $N_{\mu\nu}(Q; q^{r_{\mu\nu}})$.

Once we know that the Young diagrams μ and ν are truncated such that $\ell(\mu) \leq N_\mu$ and $\ell(\nu) \leq N_\nu$, one is able to show that the generalized Nekrasov factor can be rewritten as

$$\begin{aligned} N_{\mu\nu}(Q; q^{r_{\mu\nu}}) = &\prod_{i=1}^{N_\mu} \prod_{j=1}^{N_\nu} \frac{(Q\, q^{r_\mu \mu_i - r_\nu \nu_j} t^{j-i+1}; q^{r_{\mu\nu}})_\infty (Q\, t^{j-i}; q^{r_{\mu\nu}})_\infty}{(Q\, q^{r_\mu \mu_i - r_\nu \nu_j} t^{j-i}; q^r)_\infty (Q\, t^{j-i+1}; q^r)_\infty} \\ &\times N_{\mu\varnothing}(Q\, t^{N_\nu}; q^{r_{\mu\nu}})\, N_{\varnothing\nu}(Q\, t^{-N_\mu}, q^{r_{\mu\nu}}). \end{aligned} \tag{3.4.50}$$

This identity is crucial in establishing the equivalence between the 3d and 5d partition functions. Now, for definiteness, suppose that T^{5d} is engineered from a given *polarized* set $\mathcal{W}_\mathcal{S}$ of coweights of $\mathfrak{g}$, in the sense of Section 2.4. We then look at the decomposition of the various multiplet contributions after imposing (3.4.48). The 5d vector multiplets become

$$\prod_{a=1}^{n} z^{5d}_{V_a, \mu^a} = \prod_{a=1}^{n} \frac{z^{3d}_{V_a}(x_{\mu^a})}{z^{3d}_{V_a}(x_\varnothing)} \cdot V_{vect}, \tag{3.4.51}$$

where the first factor is nothing but the vector multiplet contribution for 3d theory. V_{vect} is all the remaining factors from 5d vector multiplet. Similarly, we can also reduce and isolate

factors from bifundamental multiplets that make up 3d bifundamental contribution and a leftover factor V_{bifund}:

$$\prod_{a<b} z^{5d}_{H_{ab},\mu^a,\mu^b} = \prod_{a<b} \left[\frac{z^{3d}_{H_{ab}}(x_{\mu^a}, x_{\mu^b})}{z^{3d}_{H_{ab}}(x_\varnothing, x_\varnothing)} \right]^{\Delta_{ab}} \cdot V_{bifund} \ . \tag{3.4.52}$$

We write the following for the contributions of the fundamental hypermultiplets and Chern-Simons term:

$$\prod_{a=1}^{n} z^{5d}_{H_a,\mu^a} = V_{fund}, \tag{3.4.53}$$

$$\prod_{a=1}^{n} z^{5d}_{CS,\mu^a} = V_{CS}. \tag{3.4.54}$$

We now collect all the leftover factors from the above reduction. After many cancellations, one can show that these factors make up a 3d hypermultiplet contribution,

$$V_{vect} V_{bifund} V_{fund} V_{CS} = \prod_{a=1}^{n} \frac{z^{3d}_{H_a}(x_{\mu^a})}{z^{3d}_{H_a}(x_\varnothing)} \ , \tag{3.4.55}$$

where $z^{3d}_{H_a}(x_{\mu^a})$ can be written compactly as:

$$z^{3d}_{H_a}(x_a, f_{a,i}) = \prod_{1\le I\le N_a} \prod_{j=1}^{|\mathcal{W}_\mathcal{S}|} \left[(v_a^{\#_{a,I}}\, e^{x_I^{(a)}}/f_j; q^{r_a})_\infty \right]^{\omega_{j,a}} \tag{3.4.56}$$

Here, $\omega_{j,a}$ is the a'th Dynkin label of the j'th coweight in $\mathcal{W}_\mathcal{S}$, with the coweights expanded in terms of fundamental coweights. For example, the $\mathfrak{g} = B_3$ coweight $\omega_1 = [-1, \ \ 1, \ \ 0]$ has $\omega_{1,1} = -1, \ \omega_{1,2} = 1, \ \omega_{1,3} = 0$, and is to be understood as minus the first fundamental coweight plus the second fundamental coweight of B_3. The requirement that the sum of the coweights in $\mathcal{W}_\mathcal{S}$ add up to zero implies that the matter contribution (3.4.56) is in fact a ratio of q-Pochhammer's. From the point of view of G^{3d}, the various $v_a^{\#_{a,I}}$ factors are fixed by R-charge conservation. In the end, the summand of the 5d gauge theory partition function becomes the summand of the 3d partition function, establishing the first half of triality.

q-deformed Toda Conformal Block and 3d Partition Function

The second part of the proof is more straightforward, as it simply consists in comparing the integrands on both sides. The q-deformed conformal block is then equal to the partition function of G^{3d}: the two-point functions of screenings in (3.3.36), (3.3.37), are the contributions of the $\mathcal{N} = 4$ vector and bifundamental multiplets in (3.2.15) and (3.2.16) to the D3 brane partition function, respectively. The number N_a of D3 branes on the a-th node maps to the number of screening charge insertions. The evaluation of the two-point of a screening and a vertex operator (3.3.44) becomes the 3d hypermultiplet contribution (3.4.56). This finishes the proof.

3.5 Quantum Affine Algebras and Defects

The above proof of triality was technically only written for the case of polarized defects of the little string theory. A natural question to ask, then, is whether triality still works for unpolarized defects. The answer is affirmative, and addressing this question in full generality turns out to have important implications for the (co)weights of $\mathfrak{g}$. Indeed, already in the case where $\mathcal{W}_{\mathcal{S}}$ characterizes a polarized defect, the matter content on node a of the 3d theory is given by (3.4.56):

$$z^{3d}_{H_a}(x_a, f_{a,i}) = \prod_{1\leq I\leq N_a}\prod_{j=1}^{|\mathcal{W}_{\mathcal{S}}|}\left[(v_a^{\#_{a,I}}\, e^{x_I^{(a)}}/f_j; q^{r_a})_\infty\right]^{\omega_{j,a}}\ , \tag{3.5.57}$$

meaning the coweight ω_j appears in a "refined" fashion. Going back to unpolarized (co)weights of the little string, they too will get refined in the triality picture, and the matter content of G^{3d} gives an explicit formula for them (though in that case, we do not have a general closed-form formula such as (3.4.56)). Does this refinement have a mathematical interpretation? The answer is given in [77]: the authors point out the existence of a deep relation between the deformed $\mathcal{W}$-algebra $\mathcal{W}_{q,t}(\mathfrak{g})$ and the representation ring of the quantum affine algebra $U_q(\hat{\mathfrak{g}})$, for $\mathfrak{g}$ a simple Lie algebra. Specifically, one would like to construct the generators of $\mathcal{W}_{q,t}(\mathfrak{g})$ as the commutant of the screening charges of the algebra. The construction of these generators is similar to the construction of irreducible finite dimensional representations $V(\Lambda)$ of $\mathfrak{g}$, where Λ is some highest weight of an irrep. However, the number of terms in a generator of $\mathcal{W}_{q,t}(\mathfrak{g})$ is in general bigger than the dimension of $V(\Lambda)$. The correct statement is that the weights appearing in the generators of $\mathcal{W}_{q,t}(\mathfrak{g})$ are the weights of some irreducible finite dimensional representation $\mathbf{V}(\Lambda)$ of the quantum affine algebra $U_q(\hat{\mathfrak{g}})$; this representation decomposes under $U_q(\mathfrak{g})$ as $\mathbf{V}(\Lambda) \cong V(\Lambda) \oplus \ldots$, where the dots are smaller irreducible representations.

The weights in the finite dimensional representations of $U_q(\hat{\mathfrak{g}})$ (or equivalently, appearing in the generators of $W_{q,t}(\mathfrak{g})$) are generically of the form:

$$: W_\Lambda\, E_{i_1}\left(z\, q^{a_1}\, v^{b_1}\right)^{-1}\, E_{i_2}\left(z\, q^{a_2}\, v^{b_2}\right)^{-1}\, \ldots\, E_{i_k}\left(z\, q^{a_k}\, v^{b_k}\right)^{-1} :\ ,$$

where E_{i_l} are simple (co)root operators, and a_i, b_i are integers[7].

It turns out that all the weights of $U_q(\hat{\mathfrak{g}})$ are explicitly realized as little string defects. As an instructive example, let us look at $\mathfrak{g} = D_4$.

Example 3.5.1. *Note that the representation theory of the four fundamental representations*

[7]Some of the terms appearing in the generators of $W_{q,t}(\mathfrak{g})$ also sometimes feature derivatives, which come from the fusion of certain vertex operators at a given position z. It would be important to understand exactly how they arise in our context.

of $U_q(\widehat{D_4})$, interpreted as representations of $U_q(D_4)$, gives:

$$\begin{aligned}\boldsymbol{V}(\omega_1) &\cong V(\omega_1)\\ \boldsymbol{V}(\omega_2) &\cong V(\omega_2)\oplus\mathbb{C}\\ \boldsymbol{V}(\omega_3) &\cong V(\omega_3)\\ \boldsymbol{V}(\omega_4) &\cong V(\omega_4)\ .\end{aligned}$$

See for instance [98] for the derivation. In particular, the quantum affine algebra and Lie algebra vector and spinor representations are isomorphic, but the second fundamental representation of $U_q(\widehat{D_4})$ is bigger than that of D_4: it also contains an extra trivial representation (denoted by $\mathbb{C}$).

This matches exactly the representation theory: the null weight appears 4 times in $V(\omega_2)$ (this is just the rank of D_4, as it should be), and then once again in $\mathbb{C}$. Using triality, we can engineer these weights explicitly, with five distinct truncations of T^{5d}'s partition function that produce a distinct potential for the matter content of G^{3d}. The recent work of [71] shows that one can equivalently recover these potentials from the computation of qq-characters of D_4. We will be more quantitative in Chapter 8.

Chapter 4

(2,0) CFT Limit and Nilpotent Orbits Classification

Because it has a scale m_s, the $(2,0)$ little string theory on $\mathcal{C}$ is not conformal. To recover the $(2,0)$ 6d CFT theory on $\mathcal{C}$, we take this string scale m_s to infinity, while keeping all moduli of the $(2,0)$ theory fixed in the process. Furthermore, if we denote by Δx the relative position of the $|\mathcal{W}_{\mathcal{S}}|$ D5 branes on $\mathcal{C}$, we then take the product $\Delta x\, m_s$ to zero.

4.1 Description of the Defects

The quiver gauge theory description of the defects is only valid at finite m_s. Taking the $(2,0)$ CFT limit $m_s \to \infty$ has drastic effects on the physics; most notably, the radius of the 5d circle $S^1(R) = 1/m_s^2 S^1(\hat{R})$ vanishes in the limit, so the theory becomes four-dimensional. We call the resulting theory $T^{5d}_{m_s\to\infty} \equiv T^{4d}$. The 4d inverse gauge couplings τ_a vanishes as well, because the combinations $\tau_a\, m_s^2$ turn out to be moduli of the $(2,0)$ CFT, which are fixed in the limit. In other words, there is no longer a Lagrangian describing the theory on the D5 branes[1]. Though an effective description as a quiver gauge theory is no longer available, a lot can be deduced about the resulting 4d theory in that limit, as we now explain.

Most notably, we conjecture that when $m_s \to \infty$, the Coulomb branch of the defect theory T^{4d} becomes a nilpotent orbit of $\mathfrak{g}$. In the next sections, we will perform extensive checks of this claim, such as dimension counting of the Coulomb branch, matching of the Bala-Carter labeling of nilpotent orbits, and computation of Seiberg–Witten curves. To arrive at nilpotent orbits, however, we first show a beautiful connection that exists between the coweights defining a little string defects and the so-called parabolic subalgebras of $\mathfrak{g}$.

[1]Note this is not the 4d limit described in [70]; there, one obtains a 4d quiver gauge theory, with the same quiver as for T^{5d}, by keeping the inverse gauge couplings τ_a finite. This does *not* decribe the $(2,0)$ theory on $\mathcal{C}$, since the moduli $\tau_a m_s^2$ then become infinite.

4.2 Parabolic Subalgebras

We will need two facts from representation theory: First, a Borel subalgebra of a Lie algebra $\mathfrak{g}$ is a maximal solvable subalgebra. We note that the Borel subalgebra can always be written as the direct sum $\mathfrak{b} = \mathfrak{h} \oplus \mathfrak{m}$; here, $\mathfrak{h}$ is a Cartan subalgebra of $\mathfrak{g}$, and $\mathfrak{m} = \sum_{\alpha \in \Phi^+} \mathfrak{g}_\alpha$, with $\mathfrak{g}_\alpha$ the root spaces associated to a given set of positive roots Φ^+. We fix the set Φ^+, which in turn fixes the Borel subalgebra $\mathfrak{b}$, for a given Lie algebra $\mathfrak{g}$.

Second, a parabolic subalgebra $\mathfrak{p}_\Theta$ is defined as a subalgebra of $\mathfrak{g}$ which contains the Borel subalgebra $\mathfrak{b}$. More precisely, let us denote the set of positive simple roots by Δ. Take an arbitrary subset $\Theta \subset \Delta$. We define $\mathfrak{p}_\Theta$ to be the subalgebra of $\mathfrak{g}$ generated by $\mathfrak{b}$ and all of the root spaces $\mathfrak{g}_\alpha$, with $\alpha \in \Delta$ or $-\alpha \in \Theta$. Then $\mathfrak{p}_\Theta$ is a parabolic subalgebra of $\mathfrak{g}$ containing $\mathfrak{b}$, and every parabolic subalgebra of $\mathfrak{g}$ containing $\mathfrak{b}$ is of the form $\mathfrak{p}_\Theta$ for some $\Theta \subset \Delta$. In fact, every parabolic subalgebra of $\mathfrak{g}$ is conjugate to one of the form $\mathfrak{p}_\Theta$ for some $\Theta \subset \Delta$.

A parabolic subalgebra also obeys a direct sum decomposition:

$$\mathfrak{p}_\Theta = \mathfrak{l}_\Theta \oplus \mathfrak{n}_\Theta \,. \tag{4.2.1}$$

We introduced $\mathfrak{n}_\Theta = \sum_{\alpha \in \Phi^+ \setminus \langle\Theta\rangle^+} \mathfrak{g}_\alpha$, which is called the nilradical of $\mathfrak{p}_\Theta$, while $\mathfrak{l}_\Theta = \mathfrak{h} \oplus \sum_{\alpha \in \langle\Theta\rangle} \mathfrak{g}_\alpha$ is called a Levi subalgebra; the subroot system $\langle\Theta\rangle$ is generated by the simple roots in Θ, while $\langle\Theta\rangle^+$ is built out of the positive roots of $\langle\Theta\rangle$. Then, it follows that $\mathfrak{n}_\Theta \cong \mathfrak{g}/\mathfrak{p}_\Theta$.

Furthermore, all Levi subalgebras of a given parabolic subalgebra are conjugate to each other [99]. We illustrate the above statements in the examples below:

Example 4.2.1. *Consider $\mathfrak{g} = A_2$ in the fundamental, three-dimensional representation. Then the elements in the Cartan subalgebra have the form*

$$\mathfrak{h} = \begin{pmatrix} * & 0 & 0 \\ 0 & * & 0 \\ 0 & 0 & * \end{pmatrix} . \tag{4.2.2}$$

We associate to a root $\alpha_{ij} = h_i - h_j$ the space $\mathbb{C}E_{ij}$, where E_{ij} is the matrix that has a 1 in the i-th row and j-th column, and zeroes everywhere else. Thus, we see that

$$\mathfrak{b} = \begin{pmatrix} * & * & * \\ 0 & * & * \\ 0 & 0 & * \end{pmatrix} , \tag{4.2.3}$$

and the parabolic subalgebras are

$$\mathfrak{p}_{\varnothing} = \mathfrak{b} = \begin{pmatrix} * & * & * \\ 0 & * & * \\ 0 & 0 & * \end{pmatrix}, \tag{4.2.4}$$

$$\mathfrak{p}_{\{\alpha_1\}} = \begin{pmatrix} * & * & * \\ * & * & * \\ 0 & 0 & * \end{pmatrix}, \tag{4.2.5}$$

$$\mathfrak{p}_{\{\alpha_2\}} = \begin{pmatrix} * & * & * \\ 0 & * & * \\ 0 & * & * \end{pmatrix}, \tag{4.2.6}$$

$$\mathfrak{p}_{\{\alpha_1,\alpha_2\}} = \mathfrak{g} = \begin{pmatrix} * & * & * \\ * & * & * \\ * & * & * \end{pmatrix}. \tag{4.2.7}$$

Let us look at the Levi decompositions of the above:

Example 4.2.2. *For $\mathfrak{g} = A_2$, we get the following decompositions:*

$$\mathfrak{p}_{\varnothing} = \begin{pmatrix} * & * & * \\ 0 & * & * \\ 0 & 0 & * \end{pmatrix} = \begin{pmatrix} * & 0 & 0 \\ 0 & * & 0 \\ 0 & 0 & * \end{pmatrix} \oplus \begin{pmatrix} 0 & * & * \\ 0 & 0 & * \\ 0 & 0 & 0 \end{pmatrix} = \mathfrak{l}_{\varnothing} \oplus \mathfrak{n}_{\varnothing}, \tag{4.2.8}$$

$$\mathfrak{p}_{\{\alpha_1\}} = \begin{pmatrix} * & * & * \\ * & * & * \\ 0 & 0 & * \end{pmatrix} = \begin{pmatrix} * & * & 0 \\ * & * & 0 \\ 0 & 0 & * \end{pmatrix} \oplus \begin{pmatrix} 0 & 0 & * \\ 0 & 0 & * \\ 0 & 0 & 0 \end{pmatrix} = \mathfrak{l}_{\{\alpha_1\}} \oplus \mathfrak{n}_{\{\alpha_1\}}, \tag{4.2.9}$$

$$\mathfrak{p}_{\{\alpha_2\}} = \begin{pmatrix} * & * & * \\ 0 & * & * \\ 0 & * & * \end{pmatrix} = \begin{pmatrix} * & 0 & 0 \\ 0 & * & * \\ 0 & * & * \end{pmatrix} \oplus \begin{pmatrix} 0 & * & * \\ 0 & 0 & 0 \\ 0 & 0 & 0 \end{pmatrix} = \mathfrak{l}_{\{\alpha_2\}} \oplus \mathfrak{n}_{\{\alpha_2\}}, \tag{4.2.10}$$

$$\mathfrak{p}_{\{\alpha_1,\alpha_2\}} = \begin{pmatrix} * & * & * \\ * & * & * \\ * & * & * \end{pmatrix} = \begin{pmatrix} * & * & * \\ * & * & * \\ * & * & * \end{pmatrix} \oplus \begin{pmatrix} 0 & 0 & 0 \\ 0 & 0 & 0 \\ 0 & 0 & 0 \end{pmatrix} = \mathfrak{l}_{\{\alpha_1,\alpha_2\}} \oplus \mathfrak{n}_{\{\alpha_1,\alpha_2\}}. \tag{4.2.11}$$

Example 4.2.3. *In table 4.1, we show the root spaces that the Borel subalgebra of A_3 is made of.*

Θ	$\mathfrak{p}_\Theta$	$\mathfrak{l}_\Theta$	$\mathfrak{n}_\Theta$
$\varnothing$	$\begin{pmatrix} * & * & * & * \\ 0 & * & * & * \\ 0 & 0 & * & * \\ 0 & 0 & 0 & * \end{pmatrix}$	$\begin{pmatrix} * & 0 & 0 & 0 \\ 0 & * & 0 & 0 \\ 0 & 0 & * & 0 \\ 0 & 0 & 0 & * \end{pmatrix}$	$\begin{pmatrix} 0 & * & * & * \\ 0 & 0 & * & * \\ 0 & 0 & 0 & * \\ 0 & 0 & 0 & 0 \end{pmatrix}$

: α_1 : $(\alpha_1+\alpha_2)$:$(\alpha_1+\alpha_2+\alpha_3)$
: α_2 : $(\alpha_2+\alpha_3)$
: α_3

Table 4.1: This table illustrates the Levi decomposition of $\mathfrak{p}_\Theta$, when Θ is the empty set and $\mathfrak{g} = A_3$. $\mathfrak{p}_\Theta$ consists of all the matrices in A_3 with zeroes in the indicated places and the other entries are arbitrary. The color code shows which positive root is denoted by which nonzero entry.

Parabolic Subalgebras from Brane Defects

We can now explain how parabolic subalgebras of $\mathfrak{g}$ arise from noncompact D5 branes: Consider a set of coweights defining a puncture,

$$\mathcal{W}_\mathcal{S} = \{\omega_i\} \ .$$

As we explained in Section 2.3, each coweight ω_i represents a distinct D5 brane. A set of simple roots Θ, as defined in the previous paragraph, is constructed as the subset of all simple roots of $\mathfrak{g}$ that have a zero inner product with every coweight of $\mathcal{W}_\mathcal{S}$.

Among the many possible sets of coweights, we look in particular for a set in the Weyl group orbit of $\mathfrak{g}$ for which $|\Theta|$ is the biggest. We call such a set of coweights distinguished. In the rest of this thesis, the sets of coweights $\mathcal{W}_\mathcal{S}$ we consider are all taken to be *distinguished*. If a given set is not distinguished, acting simultaneously on all its coweights with the Weyl group of $\mathfrak{g}$ will always turn it into a distinguished set. We provide many examples below.

Example 4.2.4. *Let us consider the following set of F_4 coweights, expanded in terms of fundamental coweights as:*

$$\mathcal{W}_\mathcal{S} = \{\omega_1 = [\ 0,\ \ 0,\ \ 1, -1],\ \ \omega_2 = [\ \ 0,\ \ 0, -1,\ \ 1]\}.$$

Both coweights have a zero inner product with α_1, α_2, so $|\Theta| = 2$. A Weyl relfection about the simple root α_4 turns the set into:

$$\mathcal{W}'_\mathcal{S} = \{\omega_1 = [\ \ 0,\ \ 0,\ \ 0,\ \ 1],\ \ \omega_2 = [\ \ 0,\ \ 0,\ \ 0, -1]\}$$

Note that this time, $|\Theta| = 3$, and that is the maximal size of Θ for this choice of defect. Therefore, we call the set $\mathcal{W}'_{\mathcal{S}}$ distinguished.

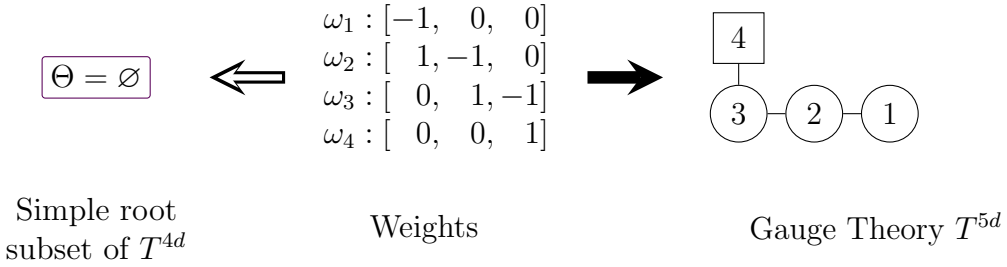

Figure 4.1: From the distinguished set of weights $\mathcal{W}_{\mathcal{S}}$, we obtain the parabolic subalgebra $\mathfrak{p}_{\varnothing}$ of A_3 in the CFT limit (in this case, the choice of weights is unique up to global $\mathbb{Z}_2$ action on the set). Reinterpreting each weight as a sum of "minus a fundamental weight plus simple roots," we obtain the 5d quiver gauge theory shown on the right. The white arrow implies we take the CFT limit on the left.

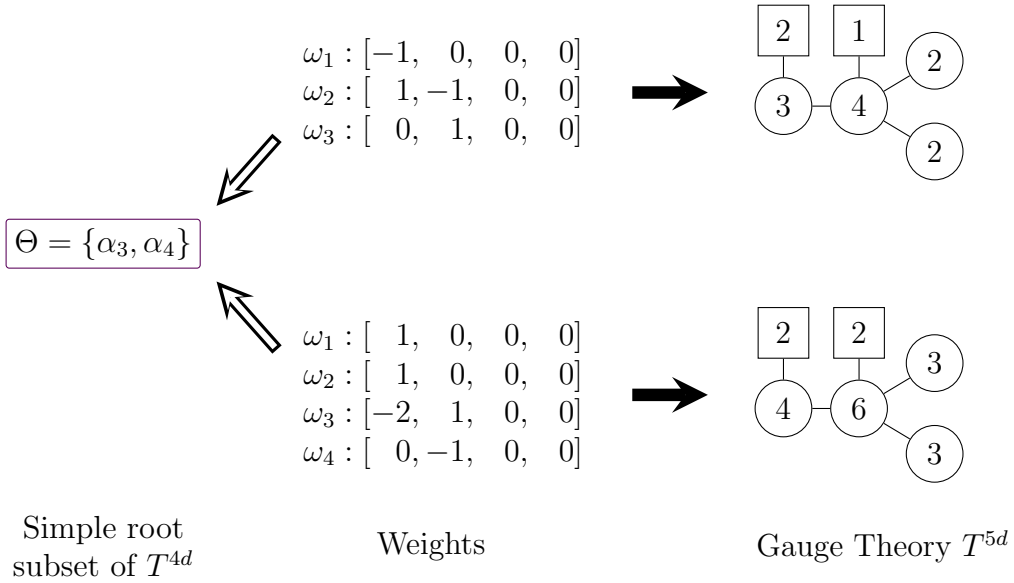

Figure 4.2: From the two distinguished sets of weights $\mathcal{W}_{\mathcal{S}}$, we read off the parabolic subalgebra $\mathfrak{p}_{\{\alpha_3,\alpha_4\}}$ of D_4 when we flow to the CFT limit. Reinterpreting each weight as a sum of "minus a fundamental weight plus simple roots," we obtain two different 5d quiver gauge theories shown on the right. The white arrows imply we take the CFT limit on the left.

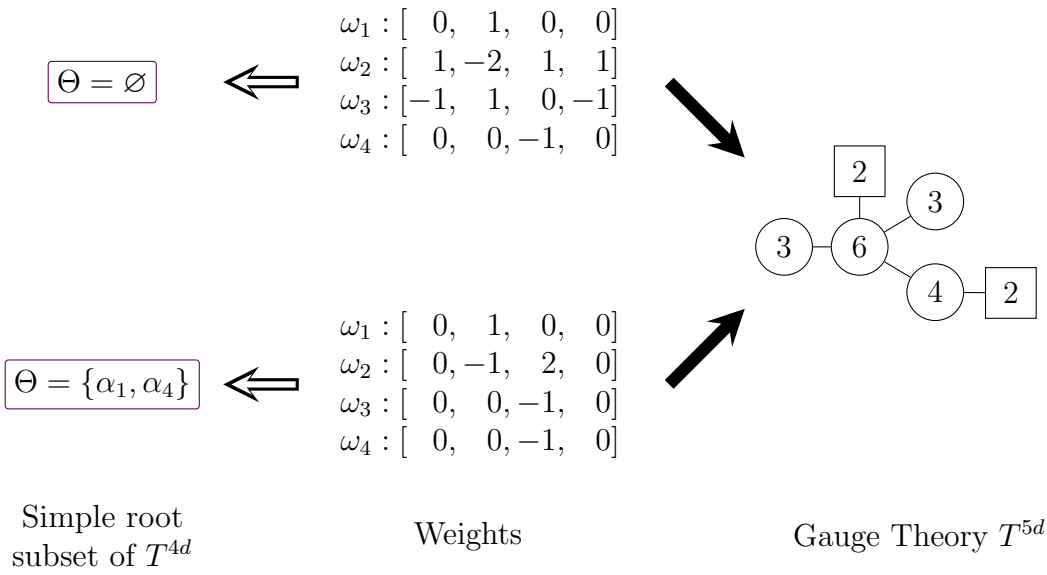

Figure 4.3: Two distinguished sets of weights $\mathcal{W}_{\mathcal{S}}$ which spell out the same quiver, but flow to two different defects in the CFT limit; we therefore see it is really the weights, and not quivers, that define a defect.

A nilradical $\mathfrak{n}_\Theta$ of $\mathfrak{g}$ occuring in the direct sum decomposition (4.2.1) always specifies the Coulomb branch of some defect T^{4d}. Starting from the weight data of the defect, the nilradical is extracted as follows: it is the direct sum of the root spaces associated to a set of positive roots $\{e_\gamma\}$ in $\mathfrak{g}$, such that

$$\langle e_\gamma, \omega_i \rangle < 0 \tag{4.2.12}$$

for at least one coweight ω_i of $\mathcal{W}_{\mathcal{S}}$. The bracket $\langle \cdot, \cdot \rangle$ is the Cartan-Killing form of $\mathfrak{g}$. In particular, the size of this set gives the complex dimension of the Coulomb branch of T^{4d}. It is important to note that the Coulomb branch is generically smaller than at finite m_s, for T^{5d}, where we had (2.4.17):

$$\sum_{\langle e_\gamma, \omega_i \rangle < 0} |\langle e_\gamma, \omega_i \rangle| \ .$$

Indeed, in the little string formula above, positive roots are counted with multiplicity, while this is not the case in the CFT limit. As a consequence, the Coulomb branch dimension of T^{4d} is at most the number of all positive roots of $\mathfrak{g}$. This decrease of the Coulomb branch is directly related to an effect we pointed out in Toda theory 3.3: there, the number of contours in the evaluation of conformal blocks was conjectured to be bigger in q-deformed Toda, as opposed to the undeformed case.

Though we do not have a direct proof of the above prescription for computing the Coulomb branch dimension of T^{4d}, we checked it explicitly for the defects of all exceptional algebras, and up to a high rank for the classical algebras.

Example 4.2.5. *We will explicitly calculate the Coulomb branch dimension of the full puncture theory of example 2.3.1, both for T^{5d} in the little string and T^{4d} in the CFT limit. Recall that the little string defect was defined by the following set of weights $\mathcal{W}_S$:*

$$\begin{aligned}
\omega_1 &= [\ \ 1, \ \ 0, \ \ 0, \ \ 0] = -w_1 + 2\alpha_1 + 2\alpha_2 + \alpha_3 + \alpha_4,\\
\omega_2 &= [-1, \ \ 1, \ \ 0, \ \ 0] = -w_1 + \alpha_1 + 2\alpha_2 + \alpha_3 + \alpha_4,\\
\omega_3 &= [\ \ 0, -1, \ \ 1, \ \ 1] = -w_1 + \alpha_1 + \alpha_2 + \alpha_3 + \alpha_4,\\
\omega_4 &= [\ \ 0, \ \ 0, -1, \ \ 0] = -w_3,\\
\omega_5 &= [\ \ 0, \ \ 0, \ \ 0, -1] = -w_4.
\end{aligned}$$

We record the negative inner products of each of the positive roots with the weights in $\mathcal{W}_S$. We write the results in the following table, where all positive inner products are replaced by 0:

$$\begin{aligned}
\langle \Phi^+, \omega_1 \rangle &\to (\ \ 0, \ \ 0, \ \ 0, \ \ 0, \ \ 0, \ \ 0, \ \ 0, \ \ 0, \ \ 0, \ \ 0, \ \ 0, \ \ 0),\\
\langle \Phi^+, \omega_2 \rangle &\to (\ \ 0, \ \ 0, \ \ 0, \ \ 0, \ \ 0, \ \ 0, \ \ 0, \ \ 0, \ \ 0, \ \ 0, \ \ 0, -1),\\
\langle \Phi^+, \omega_3 \rangle &\to (\ \ 0, \ \ 0, \ \ 0, \ \ 0, \ \ 0, \ \ 0, \ \ 0, -1, -1, \ \ 0, \ \ 0, \ \ 0),\\
\langle \Phi^+, \omega_4 \rangle &\to (-1, -1, -1, \ \ 0, -1, \ \ 0, -1, \ \ 0, \ \ 0, \ \ 0, -1, \ \ 0),\\
\langle \Phi^+, \omega_5 \rangle &\to (-1, -1, -1, -1, \ \ 0, -1, \ \ 0, \ \ 0, \ \ 0, -1, \ \ 0, \ \ 0).
\end{aligned}$$

Adding the absolute value of all these entries gives 15, the dimension of the Coulomb branch of T^{5d}. Comparing this to the quiver in Figure 2.5, this is indeed correct.

Furthermore, we see that all 12 positive roots have a negative inner product with at least one of the weights. Thus, the Coulomb branch of T^{4d} has (complex) dimension 12.

The set $\mathcal{W}_S$ is distinguished, and one can see immediately that $\Theta = \varnothing$. So the parabolic subalgebra associated to this defect is all of D_4.

Example 4.2.6. *As another example, let us look at the F_4 defect:*

$$\mathcal{W}_S = \{\omega_1 = [\ \ 0, \ \ 0, \ \ 0, \ \ 1], \ \ \omega_2 = [\ \ 0, \ \ 0, \ \ 0, -1]\}$$

First, let us compute the Coulomb branch dimension of T^{5d} in the little string and of T^{4d} in the CFT limit. ω_1 has no negative inner product with any of the positive roots, so it does not contribute to the Coulomb branch counting.

ω_2 has an inner product equal to -2 with 7 of the positive roots, and an inner product equal to -1 with 8 of the positive roots. Summing up the absolute value of these inner products, we deduce that the complex Coulomb branch dimension of T^{5d} is 22. Writing down the quiver engineered by $\mathcal{W}_S$, the Coulomb content from the gauge nodes is indeed $4 + 8 + 6 + 4 = 22$. Furthermore, we can conclude that 15 of the positive roots have a negative inner product with at least one of the weights. Thus, the Coulomb branch of T^{4d} has complex dimension 15.

The set $\mathcal{W}_S$ is distinguished, and ω_1 and ω_2 both clearly have a zero inner product with the three simple roots $\alpha_1, \alpha_2, \alpha_3$ (they have common zeros for their first three Dynkin labels). We conclude at once that $\Theta = \{\alpha_1, \alpha_2, \alpha_3\}$. Therefore, the parabolic subalgebra associated to this defect is $\mathfrak{p}_{\{\alpha_1,\alpha_2,\alpha_3\}}$.

The above discussion leads us straight to the consideration of nilpotent orbits.

4.3 Surface defects and Nilpotent Orbits

The characterization of a puncture as studied in the 6d $(2,0)$ CFT literature [46] is given in terms of a *nilpotent orbit* of the algebra: An element $X \in \mathfrak{g}$ is nilpotent if the matrix representative (in some faithful representation) is a nilpotent matrix. If X is nilpotent, then the whole orbit $\mathcal{O}_X$ of X under the adjoint action of G is nilpotent – we call this a nilpotent orbit[2]. For readers interested in details and applications, the textbook [100] serves as an excellent introduction.

A short review

For a simple Lie algebra, the number of nilpotent orbits is finite, and studying their properties leads to many connections to different branches of representation theory. For instance, for $\mathfrak{g} = A_n$, these orbits are labeled by Young diagrams with $n+1$ boxes.

An important fact is that for any nilpotent orbit $\mathcal{O}$, the closure $\overline{\mathcal{O}}$ is always a union of nilpotent orbits. Furthermore, there is a maximal orbit $\mathcal{O}_{\max}$ whose union contains all other nilpotent orbits of $\mathfrak{g}$. This allows us to define an ordering on these orbits:

Given two nilpotent orbits $\mathcal{O}_1, \mathcal{O}_2 \subset \mathfrak{g}$, we define the relation

$$\mathcal{O}_1 \preceq \mathcal{O}_2 :\Leftrightarrow \mathcal{O}_1 \subseteq \overline{\mathcal{O}_2}\ , \tag{4.3.13}$$

where $\overline{\mathcal{O}}$ is the closure in the Zariski topology. This turns the set of all nilpotent orbits into a partially ordered set.

For classical Lie algebras, this order corresponds to the dominance order of the Young diagrams used to label the orbits.

Example 4.3.1 (A_3)**.** *For an A_n nilpotent orbit labeled by a partition $[d_1, \ldots, d_k]$, a matrix representative is given by k Jordan blocks of size $d_i \times d_i$. Taking the example of $n = 3$, there are five different nilpotent orbits. Their Hasse diagram can be found below in Figure 4.4. For instance, the sub-dominant diagram $[3,1]$ labels the orbit of*

$$X_{[3,1]} = \begin{pmatrix} 0 & 1 & 0 & 0 \\ 0 & 0 & 1 & 0 \\ 0 & 0 & 0 & 0 \\ 0 & 0 & 0 & 0 \end{pmatrix}. \tag{4.3.14}$$

In [46], boundary conditions of the 6d $(2,0)$ CFT are determined by solutions to Nahm's equations. These equations admit singular solutions near a puncture which are labeled by embeddings $\rho : \mathfrak{sl}_2 \to \mathfrak{g}$. Since $\sigma_+ \in \mathfrak{sl}_2$ is nilpotent, its image $\rho(\sigma_+)$ is as well, and defines a nilpotent orbit. By the Jacobson–Morozov theorem, this gives a one-to-one correspondence between such embeddings and nilpotent orbits.

[2]Note it is the adjoint Lie *group* action that is used here, not the Lie algebra.

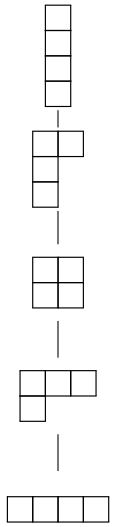

Figure 4.4: This diagram represents the inclusion relations between the nilpotent orbits of A_3.

Nilpotent orbits from Levi subalgebras

Since we now have two different constructions of surface defects, we should explain how we can relate them:

Given a parabolic subalgebra $\mathfrak{p} = \mathfrak{l} \oplus \mathfrak{n}$, the nilpotent orbit $\mathcal{O}_\mathfrak{p}$ associated to it is the maximal orbit that has a representative $X \in \mathcal{O}_\mathfrak{p}$ for which $X \in \mathfrak{n}$. This induced orbit agrees with what is referred to as the Richardson orbit of $\mathfrak{p}$.

If $\mathfrak{g}$ is a classical Lie algebra, this map can be most easily described using the semi-simple pole of the Higgs field. We represent the pole in the first fundamental representation, and assign a Young diagram to it by counting the multiplicities of the eigenvalues. For A_n, these Young diagrams are given by the sizes of the blocks making up the Levi subalgebra $\mathfrak{l}$.

To this Young diagram, we can apply a *duality map*, called the Spaltenstein map [101], and obtain another Young diagram. The map is many-to-one for all algebras except $\mathfrak{g} = A_n$, where the map is just the transposition of a Young diagram[3]. This Young diagram labels the nilpotent orbit describing a defect, according to [46]; adding the resulting nilpotent element to the Higgs field describes moving on the Coulomb branch of the theory T^{4d}, meaning we are no longer at the root of the Higgs branch. We will revisit this statement in detail when considering the explicit Seiberg–Witten curves of our defects in section 6.2.

Example 4.3.2. *Let us show how to get the nilpotent orbits of A_3 in Figure 4.4 from parabolic*

[3]Since the defects of the little string live in the weight lattice of ${}^L\mathfrak{g}$, one can also choose to work with a slightly different map, the Spaltenstein-Barbasch-Vogan map, which sends nilpotent orbits of $\mathfrak{g}$ to orbits of ${}^L\mathfrak{g}$. Ultimately, there is no difference in the resulting physics, so we choose to work with the Spaltenstein map instead, denoting defects as living in the coweight lattice of $\mathfrak{g}$, as we have done in the rest of this thesis.

subalgebras. To assign the right nilpotent orbit to them, we take the transpose of the partition describing the Levi subalgebra. The resulting Young diagram labels a nilpotent orbit, which describes a Coulomb deformation of the theory. Since this partition is the same one that is assigned to the pole of the Higgs field (in the first fundamental representation), we can also directly get the nilpotent orbit from the Higgs field data.

The correspondence we get can be read off from Table 4.2 below.

Θ	$\mathcal{O}$
$\varnothing$	[4]
$\{\alpha_i\}_{\,i=1,2,3}$	[3,1]
$\{\alpha_1, \alpha_2\}$	[2,2]
$\{\alpha_1, \alpha_3\}$	[2,1,1]
$\{\alpha_1, \alpha_2, \alpha_3\}$	[1,1,1,1]

Table 4.2: In this table, we read off which parabolic subalgebras of A_3 (labeled by a subset Θ of positive simple roots) induce which nilpotent orbits $\mathcal{O}$ (labeled by Young diagrams).

There are two issues with the above description of the Coulomb branch of T^{4d} as a nilpotent orbit. The first one is that for algebras of high rank, it quickly becomes cumbersome to extract a nilpotent orbit by assigning a Young diagram to a Higgs field as we described. Second, Young diagrams are not available to represent nilpotent orbits of exceptional Lie algebras. We remedy both problems in this next Section.

Bala–Carter Labeling of Nilpotent Orbits

The characterization of nilpotent orbits that turns out to arise naturally in the little string context was developed by Bala and Carter, and is applicable to any semi-simple Lie algebra [102, 103]. We only need the result of their analysis, so we will be brief in describing their construction. It relies once again on the use of the Levi subalgebras of $\mathfrak{g}$.

The Bala–Carter prescription is to label a nilpotent orbit $\mathcal{O}$ by the smallest Levi subalgebra $\mathfrak{l} \subset \mathfrak{g}$ that contains some representative of that orbit. When $\mathfrak{g} \neq A_n$, it can happen that this Levi subalgebra does not specify uniquely $\mathcal{O}$, so extra data is needed. The prescription is as follows: suppose a parabolic subalgebra $\mathfrak{p}$ has the usual direct sum decompostion into Levi and nilradical parts, $\mathfrak{p} = \mathfrak{l}' \oplus \mathfrak{u}$. We say $\mathfrak{p}$ is distinguished if $\dim \mathfrak{l}' = \dim (\mathfrak{u}/[\mathfrak{u}, \mathfrak{u}])$ (an example of such a $\mathfrak{p}$ is the Borel subalgebra of $\mathfrak{l}$.) Then, one can show that a nilpotent orbit $\mathcal{O}$ is uniquely determined by the Levi subalgebra $\mathfrak{l}$ *and* by a distinguished parabolic subalgebra of $[\mathfrak{l}, \mathfrak{l}]$.

If $\mathfrak{l}$ is sufficient to uniquely specify a nilpotent orbit $\mathcal{O}$, meaning $\mathfrak{l}$ contains a unique distinguished parabolic subalgebra, then $\mathcal{O}$ is said to have Bala–Carter label $\mathfrak{l}$. The orbit $\mathcal{O}$ is called the *principal nilpotent orbit* of $\mathfrak{l}$. If the orbit $\mathcal{O}$ is not uniquely determined by $\mathfrak{l}$, an

additional label specifying a distinguished parabolic subalgebra of $[\mathfrak{l},\mathfrak{l}]$ is needed (it is usually given as the number of simple roots in a Levi subalgebra of $\mathfrak{p}$).

It is remarkable that one can read off the Bala–Carter label of a nilpotent orbit just from the Dynkin labels of the coweights specifying a D5 brane defect in little string theory. To be precise, we find the following general result, for $\mathcal{W}_{\mathcal{S}}$ a distinguished set of coweights of $\mathfrak{g}$, and Θ its associated set of simple roots, as defined in the previous section:

- If $\mathcal{W}_{\mathcal{S}}$ denotes a polarized defect of the little string, then one can identify the set Θ with the Bala–Carter label of the defect. Specifically, the union of all elements of the set Θ is a subquiver of $\mathfrak{g}$, called the Bala–Carter label of this defect, written as $\mathfrak{l}_\Theta$. The Coulomb branch of T^{4d} is then a resolution of the Spaltenstein dual of $\mathcal{O}$, where $\mathcal{O}$ is the nilpotent orbit labeled by the Bala–Carter label $\mathfrak{l}_\Theta$. The orbit $\mathcal{O}$ is the principal nilpotent orbit of the Levi subalgebra $\mathfrak{l}_\Theta$.

- If $\mathcal{W}_{\mathcal{S}}$ denotes an unpolarized defect of the little string *and* $\mathfrak{g}$ is simply-laced, then one can identify the set Θ with *part of* the Bala–Carter label of the defect. To fully characterize the defect, one must also indicate which fundamental representation the coweights of $\mathcal{W}_{\mathcal{S}}$ belong in. This additional prescription is in one-to-one correspondence with specifying the extra data needed to denote the Bala–Carter label of a non-principal nilpotent orbit. Furthermore, the Coulomb branch of T^{4d} is *not* in general in the image of the Spaltenstein map.

  When $\mathfrak{g}$ is non simply-laced, it can happen that an *unpolarized* defect $\mathcal{W}_{\mathcal{S}}$ has no relation to the labeling of nilpotent orbits predicted by Bala and Carter (the nilpotent orbit is still realized physically as a Coulomb branch of some theory T^{4d}, but the Bala–Carter label for it is not readable from the simple roots set Θ of $\mathcal{W}_{\mathcal{S}}$).

We present a few Bala–Carter labels for polarized defects in Figure 4.5, and for unpolarized defects in Figure 4.6.

Example 4.3.3. *For $\mathfrak{g} = A_3$, consider the orbit of the element*

$$X = \begin{pmatrix} 0 & 1 & 0 & 0 \\ 0 & 0 & 0 & 0 \\ 0 & 0 & 0 & 1 \\ 0 & 0 & 0 & 0 \end{pmatrix}.$$

The algebra $\mathfrak{sl}_4$ has five different (conjugacy classes of) Levi subalgebras, corresponding to the five integer partitions of 4. X itself obviously is an element of the Levi subalgebra $\mathfrak{l}_{\{\alpha_1,\alpha_3\}}$:

$$\mathfrak{l}_{\{\alpha_1,\alpha_3\}} = \begin{pmatrix} * & * & 0 & 0 \\ * & * & 0 & 0 \\ 0 & 0 & * & * \\ 0 & 0 & * & * \end{pmatrix}.$$

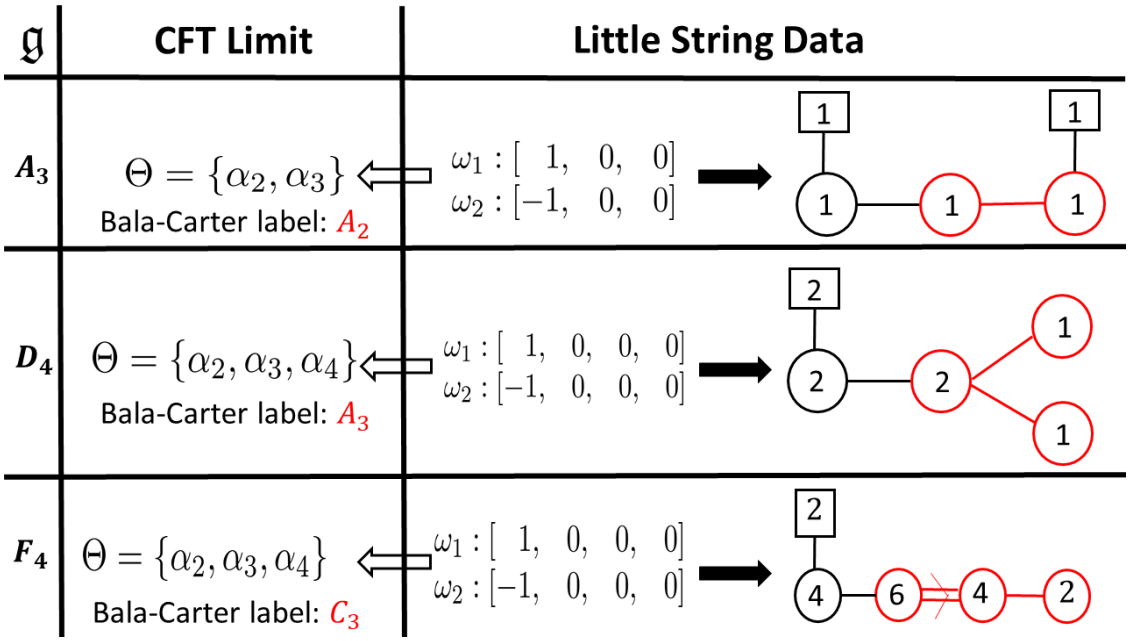

Figure 4.5: Given a distinguished set of coweights defining a defect T^{5d}, we immediately read off the Bala–Carter of the theory T^{4d}, in the CFT limit. Featured here are examples of polarized defects. Note that the Bala–Cater label forms a "subquiver" (shown in red) of the little string quiver.

This algebra contains

$$\mathfrak{l}_{\{\alpha_1\}} = \begin{pmatrix} * & * & 0 & 0 \\ * & * & 0 & 0 \\ 0 & 0 & * & 0 \\ 0 & 0 & 0 & * \end{pmatrix}.$$

Since every element in any conjugacy class of $\mathfrak{l}_{\{\alpha_1\}}$ has at most one non-trivial Jordan block, X can never be contained in any of them; thus, the orbit of X is associated to $\mathfrak{l}_{\{\alpha_1,\alpha_3\}}$ and has the Bala–Carter label $2A_1$.

Example 4.3.4. *Let us consider again our F_4 defect,*

$$\mathcal{W}_{\mathcal{S}} = \{\omega_1 = [\ 0,\ \ 0,\ \ 0,\ \ 1],\ \ \omega_2 = [\ 0,\ \ 0,\ \ 0, -1]\}.$$

One can easily check that the defect is polarized. Furthermore, we identified in the previous example that $\Theta = \{\alpha_1, \alpha_2, \alpha_3\}$. Therefore, the Bala–Carter label for the defect is B_3, and the Coulomb branch of the defect in the CFT limit is the Spaltenstein dual of the nilpotent orbit B_3, which is the orbit A_{2_s}. The orbit A_{2_s} has complex dimension 15, which confirms our previous computation of the dimension from a different method.

Some comments are in order: First, the above points imply that all nilpotent orbits are realized as the m_s to infinity limit of the Coulomb branch of some Dynkin-shaped quiver

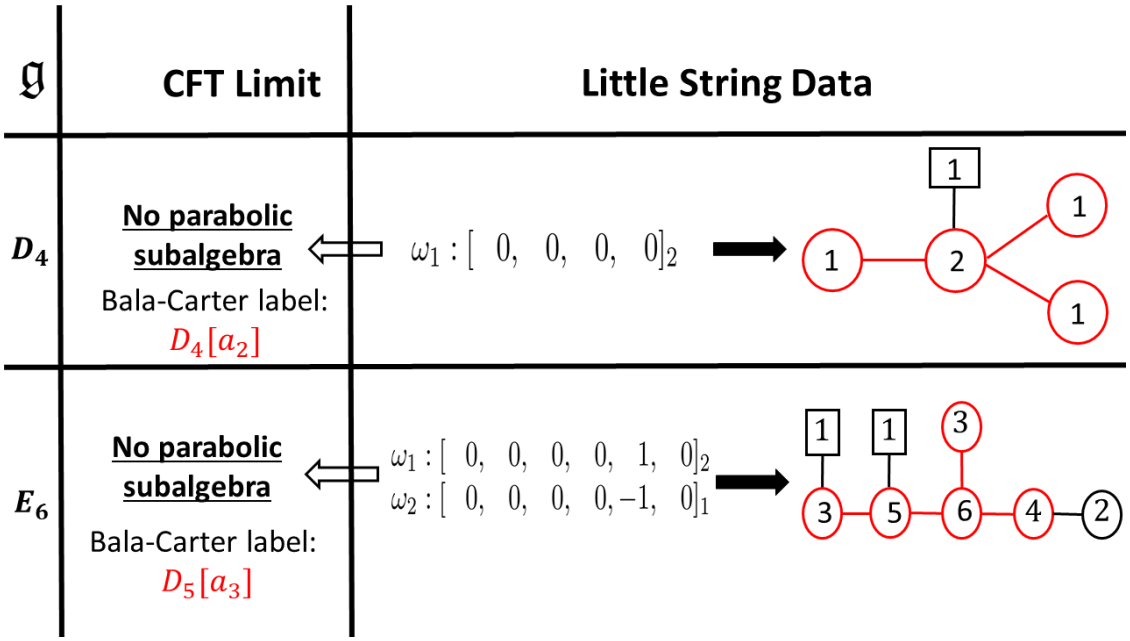

Figure 4.6: Bala–Carter labels for unpolarized defects. The subscript next to the coweights is necessary to fully specify the defects; it indicates which representation the coweights are taken in. This extra data is in one-to-one correspondence with an extra "simple root label" (written as $[a_i]$) for the Bala–Carter label.

gauge theory, with unitary gauge groups. Second, the coweight data of the D5 branes defining those quivers almost always provides a physical realization of the Bala–Carter classification of nilpotent orbits, with a few exceptions: for some non simply-laced unpolarized defects, the *labeling* predicted by Mathematics is sometimes not the same as the prediction obtained from little string Physics. We will illustrate this feature in detail for $\mathfrak{g} = G_2$ in the Examples 8.2.

4.4 Weighted Dynkin Diagrams

There is yet another way to classify nilpotent orbits of $\mathfrak{g}$, known as the so-called *weighted Dynkin diagrams*. We now show how to derive them, and make the surprising observation that all weighted Dynkin diagrams can be interpreted as physical quiver theories of the little string.

Mathematical construction

Weighted Dynkin diagrams are vectors of integers $r_i \in \{0, 1, 2\}$, where $i = 1, \ldots, \mathrm{rk}\mathfrak{g}$; thus, we get one number for each node in the Dynkin diagram of $\mathfrak{g}$. We can associate such a vector to each nilpotent orbit of $\mathfrak{g}$, and each nilpotent orbit has a unique weighted Dynkin diagram.

Note, however, that not all such labellings of the Dynkin diagram also have a nilpotent orbit corresponding to it.

To construct such a weighted Dynkin diagram, we use the following theorem by Jacobson and Morozov [104].

Remember that $\mathfrak{sl}_2$ is the algebra generated by X, Y and H with the relations

$$[H, X] = 2X, \qquad [H, Y] = -2Y, \qquad [X, Y] = H. \tag{4.4.15}$$

Every nilpotent orbit in $\mathfrak{g}$ arises as the orbit of the image of X in an embedding $\rho : \mathfrak{sl}_2 \to \mathfrak{g}$.

In other words, for any embedding $\rho : \mathfrak{sl}_2 \to \mathfrak{g}$, the element $\rho(X)$ always is a nilpotent element of $\mathfrak{g}$. The Jacobson–Morozov theorem tells us that any nilpotent orbit uniquely arises (up to conjugation) as the orbit of such an element.

This means in particular that any nilpotent orbit also determines an element $\rho(H)$, which is semi-simple (we assume it to be diagonal). For simplicity, we'll just write $\rho(H)$ as H. The (diagonal) entries of H are always integers, and allow us to read off the weighted Dynkin diagram; the entry of the i-th node is defined to be $r_i = \alpha_i(H)$, where α_i is the i-th simple root of $\mathfrak{g}$. It turns out that these numbers are always 0, 1 or 2.

Example 4.4.1. *We illustrate the above construction for the nilpotent orbit of*

$$X = \begin{pmatrix} 0 & 1 & 0 & 0 \\ 0 & 0 & 0 & 0 \\ 0 & 0 & 0 & 1 \\ 0 & 0 & 0 & 0 \end{pmatrix}$$

in $\mathfrak{sl}_4$. One first constructs H; we won't do this explicitly here (see [100] for details), but the result is

$$H = \begin{pmatrix} 1 & 0 & 0 & 0 \\ 0 & -1 & 0 & 0 \\ 0 & 0 & 1 & 0 \\ 0 & 0 & 0 & -1 \end{pmatrix}.$$

The next step is to reorder the elements in the diagonal of H in a monotonically decreasing order. The quadruple we get is $(h_1, h_2, h_3, h_4) = (1, 1, -1, -1)$.

The nodes of the Dynkin diagram are labelled by the consecutive differences of these numbers, so $r_i = h_i - h_{i+1}$. This gives us $(r_1, r_2, r_3) = (0, 2, 0)$. So the weighted Dynkin diagram in this example looks as follows:

$$0 \text{ — } 2 \text{ — } 0$$

One can generalize the above construction to all simple Lie algebras, with minor modifications.

From Weighted Dynkin Diagrams to Little String Defects

We make the following observations:

All weighted Dynkin diagrams can be interpreted as physical quiver theories: the label on each node of the weighted Dynkin diagram should be understood as the rank of a flavor symmetry group in a quiver. The quivers one reads in this way are always superconformal (in a 4d sense), and the flavor symmetry on each node is either nothing, a $U(1)$ group, or a $U(2)$ group. For instance, the full puncture, or maximal nilpotent orbit, denoted by the weighted Dynkin diagram $(2, 2, \ldots, 2, 2)$, can be understood as a quiver gauge theory with a $U(2)$ flavor attached to each node, for all semi-simple Lie algebras (see also [106]). Pushing this idea further, we find, surprisingly, that these quivers are little string defect theories T^{5d}, at finite m_s.

In the case of $\mathfrak{g} = A_n$, this correspondence between weighted Dynkin diagrams and defect theories T^{5d} can be made explicit. Indeed, all A_n weighted Dynkin diagrams are invariant under the $\mathbb{Z}_2$ outer automorphism action of the algebra; in other words, the quivers are all symmetric. For low dimensional defects, these quivers are precisely the little string quivers T^{5d} studied in this note. For instance, consider the simple puncture of A_n, generated by the set of weights $\mathcal{W}_{\mathcal{S}} = \{[1, 0, \ldots, 0]\ ,\ [-1, 0, \ldots, 0]\}$, with Bala-Carter label A_{n-1}; the weighted Dynkin diagram with this Bala-Carter label can be shown to be $(1, 0, \ldots, 0, 1)$, in standard notation. This is precisely the little string quiver T^{5d} for the simple puncture! It has a $U(1)$ flavor symmetry on the first node, and a $U(1)$ flavor symmetry on the last node, as it should. Many of the little string quivers T^{5d} of A_n, however, are not weighted Dynkin diagrams. They are the quivers not invariant under $\mathbb{Z}_2$ reflection. We claim that such theories T^{5d} can however uniquely be turned into the correct weighted Dynkin diagrams, by moving on the Higgs branch of the theory. Detailed examples are given in Appendix C.

This map between little string quivers and weighted Dynkin diagrams is one-to-one for $\mathfrak{g} = A_n$, but many-to-one for the other algebras, as a large number of different little string quivers typically describe one and the same defect in those cases. Nevertheless, the map always exists.

We now come to another important result about weighted Dynkin diagrams, motivated by their apparent connection to little string defects: the dimension of a nilpotent orbit can be easily computed from its weighted Dynkin diagram.

Dimension Formula

Recall that the "flavor symmetry rank" of a weighted Dynkin diagram never exceeds 2 (as the flavor symmetry is always a product of $U(1)$ and $U(2)$ groups only). This is a claim about the hypermultiplets of the quiver theory. There exists a "vector multiplet" counterpart to this statement, which is given by the following mathematical statement:

We interpret the weighted Dynkin diagram of a nilpotent orbit $\mathcal{O}$ as a coweight ω, written down in fundamental coweight basis. We then compute the sum of the inner products of all the positive roots of $\mathfrak{g}$ with this coweight. This gives a vector of non-negative integers.

Truncating the entries of this vector at 2 and taking the sum of the entries gives the (real) dimension of $\mathcal{O}$.

This result can be derived from the following dimension formula for nilpotent orbits[4] (see for instance [100]):

$$\dim \mathcal{O} = \dim \mathfrak{g} - \dim \mathfrak{g}_0 - \dim \mathfrak{g}_1, \tag{4.4.16}$$

where

$$\mathfrak{g}_i = \{Z \in \mathfrak{g} | [H, Z] = i \cdot Z\}, \tag{4.4.17}$$

and where H is the semisimple element in the $\mathfrak{sl}_2$ triple corresponding to $\mathcal{O}$.

Note that whenever $Z \in \mathfrak{g}_\beta$ for a root β, $[H, Z] = \beta(H)Z$. So

$$\mathfrak{g}_i = \bigoplus_{\substack{\beta \in \Phi, \\ \beta(H)=i}} \mathfrak{g}_\beta.$$

On the other hand, the inner product of the weighted Dynkin diagram coweight ω with a root β is just

$$\left\langle \sum_{i=1}^{n} \alpha_i(H)\omega_i, \beta \right\rangle = \sum_{i=1}^{n} \alpha_i(H)\langle \omega_i, \beta \rangle = \beta(H),$$

where α_i and ω_i are the simple roots and fundamental coweights of $\mathfrak{g}$, respectively. Thus, the above inner products just give us the grading 4.4.17.

The prescription we give is therefore equivalent to the dimension formula 4.4.16; namely,

$$\begin{aligned} \dim(\mathfrak{g}_1) + 2\sum_{i\geq 2} \dim(\mathfrak{g}_i) &= \dim(\mathfrak{g}_1) + \sum_{i\geq 2} \dim(\mathfrak{g}_i) + \sum_{i\leq -2} \dim(\mathfrak{g}_i) \\ &= \dim(\mathfrak{g}_1) + \dim(\mathfrak{g}) - \sum_{-1\leq i\leq 1} \dim(\mathfrak{g}_i) \\ &= \dim(\mathfrak{g}_1) + \dim(\mathfrak{g}) - 2\dim(\mathfrak{g}_1) - \dim(\mathfrak{g}_0) \\ &= \dim(\mathfrak{g}) - \dim(\mathfrak{g}_0) - \dim(\mathfrak{g}_1). \end{aligned} \tag{4.4.18}$$

Example 4.4.2. *Let us take the example of the weighted Dynkin diagram (2,1,1,2) in the algebra $\mathfrak{g} = A_4$. We write $\omega = [2, 1, 1, 2]$ as a weight in Dynkin basis. The positive roots Φ^+ of A_4, written here in Euclidean basis, are*

$$(h_1 - h_5,\ h_2 - h_5,\ h_1 - h_4,\ h_2 - h_4,\ h_3 - h_5,\ h_1 - h_3,\ h_2 - h_3,\ h_3 - h_4,\ h_4 - h_5,\ h_1 - h_2)$$

Calculating the inner product of all of these positive roots with ω gives the numbers

$$\langle \Phi^+, \omega \rangle = (6, 4, 4, 2, 3, 3, 1, 1, 2, 2).$$

Truncating at multiplicity 2, the sum of the inner products is $2 \times 8 + 1 \times 2 = 18$, which is indeed the dimension of the nilpotent orbit denoted by the diagram $(2, 1, 1, 2)$.

[4] We thank Axel Kleinschmidt for pointing out this proof to us.

Example 4.4.3. *Let us look at the weighted Dynkin diagram (0,0,0,2) in the algebra* $\mathfrak{g} = F_4$. *We therefore consider the coweight* $\omega = [0, 0, 0, 2]$, *which happens to be twice the fourth fundamental coweight of* F_4. *Let* $\Phi^{+\vee}$ *be the set of the 24 positive roots of* F_4. *Calculating the inner product of all of these positive roots with* ω *gives:*

$$\langle \Phi^{+\vee}, \omega \rangle = (4, 4, 4, 4, 2, 4, 2, 4, 4, 0, 2, 2, 0, 2, 0, 2, 0, 0, 2, 0, 0, 0, 2, 0).$$

Truncating at multiplicity 2, the sum of the inner products is $2 \times 7 + 2 \times 8 = 30$, *which is the correct real dimension of the nilpotent orbit denoted by the diagram* $(0, 0, 0, 2)$. *It is quite amazing that at finite* m_s, *in the little string, the gauge theory whose Coulomb branch flows to this orbit in the CFT limit is precisely the quiver with mass content* $(0, 0, 0, 2)$. *This is just the quiver engineered in the previous examples, from the set:*

$$\mathcal{W}_{\mathcal{S}} = \{\omega_1 = [\ \ 0, \ \ 0, \ \ 0, \ \ 1], \ \ \omega_2 = [\ \ 0, \ \ 0, \ \ 0, -1]\}.$$

Note that these results can be interpreted in the context of 3d $\mathcal{N} = 4$ theories. It is then interesting to compare this formula to the dimension of the Coulomb branch of a 3d $\mathcal{N} = 4$ quiver theory [107], which is given by a slice in the affine Grassmannian [108]. In that setup, the dimension can be calculated by the exact same procedure, coming from a monopole formula [109], but without truncating the inner products at the value 2. For conformal theories, this is simply the sum of the ranks of the gauge groups.

Lastly, we want to emphasize that the above formula we gave does not compute the Coulomb branch dimension of the defect theory T^{4d} denoted by the weighted Dynkin diagram. Instead, the Coulomb branch dimension is given by the dimension of the diagram's image under the Spaltenstein map. Since not all nilpotent orbits are in the image of the Spaltenstein map, so in many cases, it is unclear what the physical interpretation of the dimension formula should be.

Chapter 5

Little String Origin of 4d SYM Surface Defects

We now show how the description of two-dimensional surface defects in 4d $\mathcal{N} = 4$ SYM due to Gukov and Witten [1] originates from brane defects of the $(2, 0)$ little string theory. Let us first remind ourselves of their results (in this chapter, we will limit ourselves to the case where $\mathfrak{g} = ADE$, though it should be straightforward to generalize to the non simply-laced case, using the orbifold arguments of [56]).

5.1 Gukov–Witten Description of Defects

Surface defects of $\mathcal{N} = 4$ SYM are $\frac{1}{2}$-BPS operators; to describe them, one starts with a four-dimensional manifold M, which is locally $M = D \times D'$, where D is two-dimensional, and D' is a fiber to the normal bundle to D. Surface defects are then codimension two objects living on D, and located at a point on D'; they are introduced by specifying the singular behavior of the gauge field near this defect. A surface operator naturally breaks the gauge group G to a subgroup $\mathbb{L} \subset G$, called a Levi subgroup.

The story so far is in fact valid for $\mathcal{N} = 2$ SUSY, but $\mathcal{N} = 4$ SUSY has additional parameters $\vec{\beta}$ and $\vec{\gamma}$, which describe the singular behavior of the Higgs field ϕ near the surface operator; choosing $D' = \mathbb{C}$ with coordinate $z = re^{i\theta} = x_2 + ix_3$, we have:

$$A = \vec{\alpha} d\theta + \dots, \tag{5.1.1}$$

$$\phi = \frac{1}{2}\left(\vec{\beta} + i\vec{\gamma}\right)\frac{dz}{z} + \dots, \tag{5.1.2}$$

which solve the Hitchin equations [110]:

$$F = [\phi, \overline{\phi}], \tag{5.1.3}$$

$$\overline{D}_z \phi = 0 = D_z \overline{\phi}. \tag{5.1.4}$$

As written above, we have chosen a complex structure which depends holomorphically on $\beta + i\gamma$, while the Kähler structure depends on α. Quantum mechanics also requires the consideration of the Theta angle, denoted by η; by supersymmetry, it will complexify the Kähler parameter α.

S-duality is the statement that this theory is equivalent to $\mathcal{N} = 4$ gauge theory with a dual gauge group and coupling constant

$$g'_{4d} = 1/g_{4d}.$$

The action of S-duality on the surface defect parameters is a rescaling of the Higgs field residue

$$(\beta, \gamma) \to \left(\frac{4\pi}{g^2_{4d}}\right)(\beta, \gamma), \tag{5.1.5}$$

and an exchange of the gauge field and Theta angle parameters:

$$(\alpha, \eta) \to (\eta, -\alpha). \tag{5.1.6}$$

The analysis of [1] gives a second description of the surface operators of $\mathcal{N} = 4$ SYM, which will be of great relevance to us; one couples the 4d theory to a 2d non-linear sigma model on D. In the $\mathcal{N} = 4$ case, the 2d theory is a sigma model to $T^*(G/\mathcal{P})$, where $\mathcal{P} \subset G$ is a parabolic subgroup of the gauge group. The quotient describes a partial flag manifold when the Lie algebra $\mathfrak{g}$ is A_n. In the case of a general Lie algebra, the quotient is a generalized flag variety. This target space is in fact the moduli space of solutions to the Hitchin equations (5.1.3).

Then, to describe a surface operator, one can either specify the parameters (β, γ, α) for the singular Higgs and gauge fields, or spell out the sigma model $T^*(G/\mathcal{P})$. It turns out that both of these descriptions have an origin in the $(2, 0)$ little string theory, and we will now show this explicitly.

5.2 Integrable Systems, Bogomolny and Hitchin Equations

The integrable system associated to the $(2, 0)$ little string theory on $\mathcal{C}$ has two descriptions. The first is in terms of the moduli space of $\mathfrak{g}$-monopoles on $\mathbb{R} \times T^2$. The second is in terms of a Hitchin-type system on $\mathcal{C}$. These integrable systems and their relation to 5d quiver gauge theories were studied recently in [41, 42, 111], so we can focus here on the new aspect, namely, the relation to the $(2, 0)$ little string theory. The connection to integrable systems emerges upon compactifying the theory on an additional circle, which we take to have the radius R_1, so we study $(2, 0)$ little string on $\mathcal{C} \times S^1(R_1)$, with defects at points on $\mathcal{C}$, as before.

To be more quantitative, we fist note that the brane defects are solutions to Bogomolny equations on $\mathcal{C} \times S^1(R_1)$:

$$D\phi = *F. \tag{5.2.7}$$

As mentioned in Section 1.2, little string theory enjoys T-duality, so in particular, the $(2,0)$ ADE Little String of type IIB compatified on $S^1(R_1)$ is dual to the (1,1) ADE Little String of type IIA compatified on $S^1(\hat{R}_1)$ of radius $\hat{R}_1 = 1/m_s^2 R_1$. The defects are then D4 branes after T-dualizing, and are points on $\mathcal{C} \times S^1(\hat{R}_1)$. These are the $\mathfrak{g}$-monopoles, magnetically charged under the gauge field coming from the (1,1) little string. The n scalars are $\phi_a = \int_{S_a^2} m_s^3 \omega^I / g_s'$, where g_s' is the IIA string coupling, related to the IIB one by $1/g_s' = R_1 m_s / g_s$. F is the curvature of the gauge field coming from the (1,1) little string.

If we want to recover the original description of the defects as D5 branes, we can take the dual circle size $\hat{R}_1$ to be very small; the upshot is that the Bogomolny equations simplify and we recover the Hitchin equations (5.1.3) we considered previously:

$$F = [\phi, \overline{\phi}], \tag{5.2.8}$$

$$\overline{D}_z \phi = 0 = D_z \overline{\phi}. \tag{5.2.9}$$

A subtlety here is that the field ϕ got complexified in passing from D4 branes back to D5 branes. The imaginary part of ϕ is the holonomy of the (1,1) gauge field around $S^1(\hat{R}_1)$; this comes from the fact that the D4 branes are magnetically charged under the RR 3-form: $R_1 \int_{S_a^2 \times S^1(R_1)} m_s^2 \; C_{RR}^{(3)}$. In type IIB language, after T-duality, the D5 branes are charged under the RR 2-form instead: $1/\hat{R}_1 \int_{S_a^2} B_{RR}$. All in all, the Higgs field is then written in IIB variables as

$$\phi_a = (\alpha_a, \phi) = 1/\hat{R}_1 \int_{S_a^2} (m_s^2 \omega_I / g_s + i B_{RR}) = \tau_a / \hat{R}_1. \tag{5.2.10}$$

The Seiberg–Witten curve of the quiver gauge theory on the D5 branes arises as the spectral curve of the Higgs field ϕ, taken in some representation $\mathfrak{R}$ of $\mathfrak{g}$:

$$\det{}_{\mathfrak{R}} (e^{\hat{R}_1 \phi} - e^{\hat{R}_1 p}) = 0. \tag{5.2.11}$$

In the absence of monopoles, ϕ is constant: the vacuum expectation value of the Higgs field is $\hat{R}_1 \phi = \tau$.

By construction, then, the Coulomb branch of the ADE quiver theory on the D5 branes is the moduli space of monopoles on $\mathcal{C} \times S^1(\hat{R}_1)$. The D4 branes wrapping the compact 2-cycles are non-abelian monopoles, while the D4 branes wrapping non-compact cycles, are singular, Dirac monopoles [112, 113]. This is consistent with our coroot and coweight lattice interpretation of section . Now, at the root of the Higgs branch of the theory, recall that we get a description of the defects as a set of weights $\mathcal{W}_{\mathcal{S}}$ in $\mathfrak{g}$; there, all the non-abelian monopoles reduce to Dirac monopoles. The effect on ϕ of adding a Dirac monopole of charge ω_i, at a point $x_i = \hat{R}_1 \hat{\beta}_i$ on $\mathcal{C}$, is to shift:

$$e^{\hat{R}_1 \phi} \to e^{\hat{R}_1 \phi} \cdot (1 - z \, e^{-\hat{R}_1 \hat{\beta}_i})^{-w_i}. \tag{5.2.12}$$

Here, z is the complex coordinate on $\mathcal{C} = \mathbb{C}$. Thus, the Higgs field solving the Hitchin equations at the point where the Higgs and the Coulomb branches meet is

$$e^{\hat{R}_1 \phi(x)} = e^{\tau} \prod_{\omega_i^V \in \mathcal{W}_{\mathcal{S}}} (1 - z \, e^{-\hat{R}_1 \hat{\beta}_i})^{-\omega_i}. \tag{5.2.13}$$

To take the string mass m_s to infinity, we relabel $e^{\hat{R}_1\hat{\beta}_i} = z_{\mathcal{P}}\, e^{\hat{R}_1\beta_{i,\mathcal{P}}}$. We can then safely take the limit $\hat{R}_1 \to 0$; the imaginary part of ϕ decompactifies, and equation (5.2.11) becomes the spectral curve of the Hitchin integrable system [5]:

$$\det_{\mathfrak{R}}(\phi - p) = 0. \tag{5.2.14}$$

In this limit, the Higgs field near a puncture of $\mathcal{C}$ has a pole of order one, and takes the form

$$\phi(z) = \frac{\beta_0}{z} + \sum_{\mathcal{P}} \sum_{\omega_i \in \mathcal{W}_{\mathcal{P}}} \frac{\beta_{i,\mathcal{P}}\, \omega_i}{z_{\mathcal{P}} - z}, \tag{5.2.15}$$

with $\beta_0 = \tau/\hat{R}_1$ and $\mathcal{P}$ the set of punctures. Therefore, in the $(2,0)$ CFT, we have poles on $\mathcal{C}$ at $z = z_{\mathcal{P}}$, with residues

$$\beta_{\mathcal{P}} = \sum_{\omega_i \in \mathcal{W}_{\mathcal{P}}} \beta_{i,\mathcal{P}}\, \omega_i\,.$$

These residues are what we called $\beta + i\gamma$ in the $\mathcal{N} = 4$ SYM setup of eq. (5.1.2).

5.3 S-Duality of Surface Defects

To provide evidence that the surface defects of $\mathcal{N} = 4$ SYM really are branes at points on $\mathcal{C}$ in the $(2,0)$ little string, we now derive four-dimensional S-duality from T-duality of the string theory, compactified on an additional torus T^2. Here, T^2 is the product of two S^1's, one from each of the two complex planes $\mathbb{C}^2$. We label those circles as $S^1(R_1)$ and $S^1(R_2)$, of radius R_1 and R_2 respectively.

First, without any D5 branes, S-duality was derived in [56], and the line of reasoning went as follows: suppose we first compactify on, say, $S^1(R_1)$; this is what we just did in the previous section to make contact with D4 branes as magnetic monopoles. Then, we are equivalently studying the (1,1) little string on $S^1(\hat{R}_1)$. Compactifying further on $S^1(R_2)$, this theory is the same as the (1,1) little string on $S^1(R_1) \times S^1(\hat{R}_2)$, by T^2-duality. 4d SYM S-duality then naturally follows from the T^2-duality of this pair of (1,1) theories. Indeed, at low energies, both $(1,1)$ little string theories become the maximally supersymmetric 6d SYM, with gauge group dictated by $\mathfrak{g}$ and gauge coupling $1/g_{6d}^2 = m_s^2$. We wish to take the string scale m_s to infinity; in the case of the $(1,1)$ string on $S^1(\hat{R}_1)$, since $m_s^2\hat{R}_1 = 1/R_1$, the radius $\hat{R}_1$ goes to 0 in that limit. The theory then becomes 5d $\mathcal{N} = 2$ SYM, with inverse gauge coupling $1/g_{5d}^2 = 1/R_1$. After the further compactification on $S^1(R_2)$, we obtain at low energies 4d $\mathcal{N} = 4$ SYM, with inverse gauge coupling $1/g_{4d}^2 = R_2/g_{5d}^2 = R_2/R_1$. Now, the same reasoning applied to the T^2-dual theory $S^1(R_1) \times S^1(\hat{R}_2)$ gives 4d $\mathcal{N} = 4$ SYM in the m_s to infinity limit, with inverse gauge coupling $1/g_{4d}'^2 = R_1/R_2$.

Note that $1/g'_{4d} = g_{4d}$. This is just the action of S-duality on the gauge coupling of $\mathcal{N} = 4$ SYM. Writing $R_2/R_1 \equiv \mathrm{Im}(\tau')$, with τ' the modular parameter of the T^2, we see that S-duality is a consequence of T^2-duality for the pair of $(1,1)$ little string theories. An illustration of the dualities is shown in Figure 5.1.

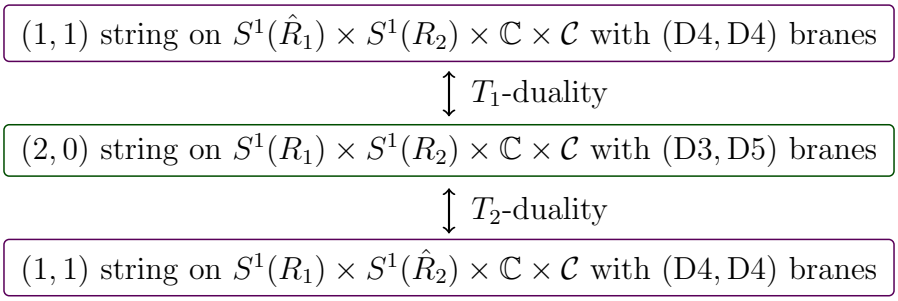

Figure 5.1: One starts with the $(1,1)$ little string theory on $T^2 \times \mathbb{C} \times \mathcal{C}$. After doing two T-dualities in the torus directions, we get the $(1,1)$ little string theory on the T-dual torus; in the low energy limit, the pair of $(1,1)$ theories gives an S-dual pair of $\mathcal{N} = 4$ SYM theories. D3 branes at a point on T^2 map to D4 branes in either $(1,1)$ theory, while D5 branes wrapping T^2 map to another set of D4 branes.

Now, we extend this argument and introduce the D5 brane defects; since the D5 branes were initially wrapping $T^2 \times \mathbb{C}$, note that we can equivalently consider the defects to be D3 branes at a point on T^2. We now argue that the S-duality action on the half BPS surface defects of SYM has its origin in the same T^2-duality of $(1,1)$ theories we presented in the previous paragraph.

First, recall that after $S^1(R_1)$ compactification, the D5 branes are charged magnetically, with period:

$$\phi_a = 1/\hat{R}_1 \int_{S_a} (m_s^2 \omega_I / g_s + i B_{RR}).$$

In type IIB variables, we call this period $\beta + i\gamma$. By T-dualizing along $S^1(R_1)$ we obtain D4 branes wrapping $S^1(R_2)$ in the $(1,1)$ little string. Now suppose we T-dualize the D5 branes along $S^1(R_2)$ instead; then we have D4 branes wrapping $S^1(R_1)$, in the T^2-dual $(1,1)$ little string. The D4 brane tensions in both $(1,1)$ theories are proportional to each other, with factor R_2/R_1. But then $(\beta, \gamma) \to R_2/R_1\,(\beta, \gamma)$ after T^2-duality. The D4 branes are then heavy, magnetic objects in one $(1,1)$ theory, while they are light, electric objects in the other. In the $m_s \to \infty$ limit, (β, γ) are the parameters of the Higgs field in 4d SYM. This is precisely the action of S-duality for the Higgs field data: $(\beta, \gamma) \to \mathrm{Im}(\tau')(\beta, \gamma)$ (5.1.5).

Second, after T^2 compactification, the D3 branes, which are points on T^2, are charged under the RR 4-form: $\int_{S_a \times \widetilde{S^1} \times S^1(R_1)} C^{(4)}_{RR}$, where $\widetilde{S^1}$ is a circle around the point defect on $\mathcal{C}$. As before, $S^1(R_1)$ is one of the 1-cycles of T^2, and S_a is a compact 2-cycle in the ALE space X. We call this period α. The D3 branes are also charged under $\int_{S_a \times \widetilde{S^1} \times S^1(R_2)} C^{(4)}_{RR}$, where $S^1(R_2)$ is the other 1-cycle of T^2; we call this period η.

Suppose we T-dualize in the $S^1(R_1)$ direction. Then α becomes the period of the RR 3-form on $S_a \times \widetilde{S^1}$; this period is in fact an electric coupling for the holonomy of the $(1,1)$ gauge field around $\widetilde{S^1}$. Also, η becomes the period of the RR 5-form on $S_a \times \widetilde{S^1} \times S^1(R_2) \times S^1(\hat{R}_1)$;

this period is in fact a magnetic coupling for the holonomy of the $(1,1)$ gauge field around $\widetilde{S^1}$. T-dualizing on $S^1(R_2)$ instead, we reach the T^2-dual $(1,1)$ theory. We see that α gets mapped to η, while η gets mapped to $-\alpha$ (the minus sign arises because the 5-form is antisymmetric). So in the end, under T^2-duality, the periods change as $(\alpha, \eta) \to (\eta, -\alpha)$.

Note that because the 1-cycles generating the T^2 appear explicitly in the definition of these periods, T^2-duality does not amount to a simple rescaling of (α, η), as was the case for (β, γ). In the low energy limit, we recover the S-duality of the gauge field and Theta angle parameters of 4d SYM α and η in the presence of a defect (5.1.6).

5.4 $T^*(G/\mathcal{P})$ Sigma Model and Coulomb Branch of Defects

We made contact with the surface defects of Gukov and Witten after compactifying the $(2,0)$ little string on T^2 and T-dualizing the D5 branes to D3 branes.

Now, Gukov and Witten showed that surface operators of $\mathcal{N} = 4$ SYM can also be described by a 2d sigma model $T^*(G/\mathcal{P})$, which is a moduli space of solutions to the Hitchin equations (5.1.3). After taking the CFT limit of the little string theory, we saw that this moduli space is also the Coulomb branch of the $(2,0)$ CFT theory on the Riemann surface $\mathcal{C}$ times a circle $S^1(R_1)$ (the radius R_1 here being very big). As an algebraic variety, this Coulomb branch is singular, while $T^*(G/\mathcal{P})$ is smooth. The statement is then that the (resolution of the) Coulomb branch of the quiver gauge theories on the D3 branes we presented, in the appropriate m_s to infinity limit, is expected to be the sigma model to $T^*(G/\mathcal{P})$. In other terms, the Coulomb branch of T^{4d}, after compactification on T^2 and below the Kaluza Klein scale of compactification, can be identified with $T^*(G/\mathcal{P})$.

Quite beautifully, we recover in the space $T^*(G/\mathcal{P})$ the parabolic subalgebras that we had identified earlier using coweights in Section 4.2[1].

As a side note, it is known ([46, 114, 115, 116]) that $T^*(G/\mathcal{P})$ is the resolution of the Higgs branch of different theories from the ones we have been considering. In the little string setup, as we reviewed, the moduli space of monopoles naturally arises as a Coulomb branch instead of a Higgs branch. A natural guess is that those two descriptions could be related by mirror symmetry, and this is indeed the case in all the cases we could explicitly checked at low rank (see also [106]). We will not investigate this point further in this thesis, but it would be important to get a clear understanding of the mirror map, when it exists.

We conclude this chapter by showing yet another way to extract a parabolic subalgebra, which relies on identifying a Levi subalgebra of $\mathfrak{g}$ from the Seiberg–Witten curve. This Levi subalgebra appears in the Levi decomposition of $\mathfrak{p}_\Theta$ as $\mathfrak{p}_\Theta = \mathfrak{l}_\Theta \oplus \mathfrak{n}_\Theta$.

Recall that the Seiberg–Witten curve of the quiver gauge theory on the D5 branes is the spectral curve of the Higgs field ϕ, taken in some representation $\mathfrak{R}$ of $\mathfrak{g}$ ([70, 69, 117]). We

[1] the Higgs field we introduced is valued in the Lie algebra $\mathfrak{g}$, so we speak here of parabolic subalgebras rather than parabolic subgroups.

described the m_s to infinity limit after which the Seiberg–Witten curve of the theory becomes the spectral curve of the Hitchin integrable system

$$\det_{\mathfrak{R}}(\phi - p) = 0.$$

At the root of the Higgs branch, where the Coulomb and Higgs branches meet, this expression simplifies: the Higgs field near a puncture of $\mathcal{C}$ has a pole of order one. After shifting this pole to $z = 0$, we get

$$0 = \det\left(p \cdot \mathbb{1} - \frac{\sum_{\omega_i \in \mathcal{W}_S} \beta_i \omega_i}{z} + \text{reg.}\right), \tag{5.4.16}$$

where $\mathcal{W}_S$ is a set of coweights (taken in fundamental representations) that adds up to zero. The β_i are mass parameters of the gauge theory, which correspond to insertion points of the D5 branes on $\mathcal{C}$.

Thus, the residue at the pole diagonalizes, and the diagonal entries can be interpreted as hypermultiplet masses. So at the root of the Higgs branch, the Higgs field is described by an honest semi-simple element of $\mathfrak{g}$. From this semi-simple element, we can once again recover a parabolic subalgebra $\mathfrak{p}$. Indeed, given a semi-simple (diagonalizable) element S (in our cases, we'll always have $S \in \mathfrak{h}$), its centralizer

$$\mathfrak{g}^S \equiv \{X \in \mathfrak{g} \,\big|\, [X, S] = 0\} \tag{5.4.17}$$

is reductive and is in fact a Levi subalgebra $\mathfrak{l}_S$ of some parabolic subalgebra $\mathfrak{p}_S$.

Since the Higgs field at a puncture of $\mathcal{C}$ has a pole with semi-simple residue, we can use this construction to associate a Levi subalgebra $\mathfrak{l}$ to a defect. The smallest parabolic subalgebra containing $\mathfrak{l}$ is then the parabolic subalgebra defining the theory. Thus, we achieved our goal of building a parabolic subalgebra, starting from a given Higgs field.

Example 5.4.1. *For $\mathfrak{g} = A_2$, assume that the Higgs field has a pole with semi-simple residue $\phi = \frac{S}{z}$ near $z = 0$. In the fundamental representation of $\mathfrak{sl}_3$, a possible choice for S is*

$$S = \begin{pmatrix} \beta & 0 & 0 \\ 0 & \beta & 0 \\ 0 & 0 & -2\beta \end{pmatrix}. \tag{5.4.18}$$

The Levi subalgebra of $\mathfrak{sl}_3$ associated to this semi-simple element is the centralizer of S, which has the form

$$\mathfrak{g}^S = \begin{pmatrix} * & * & 0 \\ * & * & 0 \\ 0 & 0 & * \end{pmatrix} = \mathfrak{l}_{\{\alpha_1\}} \tag{5.4.19}$$

The parabolic subalgebra associated to this S is then $\mathfrak{p}_{\{\alpha_1\}}$ from example 4.2.2.

Chapter 6

Surface Defect Classification and $\mathcal{W}(\mathfrak{g})$-algebras

We now revisit the previous classification of $(2,0)$ CFT defects and its relation to parabolic subalgebras from the point of view of the dual $\mathfrak{g}$-type Toda CFT.

6.1 Levi subalgebras from level-1 null states of Toda CFT

in this section, we review how to construct the null states of the $\mathfrak{g}$-type Toda CFT, and we will see that they distinguish the same parabolic subalgebras $\mathfrak{p}_\Theta$ of $\mathfrak{g}$ we encountered before. As we will explain, the set of simple roots Θ plays a very central role in the $\mathcal{W}(\mathfrak{g})$-algebra null state condition.

Note that semi-degenerate representations of the Toda CFT generated by level one null states have been studied in [118]. There, the authors studied loop and domain wall operators in four-dimensional $\mathcal{N}=2$ theories in, as well as topological defects of Toda theories, and discussed relations to codimension two defects of the 6d (2,0) CFT.

We can use the vertex operators to construct highest coweight states $|\beta\rangle$ of the $\mathcal{W}(\mathfrak{g})$-algebra by acting on the vacuum, $|\beta\rangle = \lim_{z\to 0} e^{\langle\beta,\phi(z)\rangle}|0\rangle$. These give rise to a Verma module over $|\beta\rangle$ by acting with $\mathcal{W}(\mathfrak{g})$-algebra generators. For some of the $|\beta\rangle$, these representations are degenerate, because they contain a null state; we say that $|\chi\rangle$, in the Verma module over $|\beta\rangle$, is a *level k null state* of the $\mathcal{W}(\mathfrak{g})$-algebra if for all spins s:

$$W_n^{(s)}|\chi\rangle = 0, \quad \forall n > 0, \tag{6.1.1}$$

$$W_0^{(2)}|\chi\rangle = (E_\beta + k)|\chi\rangle, \tag{6.1.2}$$

where $W_0^{(2)}|\beta\rangle = E_\beta|\beta\rangle$.

The Verma module over $|\beta\rangle$ contains such a null state at level k if the Kač determinant at level k vanishes. For any simple algebra $\mathfrak{g}$, this determinant at level k is a non-zero factor times

$$\prod_{\substack{\alpha\in\Phi\\ m,n\leq k}} \left(\langle(\beta+\alpha_+\rho+\alpha_-\rho^\vee),\alpha\rangle - \left(\frac{\langle\alpha,\alpha\rangle}{2}\, m\,\alpha_+ + n\,\alpha_-\right)\right)^{p_N(k-mn)}, \tag{6.1.3}$$

where $p_N(l)$ counts the partitions of l with N colours, Φ is the set of all roots of $\mathfrak{g}$, and ρ (resp. $\rho^\vee$) is the Weyl vector of $\mathfrak{g}$ (resp. the Weyl vector of ${}^L\mathfrak{g}$) [78]. For us, $(\alpha_+,\alpha_-) = (b, 1/b)$.

Note that this determinant is invariant only under the shifted action of the Weyl group,

$$\beta \mapsto w(\beta+\alpha_+\rho+\alpha_-\rho^\vee) - (\alpha_+\rho+\alpha_-\rho^\vee), \tag{6.1.4}$$

where w is the ordinary Weyl action.

If $\alpha=\alpha_i$ is a simple root, the condition that this determinant vanishes can be phrased as

$$\langle\beta,\alpha_i\rangle = (1-m)\alpha_+ + r\,\frac{\langle\alpha,\alpha\rangle}{2}(1-n)\alpha_-\ , \tag{6.1.5}$$

with r the highest number of arrows between two adjacent nodes in the Dynkin diagram of $\mathfrak{g}$.

We see that any β with $\langle\beta,\alpha_i\rangle = 0$ for a *simple root* α_i gives rise to a level 1 null state, and if $Q \equiv (\alpha_+ + \alpha_-) \to 0$, a null state at level 1 occurs if $\langle\beta,\alpha_i\rangle = 0$ for any $\alpha\in\Phi$. It is enough to work in this "semi-classical" limit for our purposes, so we will set Q to 0 in what follows.

We can explicitly construct these null states: Consider the *screening charge operators*

$$Q_i^\pm = \oint \frac{dz}{2\pi i}\exp(i\alpha_\pm\langle\alpha_i,\phi\rangle) \tag{6.1.6}$$

and observe that

$$[W_n^{(k)}, Q_i^\pm] = 0. \tag{6.1.7}$$

The level 1 null state is then

$$S_i^+|\beta-\alpha_+\alpha_i\rangle. \tag{6.1.8}$$

The relation to the parabolic subalgebras introduced in section 4.2 is immediate: we simply associate a generic null state $|\beta\rangle$ satisfying

$$\langle\beta,\alpha_i\rangle = 0 \quad \forall\alpha_i\in\Theta \tag{6.1.9}$$

with the parabolic subalgebra $\mathfrak{p}_\Theta$, for Θ a subset of simple roots of $\mathfrak{g}$. By the state-operator correspondence, the momentum β carried by the vertex operator $V_\beta^\vee(z)$ is simply $\beta = \sum_{i=1}^{|\mathcal{W}_\mathcal{S}|}\beta_i\,\omega_i$, as we wrote previously in equation (3.3.42). Note also that this β defines a semi-simple element in $\mathfrak{g}$; this is just the residue of the Higgs field at the puncture, as explained in Section 5.4.

It would be interesting to study the q-deformed version of (6.1.9) in the little string context; the formula for the Kač determinant is then an exponentiated version of (6.1.3) [119]. This implies that the null states can be defined analogously for the q-deformed $\mathcal{W}(\mathfrak{g})$-algebra.

We show next that these these null states induce relations in the Seiberg–Witten curve of the theory T^{4d}. Indeed, the Seiberg–Witten curve of T^{4d} (5.4.16) can be obtained from a free field realization of the $\mathcal{W}(\mathfrak{g})$-algebra. We will simply read off the null states as relations between the curve coefficients. Generically, these relations only involve semi-simple elements of the algebra $\mathfrak{g}$. We will now see these relations are still preserved when one additionally introduces certain nilpotent deformations.

6.2 Seiberg–Witten curves from $\mathcal{W}(\mathfrak{g})$-algebras

In what follows, we fix $\mathfrak{g} = A, D, E$. As we reviewed previously, the Seiberg–Witten curve of T^{4d} is the spectral curve equation

$$\det{}_{\mathfrak{R}}(\phi - p) = 0. \tag{6.2.10}$$

In our case, ϕ has a simple pole such that the residue is a semi-simple element of $\mathfrak{g}$, which we can write as

$$\beta = \sum_{\omega_i \in W_S} \beta^i \omega_i. \tag{6.2.11}$$

To find the curve near the pole, which we assume to be at $z = 0$, we can just choose some convenient representation $\mathfrak{R}$, where the residue of ϕ is diagonal, and given by $\mathrm{diag}(\beta_1, \beta_2, \ldots) \equiv M$. Then $\phi = \frac{M}{z} + A$, with A a generic element in $\mathfrak{g}$.

We now expand eq. (6.2.10) and write the curve as

$$0 = \det\left(-p \cdot \mathbb{1} + \frac{M}{z} + A\right) = (-p)^{\dim(\mathfrak{R})} + \sum_s p^{\dim(\mathfrak{R})-s} \varphi^{(s)}, \tag{6.2.12}$$

where $\varphi^{(s)}$ is a meromorphic differential, i.e. $\varphi^{(s)} = \sum_{k=0}^{s} \frac{\varphi_k^{(s)}}{z^k}$, where the $\varphi_k^{(s)}$ are regular functions of β^i and a_{ij} (the entries of A).

Since M is diagonal, this determinant just picks up the diagonal terms a_{ii} of A, which we identify with the gauge couplings of the quiver theory.

Now, we can also construct the Seiberg–Witten curve of T^{4d} from the $\mathcal{W}(\mathfrak{g})$-algebra [120, 13]: For this, we need to perform a Drinfeld–Sokolov reduction to obtain explicit $\mathcal{W}(\mathfrak{g})$-algebra generators in the free field realization[1]. Setting $Q = 0$ gives us a direct connection to the defect defined by the semi-simple element $\beta \in \mathfrak{g}$ (cf. Section 5.4): We can identify

[1]We thank Kris Thielemans for sending us his `OPEDefs.m` package [121], which allowed us to do these calculations.

the poles of the Seiberg-Witten differentials with expectation values of these $\mathcal{W}(\mathfrak{g})$ algebra generators in the state $|\beta\rangle$:

$$\varphi^{(s)} = \langle\beta|W^{(s)}|\beta\rangle. \tag{6.2.13}$$

We checked this relation explicitly for A_n and D_n theories. It would be important to extend the analysis to non simply-laced algebras as well; we leave this task to future work.

Example 6.2.1. *Let us look at the curve describing the full puncture for $\mathfrak{g} = A_2$:*

Take the fundamental three-dimensional representation of $\mathfrak{sl}_3$ and write

$$M = \begin{pmatrix} \beta_1 & 0 & 0 \\ 0 & \beta_2 & 0 \\ 0 & 0 & -\beta_1 - \beta_2 \end{pmatrix}, \quad A = \begin{pmatrix} a_{11} & a_{12} & a_{13} \\ a_{21} & a_{22} & a_{23} \\ a_{31} & a_{32} & -a_{11} - a_{22} \end{pmatrix}. \tag{6.2.14}$$

Then the curve can be expanded, and we read off the differentials. For example, $\varphi^{(2)}$, the coefficient multiplying p, has the form

$$\varphi^{(2)} = \frac{\varphi_2^{(2)}}{z^2} + \frac{\varphi_1^{(2)}}{z} + \varphi_0^{(2)}, \tag{6.2.15}$$

where

$$\varphi_2^{(2)} = \frac{1}{2}\left(\beta_1^2 + \beta_2^2 + (-\beta_1 - \beta_2)^2\right) \equiv \frac{1}{2}\beta^2, \tag{6.2.16}$$

$$\varphi_1^{(2)} = a_{11}(2\beta_1 + \beta_2) + a_{22}(\beta_1 + 2\beta_2). \tag{6.2.17}$$

Furthermore,

$$\begin{aligned} \varphi_3^{(3)} &= -\beta_1^2\beta_2 - \beta_2^2\beta_1, \\ \varphi_2^{(3)} &= a_{11}(-2\beta_1\beta_2 - \beta_2^2) + a_{22}(-2\beta_1\beta_2 - \beta_1^2). \end{aligned} \tag{6.2.18}$$

Now from the CFT side, for $\mathfrak{g} = A_2$, define $X^j = i\partial\phi^j$. In the fundamental representation, $X^1 + X^2 + X^3 = 0$. Then the generators are just the energy momentum tensor

$$T(z) = W^{(2)}(z) = \frac{1}{3}(:X^1X^1: + :X^2X^2: + :X^3X^3: - :X^1X^2: - :X^1X^3: - :X^2X^3:)$$

and the spin 3 operator

$$\begin{aligned} W^{(3)}(z) = :&\left(\frac{2}{3}X^1 - \frac{1}{3}X^2 - \frac{1}{3}X^3\right) \cdot \left(-\frac{1}{3}X^1 + \frac{2}{3}X^2 - \frac{1}{3}X^3\right) \cdot \\ &\cdot \left(-\frac{1}{3}X^1 - \frac{1}{3}X^2 + \frac{2}{3}X^3\right): . \end{aligned}$$

For the full puncture, we find at once that $\langle\beta|L_0|\beta\rangle$ *is equal to* $\varphi_2^{(2)}$ *from above, while* $\langle\beta|W_0^{(3)}|\beta\rangle$ *is equal to* $\varphi_3^{(3)}$*, as expected. For the level 1 modes, one finds*

$$\langle\beta|W_{-1}^{(2)}|\beta\rangle = (2\beta_1+\beta_2)\langle\beta|j_{-1}^1|\beta\rangle + (\beta_1+2\beta_2)\langle\beta|j_{-1}^2|\beta\rangle, \tag{6.2.19}$$

$$\langle\beta|W_{-1}^{(3)}|\beta\rangle = (-2\beta_1\beta_2-\beta_2^2)\langle\beta|j_{-1}^1|\beta\rangle + (-\beta_1^2-2\beta_1\beta_2)\langle\beta|j_{-1}^2|\beta\rangle, \tag{6.2.20}$$

where j_k^i *denotes the* k*-th mode of* X^i*.*

Observe that this has the form (6.2.18) *if we identify* $\langle\beta|j_{-1}^i|\beta\rangle$ *with the* i*-th gauge coupling constant.*

For more complicated defects, the $\mathcal{W}(\mathfrak{g})$-algebra generators will have terms that are derivatives of X — these are set to zero in the semiclassical $Q\to 0$ limit we are considering; after doing so, the reasoning is as above.

Null state relations

Punctures that are not fully generic are determined by semi-simple elements $\beta\in\mathfrak{g}$ whose Verma modules contain null states at level one. Since the eigenvalues of the level one $\mathcal{W}(\mathfrak{g})$-algebra generators appear as coefficients in the curve, the existence of these null states induces some relations between these coefficients.

For $\mathfrak{g}=A_n$ and $\mathfrak{g}=D_n$ in the fundamental representation, the pattern is easy to see. The condition $\langle\beta,\alpha\rangle=0$ for some simple root α will cause some of the entries of $M=\mathrm{diag}(\beta_1,\beta_2,\ldots)$ to be equal to each other; if the entry β_i occurs k times, we get null states by letting the operator

$$\sum_s \beta_i^s W_{-1}^{(\dim(\mathfrak{R})-s)}, \tag{6.2.21}$$

and its $k-1$ derivatives with respect to β_i, act on $|\beta\rangle$. Thus, each theory induces some characteristic null state relations which are realized in the Seiberg–Witten curve.

We now use this observation to connect these curves to nilpotent orbits: note that all the curves considered so far were written as

$$\det\left(-p\cdot\mathbb{1}+\frac{M}{z}+A\right)=0 \tag{6.2.22}$$

for some diagonal M and a generic A in $\mathfrak{g}$. In the literature, the curves considered in [47, 48, 50] have the form

$$\det\left(-p\cdot\mathbb{1}+\frac{X}{z}+A\right)=0, \tag{6.2.23}$$

where, again, A is a generic element in $\mathfrak{g}$, and X is a representative of a nilpotent orbit $\mathcal{O}_X$.

We can now simply combine these two poles and form a curve of the form

$$\det\left(-p\cdot\mathbb{1}+e\,\frac{X}{z}+\frac{M}{z}+A\right)=0, \tag{6.2.24}$$

where M is semi-simple, $X \in \mathcal{O}_X$ is nilpotent and e is a parameter. We will test the correspondence between theories defined by nilpotent orbits and theories defined by semi-simple elements from this vantage point. Recall from section 4.3 that the semi-simple element $M \in \mathfrak{g}$ induces a nilpotent orbit $\mathcal{O}$. We observe the following facts[2]:

- Whenever an orbit $\mathcal{O}' \preceq \mathcal{O}$, it is *always* possible to find an $X \in \mathcal{O}'$ such that all the null state relations of the curve (6.2.22) are still satisfied by the curve (6.2.24).
- Whenever an orbit $\mathcal{O}' \not\preceq \mathcal{O}$, it is *never* possible find an $X \in \mathcal{O}'$ such that all the null state relations of the curve (6.2.22) are still satisfied by the curve (6.2.24).

This gives a prescription for allowed deformations; from the perspective of the theory T^{4d}, this corresponds to leaving the root of the Higgs branch by turning on certain Coulomb moduli.

Example 6.2.2. *For $\mathfrak{g} = A_2$, the only interesting state is $\beta = (\beta_1, \beta_1, -2\beta_1)$; we can get the level one coefficients of the curve by setting $\beta_1 = \beta_2$ in example 6.2.1:*

$$\begin{aligned} \phi_1^{(2)} &= \langle W_{-1}^{(2)} \rangle = 3\beta_1(a_{11} + a_{22}), \\ \phi_2^{(3)} &= \langle W_{-1}^{(3)} \rangle = -3\beta_1^2(a_{11} + a_{22}), \end{aligned} \tag{6.2.25}$$

so we see that

$$\langle W_{-1}^{(3)} \rangle + \beta_1 \langle W_{-1}^{(2)} \rangle = 0. \tag{6.2.26}$$

If we now add the nilpotent element $X = \begin{pmatrix} 0 & 0 & 1 \\ 0 & 0 & 0 \\ 0 & 0 & 0 \end{pmatrix}$, then

$$\begin{aligned} \phi_1^{(2)} &= 3\beta_1(a_{11} + a_{22}) + e\, a_{31}, \\ \phi_2^{(3)} &= -3\beta_1^2(a_{11} + a_{22}) - e\, \beta_1 a_{31}, \end{aligned} \tag{6.2.27}$$

and the null state relation (6.2.26) *is still satisfied.*

Example 6.2.3. *For $\mathfrak{g} = D_4$, let $M = diag\,(\beta_1, \beta_1, \beta_2, \beta_2, -\beta_1, -\beta_1, -\beta_2, -\beta_2)$ in the fundamental representation of $\mathfrak{so}(4,4)$. The curve associated to this puncture is*

$$0 = \det\left(-p \cdot \mathbb{1} + \frac{M}{z} + A\right),$$

with A a generic $\mathfrak{so}(4,4)$ matrix. Expanded, this has the form (6.2.12) *with nontrivial, meromorphic coefficients $\phi^{(2)}$, $\phi^{(4)}$, $\phi^{(6)}$ and $\phi^{(8)}$. These satisfy the relations*

$$\phi_7^{(8)} + \beta_1^2\phi_5^{(6)} + \beta_1^4\phi_3^{(4)} + \beta_1^6\phi_1^{(2)} = 0, \tag{6.2.28}$$

$$\phi_7^{(8)} + \beta_2^2\phi_5^{(6)} + \beta_2^4\phi_3^{(4)} + \beta_2^6\phi_1^{(2)} = 0. \tag{6.2.29}$$

[2]This observation was checked on the computer for a large class of A_n and D_n defects.

A calculation on the computer now shows that the only nilpotent elements we can add to M, in the sense of (6.2.24)*, lie in the orbits* $[4,4]$*,* $[3,3,1,1]$*,* $[3,1^5]$*,* $[2^4]$ *and* $[2,1^6]$*. These are exactly the orbits lying below* $[4,4]$ *in the partial ordering of nilpotent orbits of* D_4*.*

Chapter 7

Other Realizations of Defects

Our main setup to study the little string has been to compactify type IIB on an ADE singularity. As mentioned in the earlier sections of this work, performing T-duality, we can trade an A_n singularity for $n+1$ NS5 branes. After additional T-dualities, we can naturally bring our setup to a familiar one introduced by Witten and Hanany [2]. This has the advantage of making the coweight description of the defects manifest, and motivates a new interpretation and generalization of the Hanany–Witten transition as a (co)weight addition procedure.

7.1 Brane Engineering and Weights

Let us set $\mathfrak{g} = A_n$ in this section. We consider a collection of NS5 branes separated in one direction, and extended along the non-compact direction of our Riemann surface, the cylinder. Before T-dualizing, we had D5 branes that used to wrap compact 2-cycles of the geometry. They are now D3 branes that are stretching between two NS5 branes. There were also D5 branes wrapping non-compact 2-cycles of the geometry. These become D3 branes with one end on an NS5 brane and the other end on a D5 brane, or at infinity.

The D3 brane charge can be conveniently encoded in the weights of the set $\mathcal{W}_{\mathcal{S}}$ defining a defect, and in particular, in their Dynkin labels. To see how this works, let us focus on the i-th Dynkin label of a weight. Then the following holds (see also [2]):

- A D3 brane coming from the left ending on the $i-th$ NS5 contributes -1 to the weight's i-th label.
- A D3 brane coming from the right ending on the i-th NS5 contributes $+1$ to the weight's i-th label.
- A D3 brane coming from the left ending on the $i+1$-th NS5 contributes $+1$ to the weight's i-th label.

- A D3 brane coming from the right ending on the $i+1$-th NS5 contributes -1 to the weight's i-th label.
- Finally, a D5 brane present between the i-th and $i+1$-th NS5's contributes -1 to the weight's i-th label.

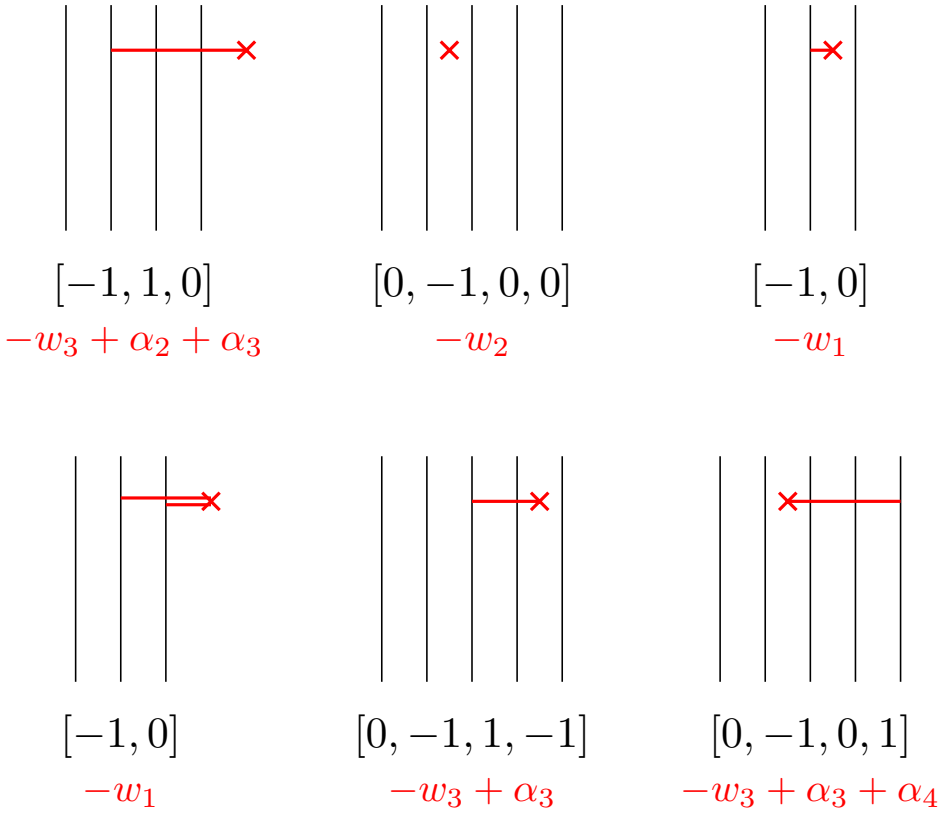

Figure 7.1: How to read off weights from a system of D3, D5, and NS5 branes.

All in all, a D3 brane stretching between a D5 brane and an NS5 brane (while possibly going through some other NS5 branes) produces a weight, whose Dynkin labels are a combination of 1's, -1's, and 0's. This construction is illustrated in figure 7.1. The map is not injective: for a given weight, there can be many distinct brane configurations. Therefore, the Dynkin labels of the weights in the set $\mathcal{W}_{\mathcal{S}}$ record the total charge of the D3 brane configuration. We recover here the statement that imposing that the sum of weights to be 0 is a statement about vanishing of D3 brane flux at infinity.

The configuration of branes spells out a quiver gauge theory at low energies, which is the expected theory T^{5d} we would write based on the weight data $\mathcal{W}_{\mathcal{S}}$. See Figure 7.2 for some examples.

7.2 Weight Addition as Generalized Hanany–Witten Transition

We now describe an effective and purely group-theoretical way to move on the Higgs branch of the defect, for any simple $\mathfrak{g}$. this makes use of the fact that a weight belonging to a fundamental representation can always be written as the sum of new weights. Each of them should be in the orbit of some fundamental weight (but the two orbits do not have to be the same).

After moving on the Higgs branch of the defect, we obtain a new defect, which reduces to the previous one at the root of the Higgs branch. When the gauge theory can be engineered using branes, this phenomenon is known as a Hanany–Witten transition [2]. There, a D5 brane passing an NS5 brane creates or removes D3 branes stretching between the two. When a brane construction is not available, the weight description we give is still valid, for an arbitrary simply laced Lie algebra.

Note that this weight addition formalism also gives a generalization of the so-called S-configuration: In the A_n case, where we have a brane picture, this statement translates immediately to the S-rule, which is then automatically satisfied. This argument is however applicable to any simple Lie algebra as well, so this gives a $\mathfrak{g}$-type S-rule.

7.3 Unpolarized Defects and Brane Web

All the fundamental representations of A_n are minuscule, so by definition, all A_n codimension-two defects are polarized; see Section 2.4. However, for the other algebras, it can also happen that a coweight in $\mathcal{W}_{\mathcal{S}}$ fails to satistfy the conditions to produce a polarized defect, in which case the resulting defect will be unpolarized. If such a coweight is picked, additional data is needed beyond simply specifying the set $\mathcal{W}_{\mathcal{S}}$; we write such coweights with a subscript denoting (minus) the representation they are taken in[1]. We show here how we can engineer unpolarized defects for a D_n theory using a $\mathbb{Z}_2$-orbifold of a A_{2n-1} brane web.

[1] the "minus" here is because every coweight we consider is written as $\omega = -w_a^\vee + \dots$

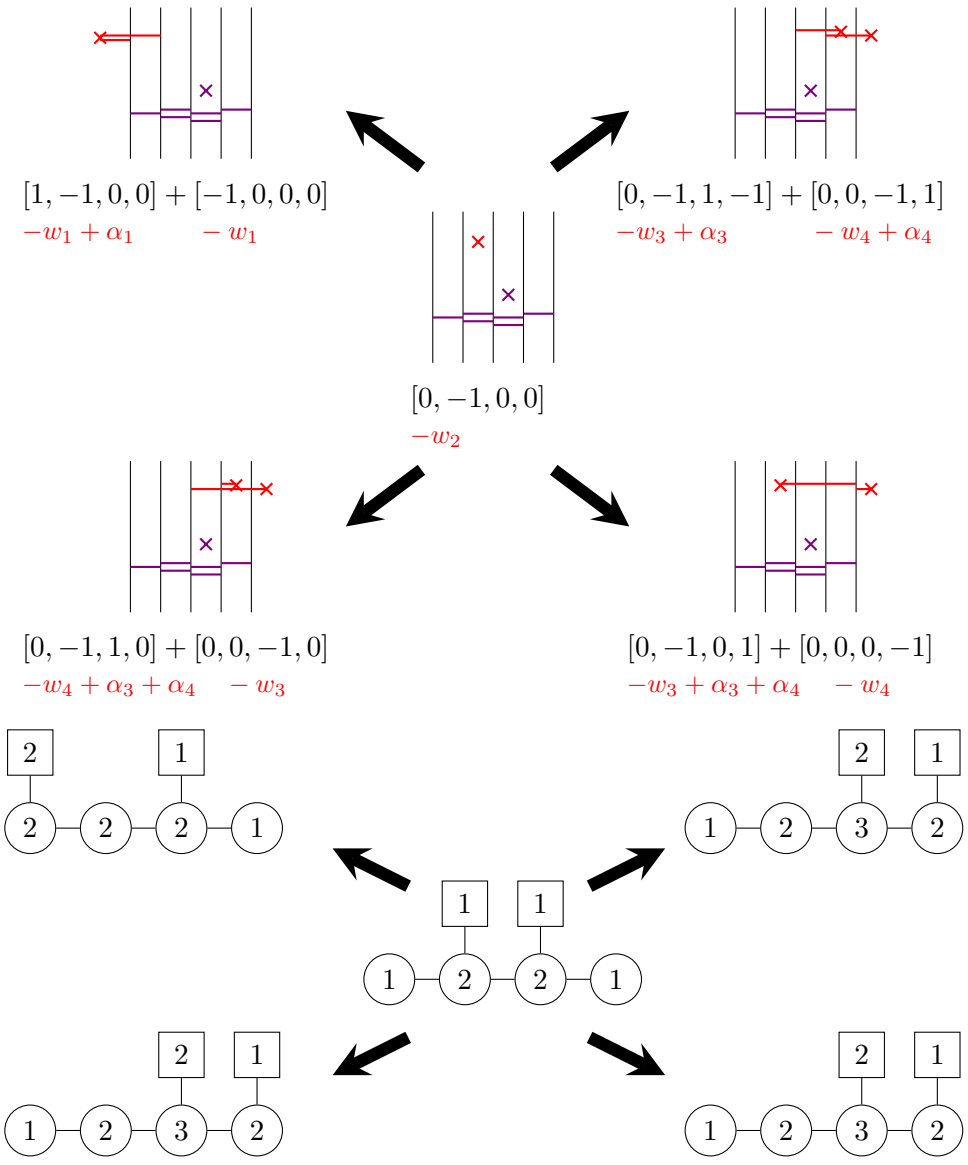

Figure 7.2: Example of a move on the Higgs branch of a defect: starting from the theory in the middle, we wrote all the theories one can obtain by replacing the weight on node 2 by a sum of two weights in fundamental representations. The top picture shows the brane realization of all the "new" defect. These all have a low-energy quiver gauge theory description (the ones shown below). At the root of the Higgs branch, the partition functions of all 5 theories is the same.

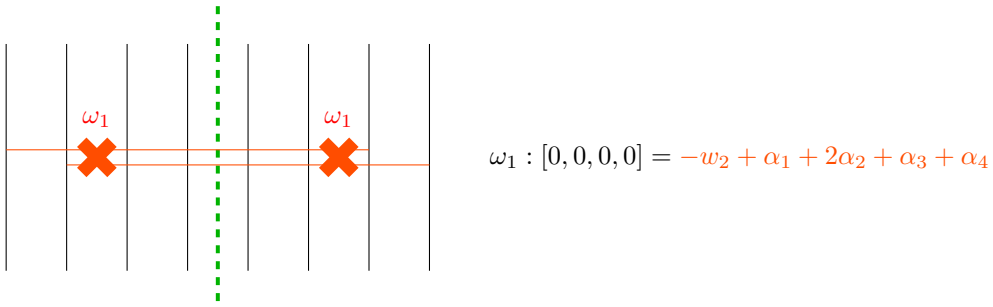

Figure 7.3: The zero weight $[0,0,0,0]$ of the D_4 algebra is the simplest example of how one constructs an unpolarized defect of the little string; on the left is pictured the type IIB brane engineering of the weight. NS5 branes are vertical black lines, D5 branes are red crosses, and D3 branes are horizontal red lines. The green dotted line produces a $\mathbb{Z}_2$-orbifold of an A_7 theory, realizing the D_4 theory. The resulting defect will be unpolarized because $[0,0,0,0]$ belongs in the $[0,1,0,0]$ representation, but is not in the Weyl group orbit of that weight.

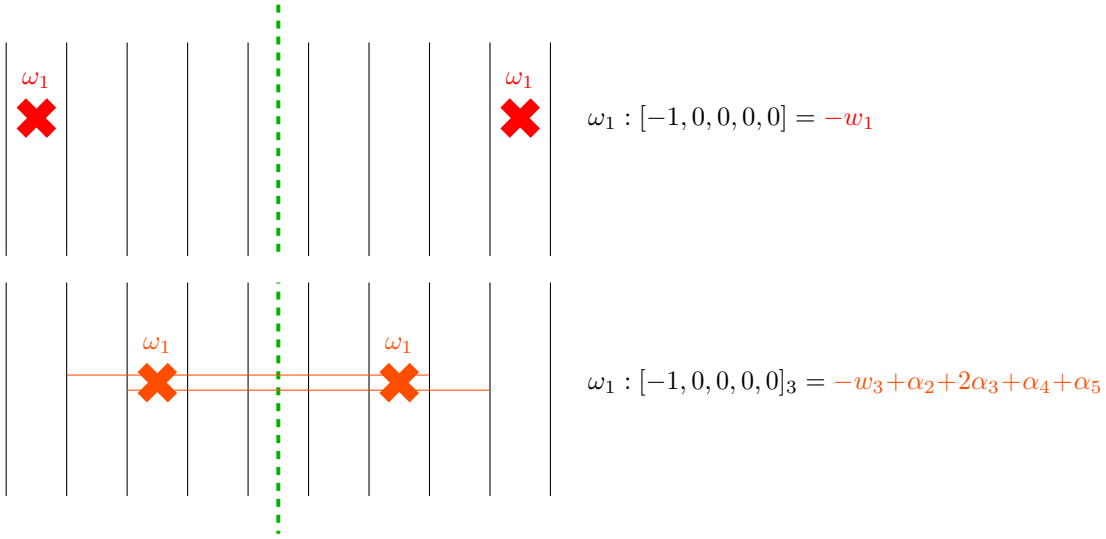

Figure 7.4: The weight $[-1,0,0,0,0]$ of D_5, with the corresponding type IIB brane engineering on the left, obtained from $\mathbb{Z}_2$-orbifolding of a A_9 theory. The weight $[-1,0,0,0,0]$ can be written in two ways. First, by placing a D5 brane between the two leftmost NS5 branes (top), the weight is written appropriately to characterize a polarized defect. This is so because $[-1,0,0,0,0]$ not only belongs in the $[1,0,0,0,0]$ representation, it is also in the Weyl group orbit of that weight. By placing the D5 brane between a different set of NS5 branes (bottom), we will obtain instead an unpolarized defect. This is so because $[-1,0,0,0,0]$ belongs in the $[0,0,1,0,0]$ representation, but is not in the Weyl group orbit of that weight. An additional subscript is added to the weight in this case, denoting (minus) the representation it belongs in.

Note that if we start with an unpolarized theory, it is always possible to move on the Higgs branch and end up with a theory that is polarized. This resulting polarized theory is of course highly specialized, since some masses have to be set equal to each other as a result. An illustration of how one can start with an unpolarized theory and arrive at a polarized theory is shown in Figure 7.5 below.

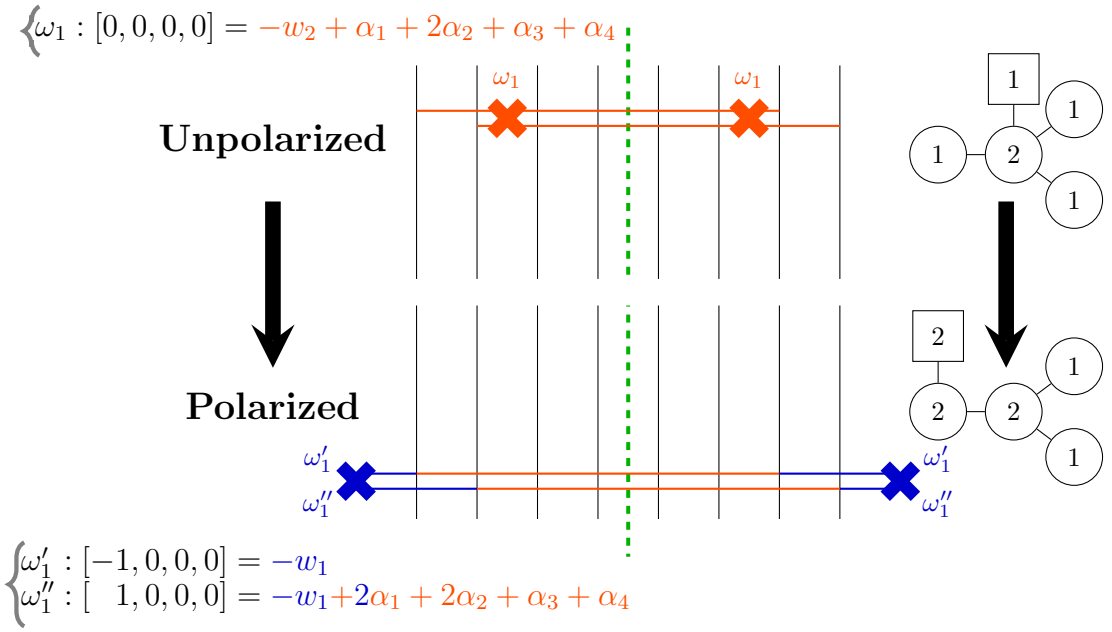

Figure 7.5: The brane picture for the null weight of D_4 (top of the figure), which makes up an unpolarized theory at low energies. It is obtained after $\mathbb{Z}_2$-orbifolding of A_7. The D5 branes sit on top of the D3 branes, and all the D3 branes are stacked together. After a Hannany–Witten transition, we end up with a polarized theory, but with the two masses equal to each other.

7.4 6d $(1,0)$ SCFTs

Consider once again type IIB string theory on the background $X \times \mathcal{C} \times \mathbb{R}^{1,3}$, where X is a resolution of the orbifold $\mathbb{C}^2/\Gamma$. This time, we choose the Riemann surface $\mathcal{C}$ to be the torus T^2. Introduce a collection of D7 branes in the string background, which further breaks suspersymmetry by half. The branes wrap a given set of compact and non-compact two-cycles of X, as well as $T^2 \times \mathbb{R}^{1,3}$ (equivalently, by T-duality in both directions of the T^2, this is a theory of D5 branes that are points on the torus, the exact setup of this thesis). The worldvolume of the 7-branes supports a six-dimensional supersymmetric gauge theory on the torus at low energies, with 8 supercharges, that is to say a 6d $(1,0)$ theory. A novelty here is

that taking the double limit $g_s \to 0$ and $m_s \to 0$, one obtains a SCFT that has a Lagrangian description as a quiver gauge theory. This is because the inverse gauge couplings on the D7 branes

$$\tau_{a,D7} = \int\limits_{S_a \times T^2} \frac{m_s^4}{g_s} \cdot \omega_{\rm vol}.$$

remain finite in the $m_s \to 0$ limit. This is in contrast to the D5 brane case, where no Lagrangian was available after taking the limit (recall indeed that $\tau_{a,D7}$ scales like $m_s^2\, \tau_{a,D5}$). We conjecture that the quiver gauge theories one obtains at low energies are intimately related to the ones we have been considering in this thesis, but this statement would need to be analyzed carefully.

Very recently, there has been a renewed interest in the study of 6d superconformal field theories with minimal supersymmetry, that is 6d $\mathcal{N} = (1,0)$ SCFTs. A classification of these theories has been proposed, based on F-theory techniques [122, 123, 124] or anomaly cancellation arguments in gauge theories [125]. Most notably, the SCFTs arise as an elliptically fibered Calabi-Yau threefold ($X \to B$) over a (non-compact) complex two-dimensional base B. The self-intersection of a curve gives the minimal gauge symmetry supported over that curve. For instance, when $\mathfrak{g} = A_n$, one first constructs the 6d SCFT theory whose tensor branch is:

$$[SU(n)] \overset{\mathfrak{su}_n}{2} \overset{\mathfrak{su}_n}{2} \ \ldots \ \overset{\mathfrak{su}_n}{2} \overset{\mathfrak{su}_n}{2} [SU(n)] \tag{7.4.1}$$

where the label 2 stands for an $O(-2)$ curve on the base of the elliptic fibration. The number of these compact curves is taken here to be arbitrarily large. There is an $SU(n)$ flavor symmetry on the left and on the right, with support on a non-compact curve.

For a given n, one can consider the RG flow for this theory, by breaking the flavor symmetry at the ends of the quiver, to obtain new conformal theories. More precisely, it can be shown that the flows are induced by nilpotent orbits; these are encoded in the tails of the quiver, denoted respectively by an orbit μ_L on the left and the orbit μ_R on the right. In the above example, both μ_R and μ_L are are the maximal nilpotent orbit of A_{n-1}, which stands for a flavor symmetry $SU(n)$ at the two ends of the quiver. A systematic analysis of these nilpotent flows was carried out for all simple algebras in [126].

When $\mathfrak{g} = A_n$, the theories obtained by RG flows are precisely the quiver gauge theories constructed in this thesis (uplifted to 6d). This is no longer the case for other algebras, but the nilpotent orbit structure of the flow remains, and it would be important to make the connection to our work precise[2].

[2]A related construction is realized using M-theory on the background $\mathbb{C}^2/\Gamma_G \times S^1_{\|} \times S^1_{\perp} \times \mathbb{R}^{4,1}$, with N M5 branes sitting at the singular point of the orbifold and at a point on $S^1_{\perp}$ while wrapping $S^1_{\|} \times \mathbb{R}^{4,1}$. Then, a reduction along $S^1_{\|}$ followed by a T-duality along $S^1_{\perp}$ brings us to a type IIB setup of D5 branes wrapping $\mathbb{R}^{4,1} \times \hat{S}^1_{\|}$. In perturbative type IIB terms, this should correspond to a fractional D5 brane realization of the 6d theories on a circle.

Chapter 8

Examples

We will now illustrate the various results of the thesis, for $\mathfrak{g}$ a simple Lie algebra.

8.1 The $\mathfrak{g}$-Type Full Puncture

We start by showcasing the Triality of Section 3.4, for a Riemann surface $\mathcal{C}$ which is the cylinder, with a full puncture on it [4]. In what follows, $n \equiv \text{rank}\,(\mathfrak{g})$.

In order to construct a single full puncture defect out of D5 branes, we pick a set $\mathcal{W}_{\mathcal{S}}$ of $n+1$ coweight vectors adding up to 0, such that the Bala-Carter label for this set is $\varnothing$. Such a defect is always polarized, in the terminology of Section 2.4. Out of the many sets of coweights that a priori satisfy this condition, we will present a set $\mathcal{W}_{\mathcal{S}}$ such that the resulting Coulomb branch of the defect is the smallest one possible.

The 5d gauge theory T^{5d} on the D5 branes, the 3d gauge theory G^{3d} on the D3 branes, and the collection of vertex operators in q-deformed Toda, are related by triality. We will see explicitly that the partition function of T^{5d} truncates to a 3-point function in the q-deformed Toda theory, with 3 primary operator insertions of generic momenta.

For each ω_i, we pick a point on the Riemann surface $\mathcal{C}$, with coordinate $x_i = R\,\beta_i$. This x_i specifies the position of the D5 brane wrapping $\omega_i = [S_i^*]$ on $\mathcal{C}$, and the masses β_i of the various matter fields in the 5d and 3d gauge theories. In the Toda theory, these parameters specify the n momenta and the position of the puncture on $\mathcal{C}$. With only 3 punctures present, we are in fact free to set this position at $z = 1$. The n 5d gauge couplings τ_a become the 3d FI parameters, or equivalently the momentum of the puncture at $z = 0$ in the Toda picture[1].

With only three punctures, no physical quantity will depend on the coordinate z itself, so we can set it to 1. The vertex operator $:\prod V_{\omega_i}(x):$ is the q-deformation of the primary operator $V_{\beta_i}(z)$. The R-charges of the 3d chiral multiplets determine all $v_a = \sqrt{q^{r_a}/t}$ factors in

[1]The n non-normalizable Coulomb moduli coming from the $U(1)$ centers in the gauge groups of T^{5d} become the ranks N_a of the 3d gauge groups of G^{3d}, which is also the number of screening charges in Toda theory; this specifies the momentum of the puncture located at $z = \infty$.

the argument of the vertex operators. These multiplets are generated from strings stretching between a D3 brane and a D5 brane wrapping S_i^*.

In the undeformed Toda CFT, the three-point of $\mathcal{W}$-algebra primaries is labeled by three momenta β_0, β, β_∞:

$$\langle V_{\beta_0}(0) V_\beta(1) V_{\beta_\infty}(\infty) \rangle \ . \tag{8.1.1}$$

If $\beta_\infty = -\beta_0 - \beta - \sum_{a=1}^n N_a \, \alpha_a^\vee / b$ for positive integers N_a (which are the ranks of the gauge groups of) we can compute the three-point function (8.1.1) in free field formalism: we simply insert N_a screening charge operators $Q_a^\vee = \int dx \, S_a^\vee(x)$:

$$\langle V^\vee_{\beta_0}(0) V^\vee_\beta(1) V^\vee_{\beta_\infty}(\infty) \prod_{a=1}^n (Q_a^\vee)^{N_a} \rangle_{free}. \tag{8.1.2}$$

Once we replace the screening charges and the vertex operators by their q-deformed counterparts, we obtain the q-deformed 3-point conformal block of the $\mathcal{W}_{q,t}(\mathfrak{g})$ algebra, as described in Section 3.3.

For definiteness, we will use the following definitions of the Cartan matrices in the examples:

$$C_{ab}^{B_n} = \begin{pmatrix} 2 & -1 & 0 & 0 & \dots & 0 \\ -1 & 2 & -1 & 0 & \dots & 0 \\ \vdots & \vdots & \vdots & \vdots & \vdots & \ddots \\ 0 & \dots & -1 & 2 & -1 & 0 \\ 0 & \dots & 0 & -1 & 2 & -2 \\ 0 & \dots & 0 & 0 & -1 & 2 \end{pmatrix} \qquad C_{ab}^{C_n} = \begin{pmatrix} 2 & -1 & 0 & 0 & \dots & 0 \\ -1 & 2 & -1 & 0 & \dots & 0 \\ \vdots & \vdots & \vdots & \vdots & \vdots & \ddots \\ 0 & \dots & -1 & 2 & -1 & 0 \\ 0 & \dots & 0 & -1 & 2 & -1 \\ 0 & \dots & 0 & 0 & -2 & 2 \end{pmatrix}$$

$$C_{ab}^{G_2} = \begin{pmatrix} 2 & -1 \\ -3 & 2 \end{pmatrix} \qquad C_{ab}^{F_4} = \begin{pmatrix} 2 & -1 & 0 & 0 \\ -1 & 2 & -2 & 0 \\ 0 & -1 & 2 & -1 \\ 0 & 0 & -1 & 2 \end{pmatrix}$$

When $\mathfrak{g}$ is simply-laced, we will use the words weights (respectively roots) and coweights (respectively coroots) interchangeably.

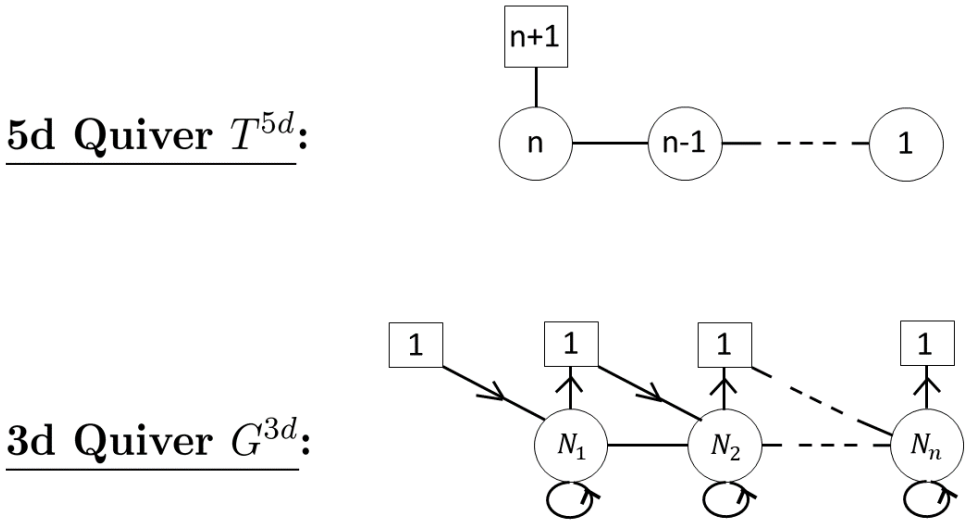

Figure 8.1: Cylinder with a full A_n puncture: 5d theory T^{5d} and 3d theory G^{3d} resulting from $\mathcal{W}_{\mathcal{S}}$.

A_n Full Puncture

For $\mathfrak{g} = A_n$, a full puncture is realized by the following set $\mathcal{W}_{\mathcal{S}}$ of $n+1$ coweights:

$$\begin{aligned}
&\omega_1 = -w_1^\vee \\
&\omega_2 = -w_1^\vee + \alpha_1^\vee \\
&\vdots \\
&\omega_n = -w_1^\vee + \alpha_1^\vee + \ldots + \alpha_{n-1}^\vee \\
&\omega_{n+1} = -w_1^\vee + \alpha_1^\vee + \ldots + \alpha_{n-1}^\vee + \alpha_n^\vee
\end{aligned} \tag{8.1.3}$$

$w_a^\vee$ is the a-th fundamental coweight, and $\alpha_a^\vee$ is the a-th coroot. Note that the set $\mathcal{W}_{\mathcal{S}}$ spans the coweight lattice. Each one of the coweights ω_a represents a distinct D5 brane wrapping a non-compact 2-cycle and some compact 2-cycles. At low energies, one can directly read off the 5d $\mathcal{N} = 1$ A_n quiver gauge theory living on the branes: the coefficients of the $\alpha_a^\vee$ give the rank of the gauge group, while the number of hypermultiplets in the fundamental representation of the a-th node is given by the number of $-w_a$. The resulting 5d quiver gauge theory is shown in figure 8.1.

We add D3 branes wrapping compact two-cycles in the homology class. The strings that stretch between D3 branes realize a 3d $\mathcal{N} = 4$ A_n quiver gauge theory, with gauge content $\prod_{a=1}^n U(N_a)$. Supersymmetry is broken to $\mathcal{N} = 2$ due to the strings stretching between the D3

and D5 branes, resulting in chiral and anti-chiral multiplets in fundamental representation of the various gauge groups. The Dynkin labels of the coweights (8.1.3) written in fundamental coweight basis encode the precise matter content of the 3d theory:

$$\begin{aligned}
\omega_1 &= [-1, \quad 0, \quad 0, \ldots, \quad 0, \quad 0] \\
\omega_2 &= [\quad 1, -1, \quad 0, \ldots, \quad 0, \quad 0] \\
&\vdots \\
\omega_n &= [\quad 0, \quad 0, \quad 0, \ldots, \quad 1, -1] \\
\omega_{n+1} &= [\quad 0, \quad 0, \quad 0, \ldots, \quad 0, \quad 1]
\end{aligned} \tag{8.1.4}$$

We obtain a 3d $\mathcal{N} = 2$ quiver gauge theory G^{3d} shown in figure 8.1. Note in passing that the set $\mathcal{W}_{\mathcal{S}}$ has no common zeros in the above notation. Acting on this set with the Weyl group will not change that, so the set is distinguished and the defect is indeed a full puncture.

The q-deformed vertex operator that realizes the full puncture is the product $: \prod_{i=1}^{n+1} V_{\omega_i}(x_i) :$, where

$$\begin{aligned}
&V_{\omega_1}(x) = W_1^{-1}(x), \\
&V_{\omega_2}(x) =: W_1^{-1}(x) E_1(xv^{-1}) : \\
&\vdots \\
&V_{\omega_n}(x) =: W_1^{-1}(x) E_1(xv^{-1}) E_2(xv^{-2}) \ldots E_{n-1}(xv^{1-n}) : \\
&V_{\omega_{n+1}}(x) =: W_1^{-1}(x) E_1(xv^{-1}) E_2(xv^{-2}) \ldots E_{n-1}(xv^{1-n}) E_n(xv^{-n}) :
\end{aligned} \tag{8.1.5}$$

The above "fundamental coweight" and "simple coroot" vertex operators were defined in section 3.3; the expression is a refinement of the relation (8.1.3). The dependence on the v factors above encodes the value of the Coulomb moduli at the triality point. Namely, let $v^{\#_{a,i}}$ be the various v factors appearing in (8.1.5). Then, the Coulomb moduli of the 5d gauge theory that truncate the partition function to the A_n q-deformed conformal block are given by

$$e_{a,i} = f_i \, t^{N_{a,i}} \, v^{\#_{a,i}} \, v^{-a} \,, \qquad a = 1, \ldots, n.$$

The Coulomb branch of the 5d theory has complex dimension $\sum_{a=1}^{n} d_a = n(n+1)/2$, with d_a the ranks of the n gauge groups. This can also be obtained from (2.4.17):

$$\sum_{\langle e_\gamma, \omega_i \rangle < 0} |\langle e_\gamma, \omega_i \rangle| = \frac{n(n+1)}{2}$$

In the above sum, one counts all positive roots that have a negative inner product with at least one of the coweights, with multiplicity. Here, all positive roots of A_n satisfy this condition, with multiplicity 1, so the right-hand side is simply the number of positive roots of A_n. This is also the number of supersymmetric vacua (or equivalently, integration contours) of the 3d theory, and the number of parameters needed to specify the 3-point of the q-deformed $\mathcal{W}_{q,t}(A_n)$ algebra.

In the CFT limit, when $m_s \to \infty$, the counting is done without multiplicity, but since each positive roots is counted once in the little string, the Coulomb branch dimension does not change. The Coulomb branch of the resulting theory T^{4d} is the maximal nilpotent orbit of A_n, with Bala-Carter label A_n. This orbit is in the image by the Spaltenstein map of the orbit denoted by $\varnothing$. This pre-image Bala–Carter label $\varnothing$ is identified at once since the set $\mathcal{W}_{\mathcal{S}}$ has no common zeros in the Dynkin labels of the different coweights, as we pointed out.

For completeness, we will also explicitly write the parabolic subalgebras in a given representation; for A_n, it is customary to do so in the fundamental representation. Therefore, the matrices will be valued in $\mathfrak{sl}(n+1)$; a star $*_i$ denotes a nonzero complex number, and the label "i" stands for the positive root e_i. A star $*_{-i}$ denotes a nonzero complex number, and the label "$-i$" stands for the negative root $-e_i$. The parabolic subalgebra is $\mathfrak{p}_\varnothing$. It is denoted by the partition $[1^{n+1}]$, which is immediately readable from the Levi subalgebra with symmetry $S(U(1)^{n+1})$.

The Levi decomposition gives:

$$\mathfrak{p}_\varnothing = \begin{pmatrix} * & *_1 & *_{1+2} & \cdots & *_{1+\ldots+(n-1)} & *_{1+\ldots+n} \\ 0 & * & *_2 & \cdots & \cdots & *_{2+\ldots+n} \\ \vdots & \ddots & \ddots & \ddots & \vdots & \vdots \\ \vdots & & \ddots & \ddots & *_{(n-1)} & *_{(n-1)+n} \\ \vdots & & & \ddots & * & *_n \\ 0 & \cdots & \cdots & \cdots & 0 & * \end{pmatrix},$$

with $\mathfrak{p}_\varnothing = \mathfrak{l}_\varnothing \oplus \mathfrak{n}_\varnothing$, where

$$\mathfrak{l}_\varnothing = \begin{pmatrix} * & 0 & \cdots & \cdots & \cdots & 0 \\ 0 & * & \ddots & & & \vdots \\ \vdots & \ddots & \ddots & \ddots & & \vdots \\ \vdots & & \ddots & \ddots & \ddots & \vdots \\ \vdots & & & \ddots & * & 0 \\ 0 & \cdots & \cdots & \cdots & 0 & * \end{pmatrix}$$

and

$$\mathfrak{n}_{\varnothing} = \begin{pmatrix} 0 & *_1 & *_{1+2} & \cdots & *_{1+\ldots+(n-1)} & *_{1+\ldots+n} \\ 0 & 0 & *_2 & \cdots & \cdots & *_{2+\ldots+n} \\ \vdots & \ddots & \ddots & \ddots & \vdots & \vdots \\ \vdots & & \ddots & \ddots & *_{(n-1)} & *_{(n-1)+n} \\ \vdots & & & \ddots & 0 & *_n \\ 0 & \cdots & \cdots & \cdots & 0 & 0 \end{pmatrix}.$$

We see explicitly that the nonzero inner products $\langle e_\gamma, \omega_i \rangle$ make up the i-th line of the nilradical $\mathfrak{n}_{\varnothing}$.

Now, from the Toda CFT perspective, we start from our set $\mathcal{W}_{\mathcal{S}}$ and recall that $\beta = \sum_{i=1}^{|\mathcal{W}_{\mathcal{S}}|} \beta_i w_i$, $\mathcal{W}_{\mathcal{S}}$ defines the Toda momentum vector β. We can write this momentum β explicitly as the semi-simple element $\mathrm{diag}(\beta_1, \beta_2, \ldots, \beta_{n+1})$, where all the entries add up to 0. One checks at once that the commutant of this element is the Levi subalgebra $\mathfrak{l}_{\varnothing}$ written above.

D_n Full Puncture

We will be more brief for the rest of the simply-laced cases. For $\mathcal{W}_{\mathcal{S}}$, we take the following collection of $n+1$ weights of D_n:

$$\begin{aligned} &\omega_1 = -w_1^\vee + \alpha_1^\vee + \alpha_2^\vee + \ldots + \alpha_{n-2}^\vee + \alpha_{n-1}^\vee + \alpha_n^\vee \\ &\omega_i = \omega_{i-1} + \alpha_{n-i}^\vee \,, \qquad i = 2, \ldots n-1 \\ &\omega_n = -w_{n-1}^\vee \\ &\omega_{n+1} = -w_n^\vee \end{aligned} \tag{8.1.6}$$

Writing each coweight above in terms of fundamental coweights, it is clear that $\mathcal{W}_{\mathcal{S}}$ has no common zeros, and acting on $\mathcal{W}_{\mathcal{S}}$ with the Weyl group will not change that, so the set is distinguished and this is indeed a full puncture.

The complex dimension of the Coulomb branch of T^{5d} (or the number of vacua of G^{3d}) is

$$\sum_{a=1}^{n} d_a = \frac{(n-1)(3n-2)}{2} = \sum_{\langle e_\gamma, \omega_i \rangle < 0} |\langle e_\gamma, \omega_i \rangle| \,.$$

In the above sum, one counts all positive roots that have a negative inner product with at least one of the coweights. Here, some of the positive roots of D_n satisfy this condition with multiplicity 1, while others satisfy it with multiplicity 2, so the answer is necessarily bigger than the number of positive roots of D_n. This is also the number of supersymmetric vacua

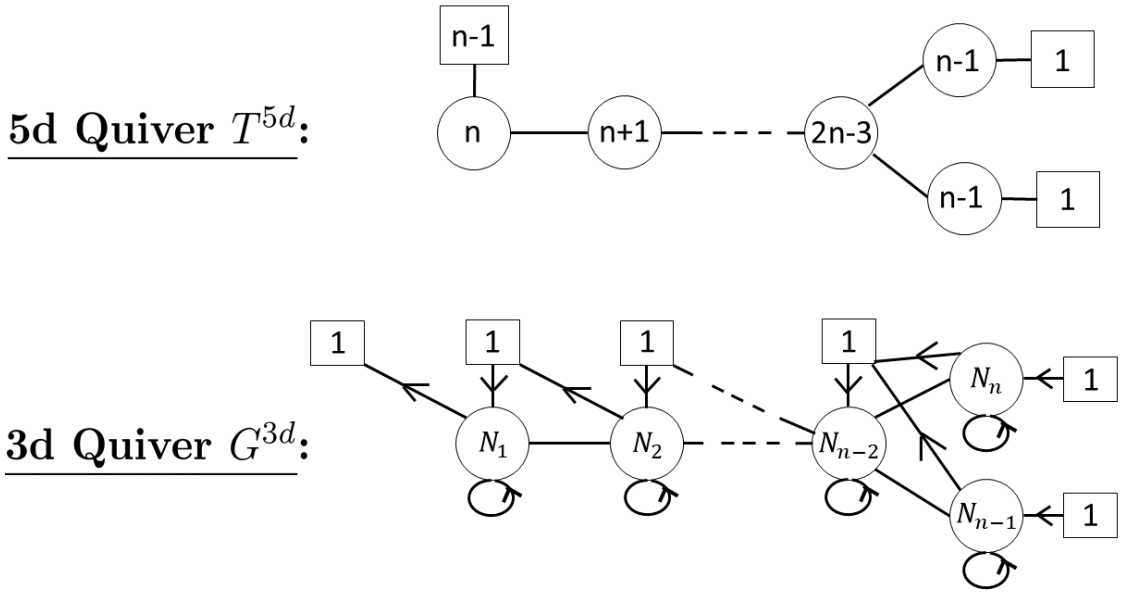

Figure 8.2: Cylinder with a full D_n puncture: 5d theory T^{5d} and 3d theory G^{3d} resulting from $\mathcal{W}_{\mathcal{S}}$.

(or equivalently, integration contours) of the 3d theory, and the number of parameters needed to specify the 3-point of the q-deformed $\mathcal{W}_{q,t}(D_n)$ algebra.

In the CFT limit, when $m_s \to \infty$, the counting is done without counting the multiplicity 2 of some of the positive roots; the Coulomb branch dimension of the D5 brane theory therefore decreases and becomes equal to the number of positive roots of D_n, which is $n^2 - n$. The Coulomb branch of the resulting theory T^{4d} is therefore the maximal nilpotent orbit of D_n. The 5d and 3d theories are shown in figure 8.2.

E_n Full Puncture

In the case of E_6, we take the set $\mathcal{W}_{\mathcal{S}}$ to be the following collection of 7 coweights:

$$\begin{aligned}
\omega_1 &= -w_5^\vee \\
\omega_2 &= -w_5^\vee + \alpha_5^\vee \\
\omega_3 &= -w_5^\vee + \alpha_1^\vee + 2\alpha_2^\vee + 3\alpha_3^\vee + 3\alpha_4^\vee + 2\alpha_5^\vee + 2\alpha_6^\vee \\
\omega_4 &= -w_5^\vee + \alpha_1^\vee + 2\alpha_2^\vee + 4\alpha_3^\vee + 3\alpha_4^\vee + 2\alpha_5^\vee + 2\alpha_6^\vee \\
\omega_5 &= -w_5^\vee + \alpha_1^\vee + 3\alpha_2^\vee + 4\alpha_3^\vee + 3\alpha_4^\vee + 2\alpha_5^\vee + 2\alpha_6^\vee \\
\omega_6 &= -w_5^\vee + 2\alpha_1^\vee + 3\alpha_2^\vee + 4\alpha_3^\vee + 3\alpha_4^\vee + 2\alpha_5^\vee + 2\alpha_6^\vee \\
\omega_7 &= -w_6^\vee
\end{aligned} \tag{8.1.7}$$

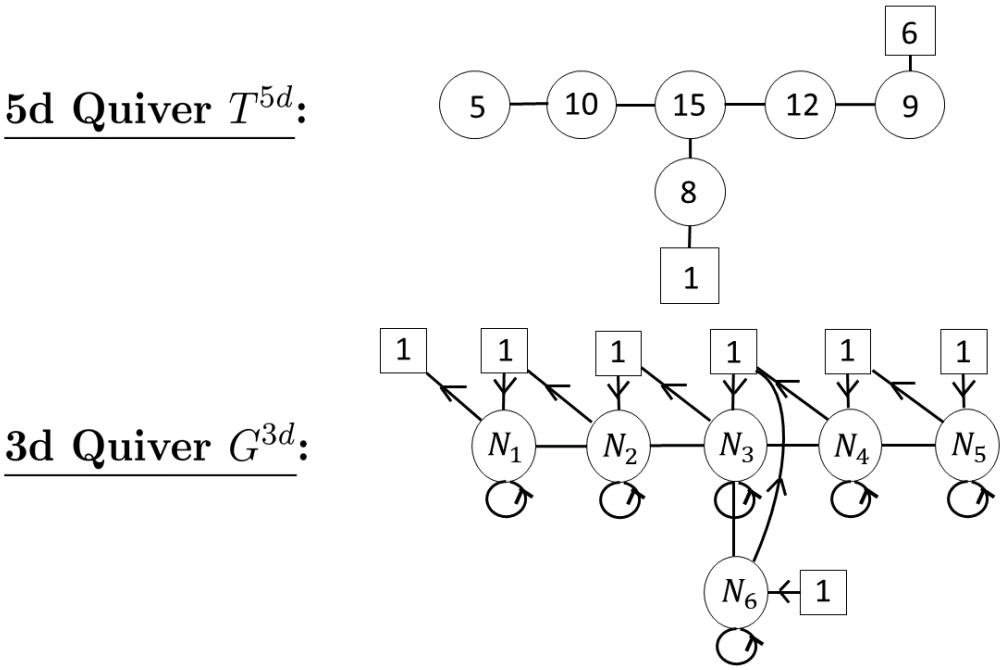

Figure 8.3: Cylinder with a full E_6 puncture: 5d theory T^{5d} and 3d theory G^{3d} resulting from $\mathcal{W}_{\mathcal{S}}$.

In the case of E_7, we take the set $\mathcal{W}_{\mathcal{S}}$ to be the following collection of 8 coweights:

$$\begin{aligned}
\omega_1 &= -w_1^\vee + 3\alpha_1^\vee + 5\alpha_2^\vee + 7\alpha_3^\vee + 6\alpha_4^\vee + 4\alpha_5^\vee + 2\alpha_6^\vee + 4\alpha_7^\vee \\
\omega_2 &= -w_1^\vee + 3\alpha_1^\vee + 5\alpha_2^\vee + 8\alpha_3^\vee + 6\alpha_4^\vee + 4\alpha_5^\vee + 2\alpha_6^\vee + 4\alpha_7^\vee \\
\omega_3 &= -w_1^\vee + 3\alpha_1^\vee + 6\alpha_2^\vee + 8\alpha_3^\vee + 6\alpha_4^\vee + 4\alpha_5^\vee + 2\alpha_6^\vee + 4\alpha_7^\vee \\
\omega_4 &= -w_1^\vee + 4\alpha_1^\vee + 6\alpha_2^\vee + 8\alpha_3^\vee + 6\alpha_4^\vee + 4\alpha_5^\vee + 2\alpha_6^\vee + 4\alpha_7^\vee \\
\omega_5 &= -w_6^\vee \\
\omega_6 &= -w_6^\vee + \alpha_6^\vee \\
\omega_7 &= -w_6^\vee + \alpha_5^\vee + \alpha_6^\vee \\
\omega_8 &= -w_7^\vee
\end{aligned} \tag{8.1.8}$$

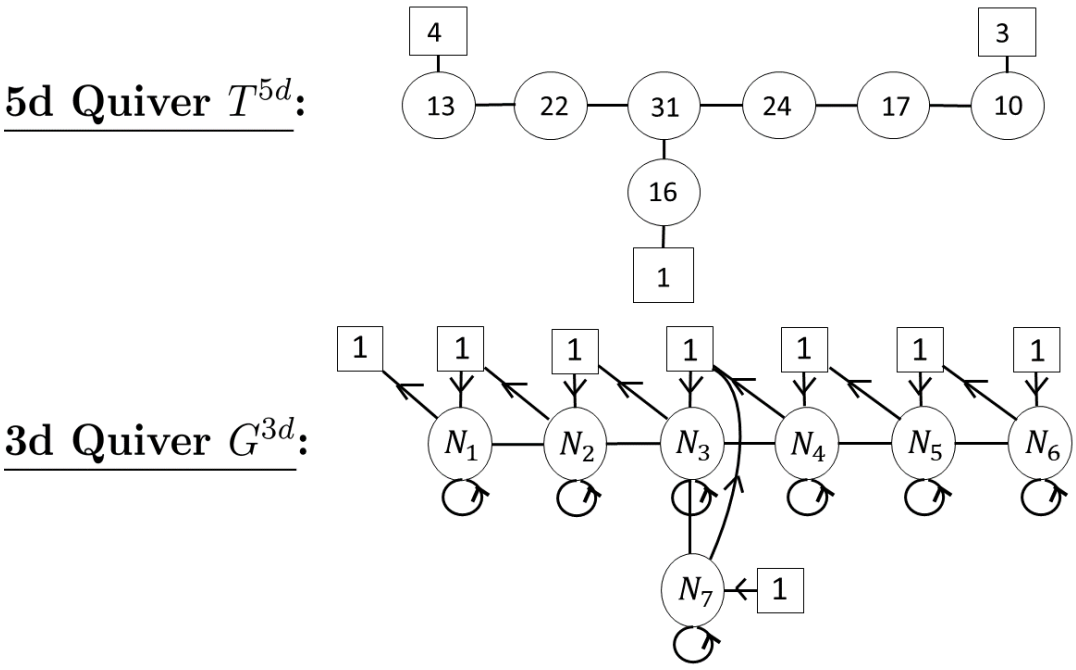

Figure 8.4: Cylinder with a full E_7 puncture: 5d theory T^{5d} and 3d theory G^{3d} resulting from $\mathcal{W}_{\mathcal{S}}$.

In the case of E_8, we take the set $\mathcal{W}_{\mathcal{S}}$ to be the following collection of 9 coweights:

$$\begin{aligned}
\omega_1 &= -w_1^\vee + 7\alpha_1^\vee + 13\alpha_2^\vee + 19\alpha_3^\vee + 16\alpha_4^\vee + 12\alpha_5^\vee + 8\alpha_6^\vee + 4\alpha_7^\vee + 10\alpha_8^\vee \\
\omega_2 &= -w_1^\vee + 7\alpha_1^\vee + 13\alpha_2^\vee + 20\alpha_3^\vee + 16\alpha_4^\vee + 12\alpha_5^\vee + 8\alpha_6^\vee + 4\alpha_7^\vee + 10\alpha_8^\vee \\
\omega_3 &= -w_1^\vee + 7\alpha_1^\vee + 14\alpha_2^\vee + 20\alpha_3^\vee + 16\alpha_4^\vee + 12\alpha_5^\vee + 8\alpha_6^\vee + 4\alpha_7^\vee + 10\alpha_8^\vee \\
\omega_4 &= -w_1^\vee + 8\alpha_1^\vee + 14\alpha_2^\vee + 20\alpha_3^\vee + 16\alpha_4^\vee + 12\alpha_5^\vee + 8\alpha_6^\vee + 4\alpha_7^\vee + 10\alpha_8^\vee \\
\omega_5 &= -w_7^\vee \\
\omega_6 &= -w_7^\vee + \alpha_7^\vee \\
\omega_7 &= -w_7^\vee + \alpha_6^\vee + \alpha_7^\vee \\
\omega_8 &= -w_7^\vee + \alpha_5^\vee + \alpha_6^\vee + \alpha_7^\vee \\
\omega_9 &= -w_8^\vee
\end{aligned} \tag{8.1.9}$$

Once again, one can check that these sets are distinguished and have no common zeros in their Dynkin labels, so these are indeed full punctures of E_n.

The complex dimension of the Coulomb branch of T^{5d} is

$$\sum_{a=1}^{n} d_a = \sum_{\langle e_\gamma, \omega_i \rangle < 0} |\langle e_\gamma, \omega_i \rangle| \ .$$

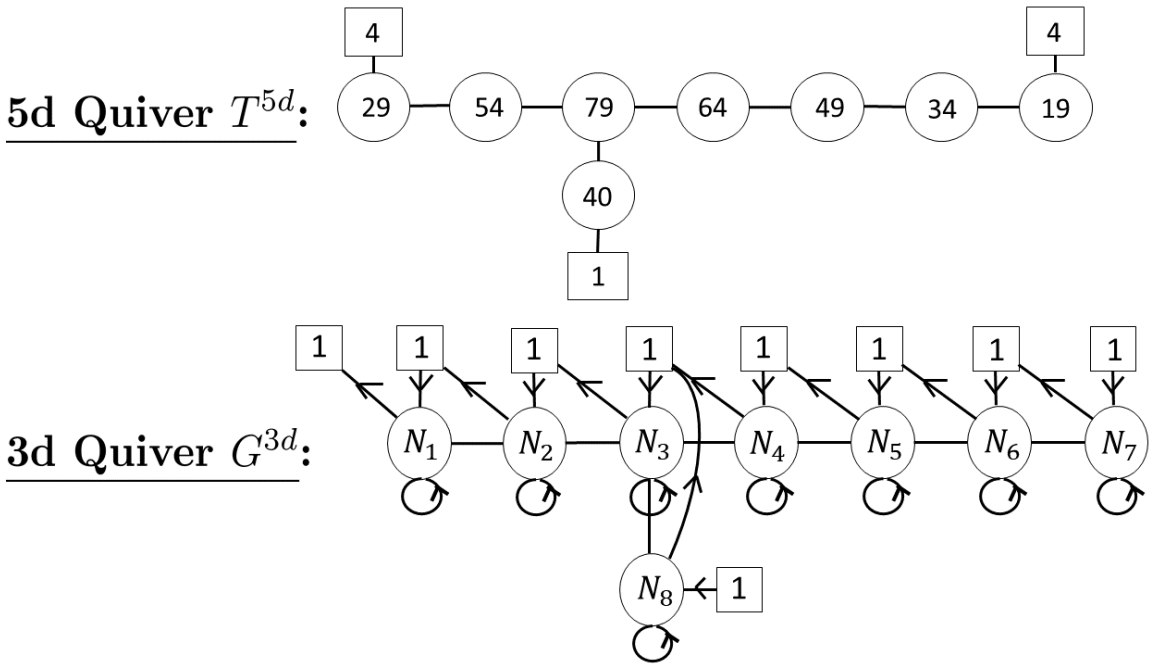

Figure 8.5: Cylinder with a full E_8 puncture: 5d theory T^{5d} and 3d theory G^{3d} resulting from $\mathcal{W}_{\mathcal{S}}$.

For E_6, we the find (using either sum) that the Coulomb branch dimension is 59. For E_7, we find that the Coulomb branch dimension is 63. For E_8, we find that the Coulomb branch dimension is 368.

In the CFT limit, when $m_s \to \infty$, the counting is done without counting the multiplicity in the sum on the right-hand side; the Coulomb branch dimension therefore decreases and becomes equal to the number of positive roots of E_n; for E_6, this is 36. For E_7, this is 63. For E_8, this is 120. The Coulomb branch of the resulting theory T^{4d} is the maximal nilpotent orbit of E_n. The 5d and 3d theories are shown in figures 8.3, 8.4, and 8.5.

G_2 Full Puncture

For G_2, we take the set $\mathcal{W}_{\mathcal{S}}$ to be the following collection of 3 coweights:

$$\begin{aligned} \omega_1 &= -w_1^\vee + 4\alpha_1^\vee + 6\alpha_2^\vee \\ \omega_2 &= -w_2^\vee + \alpha_2^\vee \\ \omega_3 &= -w_2^\vee \end{aligned} \tag{8.1.10}$$

The Dynkin labels of the coweights (8.1.10) expanded in terms of fundamental coweights

5d Quiver T^{5d}:

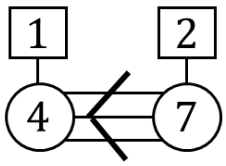

3d Quiver G^{3d}:

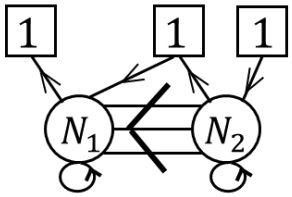

Figure 8.6: Cylinder with a full G_2 puncture: 5d theory T^{5d} and 3d theory G^{3d} resulting from $\mathcal{W}_{\mathcal{S}}$.

encode the precise matter content of the 3d theory:

$$\begin{aligned} \omega_1 &= [\ \ 1, \ \ 0] \\ \omega_2 &= [-1, \ \ 1] \\ \omega_3 &= [\ \ 0, -1] \end{aligned} \tag{8.1.11}$$

We obtain the 3d $\mathcal{N}=2$ quiver gauge theory G^{3d} shown in figure 8.6. The q-deformed vertex operator that realizes the full puncture is the product $:\prod_{i=1}^{3} V_{\omega_i}(x_i):$, where

$$\begin{aligned} V_{\omega_1}(x) = :\, & W_1^{-1}(x) E_1(xv^{-1}) E_2(xv^{-2}q^{-1/2}) E_2(xv^{-2}q^{-3/2}) E_2(xv^{-2}q^{-5/2}) E_1(xv^{-3}q^{-1}) \\ & E_1(xv^{-3}q^{-2}) E_2(xv^{-4}q^{-3/2}) E_2(xv^{-4}q^{-5/2}) E_2(xv^{-4}q^{-7/2}) E_1(xv^{-5}q^{-3}) : \\ V_{\omega_2}(x) = :\, & W_2^{-1}(x) E_2(xq^{-1/2}) : \\ V_{\omega_3}(x) = :\, & W_2^{-1}(x) : \end{aligned} \tag{8.1.12}$$

The above "fundamental coweight" and "simple coroot" vertex operators were defined in section 3.3; the expression is a refinement of the relation (8.1.10). The dependence on the v and q factors encodes the value of the Coulomb moduli at the triality point. Namely, let $v^{\#_{a,I}}\, q^{\#'_{a,I}}$ be the various v and q factors appearing in the E_a operators of (8.1.12). Then, the Coulomb moduli of the 5d gauge theory that truncate the partition function to the G_2

q-deformed conformal block are given by:

$$e_{a,I} = f_I \, t^{N_{a,I}} \, v^{\#_{a,I}} \, q^{\#'_{a,I}} \, v^{2-a} \, q^{(a-1)/2} \, , \qquad a = 1, 2 \, .$$

Recall that in our notation, $a = 1$ is gauge node designating the short root, while $a = 2$ designates the long root.

The Coulomb branch of the 5d theory has complex dimension:

$$\sum_{a=1}^{2} d_a = 11 = \sum_{\langle e_\gamma, \omega_i \rangle < 0} |\langle e_\gamma, \omega_i \rangle| \ ,$$

with d_a the ranks of the 2 gauge groups. In the right-hand sum, one counts all positive roots that have a negative inner product with at least one of the coweights. This is also the number of supersymmetric vacua (or equivalently, integration contours) of the 3d theory, and the number of parameters needed to specify the 3-point of the q-deformed $\mathcal{W}_{q,t}(G_2)$ algebra.

In the CFT limit, when $m_s \to \infty$, the counting is done without multiplicity. The Coulomb branch dimension therefore decreases and becomes equal to the number of positive roots of G_2, which is 6. The Coulomb branch of the resulting theory T^{4d} is the maximal nilpotent orbit of G_2, with Bala-Carter label G_2. Because the defect is polarized, its Coulomb branch must be in the image of the Spaltenstein map. In our case, the full puncture Coulomb branch is the image of the orbit denoted by $\varnothing$. This pre-image Bala–Carter label $\varnothing$ is identified at once by acting on $\mathcal{W}_{\mathcal{S}}$ with the Weyl group and noticing the set never has any common zeros in the Dynkin labels of the different coweights.

F_4 Full Puncture

For F_4, we take the set $\mathcal{W}_{\mathcal{S}}$ to be the following collection of 5 coweights:

$$\begin{aligned}
\omega_1 &= -w_4^\vee + 4\alpha_1^\vee + 8\alpha_2^\vee + 6\alpha_3^\vee + 4\alpha_4^\vee \\
\omega_2 &= -w_4^\vee + 4\alpha_1^\vee + 8\alpha_2^\vee + 6\alpha_3^\vee + 3\alpha_4^\vee \\
\omega_3 &= -w_1^\vee + \alpha_1^\vee + \alpha_2^\vee \\
\omega_4 &= -w_1^\vee + \alpha_1^\vee \\
\omega_5 &= -w_1^\vee
\end{aligned} \tag{8.1.13}$$

The Dynkin labels of the coweights 8.1.13 expanded in terms of fundamental coweights encode the precise matter content of the 3d theory:

$$\begin{aligned}
\omega_1 &= [\ \ 0, \ \ 0, \ \ 0, \ \ 1] \\
\omega_2 &= [\ \ 0, \ \ 0, \ \ 1, -1] \\
\omega_3 &= [\ \ 0, \ \ 1, -1, \ \ 0] \\
\omega_4 &= [\ \ 1, -1, \ \ 0, \ \ 0] \\
\omega_5 &= [-1, \ \ 0, \ \ 0, \ \ 0]
\end{aligned} \tag{8.1.14}$$

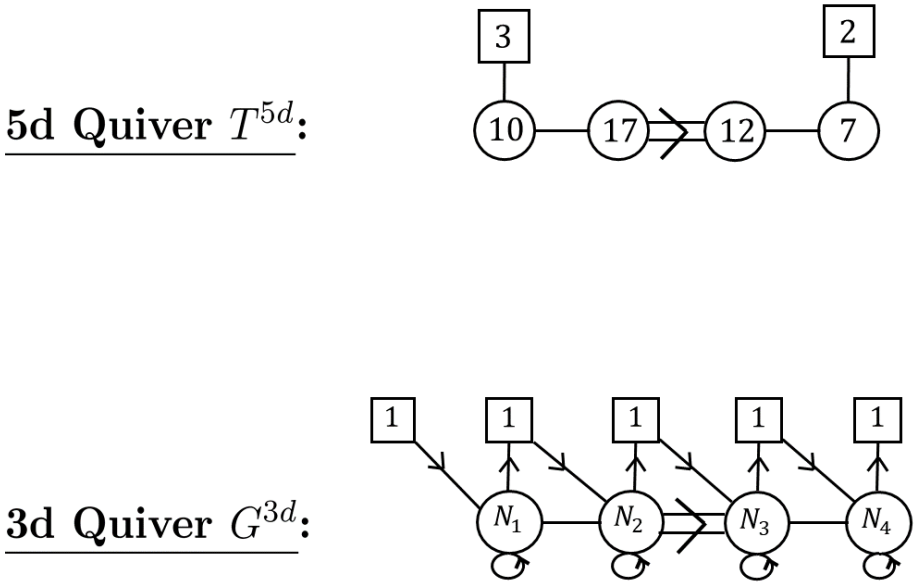

Figure 8.7: Cylinder with a full F_4 puncture: 5d theory T^{5d} and 3d theory G^{3d} resulting from $\mathcal{W}_{\mathcal{S}}$.

We obtain the quiver gauge theory G^{3d} shown in figure 8.7.

The q-deformed vertex operator that realizes the full puncture is the product $:\prod_{i=1}^{5} V_{\omega_i}(x_i):$, where

$$\begin{aligned}
V_{\omega_1}(x) =: & W_4^{-1}(x)E_4(xv^{-1})E_3(xv^{-2})E_2(xv^{-3}q^{-1/2})E_2(xv^{-3}q^{-3/2})E_1(xv^{-4}q^{-1}) \\
& E_3(xv^{-4}q^{-1})E_1(xv^{-4}q^{-2})E_4(xv^{-5}q^{-1})E_2(xv^{-5}q^{-3/2})E_2(xv^{-5}q^{-5/2})E_3(xv^{-6}q^{-1}) \\
& E_3(xv^{-6}q^{-2})E_2(xv^{-7}q^{-3/2})E_4(xv^{-7}q^{-2})E_2(xv^{-7}q^{-5/2})E_1(xv^{-8}q^{-2})E_1(xv^{-8}q^{-3}) \\
& E_3(xv^{-8}q^{-3})E_2(xv^{-9}q^{-5/2})E_2(xv^{-9}q^{-7/2})E_3(xv^{-10}q^{-3})E_4(xv^{-11}q^{-3}) : \\
V_{\omega_2}(x) =: & W_4^{-1}(x)E_4(xv^{-1})E_3(xv^{-2})E_2(xv^{-3}q^{-1/2})E_2(xv^{-3}q^{-3/2})E_1(xv^{-4}q^{-1}) \\
& E_3(xv^{-4}q^{-1})E_1(xv^{-4}q^{-2})E_4(xv^{-5}q^{-1})E_2(xv^{-5}q^{-3/2})E_2(xv^{-5}q^{-5/2})E_3(xv^{-6}q^{-1}) \\
& E_3(xv^{-6}q^{-2})E_2(xv^{-7}q^{-3/2})E_4(xv^{-7}q^{-2})E_2(xv^{-7}q^{-5/2})E_1(xv^{-8}q^{-2})E_1(xv^{-8}q^{-3}) \\
& E_3(xv^{-8}q^{-3})E_2(xv^{-9}q^{-5/2})E_2(xv^{-9}q^{-7/2})E_3(xv^{-10}q^{-3}) : \\
V_{\omega_3}(x) =: & W_1^{-1}(x)E_1(xv^{-4}q^{-1})E_2(xv^{-5}q^{-3/2}) : \\
V_{\omega_4}(x) =: & W_1^{-1}(x)E_1(xv^{-4}q^{-1}) : \\
V_{\omega_5}(x) =: & W_1^{-1}(x) :
\end{aligned} \tag{8.1.15}$$

The above expression is a refinement of the relation (8.1.13). The dependence on the v and q

factors encodes the value of the Coulomb moduli at the triality point. Namely, let $v^{\#_{a,I}}\, q^{\#'_{a,I}}$ be the various v and q factors appearing in the E_a operators of (8.1.15). Then, the Coulomb moduli of the 5d gauge theory that truncate the partition function to the F_4 q-deformed conformal block are given by:

$$\begin{aligned} e_{a,I} &= f_I\, t^{N_{a,I}}\, v^{\#_{a,I}}\, q^{\#'_{a,I}}\, v^{5-a}\, q^{(3-a)/2}\,, \qquad a = 1,2 \\ e_{a,I} &= f_I\, t^{N_{a,I}}\, v^{\#_{a,I}}\, q^{\#'_{a,I}}\, v^{5-a}\, q^{(3-a)/2}\,, \qquad a = 3,4 \end{aligned} \tag{8.1.16}$$

In our notation, $a = 1, 2$ designate the long roots, while $a = 3, 4$ designate the short roots.

The Coulomb branch of the 5d theory has complex dimension:

$$\sum_{a=1}^{4} d_a = 46 = \sum_{\langle e_\gamma, \omega_i\rangle < 0} |\langle e_\gamma, \omega_i\rangle|\ ,$$

with d_a the ranks of the 4 gauge groups. In the right-hand sum, one counts all positive roots that have a negative inner product with at least one of the coweights. This is also the number of supersymmetric vacua (or equivalently, integration contours) of the 3d theory, and the number of parameters needed to specify the 3-point of the q-deformed $\mathcal{W}_{q,t}(F_4)$ algebra.

In the CFT limit, when $m_s \to \infty$, the counting is done without multiplicity. The Coulomb branch dimension therefore decreases and becomes equal to the number of positive roots of F_4, which is 24. The Coulomb branch of the resulting theory T^{4d} is the maximal nilpotent orbit of F_4, with Bala–Carter label F_4. Because the defect is polarized, its Coulomb branch must be in the image of the Spaltenstein map. In our case, the full puncture Coulomb branch is the image of the orbit denoted by $\varnothing$. This pre-image Bala–Carter label $\varnothing$ is identified at once by acting on $\mathcal{W}_{\mathcal{S}}$ with the Weyl group and noticing the set never has any common zeros in the Dynkin labels of the different coweights.

B_n Full Puncture

For B_n, we take the set $\mathcal{W}_{\mathcal{S}}$ to be the following collection of $n+1$ coweights:

$$\begin{aligned} \omega_1 &= -w_1^\vee + \alpha_1^\vee + \alpha_2^\vee + \ldots + \alpha_{n-1}^\vee + \alpha_n^\vee \\ \omega_i &= \omega_{i-1} + \alpha_{n-i+1}^\vee\,, \qquad i = 2, \ldots n \\ \omega_{n+1} &= -w_n^\vee \end{aligned} \tag{8.1.17}$$

The Dynkin labels of the coweights (8.1.17) expanded in terms of fundamental coweights encode the precise matter content of the 3d theory:

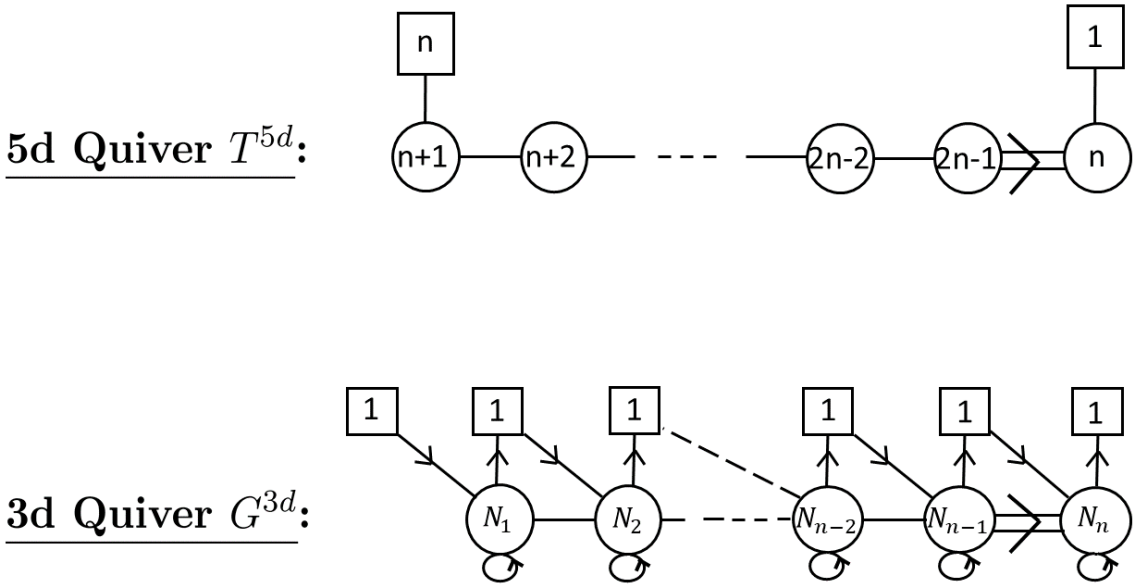

Figure 8.8: Cylinder with a full B_n puncture: 5d theory T^{5d} and 3d theory G^{3d} resulting from $\mathcal{W}_{\mathcal{S}}$.

$$\begin{aligned}
\omega_1 &= [\ 0,\ 0,\ 0,\dots,\ 0,-1,\ 1]\\
\omega_2 &= [\ 0,\ 0,\ 0,\dots,-1,\ 1,\ 0]\\
&\ \ \vdots\\
\omega_{n-2} &= [\ 0,-1,\ 1,\dots,\ 0,\ 0,\ 0]\\
\omega_{n-2} &= [\ 0,-1,\ 1,\dots,\ 0,\ 0,\ 0]\\
\omega_{n-1} &= [-1,\ 1,\ 0,\dots,\ 0,\ 0,\ 0]\\
\omega_{n+1} &= [\ 0,\ 0,\ 0,\dots,\ 0,\ 0,-1]
\end{aligned} \tag{8.1.18}$$

We obtain the quiver gauge theory G^{3d} shown in figure 8.8.

The q-deformed vertex operator that realizes the full puncture is the product $:\prod_{i=1}^{n+1} V_{\omega_i}(x_i):$, where

$$\begin{aligned}
V_{\omega_1}(x) &=: W_1^{-1}(x)E_1(xv^{-1}q^{-1/2})E_2(xv^{-2}q^{-1})\dots E_{n-1}(xv^{1-n}q^{(-n+1)/2})E_n(xv^{-n}q^{(-n+1)/2}):\\
V_{\omega_i}(x) &=: V_{\omega_{i-1}}(x)E_{n-i+1}(xv^{-n-i+1}q^{(-n-i+3)/2}): \qquad i=2,\dots,n\\
V_{\omega_{n+1}}(x) &=: W_n^{-1}(x):
\end{aligned} \tag{8.1.19}$$

The above expression is a refinement of the relation (8.1.17). The dependence on the v and q factors encodes the value of the Coulomb moduli at the triality point. Namely, let $v^{\#_{a,I}}\, q^{\#'_{a,I}}$

be the various v and q factors appearing in the E_a operators of (8.1.19). Then, the Coulomb moduli of the 5d gauge theory that truncate the partition function to the B_n q-deformed conformal block are given by:

$$\begin{aligned} e_{a,I} &= f_I\, t^{N_{a,I}}\, v^{\#_{a,I}}\, q^{\#'_{a,I}}\, v^{2-a}\, q^{(2-a)/2}\,, \qquad a = 1, \ldots, n-1 \\ e_{n,I} &= f_I\, t^{N_{n,I}}\, v^{\#_{n,I}}\, q^{\#'_{n,I}}\, v^{2-n}\, q^{(3-n)/2} \end{aligned} \tag{8.1.20}$$

In our notation, $a = 1, \ldots, n-1$ designate the long roots, while $a = n$ designates the short root.

The Coulomb branch of the 5d theory has complex dimension:

$$\sum_{a=1}^{n} d_a = \frac{n(3n-1)}{2} = \sum_{\langle e_\gamma, \omega_i \rangle < 0} |\langle e_\gamma, \omega_i \rangle| \ ,$$

with d_a the ranks of the n gauge groups. In the right-hand sum, one counts all positive roots that have a negative inner product with at least one of the coweights. This is also the number of supersymmetric vacua (or equivalently, integration contours) of the 3d theory, and the number of parameters needed to specify the 3-point of the q-deformed $\mathcal{W}_{q,t}(B_n)$ algebra.

In the CFT limit, when $m_s \to \infty$, the counting is done without multiplicity. The Coulomb branch dimension therefore decreases and becomes equal to the number of positive roots of B_n, which is n^2. The Coulomb branch of the resulting theory T^{4d} is the maximal nilpotent orbit of B_n, with Bala-Carter label B_n. Because the defect is polarized, its Coulomb branch must be in the image of the Spaltenstein map. In our case, the full puncture Coulomb branch is the image of the orbit denoted by $\varnothing$. This pre-image Bala–Carter label $\varnothing$ is identified at once by acting on $\mathcal{W}_{\mathcal{S}}$ with the Weyl group and noticing the set never has any common zeros in the Dynkin labels of the different coweights.

C_n Full Puncture

For C_n, we take the set $\mathcal{W}_{\mathcal{S}}$ to be the following collection of $n+1$ coweights:

$$\begin{aligned} \omega_1 &= -w_1^\vee + \alpha_1^\vee + \alpha_2^\vee + \ldots + \alpha_{n-2}^\vee + 2\alpha_{n-1}^\vee + 2\alpha_n^\vee \\ \omega_i &= \omega_{i-1} + \alpha_{n-i}^\vee\,, \qquad i = 2, \ldots n-1 \\ \omega_n &= -w_n^\vee + \alpha_n^\vee \\ \omega_{n+1} &= -w_n^\vee \end{aligned} \tag{8.1.21}$$

The Dynkin labels of the coweights (8.1.21) expanded in terms of fundamental coweights encode the precise matter content of the 3d theory:

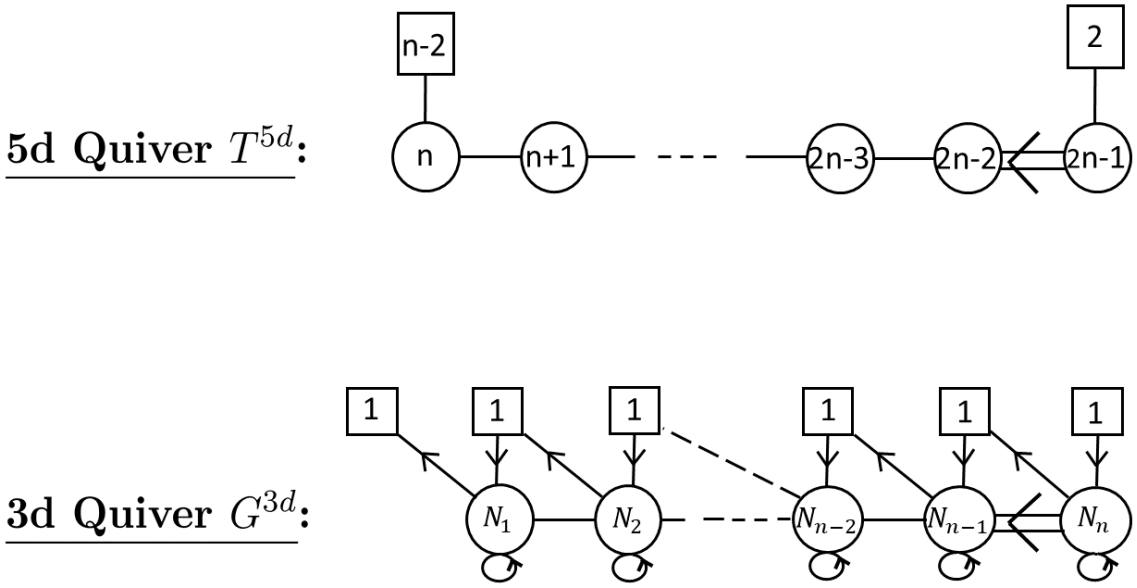

Figure 8.9: Cylinder with a full C_n puncture: 5d theory T^{5d} and 3d theory G^{3d} resulting from $\mathcal{W}_{\mathcal{S}}$.

$$\begin{aligned}
\omega_1 &= [\ 0,\ 0,\dots,\ 0,-1,\ 1,\ 0] \\
\omega_2 &= [\ 0,\ 0,\dots,-1,\ 1,\ 0,\ 0] \\
&\vdots \\
\omega_{n-2} &= [-1,\ 1,\dots,\ 0,\ 0,\ 0,\ 0] \\
\omega_{n-1} &= [\ 1,\ 0,\dots,\ 0,\ 0,\ 0,\ 0] \\
\omega_n &= [\ 0,\ 0,\dots,\ 0,\ 0,-1,\ 1] \\
\omega_{n+1} &= [\ 0,\ 0,\dots,\ 0,\ 0,\ 0,-1]
\end{aligned} \tag{8.1.22}$$

We obtain the quiver gauge theory G^{3d} shown in figure 8.9.

The q-deformed vertex operator that realizes the full puncture is the product $:\prod_{i=1}^{n+1} V_{\omega_i}(x_i):$, where

$$\begin{aligned}
V_{\omega_1}(x) =: & W_1^{-1}(x)E_1(xv^{-1})E_2(xv^{-2})\dots E_{n-1}(xv^{-n})E_n(xv^{-n}) \\
& E_n(xv^{1-n}q^{-1})E_{n-1}(xv^{-n-1}q^{-1}) : \\
V_{\omega_i}(x) =: & V_{\omega_{i-1}}(x)E_{n-i}(xv^{-n-i}q^{-1}) : \qquad i = 2,\dots,n-1 \\
V_{\omega_n}(x) =: & W_n^{-1}(x)E_n(xv^2) : \\
V_{\omega_{n+1}}(x) =: & W_n^{-1}(x) :
\end{aligned} \tag{8.1.23}$$

The above expression is a refinement of the relation (8.1.21). The dependence on the v and q factors encodes the value of the Coulomb moduli at the triality point. Namely, let $v^{\#_{a,I}}\, q^{\#'_{a,I}}$ be the various v and q factors appearing in the E_a operators of (8.1.23). Then, the Coulomb moduli of the 5d gauge theory that truncate the partition function to the C_n q-deformed conformal block are given by:

$$e_{a,I} = f_I\, t^{N_{a,I}}\, v^{\#_{a,I}}\, q^{\#'_{a,I}}\, v^{2-a}\,, \qquad a = 1, \ldots, n$$

In our notation, $a = 1, \ldots, n-1$ designate the short roots, while $a = n$ designates the long root.

The Coulomb branch of the 5d theory has complex dimension:

$$\sum_{a=1}^{n} d_a = \frac{n(3n-1)}{2} = \sum_{\langle e_\gamma, \omega_i\rangle < 0} |\langle e_\gamma, \omega_i\rangle| \ ,$$

with d_a the ranks of the n gauge groups. Note it is the same as for the B_n full puncture. In the right-hand sum, one counts all positive roots that have a negative inner product with at least one of the coweights. This is also the number of supersymmetric vacua (or equivalently, integration contours) of the 3d theory, and the number of parameters needed to specify the 3-point of the q-deformed $\mathcal{W}_{q,t}(C_n)$ algebra.

In the CFT limit, when $m_s \to \infty$, the counting is done without multiplicity. The Coulomb branch dimension therefore decreases and becomes equal to the number of positive roots of C_n, which is n^2. The Coulomb branch of the resulting theory T^{4d} is the maximal nilpotent orbit of C_n, with Bala-Carter label C_n. Because the defect is polarized, its Coulomb branch must be in the image of the Spaltenstein map. In our case, the full puncture Coulomb branch is the image of the orbit denoted by $\varnothing$. This pre-image Bala–Carter label $\varnothing$ is identified at once by acting on $\mathcal{W}_{\mathcal{S}}$ with the Weyl group and noticing the set never has any common zeros in the Dynkin labels of the different coweights.

8.2 All Punctures of the G_2 Little String and CFT Limit

We present here the classification of defects of the $\mathfrak{g} = G_2$ little string theory, along with their conjectured CFT limit. The defects are generated by D5 branes wrapping non-compact 2-cycles of a resolved D_4 singularity; more precisely, we consider a nontrivial fibration of the resolved D_4 over $\mathbb{C}^2 \times \mathcal{C}$, and as one goes around the origin of one of the planes $\mathbb{C}$ wrapped by the branes, the singularity goes back to itself, up to $\mathbb{Z}_3$ outer automorphism group action.

The resulting defects are labeled by coweights of G_2, which are weights of ${}^L G_2 = G_2$. We find that there are exactly two "distinct" unpolarized defects, both generated by the zero weight $[\ 0,\ \ 0]$, taken once in each of the two fundamental representations. The Coulomb branch of each featured quiver gauge theory T_{5d} flows to a nilpotent orbit of G_2 in the CFT limit; all nilpotent orbits of G_2 turn out to be physically realized in this way.

Furthermore, we illustrate G_2 triality, by considering the little string on the cylinder with one of the punctures of figure 8.10.

The $\varnothing$ Orbit

The first puncture we study was studied in the previous section, so we will be brief: it is realized with three D5 branes, labeled by the following set $\mathcal{W}_{\mathcal{S}}$:

$$\begin{aligned}\omega_1 &= -w_1^\vee + 4\alpha_1^\vee + 6\alpha_2^\vee = [\ \ 1,\ \ 0]\\ \omega_2 &= -w_2^\vee + \alpha_2^\vee = [-1,\ \ 1]\\ \omega_3 &= -w_2^\vee = [\ \ 0, -1]\end{aligned}$$

All the elements of $\mathcal{W}_{\mathcal{S}}$ are in the Weyl group orbit of the fundamental representation they belong in, so the defect is polarized. Moreover, the set is distinguished, as can be checked by acting on all elements of $\mathcal{W}_{\mathcal{S}}$ simultaneously with the Weyl group of G_2. The fundamental matter content of T^{5d} is:

$$\prod_{1\leq I\leq d_1} N_{\emptyset\mu_I^1}(v^2\, f_1/e_{1,I}; q) \prod_{1\leq I\leq d_2} N_{\emptyset\mu_I^2}(v_3^2\, f_2/e_{2,I}; q^3) \prod_{1\leq I\leq d_2} N_{\emptyset\mu_I^2}(v_3^2\, f_3/e_{2,I}; q^3).$$

The truncation of T^{5d}'s partition function to a 3d theory's partition function is achieved by setting:

$$\begin{aligned} e_{1,1} &= q^{-0}v^{-0}t^{N_{1,1}}\, f_1 & e_{2,1} &= q^{-0}v^{-2}t^{N_{2,1}}\, f_1\\ e_{1,2} &= q^{-1}v^{-2}t^{N_{1,2}}\, f_1 & e_{2,2} &= q^{-1}v^{-2}t^{N_{2,2}}\, f_1\\ e_{1,3} &= q^{-2}v^{-2}t^{N_{1,3}}\, f_1 & e_{2,3} &= q^{-2}v^{-2}t^{N_{2,3}}\, f_1\\ e_{1,4} &= q^{-3}v^{-4}t^{N_{1,4}}\, f_1 & e_{2,4} &= q^{-1}v^{-4}t^{N_{2,4}}\, f_1\\ & & e_{2,5} &= q^{-2}v^{-4}t^{N_{2,5}}\, f_1\\ & & e_{2,6} &= q^{-3}v^{-4}t^{N_{2,6}}\, f_1\\ & & e_{2,7} &= q^{-0}v^{-0}t^{N_{2,7}}\, f_2 \end{aligned}$$

The resulting 3d partition function has fundamental matter content given exactly by (3.4.56).

We now turn to the CFT limit: there are no common zeros in the distinguished set $\mathcal{W}_{\mathcal{S}}$, so the Bala–Carter label associated to this polarized defect is $\varnothing$. The Coulomb branch dimension is then given by the Spaltenstein dual of this orbit, which is G_2, of complex dimension 6. This is confirmed by the fact that all 6 positive roots have a negative inner product with at least one of the weights. The momentum of the associated vertex operator in G_2-Toda theory is $\beta = \sum_{i=1}^3 \beta_i\, \omega_i$. Moreover, the weighted Dynkin diagram for the orbit G_2 is $(2, 2)$; this is not the mass content of the quiver T^{5d} we wrote down (the mass content being $(1, 2)$), but can be obtained from ours by generalized Hanany-Witten transitions (see [54] for details on this procedure).

The A_1 Orbit

Consider two D5 branes labeled by the following set $\mathcal{W}_{\mathcal{S}}$:

$$\begin{aligned}\omega_1 &= -w_2^\vee + 2\alpha_1^\vee + 4\alpha_2^\vee = [\ \ 0,\ \ 1]\\ \omega_2 &= -w_2^\vee = [\ \ 0, -1]\end{aligned}$$

All the elements of $\mathcal{W}_{\mathcal{S}}$ are in the Weyl group orbit of the fundamental representation they belong in, so the defect is polarized. Moreover, the set is distinguished, as can be checked easily. The fundamental matter content of T^{5d} is:

$$\prod_{1\le I\le d_2} N_{\emptyset\mu_I^2}(v_3^2\, f_1/e_{2,I}; q^3) \prod_{1\le I\le d_2} N_{\emptyset\mu_I^2}(v_3^2\, f_2/e_{2,I}; q^3).$$

The truncation of T^{5d}'s partition function to a 3d theory's partition function is achieved by setting:

$$\begin{aligned} e_{1,1} &= q^{-0}v^{-0}t^{N_{1,1}}\, f_1 & e_{2,1} &= q^{-0}v^{-0}t^{N_{2,1}}\, f_1\\ e_{1,2} &= q^{-1}v^{-2}t^{N_{1,2}}\, f_1 & e_{2,2} &= q^{-0}v^{-2}t^{N_{2,2}}\, f_1\\ & & e_{2,3} &= q^{-1}v^{-2}t^{N_{2,3}}\, f_1\\ & & e_{2,4} &= q^{-1}v^{-4}t^{N_{2,4}}\, f_1 \end{aligned}$$

The resulting 3d partition function has fundamental matter content given exactly by (3.4.56).

We now turn to the CFT limit: there is a common zero in the first Dynkin label of the distinguished set $\mathcal{W}_{\mathcal{S}}$, so the Bala–Carter label associated to this polarized defect is A_1. The Coulomb branch dimension is then given by the Spaltenstein dual of this orbit, which is $G_2(a_1)$, of complex dimension 5. This is confirmed by the fact that all but the positive (simple) root α_1 have a negative inner product with ω_2, and ω_1 does not have a negative inner product with α_1 either, so one of the six positive roots is not counted. The momentum of the associated vertex operator in G_2-Toda theory is $\beta = \sum_{i=1}^2 \beta_i\, \omega_i$. Note that this defect characterizes a level 1 null state of G_2-Toda:

$$\langle \beta, \alpha_1 \rangle = 0$$

Finally, note that the weighted Dynkin diagram for the $G_2(a_1)$ nilpotent orbit is precisely the mass content $(0, 2)$ of the little string quiver T^{5d} we wrote.

The A_{1_s} Orbit

Consider two D5 branes labeled by the following set $\mathcal{W}_{\mathcal{S}}$:

$$\begin{aligned}\omega_1 &= -w_1^\vee + 4\alpha_1^\vee + 6\alpha_2^\vee = [\ \ 1,\ \ 0]\\ \omega_2 &= -w_1^\vee = [-1,\ \ 0]\end{aligned}$$

All the elements of $\mathcal{W}_{\mathcal{S}}$ are in the Weyl group orbit of the fundamental representation they belong in, so the defect is polarized. Moreover, the set is distinguished, as can be checked easily. The fundamental matter content of T^{5d} is:

$$\prod_{1\leq I\leq d_1} N_{\emptyset\mu_I^1}(v^2\, f_1/e_{1,I};q) \prod_{1\leq I\leq d_1} N_{\emptyset\mu_I^1}(v^2\, f_2/e_{1,I};q).$$

The truncation of T^{5d}'s partition function to a 3d theory's partition function is achieved by setting:

$$\begin{aligned} e_{1,1} &= q^{-0}v^{-0}t^{N_{1,1}}\, f_1 & e_{2,1} &= q^{-0}v^{-2}t^{N_{2,1}}\, f_1 \\ e_{1,2} &= q^{-1}v^{-2}t^{N_{1,2}}\, f_1 & e_{2,2} &= q^{-1}v^{-2}t^{N_{2,2}}\, f_1 \\ e_{1,3} &= q^{-2}v^{-2}t^{N_{1,3}}\, f_1 & e_{2,3} &= q^{-2}v^{-2}t^{N_{2,3}}\, f_1 \\ e_{1,4} &= q^{-3}v^{-4}t^{N_{1,4}}\, f_1 & e_{2,4} &= q^{-1}v^{-4}t^{N_{2,4}}\, f_1 \\ & & e_{2,5} &= q^{-2}v^{-4}t^{N_{2,5}}\, f_1 \\ & & e_{2,6} &= q^{-3}v^{-4}t^{N_{2,6}}\, f_1 \end{aligned}$$

The resulting 3d partition function has fundamental matter content given exactly by (3.4.56).

We now turn to the CFT limit: there is a common zero in the second Dynkin label of the distinguished set $\mathcal{W}_{\mathcal{S}}$, so the Bala–Carter label associated to this polarized defect is $A_{1,s}$. It is a distinct label from A_1 in the previous example, since we must distinguish between the short and the long root. The Coulomb branch dimension is then given by the Spaltenstein dual of this orbit, which is $G_2(a_1)$, of complex dimension 5 (this is the same as in the A_1 case.) This is confirmed by the fact that all but the positive (simple) root α_2 have a negative inner product with ω_2, and ω_1 does not have a negative inner product with α_2 either, so one of the six positive roots is not counted. The momentum of the associated vertex operator in G_2-Toda theory is $\beta = \sum_{i=1}^{2} \beta_i\, \omega_i$. Note that this defect characterizes a level 1 null state of G_2-Toda:

$$\langle \beta, \alpha_2 \rangle = 0$$

The $G_2(a1)$ Orbit

Consider one D5 brane labeled by the following set $\mathcal{W}_{\mathcal{S}}$:

$$\omega_1 = -w_2^\vee + 1\alpha_1^\vee + 2\alpha_2^\vee = [\ \ 0,\ \ 0]_2$$

The null coweight is in its own Weyl group orbit, so the defect is unpolarized. The fundamental matter content of T^{5d} is:

$$\prod_{1\leq I\leq d_2} N_{\emptyset\mu_I^2}(v_3^2\, f_1/e_{2,I};q^3).$$

The truncation of T^{5d}'s partition function to a 3d theory's partition function is achieved by setting:

$$e_{1,1} = q^{-0}v^{-0}t^{N_{1,1}}\, f_1 \qquad e_{2,1} = q^{-0}v^{-0}t^{N_{2,1}}\, f_1$$
$$e_{2,2} = q^{-0}v^{-2}t^{N_{2,2}}\, f_1$$

A 3d matter contribution survives this truncation, even with $\mathcal{W}_\mathcal{S}$ containing only the zero coweight. This is because the defect is unpolarized, so refinement due to q and v factors crucially enter the computation. The resulting potential is precisely a refinement of the coweight $[\ 0,\ \ 0]_2$, understood here as $[\ 0,\ \ 0]_2 = [\ 0,\ \ 1] + [\ 0, -1]$, and a potential survives, as pictured in 8.10; see Section 8.4 below.

We now turn to the CFT limit: the coweight $[\ 0,\ \ 0]_2$ has only zeros as Dynkin labels, so part of the Bala–Carter label is G_2. The extra label "2" on the coweight, denoting the fundamental representation of ${}^L G_2$ the coweight is taken in, is in one-to-one correspondence with an extra simple root label in the Bala–Carter classification. All in all, the label is $G_2(a_1)$. Because this is an unpolarized defect, there is no reason to expect that the Coulomb branch dimension of T^{4d} should be given by the Spaltenstein dual of this orbit, (namely, $G_2(a_1)$ itself), and this is indeed not the case. The Coulomb branch of T^{4d} is in fact the orbit A_1, of complex dimension 3. This can be argued from the T^{5d} quiver, which already has complex Coulomb dimension 3. Since the dimension of the Coulomb branch can only decrease in the $m_s \to \infty$ limit, this is the right orbit. Note A_1 is *not* in the image of the Spaltenstein map. Finally, the weighted Dynkin diagram for this orbit is $(0, 1)$, which is the mass content of the quiver T^{5d} we wrote down. For more details on dimension counting for unpolarized defects, see [35].

Bala–Carter Labels and Unpolarized Classification

From the above discussion, it may seem like one of the nilpotent orbits of G_2 is not realized as the Coulomb branch of some defect theory T^{4d}; namely, the orbit A_{1_s} has complex dimension 4, is not in the image of the Spaltenstein map, and did not appear so far. However, we conjecture that this orbit is realized as follows:

Consider one D5 brane labeled by the set $\mathcal{W}_\mathcal{S}$:

$$\omega_1 = -w_1^\vee + 2\alpha_1^\vee + 3\alpha_2^\vee = [\ 0,\ \ 0]_1$$

This is a different way to produce the null coweight, taken this time in the representation labeled by the first fundamental coweight $[\ 1,\ \ 0]$. In our terminology, this defect must be unpolarized. The fundamental matter content of T^{5d} is:

$$\prod_{1\le I\le d_1} N_{\emptyset\mu_I^1}(v^2\, f_1/e_{1,I}; q).$$

The truncation of T^{5d}'s partition function to a q-deformed conformal block with the appropriate vertex operator is achieved by setting:

$$\begin{aligned} e_{1,1} &= q^{-0}v^{-0}t^{N_{1,1}}\, f_1 & e_{2,1} &= q^{-0}v^{-2}t^{N_{2,1}}\, f_1 \\ e_{1,2} &= q^{-1}v^{-2}t^{N_{1,2}}\, f_1 & e_{2,2} &= q^{-1}v^{-2}t^{N_{2,2}}\, f_1 \\ & & e_{2,3} &= q^{-1}v^{-4}t^{N_{2,3}}\, f_1 \end{aligned}$$

A potential survives this truncation, even with $\mathcal{W}_{\mathcal{S}}$ containing only the zero coweight. This is because the defect is unpolarized, so refinement due to q and v factors crucially enter the computation. The resulting potential is precisely a refinement of the coweight $[\ 0,\ \ 0]_1$, as pictured in 8.10. We predict that this truncation is not unique, however (even up to permutation of the Coulomb parameters), because two other "null weights" are present in the $[\ 1,\ \ 0]$ qq-character of G_2. Each of the three null weights is a distinct element in the $U_q(\hat{G}_2)$ sense. It would be important to study carefully thte other truncations and study their flow to the nilpotent orbit A_{1_s}. We leave this task to future work. See also Section 8.4 below.

We now turn to the CFT limit: we claim that this defect is distinct from the previous unpolarized one, which was engineered by $[\ 0,\ \ 0]_2$. We predict that the Coulomb branch of T^{4d} is in fact the orbit A_{1_s}, of complex dimension 4. This is consistent with dimension counting, and the weighted Dynkin diagram for this orbit is $(1, 0)$, which is precisely the mass content of the quiver theory T^{5d}. Note this orbit is *not* in the image of the Spaltenstein map.

8.3 Non-Simply Laced Triality from Folding

Recall that if $\mathfrak{g}'$ is a simply-laced Lie algebra, and $\mathfrak{g}$ a subalgebra of $\mathfrak{g}'$ invariant under the action of the outer automorphism group of $\mathfrak{g}'$, then these automorphisms of $\mathfrak{g}'$ are in one-to-one correspondence with the automorphisms of the Dynkin diagram of $\mathfrak{g}'$. The resulting non simply-laced subalgebra $\mathfrak{g}$ is then obtained by "folding" the Dynkin diagram of $\mathfrak{g}'$.

It turns out that this folding procedure carries through algebraically, so one can engineer 5d non simply-laced quiver gauge theories from their simply-laced counterparts. The truncation of partitions in the 5d theory is preserved by this folding, so triality to a 3d non simply-laced gauge theory can be explicitly described as a folding operation. In this section, we illustrate this fact with a highly non-trivial example: we show that the $\mathbb{Z}_2$ folding of a E_6 theory leads to a F_4 defect.

Our starting theory will be the following polarized defect $\mathcal{W}_{\mathcal{S}}$ of E_6, engineered by two D5 branes:

$$\begin{aligned} \omega_1 &= -w_6^\vee + 2\alpha_1^\vee + 4\alpha_2^\vee + 6\alpha_3^\vee + 4\alpha_4^\vee + 2\alpha_5^\vee + 4\alpha_6^\vee \\ \omega_2 &= -w_6^\vee \end{aligned}$$

Equivalently, decomposed in terms of fundamental coweights, these read:

$$\begin{aligned}\omega_1 &= [\ \ 0,\ \ 0,\ \ 0,\ \ 0,\ \ 0,\ \ 1]\\ \omega_2 &= [\ \ 0,\ \ 0,\ \ 0,\ \ 0,\ \ 0,-1]\end{aligned}$$

The resulting 5d quiver $T^{5d}_{E_6}$ is shown in figure 8.11. After $\mathbb{Z}_2$ folding, the nodes 3 and 6 now designate long roots (being invariant under the outer automorphism action) and we obtain an F_4 defect theory $T^{5d}_{F_4}$, with coweights:

$$\begin{aligned}\omega_1' &= -w_1^\vee + 4\alpha_1^\vee + 6\alpha_2^\vee + 4\alpha_3^\vee + 2\alpha_4^\vee\\ \omega_2' &= -w_1^\vee\end{aligned}$$

Equivalently, decomposed in terms of fundamental coweights, these read:

$$\begin{aligned}\omega_1 &= [\ \ 1,\ \ 0,\ \ 0,\ \ 0]\\ \omega_2 &= [-1,\ \ 0,\ \ 0,\ \ 0]\end{aligned}$$

The fundamental matter content of $T^{5d}_{E_6}$ is

$$\prod_{1\le I\le d_6} N_{\emptyset\mu_I^6}(v^2\, f_1/e_{6,I};q).$$

We now show that the truncation scheme of the $T^{5d}_{E_6}$ theory at the triality point are preserved by the folding operation. Namely, we set the Coulomb parameters of $T^{5d}_{E_6}$ to:

$$\begin{aligned}
&e_{1,1} = v^{-6}t^{N_{1,1}}\, f_1 && e_{2,1} = v^{-4}t^{N_{2,1}}\, f_1 && e_{3,1} = v^{-2}t^{N_{3,1}}\, f_1\\
&e_{1,2} = v^{-10}t^{N_{1,2}}\, f_1 && e_{2,2} = v^{-6}t^{N_{2,2}}\, f_1 && e_{3,2} = v^{-4}t^{N_{3,2}}\, f_1\\
& && e_{2,3} = v^{-8}t^{N_{2,3}}\, f_1 && e_{3,3} = v^{-6}t^{N_{3,3}}\, f_1\\
& && e_{2,4} = v^{-10}t^{N_{2,4}}\, f_1 && e_{3,4} = v^{-6}t^{N_{3,4}}\, f_1\\
& && && e_{3,5} = v^{-8}t^{N_{3,5}}\, f_1\\
& && && e_{3,6} = v^{-10}t^{N_{3,6}}\, f_1
\end{aligned}$$

$$\begin{aligned}
&e_{4,1} = v^{-4}t^{N_{4,1}}\, f_1 && e_{5,1} = v^{-6}t^{N_{5,1}}\, f_1 && e_{6,1} = v^{-0}t^{N_{6,1}}\, f_1\\
&e_{4,2} = v^{-6}t^{N_{4,2}}\, f_1 && e_{5,2} = v^{-10}t^{N_{5,2}}\, f_1 && e_{6,2} = v^{-4}t^{N_{6,2}}\, f_1\\
&e_{4,3} = v^{-8}t^{N_{4,3}}\, f_1 && && e_{6,3} = v^{-6}t^{N_{6,3}}\, f_1\\
&e_{4,4} = v^{-10}t^{N_{4,4}}\, f_1 && && e_{6,4} = v^{-10}t^{N_{6,4}}\, f_1
\end{aligned}$$

The resulting 3d theory is shown in the right column of figure 8.11. Now, notice that the above v factors used in the truncation are identical on nodes 1 and 5, and identical and nodes 2 and 4. These become the v factors of $T^{5d}_{F_4}$ for the two short roots. The v factors on nodes 3 and 6 become the v factors of $T^{5d}_{F_4}$ for the two long roots.

There is one slight caveat: a bifundamental hypermultiplet truncating a partition on the long root 2 starting from the long root 1 is now accompanied by a q^{-1} factor in the argument of the Nekrasov factors in the 5d partition function. With this adjustment, we obtain the following truncation scheme for $T^{5d}_{F_4}$:

$$
\begin{aligned}
e_{1,1} &= q^{-0}v^{-0}t^{M_{1,1}}\, f_1 & \qquad e_{2,1} &= q^{-1}v^{-2}t^{M_{2,1}}\, f_1\\
e_{1,2} &= q^{-1}v^{-4}t^{M_{1,2}}\, f_1 & \qquad e_{2,2} &= q^{-1}v^{-4}t^{M_{2,2}}\, f_1\\
e_{1,3} &= q^{-1}v^{-6}t^{M_{1,3}}\, f_1 & \qquad e_{2,3} &= q^{-1}v^{-6}t^{M_{2,3}}\, f_1\\
e_{1,4} &= q^{-2}v^{-10}t^{M_{1,4}}\, f_1 & \qquad e_{2,4} &= q^{-2}v^{-6}t^{M_{2,4}}\, f_1\\
& & \qquad e_{2,5} &= q^{-2}v^{-8}t^{M_{2,5}}\, f_1\\
& & \qquad e_{2,6} &= q^{-2}v^{-10}t^{M_{2,6}}\, f_1
\end{aligned}
$$

$$
\begin{aligned}
e_{3,1} &= q^{-1}v^{-4}t^{M_{3,1}}\, f_1 & \qquad e_{4,1} &= q^{-1}v^{-6}t^{M_{4,1}}\, f_1\\
e_{3,2} &= q^{-1}v^{-6}t^{M_{3,2}}\, f_1 & \qquad e_{4,2} &= q^{-2}v^{-10}t^{M_{4,2}}\, f_1\\
e_{3,3} &= q^{-2}v^{-8}t^{M_{3,3}}\, f_1 & &\\
e_{3,4} &= q^{-2}v^{-10}t^{M_{3,4}}\, f_1 & &
\end{aligned}
$$

The resulting 3d theory G^{3d} is shown in the right column of figure 8.11.

8.4 Unpolarized Defects of G_2 and the Quantum Affine Algebra $U_q(\widehat{G_2})$

Here, we illustrate how we can produce of a null coweight of G_2 as obtained from the triality procedure. The null weight we will obtained will naturally be "refined," and it will appear in the construction of the generators of $\mathcal{W}_{q,t}(G_2)$. The expression we will obtain can be recovered from other methods, such as the G_2 qq-characters; see [71, 77] for details.

For concreteness, let $\mathcal{W}_{\mathcal{S}}$ be the set $\omega = [\ \ 0,\ \ 0]_2$ we studied above, with T^{5d} the 5d quiver engineered at the top of figure 8.10. Because the only coweight of $\mathcal{W}_{\mathcal{S}}$ is the null coweight, one would naively think that there is no matter left after truncation of the partition function to the resulting 3d theory, meaning the presence of the D5 brane would not be felt by the compact D3 branes. This is however not the case: in the little string theory, a refinement due to q and v factors results in chiral and anti-chiral matter in G^{3d}, and one ends up with a "refinement" of the coweight $[\ \ 0,\ \ 0]_2$. Namely, we perform the truncation of the 5d partition function by setting:

$$
\begin{aligned}
e_{1,1} &= q^{-0}v^{-0}t^{N_{1,1}}\, f_1 & \qquad e_{2,1} &= q^{-0}v^{-0}t^{N_{2,1}}\, f_1\\
& & \qquad e_{2,2} &= q^{-0}v^{-2}t^{N_{2,2}}\, f_1\ .
\end{aligned}
$$

We obtain the partition function of a 3d theory G^{3d} with fundamental matter $z^{3d}_{H_2}(x_{\mu^2})/z^{3d}_{H_2}(x_\varnothing)$, where

$$z^{3d}_{H_2}(x_2) = \prod_{1\leq I\leq N_2} \frac{(v^2\, q\, e^{x_I^{(2)}}/f_1; q^3)_\infty}{(q^2\, e^{x_I^{(2)}}/f_1; q^3)_\infty} \,. \tag{8.4.24}$$

This gives a physical construction of the weight $[\ \ 0,\ \ 0]_2$ as it appears in the representation theory of $U_q(\widehat{G_2})$. It is of the expected form, after rescaling of q and v, as suggested by the relevant term in the $[\ \ 0,\ \ 1]$ qq-character of G_2. Note that we recover the unrefined null coweight (and therefore a trivial potential) in the limit $qv^{-2} = 1$.

In this fashion, one can derive the full representation theory content of any finite-dimensional integral representation of a quantum affine algebra $U_q(\hat{\mathfrak{g}})$, for any simple Lie algebra $\mathfrak{g}$.

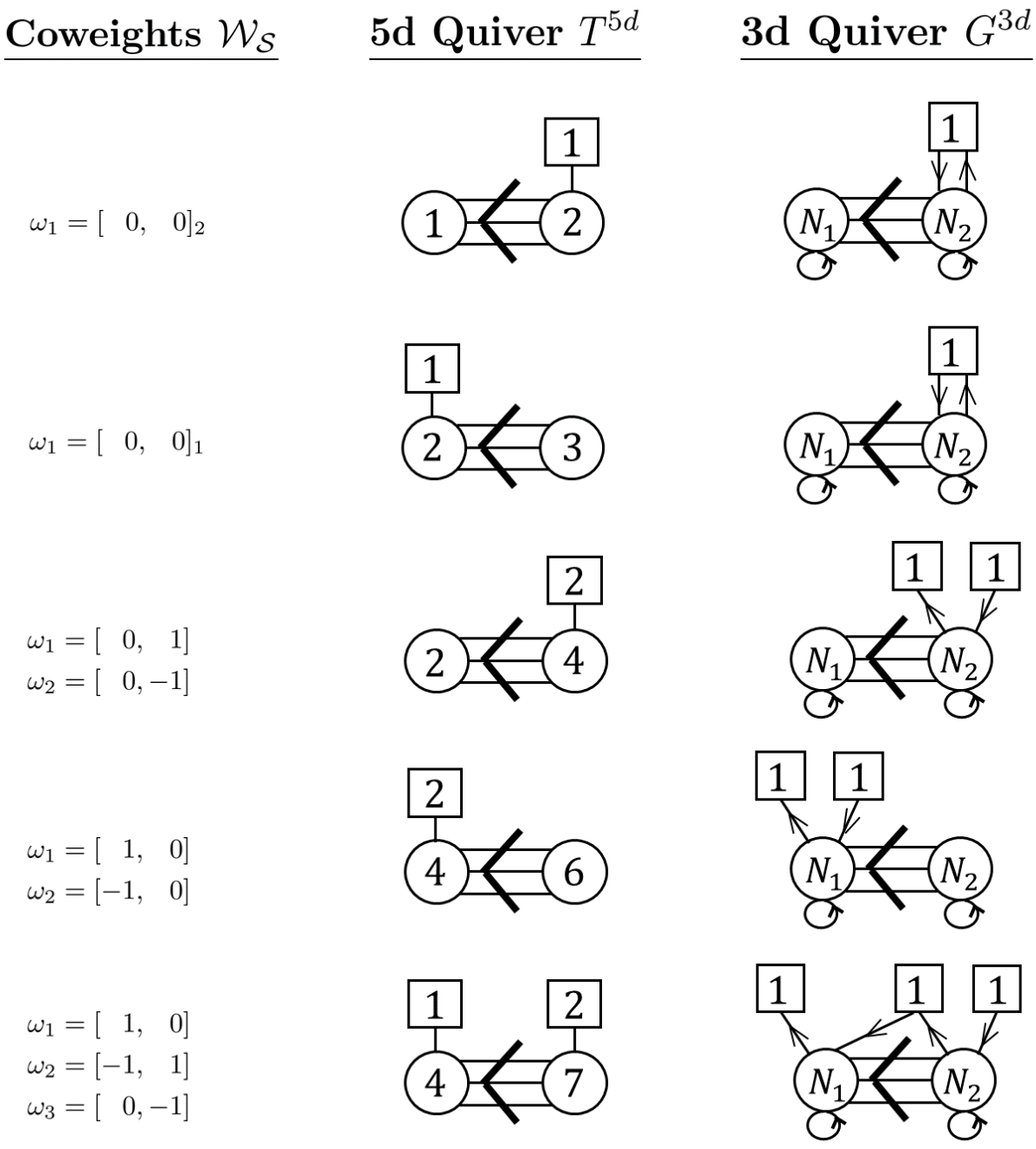

Figure 8.10: Defects of the G_2 Little String

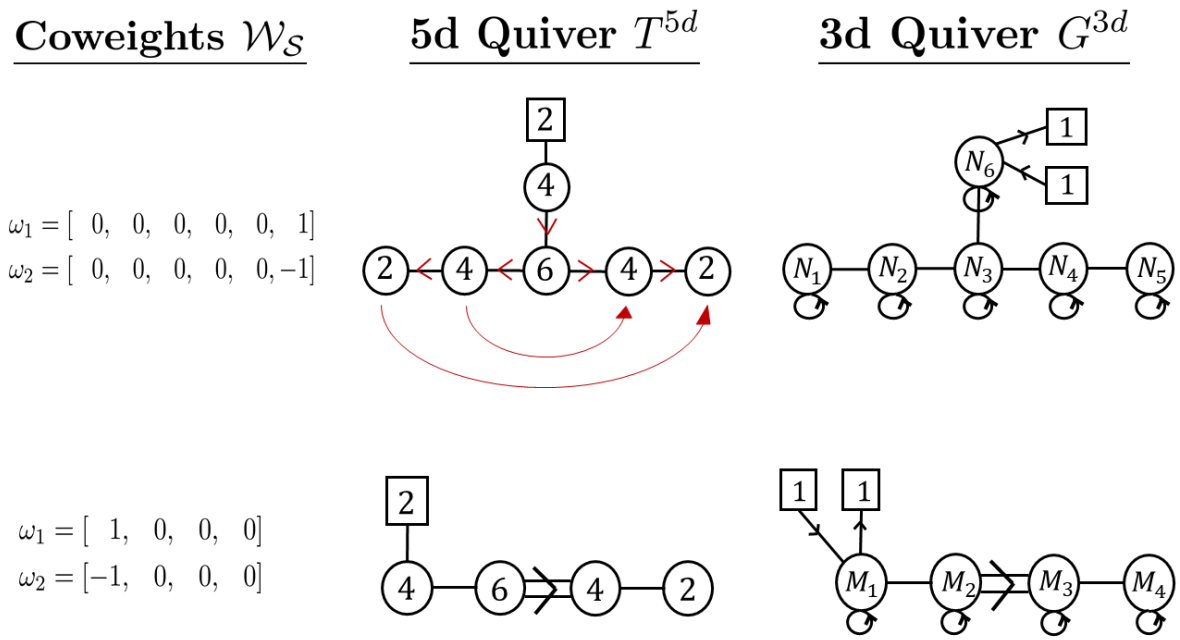

Figure 8.11: Folding of a E_6 little string defect and the resulting F_4 defect. The 3d theory at the triality locus is shown on the right.

8.5 All Punctures of the E_n Little String and CFT Limit

As an application of the Bala–Carter classification, we present a table of the defects of the E_n little string. Unpolarized defects are shaded in yellow. For each defect type, we give a set $\mathcal{W}_\mathcal{S}$ of weights, along with the low energy 5d quiver gauge theory T^{5d} on the D5 branes that results from it. The Bala–Carter label that designates the nilpotent orbit in the CFT limit $m_s \to \infty$ is written in the left column. Each set $\mathcal{W}_\mathcal{S}$ is a distinguished set, in the sense of section 4.2; in particular, the (co)weights ω_i of $\mathcal{W}_\mathcal{S}$ satisfy

$$\langle \beta, \alpha_i \rangle = 0 \quad \forall \alpha_i \in \Theta,$$

with $\beta = \sum_{i=1}^{|\mathcal{W}_\mathcal{S}|} \beta_i \, \omega_i$. This constraint has an interpretation as a level 1 null state condition of $\mathfrak{g}$-Toda. For unpolarized defects, a subscript is added to the weights, specifying the representation they are taken in. This corresponds to giving the additional simple root label a_i in the Bala–Carter picture. For polarized defects, no subscript is needed for the weights.

The dual orbit is the orbit describing the Coulomb branch of T^{4d}; for polarized defects, this is given by the Spaltenstein dual of the Bala–Carter label. For unpolarized defects, these dual orbits had to be conjectured based on other approaches, such as dimension counting. The dimension of this dual orbit describing the Coulomb branch is given by d.

Note the quivers are either literally the weighted Dynkin diagrams as given in the literature, or are quivers that can be made to be weighted Dynkin diagrams after moving on the Higgs branch.

Table 8.1: Results for E_6

Orbit	Weights	Quiver	Dual orbit	d
0	$\begin{bmatrix} 0, & 0, & 0, & 0, & 0, & -1] \\ [-1, & 0, & 0, & 0, & -1, & 1] \\ [1, & 0, & 0, & -1, & 0, & 1] \\ [0, & -1, & 0, & 0, & 1, & 1] \\ [0, & 1, & -1, & 1, & 0, & 0] \\ [0, & 0, & 1, & 0, & 0, & -1] \\ [0, & 0, & 0, & 0, & 0, & -1] \end{bmatrix}$	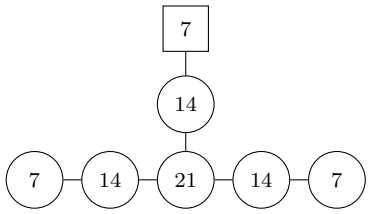	E_6	72
A_1	$\begin{bmatrix} 0, & 0, & 0, & 0, & -1, & 0] \\ [0, & 0, & 0, & -1, & 1, & 0] \\ [0, & 1, & 0, & -1, & 0, & 0] \\ [0, & 0, & 0, & 1, & 0, & -1] \\ [0, & 0, & -1, & 1, & 0, & 1] \\ [0, & -1, & 1, & 0, & 0, & 0] \end{bmatrix}$	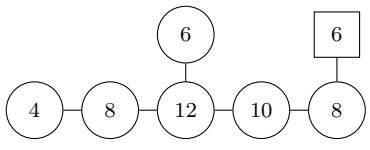	$E_6(a_1)$	70

Table 8.1: Results for E_6

Orbit	Weights	Quiver	Dual orbit	d
$2A_1$	$\begin{bmatrix} 0, & 0, & 0, & 1, & -1, & -1] \\ [& 0, & 0, & 0, & 0, & 1, & -1] \\ [& 0, & -1, & 0, & 0, & 0, & 1] \\ [& 0, & 1, & 0, & -1, & 0, & 0] \\ [& 0, & 0, & 0, & 0, & 0, & 1] \end{bmatrix}$	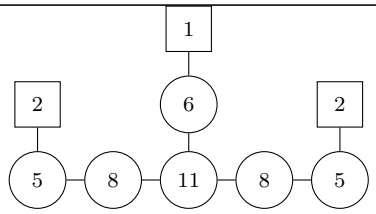	D_5	68
$3A_1$	$\begin{bmatrix} 0, & -1, & 0, & 0, & 0, & 0] \\ [& 0, & 2, & 0, & -1, & 0, & -2] \\ [& 0, & -1, & 0, & 1, & 0, & 1] \\ [& 0, & 0, & 0, & 0, & 0, & 1] \end{bmatrix}$	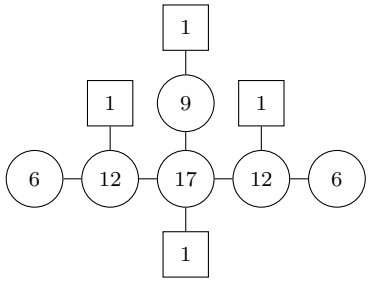	$E_6(a_3)$	66
A_2	$\begin{bmatrix} 0, & 0, & 1, & -1, & 0, & -1] \\ [& 0, & 0, & 0, & 0, & -1, & 0] \\ [& 0, & 0, & 0, & -1, & 2, & 0] \\ [& 0, & 0, & -1, & 2, & -1, & 0] \\ [& 0, & 0, & 0, & 0, & 0, & 1] \end{bmatrix}$	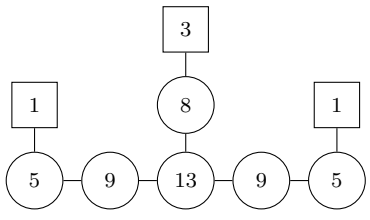	$E_6(a_3)$	66
$A_2 + A_1$	$\begin{bmatrix} 0, & 0, & 0, & 0, & 1, & -1] \\ [& 0, & 0, & 0, & 0, & -1, & 0] \\ [& 0, & 0, & -1, & 0, & 0, & 2] \\ [& 0, & 0, & 1, & 0, & 0, & -1] \end{bmatrix}$	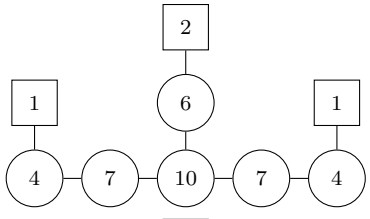	$D_5(a_1)$	64
$2A_2$	$\begin{bmatrix} 0, & 0, & 0, & 0, & 0, & -1] \\ [& 0, & 0, & -1, & 0, & 0, & 2] \\ [& 0, & 0, & 1, & 0, & 0, & -1] \end{bmatrix}$	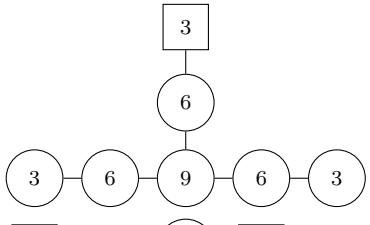	D_4	60
$A_2 + 2A_1$	$\begin{bmatrix} 0, & 0, & 0, & 0, & 1, & 0] \\ [& 0, & 0, & -1, & 0, & 1, & 0] \\ [& 0, & 0, & 1, & 0, & -2, & 0] \end{bmatrix}$	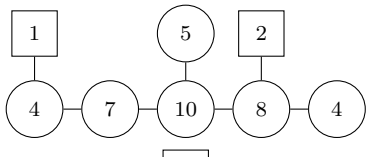	$A_4 + A_1$	62
A_3	$\begin{bmatrix} 0, & 0, & 0, & 0, & -1, & 0] \\ [& 0, & 0, & 0, & -1, & 1, & 0] \\ [& 0, & 0, & 0, & 1, & 0, & -1] \\ [& 0, & 0, & 0, & 0, & 0, & 1] \end{bmatrix}$	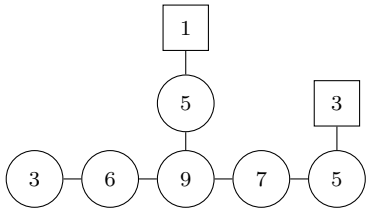	A_4	60

Table 8.1: Results for E_6

Orbit	Weights	Quiver	Dual orbit	d
$2A_2 + A_1$	$\begin{bmatrix} 0, & 0, -1, & 0, & 0, & 0] \\ [0, & 0, & 1, & 0, & 0, & 0] \end{bmatrix}$	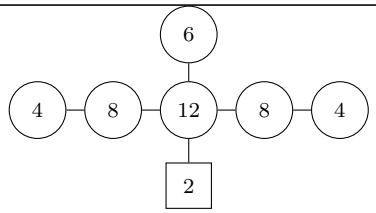	$D_4(a_1)$	58
$A_3 + A_1$	$\begin{bmatrix} 0, & 0, & 0, -1, & 0, & 0] \\ [0, & 0, & 0, & 1, & 0, -1] \\ [0, & 0, & 0, & 0, & 0, & 1] \end{bmatrix}$	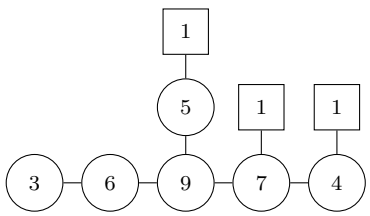	$D_4(a_1)$	58
$D_4(a_1)$	$\begin{bmatrix} 0, & 0, & 0, & 0, & 1, & 0]_1 \\ [-1, & 0, & 0, & 0, -1, & 0]_3 \\ [1, & 0, & 0, & 0, & 0, & 0]_5 \end{bmatrix}$	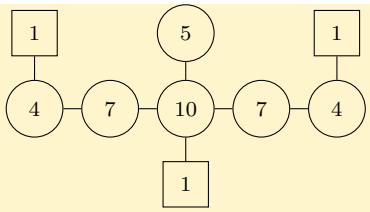	$2A_2 + A_1$	54
A_4	$\begin{bmatrix} 0, & 0, & 0, & 0, & 2, -1] \\ [0, & 0, & 0, & 0, -1, & 0] \\ [0, & 0, & 0, & 0, -1, & 1] \end{bmatrix}$	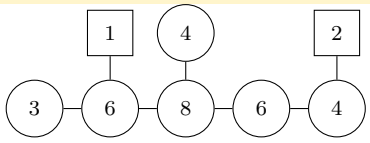	A_3	52
D_4	$\begin{bmatrix} 0, & 0, & 0, & 0, -1, & 0] \\ [-1, & 0, & 0, & 0, & 1, & 0] \\ [1, & 0, & 0, & 0, & 0, & 0] \end{bmatrix}$	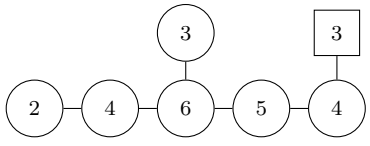	$2A_2$	48
$A_4 + A_1$	$\begin{bmatrix} 0, & 0, & 0, & 1, & 0, & 0] \\ [0, & 0, & 0, -1, & 0, & 0] \end{bmatrix}$	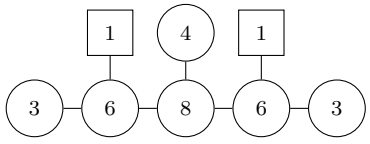	$A_2 + 2A_1$	50
A_5	$\begin{bmatrix} 0, & 0, & 0, & 0, & 0, -1] \\ [0, & 0, & 0, & 0, & 0, & 1] \end{bmatrix}$	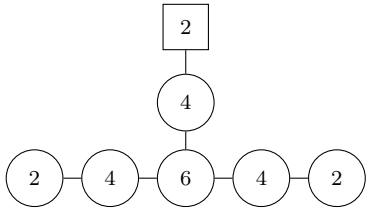	A_2	42
$D_5(a_1)$	$\begin{bmatrix} 0, & 0, & 0, & 0, & 1, & 0]_1 \\ [0, & 0, & 0, & 0, -1, & 0]_2 \end{bmatrix}$	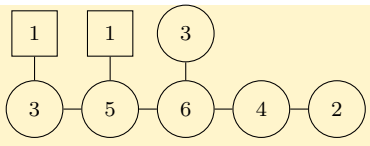	$A_2 + A_1$	46

Table 8.1: Results for E_6

Orbit	Weights	Quiver	Dual orbit	d
$E_6(a_3)$	$[\ 0,\ 0,\ 0,\ 0,\ 0,\ 0]_3$	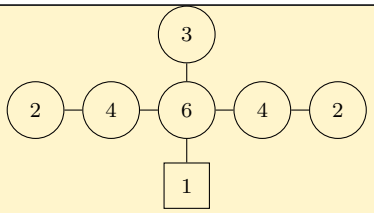	$3A_1$	40
D_5	$[\ 0,\ 0,\ 0,\ 0,\ 1,\ 0]$ $[\ 0,\ 0,\ 0,\ 0,-1,\ 0]$	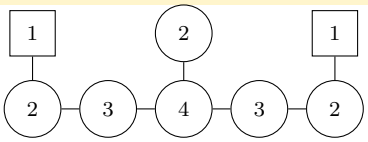	$2A_1$	32
$E_6(a_1)$	$[\ 0,\ 0,\ 0,\ 0,\ 0,\ 0]_7$	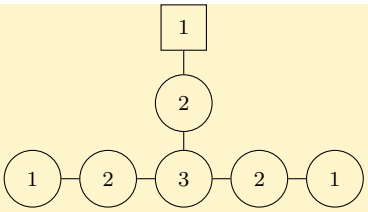	A_1	22

Table 8.2: Results for E_7

Orbit	Weights	Quiver	Dual orbit	d
0	$\begin{bmatrix}-1,&0,&0,&0,&0,&0,&0\\ 1,&0,&0,&-1,&0,&1,&0\\ 0,&-1,&1,&0,&0,&-1,&0\\ -1,&1,&0,&0,&0,&-1,&0\\ 0,&0,&0,&0,&0,&1,&0\\ 0,&0,&-1,&1,&0,&0,&1\\ 1,&0,&-1,&1,&-1,&0,&0\\ 0,&0,&1,&-1,&1,&0,&-1\end{bmatrix}$	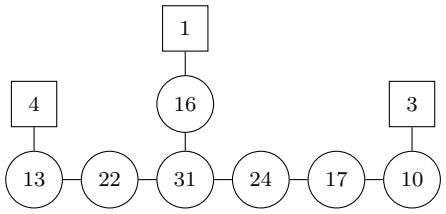	E_7	126
A_1	$\begin{bmatrix}-1,&0,&0,&0,&0,&0,&0\\ 1,&0,&0,&-1,&0,&1,&0\\ 0,&-1,&1,&0,&0,&-1,&0\\ -1,&1,&0,&0,&0,&-1,&0\\ 0,&0,&0,&0,&0,&1,&0\\ 0,&0,&-1,&1,&0,&0,&1\\ 1,&0,&0,&0,&0,&0,&-1\end{bmatrix}$	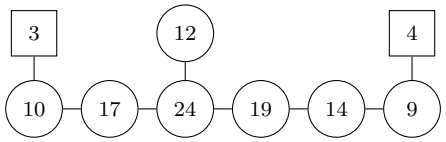	$E_7(a_1)$	124
$2A_1$	$\begin{bmatrix}-1,&0,&0,&0,&0,&0,&0\\ 1,&0,&0,&-1,&0,&1,&0\\ 0,&-1,&1,&0,&0,&-1,&0\\ -1,&1,&0,&0,&0,&-1,&0\\ 1,&0,&-1,&1,&0,&0,&0\\ 0,&0,&0,&0,&0,&1,&0\end{bmatrix}$	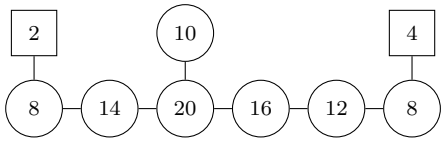	$E_7(a_2)$	122
$3A_1b$	$\begin{bmatrix}0,&0,&0,&0,&-1,&0,&0\\ 0,&0,&-1,&0,&1,&0,&0\\ -2,&0,&1,&0,&0,&0,&0\\ 2,&-2,&1,&0,&0,&0,&0\\ 0,&2,&-1,&0,&0,&0,&0\end{bmatrix}$	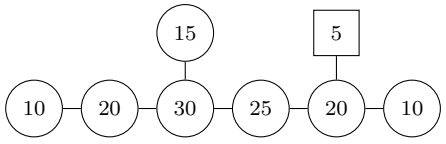	E_6	120
$3A_1a$	$\begin{bmatrix}0,&0,&0,&0,&-1,&0,&0\\ 0,&0,&-1,&0,&1,&0,&0\\ 0,&-1,&1,&0,&1,&-2,&0\\ 0,&-1,&1,&0,&-1,&2,&0\\ 0,&2,&-1,&0,&0,&0,&0\end{bmatrix}$	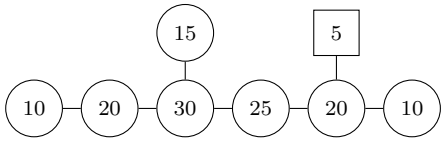	$E_7(a_3)$	120
A_2	$\begin{bmatrix}0,&0,&0,&0,&0,&-1,&0\\ 0,&0,&0,&0,&-1,&1,&0\\ 0,&0,&0,&0,&1,&0,&-1\\ 0,&0,&-1,&0,&1,&0,&1\\ 0,&0,&1,&-1,&0,&0,&0\\ 0,&0,&0,&1,&-1,&0,&0\end{bmatrix}$	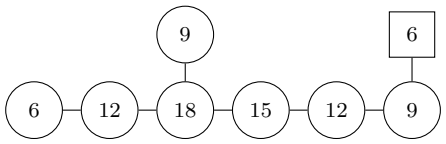	$E_7(a_3)$	120
$4A_1$	$\begin{bmatrix}0,&0,&-1,&0,&0,&0,&0\\ 0,&0,&1,&0,&-3,&0,&0\\ 2,&0,&-1,&0,&2,&0,&0\\ -2,&0,&1,&0,&1,&0,&0\end{bmatrix}$	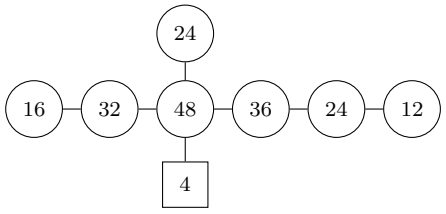	$E_6(a_1)$	118
A_2+A_1	$\begin{bmatrix}0,&0,&1,&-1,&0,&-1,&0\\ 0,&0,&-1,&0,&0,&0,&0\\ 0,&0,&-1,&2,&-2,&2,&0\\ 0,&0,&1,&-1,&1,&-1,&0\\ 0,&0,&0,&0,&1,&0,&0\end{bmatrix}$	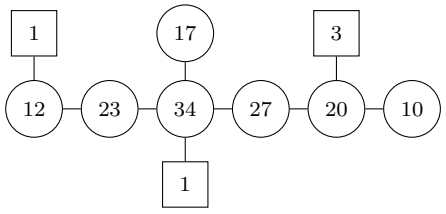	$E_6(a_1)$	118

Table 8.2: Results for E_7

Orbit	Weights	Quiver	Dual orbit	d
A_2+2A_1	$\begin{bmatrix} 0, & 0, & 0, & 0, & 1, & -2, & 0 \\ 0, & 0, & -1, & 0, & 0, & 1, & 0 \\ 0, & 0, & 0, & 0, & 1, & 0, & 0 \\ 0, & 0, & 1, & 0, & -2, & 1, & 0 \end{bmatrix}$	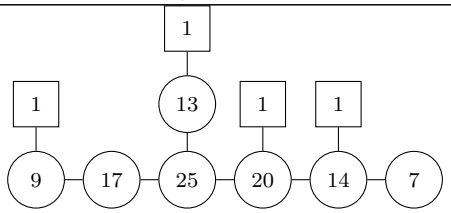	$E_7(a_4)$	116
A_3	$\begin{bmatrix} 0, & 0, & 0, & 1, & -1, & 0, & -1 \\ 0, & 0, & 0, & -1, & 1, & 0, & 0 \\ 0, & 0, & 0, & 0, & -1, & 0, & 1 \\ 0, & 0, & 0, & 0, & 1, & -1, & 0 \\ 0, & 0, & 0, & 0, & 0, & 1, & 0 \end{bmatrix}$	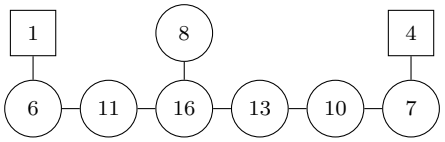	$D_6(a_1)$	114
$2A_2$	$\begin{bmatrix} 0, & 0, & -1, & 1, & 0, & 0, & 0 \\ 0, & 0, & 0, & 0, & 0, & 0, & -1 \\ 0, & 0, & 0, & -1, & 0, & 0, & 2 \\ 0, & 0, & 1, & 0, & 0, & 0, & -1 \end{bmatrix}$	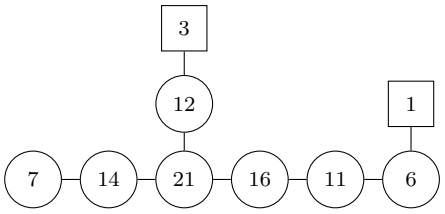	D_5+A_1	114
A_2+3A_1	$\begin{bmatrix} 0, & 0, & 0, & 0, & -1, & 0, & 0 \\ 0, & 0, & -1, & 0, & 2, & 0, & 0 \\ 0, & 0, & 1, & 0, & -1, & 0, & 0 \end{bmatrix}$	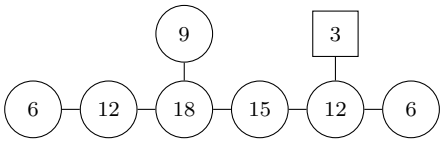	A_6	114
A_3b+A_1b	$\begin{bmatrix} -1, & 0, & 0, & 0, & 0, & 0, & 0 \\ 1, & 0, & 0, & 0, & -1, & 0, & 0 \\ 1, & -1, & 0, & 0, & 1, & 0, & 0 \\ -1, & 1, & 0, & 0, & 0, & 0, & 0 \end{bmatrix}$	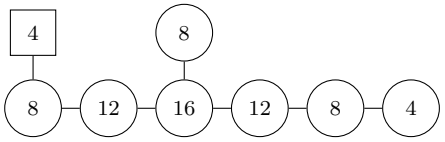	D_5	112
$2A_2+A_1$	$\begin{bmatrix} 0, & 0, & -1, & 0, & 0, & 0, & 0 \\ 0, & 0, & 1, & 0, & 0, & -1, & 0 \\ 0, & 0, & 0, & 0, & 0, & 1, & 0 \end{bmatrix}$	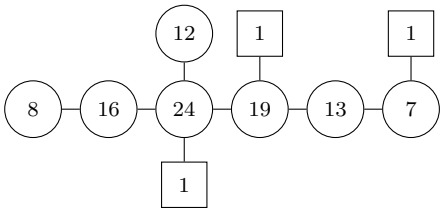	$E_7(a_5)$	112
A_3a+A_1a	$\begin{bmatrix} 0, & -1, & 0, & 0, & 1, & 0, & 0 \\ 0, & 0, & 0, & 0, & -1, & 0, & 0 \\ 0, & 0, & 0, & 0, & 1, & -1, & 0 \\ 0, & 1, & 0, & 0, & -1, & 1, & 0 \end{bmatrix}$	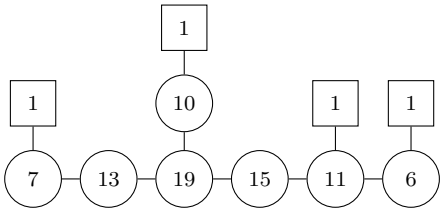	$E_7(a_5)$	112
$D_4(a_1)$	$\begin{bmatrix} 1, & 0, & 0, & 0, & 0, & 0, & 0 \end{bmatrix}_1$ $\begin{bmatrix} -1, & 0, & 0, & 0, & -1, & 0, & 0 \end{bmatrix}_3$ $\begin{bmatrix} 0, & 0, & 0, & 0, & 0, & 1, & 0 \end{bmatrix}_6$ $\begin{bmatrix} 0, & 0, & 0, & 0, & 1, & -1, & 0 \end{bmatrix}_6$	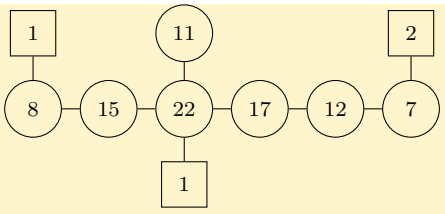	$D_6(a_2)$	110

Table 8.2: Results for E_7

Orbit	Weights	Quiver	Dual orbit	d
$A_3 + 2A_1$	$\begin{bmatrix} 0, & 1, -1, & 0, & 0, & 0, & 0 \\ 0, -1, & 0, & 0, & 0, & 0, & 0 \\ 0, & 0, & 1, & 0, & 0, & 0 \end{bmatrix}$	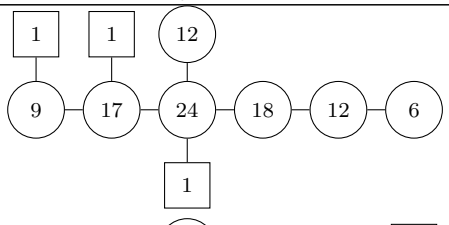	$E_6(a_3)$	110
D_4	$\begin{bmatrix} 0, & 0, & 0, & 0, & 0, -1, & 0 \\ -1, & 0, & 0, & 0, & 0, & 1, & 0 \\ 1, & 0, & 0, & 0, -1, & 1, & 0 \\ 0, & 0, & 0, & 0, & 1, -1, & 0 \end{bmatrix}$	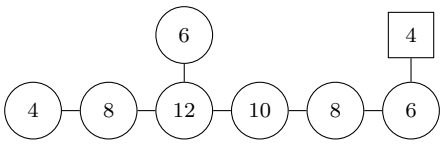	A_5b	102
$D_4(a_1)+A_1$	$\begin{bmatrix} 1, & 0, & 0, & 0, & 0, & 0, & 0 \\ -1, & 0, & 0, & 0, -1, & 0, & 0 \\ 0, & 0, & 0, & 0, & 1, & 0, & 0 \end{bmatrix}_{1,3,5}$	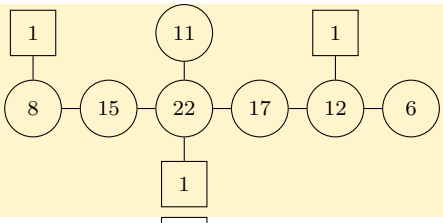	A_5a	108
$A_3 + A_2$	$\begin{bmatrix} 0, & 0, & 0, -1, & 0, & 0, & 1 \\ 0, & 0, & 0, & 1, & 0, & 0, -2 \\ 0, & 0, & 0, & 0, & 0, & 0, & 1 \end{bmatrix}$	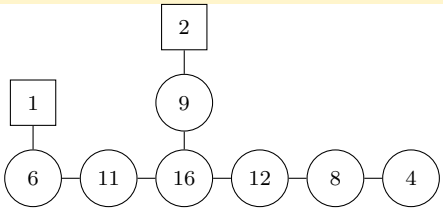	$D_5(a_1)+A_1$	108
A_4	$\begin{bmatrix} 0, & 0, & 0, & 0, & 0, -1, & 0 \\ 0, & 0, & 0, & 0, -1, & 1, & 0 \\ 0, & 0, & 0, & 0, & 1, & 0, -1 \\ 0, & 0, & 0, & 0, & 0, & 0, & 1 \end{bmatrix}$	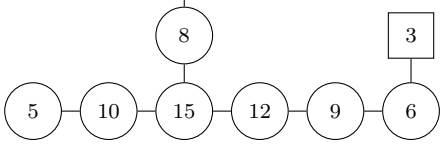	$D_5(a_1)$	106
$A_3+A_2+A_1$	$\begin{bmatrix} 0, & 0, -1, & 0, & 0, & 0, & 0 \\ 0, & 0, & 1, & 0, & 0, & 0, & 0 \end{bmatrix}$	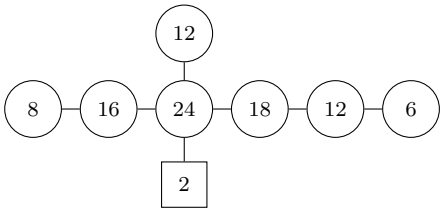	$A_4 + A_2$	106
A_5b	$\begin{bmatrix} -1, & 0, & 0, & 0, & 0, & 0, & 0 \\ 2, -1, & 0, & 0, & 0, & 0, & 0, & 0 \\ -1, & 1, & 0, & 0, & 0, & 0, & 0 \end{bmatrix}$	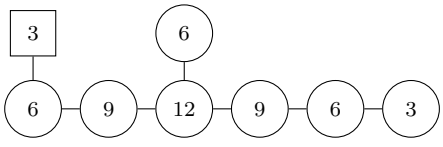	D_4	96
$D_4 + A_1$	$\begin{bmatrix} -1, & 0, & 0, & 0, & 0, & 0, & 0 \\ 1, & 0, & 0, & 0, -1, & 0, & 0 \\ 0, & 0, & 0, & 0, & 1, & 0, & 0 \end{bmatrix}$	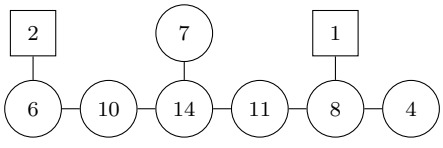	A_4	100

Table 8.2: Results for E_7

Orbit	Weights	Quiver	Dual orbit	d
$A_4 + A_1$	$\begin{bmatrix} 0, & 0, & 0, & 0, -1, & 0, & 0 \\ 0, & 0, & 0, & 0, & 1, & 0, -1 \\ 0, & 0, & 0, & 0, & 0, & 0, & 1 \end{bmatrix}$	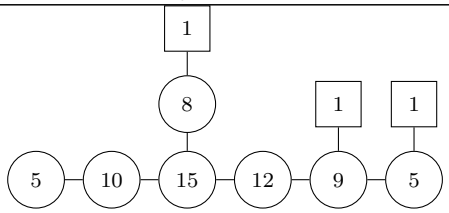	$A_4 + A_1$	104
$D_5(a_1)$	$\begin{bmatrix} 1, & 0, & 0, & 0, & 0, & 0, & 0 \\ -1, & 0, & 0, & 0, & 0, & -1, & 0 \\ 0, & 0, & 0, & 0, & 0, & 1, & 0 \end{bmatrix}_{1,4,6}$	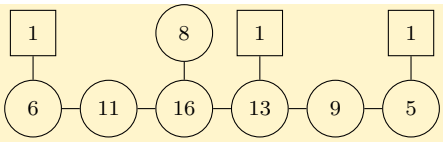	A_4	100
$A_4 + A_2$	$\begin{bmatrix} 0, & 0, & 0, -1, & 0, & 0, & 0 \\ 0, & 0, & 0, & 1, & 0, & 0, & 0 \end{bmatrix}$	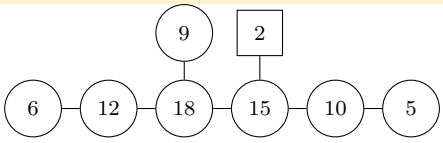	$A_3+A_2+A_1$	100
A_5a	$\begin{bmatrix} 0, & 0, & 0, & 0, & 0, & 1, -1 \\ 0, & 0, & 0, & 0, & 0, -1, & 0 \\ 0, & 0, & 0, & 0, & 0, & 0, & 1 \end{bmatrix}$	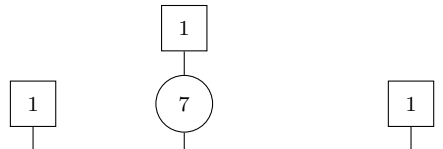	$D_4(a_1)+A_1$	96
$A_5 + A_1$	$\begin{bmatrix} 0, -1, & 0, & 0, & 0, & 0, & 0 \\ 0, & 1, & 0, & 0, & 0, & 0, & 0 \end{bmatrix}$	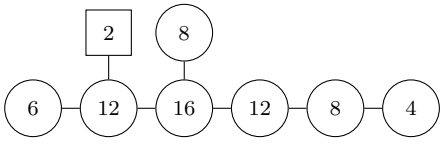	$D_4(a_1)$	94
$D_5(a_1)+A_1$	$\begin{bmatrix} 0, & 0, & 0, & 0, -1, & 0, & 0 \\ 0, & 0, & 0, & 0, & 1, & 0, & 0 \end{bmatrix}_{3,5}$	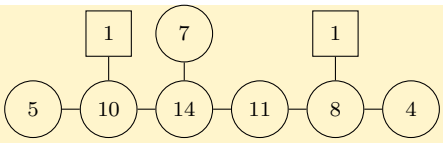	$A_3 + A_2$	98
$D_6(a_2)$	$\begin{bmatrix} 1, & 0, & 0, & 0, & 0, & 0, & 0 \\ -1, & 0, & 0, & 0, & 0, & 0, & 0 \end{bmatrix}_{1,3}$	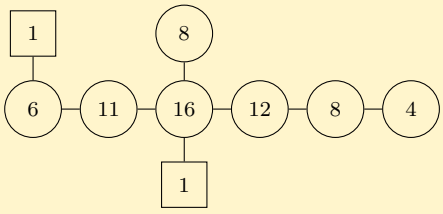	$A_3a + A_1a$	92
$E_6(a_3)$	$\begin{bmatrix} 0, & 0, & 0, & 0, & 0, -1, & 0 \\ 0, & 0, & 0, & 0, & 0, & 1, & 0 \end{bmatrix}_{4,6}$	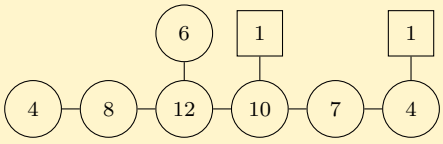	$A_3 + 2A_1$	94
D_5	$\begin{bmatrix} 0, & 0, & 0, & 0, -1, & 0, & 0 \\ 0, & 0, & 0, & 0, & 1, -1, & 0 \\ 0, & 0, & 0, & 0, & 0, & 1, & 0 \end{bmatrix}$	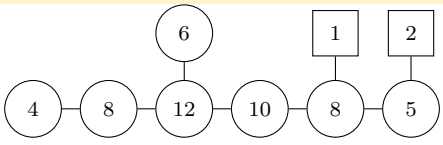	$A_3b + A_1b$	86

Table 8.2: Results for E_7

Orbit	Weights	Quiver	Dual orbit	d
$E_7(a_5)$	$[0, 0, 0, 0, 0, 0, 0]_2$ $[0, 0, 0, 0, 0, 0, 0]_5$	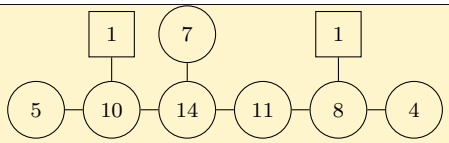	$2A_2 + A_1$	90
A_6	$[0, 0, 0, 0, 0, 0, -1]$ $[0, 0, 0, 0, 0, 0, 1]$	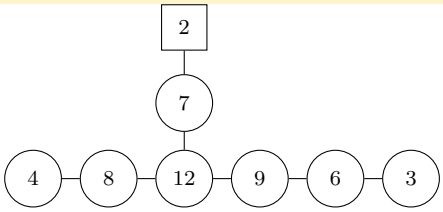	$A_2 + 3A_1$	84
$D_5 + A_1$	$[0, 0, 0, 0, -1, 0, 0]$ $[0, 0, 0, 0, 1, 0, 0]$	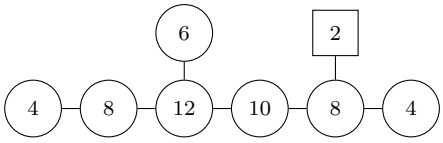	$2A_2$	84
$D_6(a_1)$	$[1, 0, 0, 0, 0, 0, 0]_1$ $[-1, 0, 0, 0, 0, 0, 0]_5$	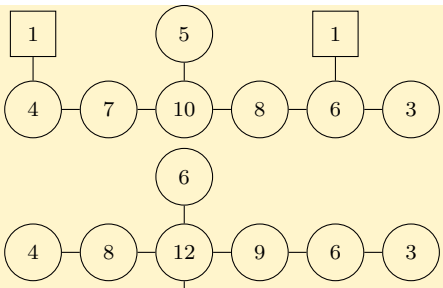	A_3	84
$E_7(a_4)$	$[0, 0, 0, 0, 0, 0, 0]_3$		$A_2 + 2A_1$	82
D_6	$[-1, 0, 0, 0, 0, 0, 0]$ $[1, 0, 0, 0, 0, 0, 0]$	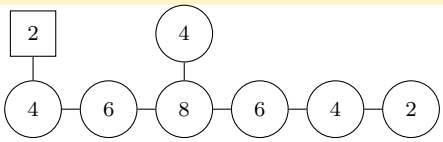	A_2	66
$E_6(a_1)$	$[0, 0, 0, 0, 0, 1, 0]_6$ $[0, 0, 0, 0, 0, -1, 0]_7$	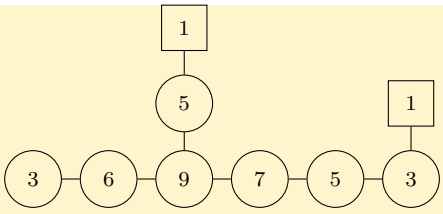	$4A_1$	70
E_6	$[0, 0, 0, 0, 0, -1, 0]$ $[0, 0, 0, 0, 0, 1, 0]$	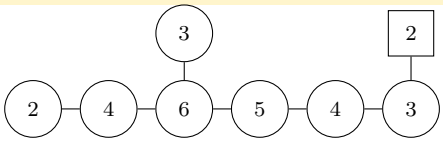	$3A_1b$	54
$E_7(a_3)$	$[0, 0, 0, 0, 0, 0, 0]_2$	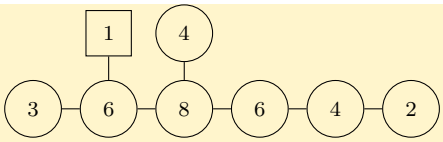	$3A_1a$	64

Table 8.2: Results for E_7

Orbit	Weights	Quiver	Dual orbit	d
$E_7(a_2)$	$[\ 0,\ 0,\ 0,\ 0,\ 0,\ 0,\ 0]_5$	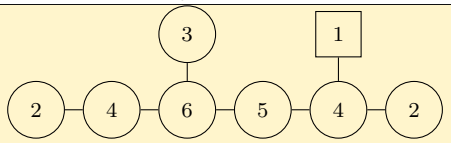	$2A_1$	52
$E_7(a_1)$	$[\ 0,\ 0,\ 0,\ 0,\ 0,\ 0,\ 0]_1$	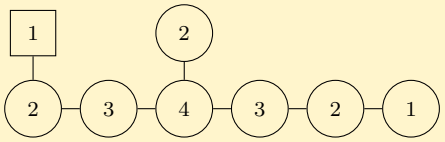	A_1	34

Table 8.3: Results for E_8

Orbit	Weights	Quiver	Dual orbit	d
0	$\begin{bmatrix} -1, & 0, & 0, & 0, & 0, & 0, & 0, & 0 \\ 1, & -1, & 1, & -1, & 0, & 0, & 0, & 0 \\ 0, & 1, & -1, & 1, & 0, & -1, & 0, & 0 \\ -1, & -1, & 1, & -1, & 0, & 1, & -1, & 0 \\ 1, & 2, & -2, & 1, & 0, & 0, & 1, & 0 \\ -1, & 0, & 0, & 1, & -1, & 0, & 0, & -1 \\ 1, & -1, & 0, & 0, & 1, & 0, & 0, & 1 \\ 0, & 0, & 2, & -2, & 0, & 0, & 0, & -1 \\ 0, & 0, & -1, & 1, & 0, & 0, & 0, & 1 \\ -1, & 0, & 0, & 0, & 0, & 0, & 0, & 0 \\ 1, & -1, & 1, & -1, & 0, & 0, & 0, & 0 \\ 0, & 1, & -1, & 1, & 0, & -1, & 0, & 0 \\ 0, & 1, & -1, & 0, & 0, & 1, & 0, & 0 \\ -1, & 0, & 0, & 1, & -1, & 0, & 0, & -1 \\ 1, & -1, & 0, & 0, & 1, & 0, & 0, & 1 \\ 0, & 0, & 2, & -2, & 0, & 0, & 0, & -1 \\ 0, & 0, & -1, & 1, & 0, & 0, & 0, & 1 \\ -1, & 0, & 0, & 0, & 0, & 0, & 0, & 0 \\ 1, & -1, & 1, & -1, & 0, & 0, & 0, & 0 \\ 0, & 1, & -1, & 1, & 0, & -1, & 0, & 0 \\ 0, & 1, & -1, & 0, & 0, & 1, & 0, & 0 \\ 0, & -1, & 0, & 1, & 0, & 0, & 0, & 0 \\ 0, & 0, & 2, & -2, & 0, & 0, & 0, & -1 \\ 0, & 0, & -1, & 1, & 0, & 0, & 0, & 1 \\ -1, & 0, & 0, & 0, & 0, & 0, & 0, & 0 \\ 1, & -1, & 1, & -1, & 0, & 0, & 0, & 0 \\ 0, & 1, & -1, & 1, & 0, & -1, & 0, & 0 \\ 0, & 1, & -1, & 0, & 0, & 1, & 0, & 0 \\ 0, & -1, & 0, & 1, & 0, & 0, & 0, & 0 \\ 0, & 0, & 1, & -1, & 0, & 0, & 0, & 0 \\ 2, & 0, & 0, & -1, & 0, & -1, & 0, & 0 \\ 0, & 0, & 0, & 0, & 0, & -1, & 0, & 0 \\ -1, & 0, & 0, & 0, & -1, & 3, & -1, & 0 \\ 0, & 0, & 0, & 0, & 2, & -2, & 0, & -1 \\ 0, & 0, & 0, & 0, & 0, & -1, & 1, & 0 \\ 0, & 0, & 0, & 0, & 0, & 0, & 1, & 0 \\ -1, & 0, & 0, & 1, & 0, & 0, & 0, & 0 \end{bmatrix}$	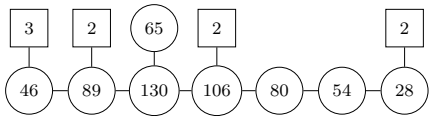	E_8	240
A_1	$\begin{bmatrix} -1, & 0, & 0, & 0, & 0, & 0, & 0, & 0 \\ 1, & -1, & 1, & -1, & 0, & 0, & 0, & 0 \\ 0, & 1, & -1, & 1, & 0, & -1, & 0, & 0 \\ 0, & 1, & -1, & 0, & 0, & 1, & 0, & 0 \\ -1, & 0, & 0, & 1, & -1, & 0, & 0, & -1 \\ 1, & -1, & 0, & 0, & 1, & 0, & 0, & 1 \\ 0, & 0, & 2, & -2, & 0, & 0, & 0, & -1 \\ 0, & 0, & -1, & 1, & 0, & 0, & 0, & 1 \\ -1, & 0, & 0, & 0, & 0, & 0, & 0, & 0 \\ 1, & -1, & 1, & -1, & 0, & 0, & 0, & 0 \\ 0, & 1, & -1, & 1, & 0, & -1, & 0, & 0 \\ 0, & 1, & -1, & 0, & 0, & 1, & 0, & 0 \\ 0, & -1, & 0, & 1, & 0, & 0, & 0, & 0 \\ 0, & 0, & 2, & -2, & 0, & 0, & 0, & -1 \\ 0, & 0, & -1, & 1, & 0, & 0, & 0, & 1 \\ -1, & 0, & 0, & 0, & 0, & 0, & 0, & 0 \\ 1, & -1, & 1, & -1, & 0, & 0, & 0, & 0 \\ 0, & 1, & -1, & 1, & 0, & -1, & 0, & 0 \\ 0, & 1, & -1, & 0, & 0, & 1, & 0, & 0 \\ 0, & -1, & 0, & 1, & 0, & 0, & 0, & 0 \\ 0, & 0, & 1, & -1, & 0, & 0, & 0, & 0 \\ 2, & 0, & 0, & -1, & 0, & -1, & 0, & 0 \\ 0, & 0, & 0, & 0, & 0, & -1, & 0, & 0 \\ -1, & 0, & 0, & 0, & -1, & 3, & -1, & 0 \\ 0, & 0, & 0, & 0, & 2, & -2, & 0, & -1 \\ 0, & 0, & 0, & 0, & 0, & -1, & 1, & 0 \\ 0, & 0, & 0, & 0, & 0, & 0, & 1, & 0 \\ -1, & 0, & 0, & 1, & 0, & 0, & 0, & 0 \end{bmatrix}$	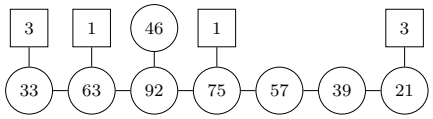	$E_8(a_1)$	238
$2A_1$	$\begin{bmatrix} -1, & 0, & 0, & 0, & 0, & 0, & 0, & 0 \\ 1, & -1, & 1, & -1, & 0, & 0, & 0, & 0 \\ 0, & 1, & -1, & 1, & 0, & -1, & 0, & 0 \\ 0, & 1, & -1, & 0, & 0, & 1, & 0, & 0 \\ 0, & -1, & 0, & 1, & 0, & 0, & 0, & 0 \\ 0, & 0, & 2, & -2, & 0, & 0, & 0, & -1 \\ 0, & 0, & -1, & 1, & 0, & 0, & 0, & 1 \\ -1, & 0, & 0, & 0, & 0, & 0, & 0, & 0 \\ 1, & -1, & 1, & -1, & 0, & 0, & 0, & 0 \\ 0, & 1, & -1, & 1, & 0, & -1, & 0, & 0 \\ 0, & 1, & -1, & 0, & 0, & 1, & 0, & 0 \\ 0, & -1, & 0, & 1, & 0, & 0, & 0, & 0 \\ 0, & 0, & 1, & -1, & 0, & 0, & 0, & 0 \\ 2, & 0, & 0, & -1, & 0, & -1, & 0, & 0 \\ 0, & 0, & 0, & 0, & 0, & -1, & 0, & 0 \\ -1, & 0, & 0, & 0, & -1, & 3, & -1, & 0 \\ 0, & 0, & 0, & 0, & 2, & -2, & 0, & -1 \\ 0, & 0, & 0, & 0, & 0, & -1, & 1, & 0 \\ 0, & 0, & 0, & 0, & 0, & 0, & 1, & 0 \\ -1, & 0, & 0, & 1, & 0, & 0, & 0, & 0 \end{bmatrix}$	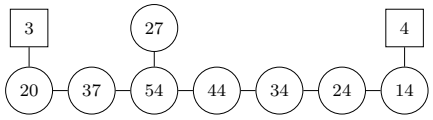	$E_8(a_2)$	236
$3A_1$	$\begin{bmatrix} -1, & 0, & 0, & 0, & 0, & 0, & 0, & 0 \\ 1, & -1, & 1, & -1, & 0, & 0, & 0, & 0 \\ 0, & 1, & -1, & 1, & 0, & -1, & 0, & 0 \\ 0, & 1, & -1, & 0, & 0, & 1, & 0, & 0 \\ 0, & -1, & 0, & 1, & 0, & 0, & 0, & 0 \\ 0, & 0, & 1, & -1, & 0, & 0, & 0, & 0 \\ 2, & 0, & 0, & -1, & 0, & -1, & 0, & 0 \\ 0, & 0, & 0, & 0, & 0, & -1, & 0, & 0 \\ -1, & 0, & 0, & 0, & -1, & 3, & -1, & 0 \\ 0, & 0, & 0, & 0, & 2, & -2, & 0, & -1 \\ 0, & 0, & 0, & 0, & 0, & -1, & 1, & 0 \\ 0, & 0, & 0, & 0, & 0, & 0, & 1, & 0 \\ -1, & 0, & 0, & 1, & 0, & 0, & 0, & 0 \end{bmatrix}$	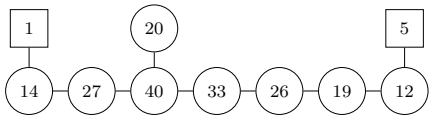	$E_8(a_3)$	234
A_2	$\begin{bmatrix} -1, & 0, & 0, & 0, & 0, & 0, & 0, & 0 \\ 1, & -1, & 1, & -1, & 0, & 0, & 0, & 0 \\ 0, & 1, & -1, & 1, & 0, & -1, & 0, & 0 \\ 0, & 1, & -1, & 0, & 0, & 1, & 0, & 0 \\ 0, & -1, & 0, & 1, & 0, & 0, & 0, & 0 \\ 0, & 0, & 2, & -2, & 0, & 0, & 0, & -1 \\ 0, & 0, & -1, & 1, & 0, & 0, & 0, & 1 \\ -1, & 0, & 0, & 0, & 0, & 0, & 0, & 0 \\ 1, & -1, & 1, & -1, & 0, & 0, & 0, & 0 \\ 0, & 1, & -1, & 1, & 0, & -1, & 0, & 0 \\ 0, & 1, & -1, & 0, & 0, & 1, & 0, & 0 \\ 0, & -1, & 0, & 1, & 0, & 0, & 0, & 0 \\ 0, & 0, & 1, & -1, & 0, & 0, & 0, & 0 \\ 2, & 0, & 0, & -1, & 0, & -1, & 0, & 0 \\ 0, & 0, & 0, & 0, & 0, & -1, & 0, & 0 \\ -1, & 0, & 0, & 0, & -1, & 3, & -1, & 0 \\ 0, & 0, & 0, & 0, & 2, & -2, & 0, & -1 \\ 0, & 0, & 0, & 0, & 0, & -1, & 1, & 0 \\ 0, & 0, & 0, & 0, & 0, & 0, & 1, & 0 \\ -1, & 0, & 0, & 1, & 0, & 0, & 0, & 0 \end{bmatrix}$	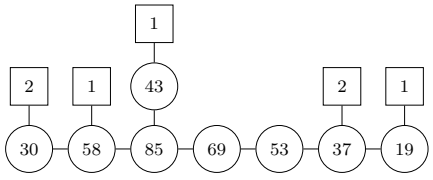	$E_8(a_3)$	234
$4A_1$	$\begin{bmatrix} 0, & -1, & 0, & 0, & 0, & -1, & 0, & 1 \\ 0, & -1, & 0, & 0, & 0, & -1, & 0, & 1 \\ 0, & 3, & 0, & -1, & 0, & 1, & 0, & -3 \\ 0, & -1, & 0, & 1, & 0, & 1, & 0, & 0 \\ 0, & 0, & 0, & 0, & 0, & 0, & 0, & 1 \end{bmatrix}$	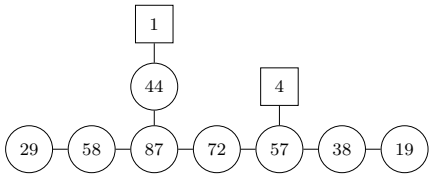	$E_8(a_4)$	232
$A_2 + A_1$	$\begin{bmatrix} 0, & 0, & 0, & -1, & 0, & 0, & 0, & 0 \\ 0, & 0, & 0, & 0, & -1, & 1, & 0, & 0 \\ -1, & 0, & 0, & 0, & 1, & -1, & 0, & 0 \\ 0, & 0, & 0, & 1, & -1, & 0, & 0, & 0 \\ 1, & 0, & 0, & 0, & 1, & 0, & 0, & -1 \\ 0, & 0, & 0, & 0, & 0, & 0, & 0, & 1 \end{bmatrix}$	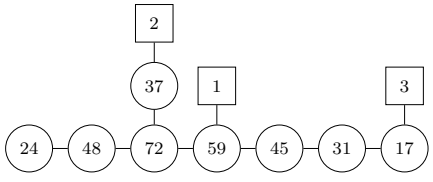	$E_8(a_4)$	232

Table 8.3: Results for E_8

Orbit	Weights	Quiver	Dual orbit	d
$A_2 + 2A_1$	$\begin{bmatrix} 0, & 0, & 1, & 0, -3, & 0, & 0, & 0] \\ [0, & 0, & 0, & 0, & 1, & 0, -1, & 0] \\ [0, & 0, & 0, & 0, & 1, & 0, & 0, -1] \\ [0, & 0, -1, & 0, & 1, & 0, & 0, & 1] \\ [0, & 0, & 0, & 0, & 0, & 1, & 0, & 0] \end{bmatrix}$	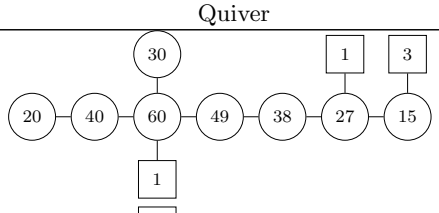	$E_8(b_4)$	230
A_3	$\begin{bmatrix} 2, & 0, & 0, -1, & 0, -1, & 0, & 0] \\ [0, & 0, & 0, & 0, & 0, -1, & 0, & 0] \\ [-1, & 0, & 0, & 0, -1, & 3, -1, & 0] \\ [0, & 0, & 0, & 0, & 1, -1, & 0, & 0] \\ [0, & 0, & 0, & 0, & 0, & 0, & 1, & 0] \\ [-1, & 0, & 0, & 1, & 0, & 0, & 0, & 0] \end{bmatrix}$	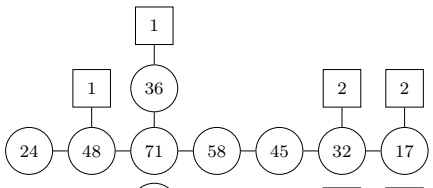	$E_7(a_1)$	228
$A_2 + 3A_1$	$\begin{bmatrix} 0, & 0, & 0, & 0, & 0, -1, & 0, & 0] \\ [0, & 1, & 0, -2, & 0, & 2, & 0, & 0] \\ [0, & 0, & 0, & 1, & 0, -1, & 0, & 0] \\ [0, -1, & 0, & 1, & 0, & 0, & 0, & 0] \end{bmatrix}$	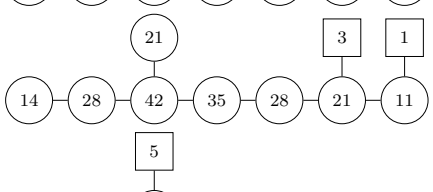	$E_8(a_5)$	228
$2A_2$	$\begin{bmatrix} 0, & 0, & 0, & 0, & 0, & 0, & 0, -1] \\ [0, & 0, & 0, & 0, & 0, & 0, & 0, -1] \\ [0, & 0, -2, & 0, & 0, & 2, -1, & 3] \\ [0, & 0, & 1, & 0, & 0, -2, & 1, & 0] \\ [0, & 0, & 1, & 0, & 0, & 0, & 0, -1] \end{bmatrix}$	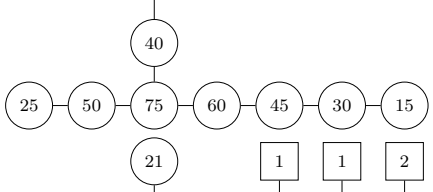	$E_8(a_5)$	228
$2A_2 + A_1$	$\begin{bmatrix} 0, & 0, -1, & 0, & 0, & 1, & 0, & 0] \\ [0, & 0, & 0, & 0, & 0, & 1, & 0, & 0] \\ [0, & 0, & 1, & 0, & 0, -1, & 0, -1] \\ [0, & 0, & 0, & 0, & 0, -1, & 0, & 1] \end{bmatrix}$	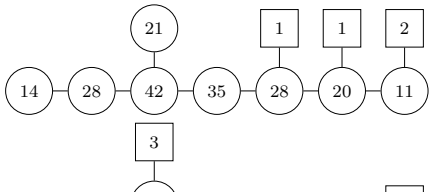	$E_8(b_5)$	226
$A_3 + A_1$	$\begin{bmatrix} 0, & 0, & 0, & 0, & 0, & 0, -1, & 0] \\ [0, & 0, & 0, & 0, & 0, & 1, & 0, -1] \\ [0, & 0, & 0, & 0, & 0, & 0, & 0, -1] \\ [0, & 0, & 0, & 1, & 0, -2, & 2, & 0] \\ [0, & 0, & 0, -1, & 0, & 1, -1, & 2] \end{bmatrix}$	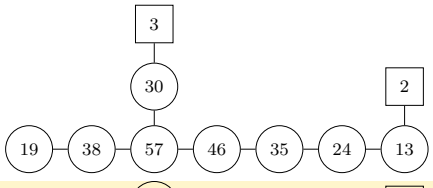	$E_8(b_5)$	226
$D_4(a_1)$	$\begin{bmatrix} 0, & 0, & 0, & 0, -1, & 1, & 0, & 0] \\ [0, & 0, & 0, & 0, & 0, & 0, & 1, & 0] \\ [0, & 0, & 0, & 0, & 0, & 1, -1, & 0] \\ [1, & 0, & 0, & 0, & 0, -1, & 0, & 0] \\ [-1, & 0, & 0, & 0, & 1, -1, & 0, & 0] \end{bmatrix}$	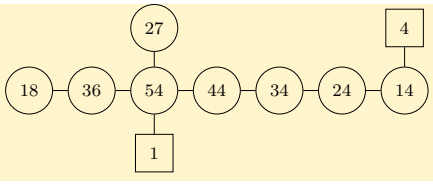	$E_8(b_5)$	226
D_4	$\begin{bmatrix} 0, & 0, & 0, & 0, & 0, & 0, -1, & 0] \\ [0, & 0, & 0, & 0, & 0, -1, & 1, & 0] \\ [-1, & 0, & 0, & 0, & 0, & 1, & 0, & 0] \\ [1, & 0, & 0, & 0, -1, & 1, & 0, & 0] \\ [0, & 0, & 0, & 0, & 1, -1, & 0, & 0] \end{bmatrix}$	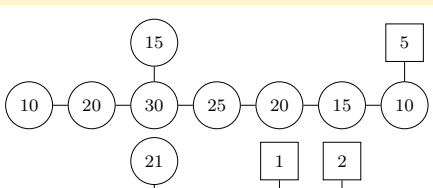	E_6	216
$2A_2 + 2A_1$	$\begin{bmatrix} 0, & 0, -1, & 0, & 0, & 1, & 0, & 0] \\ [0, & 0, & 1, & 0, & 0, -2, & 0, & 0] \\ [0, & 0, & 0, & 0, & 0, & 1, & 0, & 0] \end{bmatrix}$	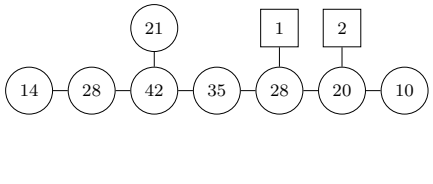	$E_8(a_6)$	224

Table 8.3: Results for E_8

Orbit	Weights	Quiver	Dual orbit	d
$A_3 + 2A_1$	$\begin{bmatrix} 0, & 0, & 0, & 1, & 0, & 0, & 0, -2] \\ [0, & 0, & 0, & 0, & 0, -1, & 0, & 0] \\ [0, & 0, & 0, -1, & 0, & 1, & 0, & 1] \\ [0, & 0, & 0, & 0, & 0, & 0, & 0, & 1] \end{bmatrix}$	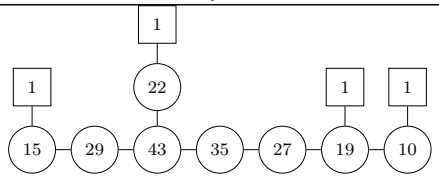	$E_8(a_6)$	224
$D_4(a_1)+A_1$	$\begin{bmatrix} 0, & 0, & 0, & 0, -1, & 1, & 0, & 0] \\ [0, & 0, & 0, & 0, & 0, & 1, & 0, & 0] \\ [1, & 0, & 0, & 0, & 0, -1, & 0, & 0] \\ [-1, & 0, & 0, & 0, & 1, -1, & 0, & 0] \end{bmatrix}$	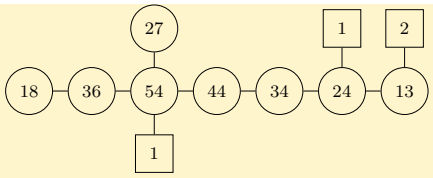	$E_8(a_6)$	224
$A_3 + A_2$	$\begin{bmatrix} 0, & 0, & 0, -1, & 0, & 0, & 0, & 1] \\ [0, & 0, & 0, & 1, & 0, & 0, & 0, -2] \\ [0, & 0, & 0, & 0, & 0, & 0, -1, & 1] \\ [0, & 0, & 0, & 0, & 0, & 1, & 0] \end{bmatrix}$	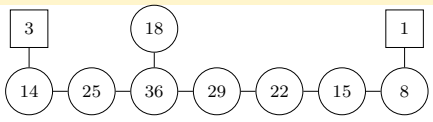	$D_7(a_1)$	222
A_4	$\begin{bmatrix} 0, & 0, & 0, & 0, & 0, & 0, & 0, -1] \\ [0, & 0, & 0, & 0, & 1, & 0, & 0, -2] \\ [0, & 0, & 0, & 0, & 1, -1, & -2, & 1] \\ [0, & 0, & 0, & 0, & 0, -2, & 3, & 1] \\ [0, & 0, & 0, & 0, -2, & 3, -1, & 1] \end{bmatrix}$	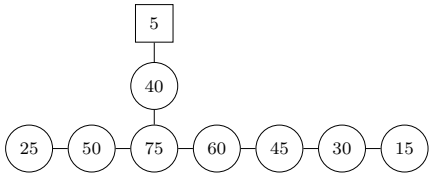	$E_7(a_3)$	220
$A_3+A_2+A_1$	$\begin{bmatrix} 0, -1, & 0, & 0, & 0, & 0, & 0, & 0] \\ [0, & 2, & 0, -1, & 0, & 0, & 0, & 0] \\ [0, -1, & 0, & 1, & 0, & 0, & 0, & 0] \end{bmatrix}$	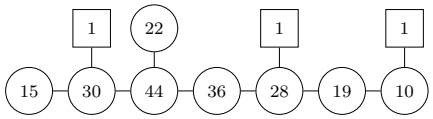	$E_8(b_6)$	220
$D_4 + A_1$	$\begin{bmatrix} -1, & 0, & 0, & 0, & 0, & 0, & 0, & 0] \\ [1, & 0, & 0, & 0, -1, & 0, & 0, & 0] \\ [0, & 0, & 0, & 0, & 1, & 0, -1, & 0] \\ [0, & 0, & 0, & 0, & 0, & 0, & 1, & 0] \end{bmatrix}$	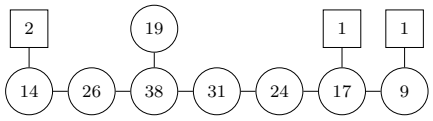	$E_6(a_1)$	214
$D_4(a_1)+A_2$	$\begin{bmatrix} 1, & 0, & 0, & 0, & 0, & 0, & 0, & 0] \\ [-1, & 0, & 0, & 0, & 1, & 0, & 0, & 0] \\ [0, & 0, & 0, & 0, -1, & 0, & 0, & 0] \end{bmatrix}$	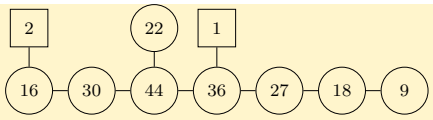	A_7	218
$A_4 + A_1$	$\begin{bmatrix} 0, & 0, & 0, & 0, -1, & 0, & 1, & 0] \\ [0, & 0, & 0, & 0, & 0, & 0, -1, & 0] \\ [0, & 0, & 0, & 0, & 1, & 0, & 0, -1] \\ [0, & 0, & 0, & 0, & 0, & 0, & 0, & 1] \end{bmatrix}$	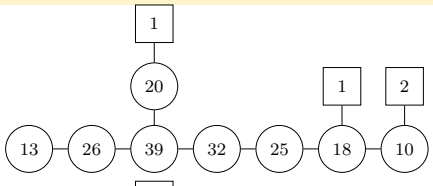	$E_6(a_1)+A_1$	218
$2A_3$	$\begin{bmatrix} 0, & 0, & 0, -1, & 0, & 0, & 0, & 1] \\ [0, & 0, & 0, & 1, & 0, & 0, & 0, -2] \\ [0, & 0, & 0, & 0, & 0, & 0, & 0, & 1] \end{bmatrix}$	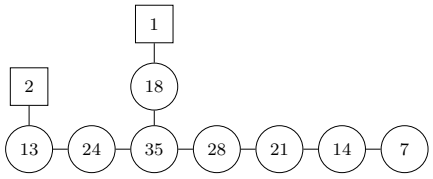	$D_7(a_2)$	216
$D_5(a_1)$	$\begin{bmatrix} 0, & 0, & 0, & 0, & 0, & 0, & 1, & 0] \\ [0, & 0, & 0, & 0, -1, & 2, -1, & 0] \\ [0, & 0, & 0, & 0, & 1, -1, & -1, & 0] \\ [0, & 0, & 0, & 0, & 0, -1, & 1, & 0] \end{bmatrix}$	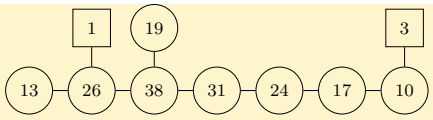	$E_6(a_1)$	214

Table 8.3: Results for E_8

Orbit	Weights	Quiver	Dual orbit	d
$A_4 + 2A_1$	$\begin{bmatrix} 0, & 1, -1, & 0, & 0, & 0, & 0, & 0, & 0 \\ 0, -1, & 0, & 0, & 0, & 0, & 0, & 0, & 0 \\ 0, & 0, & 1, & 0, & 0, & 0, & 0, & 0 \end{bmatrix}$	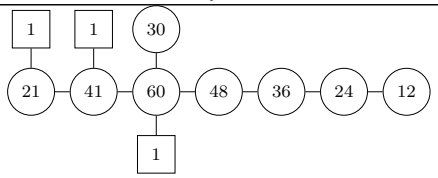	$D_7(a_2)$	216
$A_4 + A_2$	$\begin{bmatrix} 0, & 0, & 1, & 0, & 0, & 0, & 0, -2 \\ 0, & 0, -1, & 0, & 0, & 0, & 0, & 1 \\ 0, & 0, & 0, & 0, & 0, & 0, & 0, & 1 \end{bmatrix}$	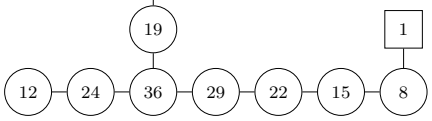	$D_5 + A_2$	214
A_5	$\begin{bmatrix} 0, & 0, & 0, & 0, & 0, & 0, -1, & 0 \\ 0, & 0, & 0, & 0, & 0, -1, & 1, & 0 \\ 0, & 0, & 0, & 0, & 0, & 1, & 0, -1 \\ 0, & 0, & 0, & 0, & 0, & 0, & 0, & 1 \end{bmatrix}$	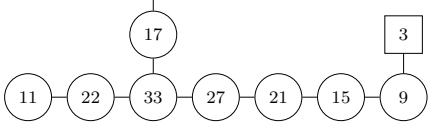	$D_6(a_1)$	210
$D_5(a_1) + A_1$	$\begin{bmatrix} 0, & 0, & 0, & 0, -1, & 0, & 1, & 0 \\ 0, & 0, & 0, & 0, & 1, & 0, & 0, & 0 \\ 0, & 0, & 0, & 0, & 0, & 0, -1, & 0 \end{bmatrix}$	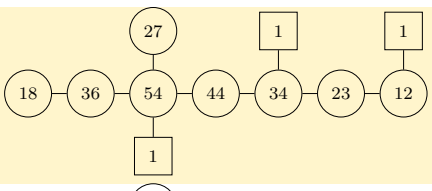	$E_7(a_4)$	212
$A_4 + A_2 + A_1$	$\begin{bmatrix} 0, & 0, -1, & 0, & 0, & 0, & 0, & 0 \\ 0, & 0, & 1, & 0, & 0, & 0, & 0, & 0 \end{bmatrix}$	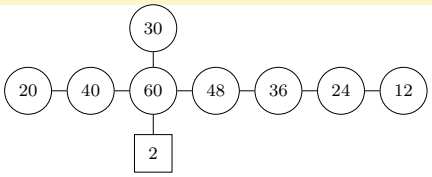	$A_6 + A_1$	212
$D_4 + A_2$	$\begin{bmatrix} -1, & 0, & 0, & 0, & 0, & 0, & 0, & 0 \\ 1, & 0, & 0, & 0, -1, & 0, & 0, & 0 \\ 0, & 0, & 0, & 0, & 1, & 0, & 0, & 0 \end{bmatrix}$	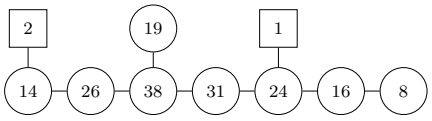	A_6	210
$E_6(a_3)$	$\begin{bmatrix} 0, & 0, & 0, & 0, & 0, -1, -1, & 0 \\ 0, & 0, & 0, & 0, & 0, & 1, & 0, & 0 \\ 0, & 0, & 0, & 0, & 0, & 0, & 1, & 0 \end{bmatrix}$	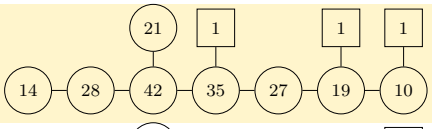	$D_5 + A_1$	208
D_5	$\begin{bmatrix} 0, & 0, & 0, & 0, & 0, & 0, -1, & 0 \\ 0, & 0, & 0, & 0, & 0, & 1, -2, & 1, & 0 \\ 0, & 0, & 0, & 0, & 0, -1, & 1, & 1, & 0 \\ 0, & 0, & 0, & 0, & 0, & 0, & 1, -1, & 0 \end{bmatrix}$	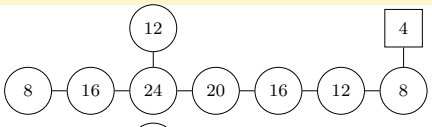	D_5	200
$A_4 + A_3$	$\begin{bmatrix} 0, & 0, & 0, -1, & 0, & 0, & 0, & 0 \\ 0, & 0, & 0, & 1, & 0, & 0, & 0, & 0 \end{bmatrix}$	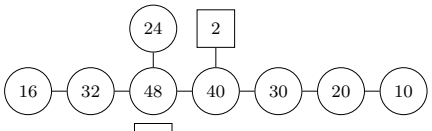	$E_8(a_7)$	208
$A_5 + A_1$	$\begin{bmatrix} 0, & 0, & 0, & 0, & 0, -1, & 0, & 0 \\ 0, & 0, & 0, & 0, & 0, & 1, & 0, -1 \\ 0, & 0, & 0, & 0, & 0, & 0, & 0, & 1 \end{bmatrix}$	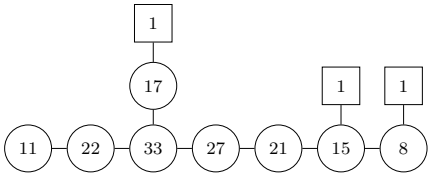	$E_8(a_7)$	208

Table 8.3: Results for E_8

Orbit	Weights	Quiver	Dual orbit	d
$D_5(a_1)+A_2$	$\begin{bmatrix} 0, & 0, & 0, & 0, & 0, & -1, & 0, & 0, & 0 \\ 0, & 0, & 0, & 0, & 0, & 1, & 0, & 0, & 0 \end{bmatrix}$	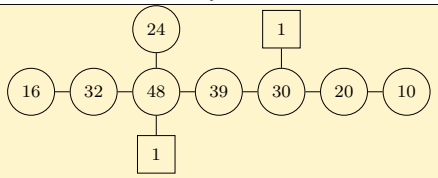	$E_7(a_5)$	206
$D_6(a_2)$	$\begin{bmatrix} 1, & 0, & 0, & 0, & 0, & 0, & 0, & 0, & 0 \\ -1, & 0, & 0, & 0, & 0, & 0, & -1, & 0, & 0 \\ 0, & 0, & 0, & 0, & 0, & 0, & 1, & 0, & 0 \end{bmatrix}$	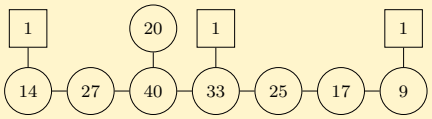	$D_5(a_1)+A_2$	202
$E_6(a_3)+A_1$	$\begin{bmatrix} 0, & 0, & 0, & 0, & 0, & 0, & -1, & 0, & 0 \\ 0, & 0, & 0, & 0, & 0, & 0, & 1, & 0, & 0 \end{bmatrix}$	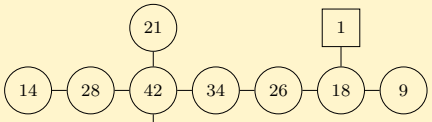	A_5+A_1	202
$E_7(a_5)$	$\begin{bmatrix} 0, & 0, & 0, & 0, & 0, & 0, & 0, & -1, & 0 \\ 0, & 0, & 0, & 0, & 0, & 0, & 0, & 1, & 0 \end{bmatrix}$	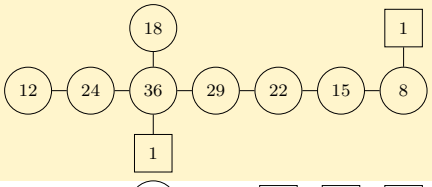	A_4+A_3	200
D_5+A_1	$\begin{bmatrix} 0, & 0, & 0, & 0, & -1, & 0, & 0, & 0 \\ 0, & 0, & 0, & 0, & 1, & 0, & -1, & 0 \\ 0, & 0, & 0, & 0, & 0, & 0, & 1, & 0 \end{bmatrix}$	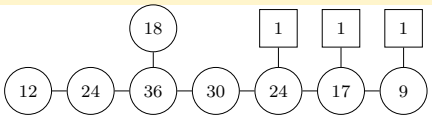	$E_6(a_3)$	198
$E_8(a_7)$	$\begin{bmatrix} 0, & 0, & 0, & 0, & 0, & 0, & 0, & 0 \\ 0, & 0, & 0, & 0, & 0, & 0, & 0, & 0 \end{bmatrix}$	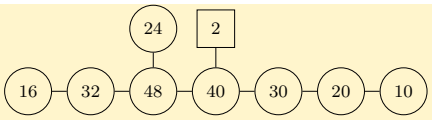	$E_8(a_7)$	208
A_6	$\begin{bmatrix} 0, & 0, & 0, & 0, & 0, & 0, & 0, & 1, & -1 \\ 0, & 0, & 0, & 0, & 0, & 0, & 0, & -1, & 0 \\ 0, & 0, & 0, & 0, & 0, & 0, & 0, & 0, & 1 \end{bmatrix}$	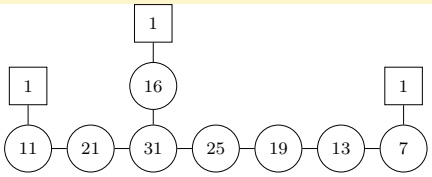	D_4+A_2	198
$D_6(a_1)$	$\begin{bmatrix} 1, & 0, & 0, & 0, & 0, & 0, & 0, & 0, & 0 \\ -1, & 0, & 0, & 0, & 0, & 0, & 0, & -1, & 0 \\ 0, & 0, & 0, & 0, & 0, & 0, & 0, & 1, & 0 \end{bmatrix}$	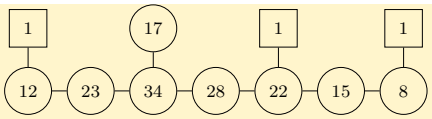	A_5	196
A_6+A_1	$\begin{bmatrix} 0, & -1, & 0, & 0, & 0, & 0, & 0, & 0 \\ 0, & 1, & 0, & 0, & 0, & 0, & 0, & 0 \end{bmatrix}$	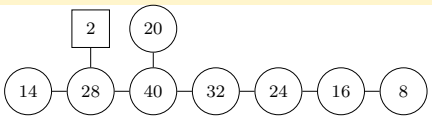	$A_4+A_2+A_1$	196
$E_7(a_4)$	$\begin{bmatrix} 0, & 0, & 0, & 0, & 0, & 0, & -1, & 0 \\ 0, & 0, & 0, & 0, & 0, & 0, & 1, & 0 \end{bmatrix}$	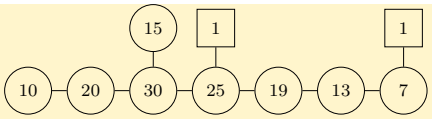	$D_5(a_1)+A_1$	196
$E_6(a_1)$	$\begin{bmatrix} 0, & 0, & 0, & 0, & 0, & 0, & -1, & 0 \\ 0, & 0, & 0, & 0, & 0, & 1, & 0, & 0 \\ 0, & 0, & 0, & 0, & 0, & -1, & 1, & 0 \end{bmatrix}$	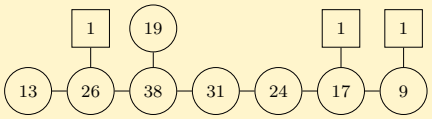	D_4+A_1	184

Table 8.3: Results for E_8

Orbit	Weights	Quiver	Dual orbit	d
$D_5 + A_2$	$\begin{bmatrix} 0, & 0, & 0, & 0, & 0, & -1, & 0, & 0, & 0 \\ 0, & 0, & 0, & 0, & 0, & 1, & 0, & 0, & 0 \end{bmatrix}$	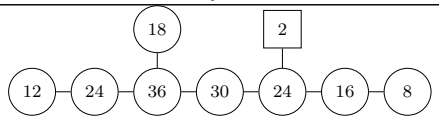	$A_4 + A_2$	194
D_6	$\begin{bmatrix} -1, & 0, & 0, & 0, & 0, & 0, & 0, & 0, & 0 \\ 1, & 0, & 0, & 0, & 0, & 0, & -1, & 0, & 0 \\ 0, & 0, & 0, & 0, & 0, & 0, & 1, & 0, & 0 \end{bmatrix}$	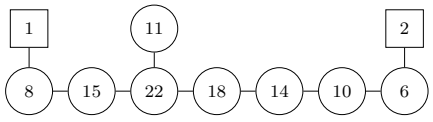	A_4	180
E_6	$\begin{bmatrix} 0, & 0, & 0, & 0, & 0, & -1, & 0, & 0 \\ 0, & 0, & 0, & 0, & 0, & 1, & -1, & 0 \\ 0, & 0, & 0, & 0, & 0, & 0, & 1, & 0 \end{bmatrix}$	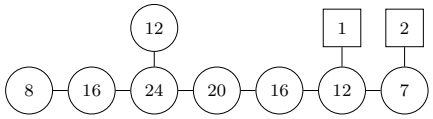	D_4	168
$D_7(a_2)$	$\begin{bmatrix} 1, & 0, & 0, & 0, & 0, & 0, & 0, & 0 \\ -1, & 0, & 0, & 0, & 0, & 0, & 0, & 0 \end{bmatrix}$	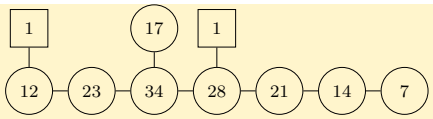	$2A_3$	188
A_7	$\begin{bmatrix} 0, & 0, & 0, & 0, & 0, & 0, & 0, & -1 \\ 0, & 0, & 0, & 0, & 0, & 0, & 0, & 1 \end{bmatrix}$	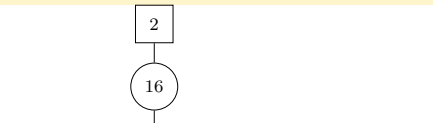	$D_4(a_1)+A_2$	184
$E_6(a_1)+A_1$	$\begin{bmatrix} 0, & 0, & 0, & 0, & 0, & -1, & 0, & 0 \\ 0, & 0, & 0, & 0, & 0, & 1, & 0, & 0 \end{bmatrix}$	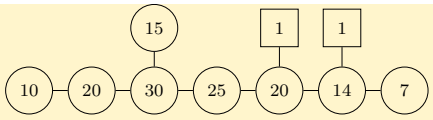	$A_4 + A_1$	188
$E_7(a_3)$	$\begin{bmatrix} 0, & 0, & 0, & 0, & 0, & 0, & -1, & 0 \\ 0, & 0, & 0, & 0, & 0, & 0, & 1, & 0 \end{bmatrix}$	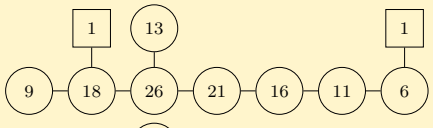	A_4	180
$E_8(b_6)$	$\begin{bmatrix} 0, & 0, & 0, & 0, & 0, & 0, & 0, & 0 \end{bmatrix}$	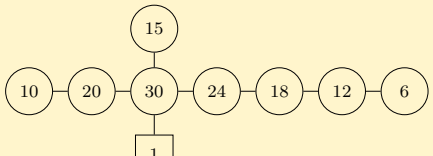	$A_3+A_2+A_1$	182
$D_7(a_1)$	$\begin{bmatrix} 1, & 0, & 0, & 0, & 0, & 0, & 0, & 0 \\ -1, & 0, & 0, & 0, & 0, & 0, & 0, & 0 \end{bmatrix}$	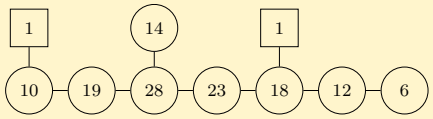	$A_3 + A_2$	178
$E_6 + A_1$	$\begin{bmatrix} 0, & 0, & 0, & 0, & 0, & -1, & 0, & 0 \\ 0, & 0, & 0, & 0, & 0, & 1, & 0, & 0 \end{bmatrix}$	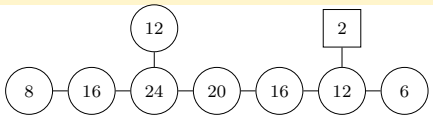	$D_4(A_1)$	166
$E_7(a_2)$	$\begin{bmatrix} 0, & 0, & 0, & 0, & 0, & 0, & -1, & 0 \\ 0, & 0, & 0, & 0, & 0, & 0, & 1, & 0 \end{bmatrix}$	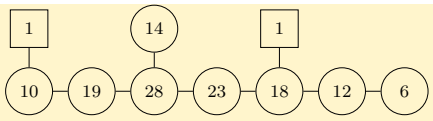	$A_3 + A_1$	164

Table 8.3: Results for E_8

Orbit	Weights	Quiver	Dual orbit	d
$E_8(a_6)$	[0, 0, 0, 0, 0, 0, 0, 0]	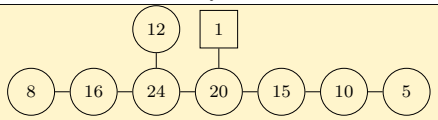	$2A_2 + 2A_1$	168
D_7	[−1, 0, 0, 0, 0, 0, 0, 0] [1, 0, 0, 0, 0, 0, 0, 0]	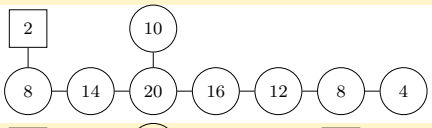	$2A_2$	156
$E_8(b_5)$	[0, 0, 0, 0, 0, 0, 0, 0] [0, 0, 0, 0, 0, 0, 0, 0]	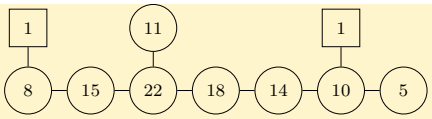	$2A_2 + A_1$	162
$E_7(a_1)$	[0, 0, 0, 0, 0, 0, 0, −1, 0] [0, 0, 0, 0, 0, 0, 0, 1, 0]	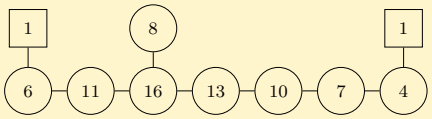	A_3	148
$E_8(a_5)$	[0, 0, 0, 0, 0, 0, 0, 0]	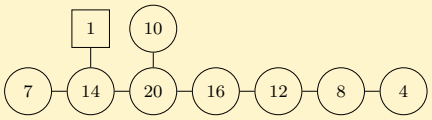	$A_2 + 3A_1$	154
$E_8(b_4)$	[0, 0, 0, 0, 0, 0, 0, 0]	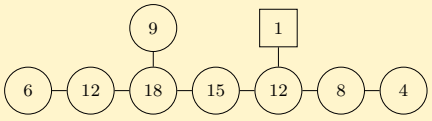	$A_2 + 2A_1$	146
E_7	[0, 0, 0, 0, 0, 0, 0, −1, 0] [0, 0, 0, 0, 0, 0, 0, 1, 0]	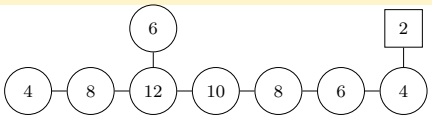	A_2	114
$E_8(a_4)$	[0, 0, 0, 0, 0, 0, 0, 0]	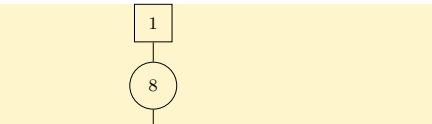	$4A_1$	128
$E_8(a_3)$	[0, 0, 0, 0, 0, 0, 0, 0]	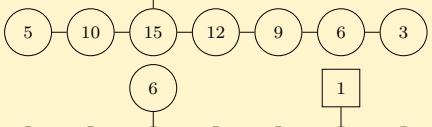	$3A_1$	112
$E_8(a_2)$	[0, 0, 0, 0, 0, 0, 0, 0]	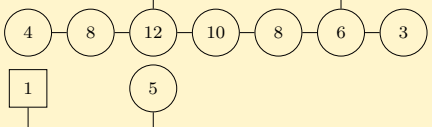	$2A_1$	92
$E_8(a_1)$	[0, 0, 0, 0, 0, 0, 0, 0]	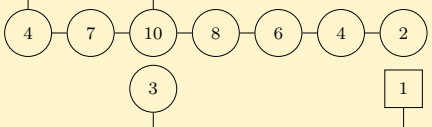	A_1	58

Chapter 9

Conclusions and Future Directions

In this thesis, we provided a classification of codimension 2 defects of the $(2,0)$ little string theory compactified on a Riemann surface. We showed that the defects are D5 branes wrapping certain 2-cycles of a resolved singularity in type IIB string theory. They are labeled by coweights of $\mathfrak{g}$, and have a low energy description as a 5d quiver gauge theory of type $\mathfrak{g}$. After going to root of the Higgs branch and introducing D3 branes, we proved that the partition function of the 5d theory is equal to the 3d partition function of the 3d theory on the D3 branes. We proved further that the partition function at this point of the moduli space is equal to a q-deformed conformal block of $\mathfrak{g}$-type Toda theory.

Taking the CFT limit $m_s \to \infty$, we showed that the Coulomb branch of any D5 brane defect flows to a nilpotent orbit of $\mathfrak{g}$, and derived the Bala–Carter classification of these orbits from Physics. We discussed the implications from the point of view of the Toda CFT. A related application is the string theory derivation of the description of surface defects due to Gukov and Witten, and its S-duality.

We think it is worthwhile to use our setup to answer a variety of problems. We list only a few here.

– As mentioned in 7.4, the introduction of D7 branes should give a perturbative handle on the description of 6d $(1,0)$ little string theories and CFTs. It would be crucial to make that statement precise.

– Introducing D9 branes naturally leads to small E_8 instanton physics, as can be shown by applying various dualities to our setup.

– Introducing D1 branes modifies the 5d partition function on the D5 branes in such a way that it becomes a qq-character of $\mathfrak{g}$, introduced recently in [127]. This is work in progress.

– Elliptic stable envelopes were defined in [30]. The envelopes provide boundary conditions for the 3d fields living on the D3 branes in the $(2,0)$ little string. It would be interesting to study these envelopes in the presence of D5 branes, for generic quiver gauge theories. One could hope to derive new dualities in the process.

– Related to the above point, let us mention that the results of this thesis are relevant to a correspondence known as geometric Langlands, which aims to prove an equivalence between specific categories associated to a connected complex Lie group and its Langlands

dual. This duality can be phrased in the context of two-dimensional conformal field theories on a Riemann surface: on one side, one considers the center of the affine Kac-Moody algebra $\widehat{{}^L\mathfrak{g}}$ at level ${}^Lk = -{}^Lh^\vee$; on the other side, one considers the classical W-algebra $\mathcal{W}_\infty(\mathfrak{g})$. Recently, a two-parameter deformation of the geometric Langlands correspondence has been proposed [31]: the first side of the duality becomes the quantum affine algebra $\mathcal{U}_\hbar(\widehat{{}^L\mathfrak{g}})$, a quantum deformation by the parameter $\hbar$ of the universal enveloping algebra of $\widehat{{}^L\mathfrak{g}}$. The other side becomes the W-algebra $\mathcal{W}_{q,t}(\mathfrak{g})$ mentioned above:

$$\mathcal{U}_\hbar(\widehat{{}^L\mathfrak{g}}) \longleftrightarrow \mathcal{W}_{q,t}(\mathfrak{g})$$

In particular, evidence was found that the conformal blocks of the two theories should be the same. A natural and important generalization is to introduce ramifications at points on the Riemann surface in this picture. These ramifications are nothing but the D5 branes we study in this thesis, so our results provide an explicit realization of the objects on the right-hand side of the duality. We leave it to future work to analyze the left-hand side and prove the correspondence with ramifications.

Appendix A

ADE Classification of Surface Singularities

A.1 Discrete Subgroups of $SU(2)$

Let Γ be a discrete group of $SU(2)$, and $(z_1, z_2) \in \mathbb{C}^2$.

The G-invariant polynomial functions make up a subalgebra called the invariant ring. In the case of Γ, the invariant ring is generated by three elements $(X, Y, Z) \in \mathbb{C}^3$, which satisfy a single relation $f(X, Y, Z) = 0$. The quotient structure of the algebraic ring $\mathbb{C}/\langle f \rangle$ is preserved by the isomorphism $(z_1, z_2) \to (X(z_1, z_2),\ Y(z_1, z_2),\ Z(z_1, z_2))$, and we can therefore identify:

$$\frac{\mathbb{C}}{\langle f \rangle} \simeq \frac{\mathbb{C}^2}{\Gamma} \tag{A.1.1}$$

Example A.1.1. *We consider the cyclic subgroup of $SU(2)$ of order $k+1$. The action of $\mathbb{Z}_{k+1}$ on $\mathbb{C}^2$ can be described by the generator $\xi_{k+1} \equiv \exp(2\pi i/(k+1))$, where ξ_{k+1} is a primitive $k+1$-th root of unity. Powers of ξ_{k+1} are irreducible representations of $\mathbb{Z}_{k+1}$; there*

Algebra	Γ	$\lvert\Gamma\rvert$	$f(X, Y, Z) = 0$
A_k	$\mathbb{Z}_{k+1}$	$k+1$	$X^2 + Y^2 + Z^{k+1} = 0$
D_k	$\mathbb{D}_{k-2}$	$4k-8$	$X^2 + Y^2\,Z + Z^{k-1} = 0$
E_6	$\mathbb{T}$	24	$X^2 + Y^3 + Z^4 = 0$
E_7	$\mathbb{O}$	48	$X^2 + Y^3 + Y\,Z^3 = 0$
E_8	$\mathbb{I}$	120	$X^2 + Y^3 + Z^5 = 0$

Table A.1: Relation between the finite subgroups Γ of $SU(2)$ and the corresponding orbifold singularity.

exists a two-dimensional reducible representation written in diagonal form as:

$$\begin{pmatrix} \xi_{k+1} & 0 \\ 0 & \xi_{k+1}^{-1} \end{pmatrix} \tag{A.1.2}$$

The orbits of $\mathbb{Z}_{k+1}$ *on* $\mathbb{C}^2$ *are* $(z_1, z_2) \sim (\xi_{k+1}\, z_1,\ \ \xi_{k+1}^{-1}\, z_2)$. *Let us define:*

$$U \equiv z_1^{k+1}\,, \tag{A.1.3}$$

$$V \equiv z_2^{k+1}\,, \tag{A.1.4}$$

$$Z \equiv z_1\, z_2\ . \tag{A.1.5}$$

The orbifold $\mathbb{C}^2/\mathbb{Z}_{k+1}$ *can then be described algebraically: we say that* U, V, Z *are the generators of the* $\mathbb{Z}_{k+1}$*-invariant polynomials, related to each other by the following constraint:*

$$U\, V = Z^{k+1}\ . \tag{A.1.6}$$

With the change of variables $U \equiv X + i\, Y$ and $V \equiv -X + i\, Y$, one obtains the first line of Table A.1.

A.2 McKay Correspondence and String Theory

As in the last section, let Γ be a finite subgroup of $SU(2)$. Let R_a be the irreducible representations of Γ, with associated characters χ_a, $a = 1, \ldots, k$. Let R be the faithful representation given by the embedding $\Gamma \to SU(2)$. The McKay graph associated to Γ is a quiver diagram of k nodes and n_{ab} lines from the node R_a to R_b, where n_{ab} can be obtained from the decomposition:

$$R \otimes R_a = \bigoplus_b n_{ab}\, R_b \tag{A.2.7}$$

Here, the graph is not oriented and $n_{ab} = n_{ba}$, though this is not the case for a more general finite group.

The McKay correspondence states that there is a one-to-one mapping between the McKay graph of Γ and the affine Dynkin diagram of the simply-laced Lie algebra labeling the associated singularity. We will not prove this statement, but choose instead to illustrate it below in the case of an A_k singularity. For more details, see [128].

Example A.2.1. *In the case where* $\Gamma = \mathbb{Z}_{k+1}$*, the faithful representation* R *given by the embedding* $\Gamma \to SU(2)$ *was written in the previous section:*

$$R = \begin{pmatrix} \xi & 0 \\ 0 & \xi^{-1} \end{pmatrix}\,, \qquad \xi^{k+1} = 1\ . \tag{A.2.8}$$

The one-dimensional irreducible representations are ξ^a*, with* $a = 1, \ldots, k$. *To get the McKay graph, we compute at once:*

$$R \otimes \xi^a = \begin{pmatrix} \xi & 0 \\ 0 & \xi^{-1} \end{pmatrix} \otimes \xi^a = \begin{pmatrix} \xi^{a+1} & 0 \\ 0 & \xi^{a-1} \end{pmatrix} \tag{A.2.9}$$

There are then k nodes in the McKay graph, where the a-th node is connected to the $(a-1)$-th and the $(a+1)$-th ones, see figure A.1 below. We recognize the Dynkin diagram of the affine Lie Algebra $\hat{A}_k$:

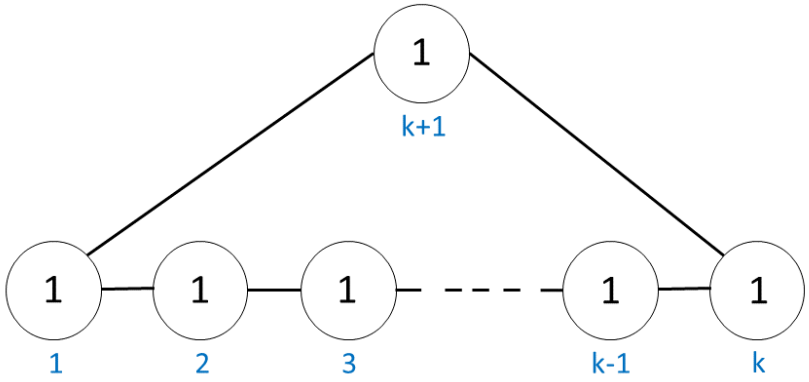

Figure A.1: The McKay graph for $\mathbb{Z}_{k+1}$ is the Dynkin diagram of the $\hat{A}_k$ affine Lie algebra. The label "1" inside the a-th node denotes the dimension of the a-th irreducible representation, and the label under node labels the power of ξ. With this convention, the $k+1$-th node denotes the generator $\xi^{k+1} = 1$, so the corresponding representation attached to this node is the identity.

So-called Asymptotically Locally Euclidean (ALE) spaces are ubiquitous in string theory. Indeed, they describe blowups of K3 singularities which are the ADE-orbifolds $\mathbb{C}^2/\Gamma$ we have been considering; these spaces are therefore natural backgrounds to compactify a string theory on. Most notably, Yang-Mills instantons and the metric can be computed explicitly on such ALE spaces using an ADHM construction [129].

In the seminal work [61], Douglas and Moore considered the compactification of type IIB string theory on such ALE spaces, and showed that by introducing D-branes, one obtains an effective field theory that probes the singular and the resolved geometry (see also [130]). Remarkably, the world-volume theory on the branes is not a $U(k)$ gauge theory, as one might have naively guessed, but rather a quiver gauge theory; the shape of the quiver is an ADE Dynkin diagram, corresponding to the choice of Γ dictated by the McKay correspondence. The gauge group is then of the form $\prod_{a=1}^{k} U(k_a)$, with k_a the dimension of the irreducible representation on the a-th node.

Appendix B

Null Weight Multiplicity

We make a comment about the multiplicity of the zero weight in unpolarized defects. This is for instance relevant for two of the E_n defects presented in the previous section 8.5: one has Bala–Carter label $E_7(a_5)$ in $\mathfrak{g} = E_7$, and the other has Bala–Carter label $E_8(b_5)$ in $\mathfrak{g} = E_8$. For both of these, $\mathcal{W}_{\mathcal{S}}$ is the set of the zero weight only, but appearing *twice*. In the little string, at finite m_s, defects add up in a linear fashion. If a subset of weights in $\mathcal{W}_{\mathcal{S}}$ adds up to zero, then one is simply describing more than one elementary defect. In the case of polarized defects, where a direct Toda interpretation is available, we would refer to this situation as a composite defect made up of two elementary defects. We note here that for the two unpolarized defects we mentioned, this is not the case. In both cases, the zero weight is required to appear twice and does characterize a single "exotic" defect, with Bala–Carter label given above. In particular, $E_7(a_5)$ and $E_8(b_5)$ are not engineered in the little string as the sum of two elementary defects with a single zero weight. See Figure B.1 for the example of $E_7(a_5)$.

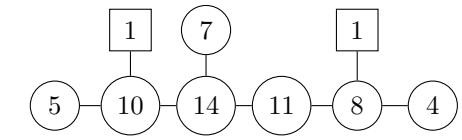

$\omega_1 : [0,0,0,0,0,0,0]$
$\omega_2 : [0,0,0,0,0,0,0]$

Bala–Carter label: $E_7(a_5)$

Coulomb dim. of T^{4d}: 45

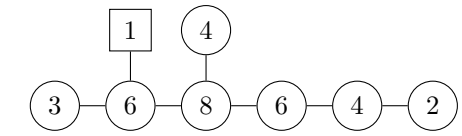

$\omega_1 : [0,0,0,0,0,0,0]$

Bala–Carter label: $E_7(a_3)$

Coulomb dim. of T^{4d}: 32

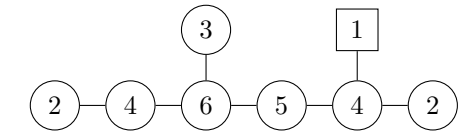

$\omega_2 : [0,0,0,0,0,0,0]$

Bala–Carter label: $E_7(a_2)$

Coulomb dim. of T^{4d}: 26

Figure B.1: In the little string, at finite m_s, defects add up in a linear fashion. For instance, the E_7 defect shown on top is the sum of the two defects shown under it. For polarized defects, we usually refer to this situation as two punctures on the cylinder, each labeled by the zero weight. However, in the $m_s \to \infty$, the defect really should be thought of as a single "exotic" puncture on the cylinder, given by a combination of the two zero weights, which cannot be split apart. As a quick check, this is confirmed by noting that the Coulomb branch dimension of T^{4d} is not additive.

Appendix C

Explicit Construction of A_n Little String Defects as Weighted Dynkin Diagrams

Many of the little string quivers T^{5d} of A_n are not weighted Dynkin diagrams (and there is no a priori reason why they should be).

However, as reviewed in Section 7.2, we can use the fact that a weight in a fundamental representation can always be written as the sum of new weights in possibly different fundamental representations. As we argued, in the context of brane engineering of A_n theories, this weight addition procedure reproduces Hanany–Witten transitions.

It turns out that all A_n little string quivers that are not symmetric under $\mathbb{Z}_2$ reflection can in fact be uniquely written as weighted Dynkin diagrams with correct Bala–Carter label after such a weight addition procedure. For instance, one can show that the full puncture of A_n, with Bala–Carter label $\varnothing$, can be symmetrized uniquely to give the weighted Dynkin diagram $(2, 2, \ldots, 2, 2)$. See figures C.2 and C.3.

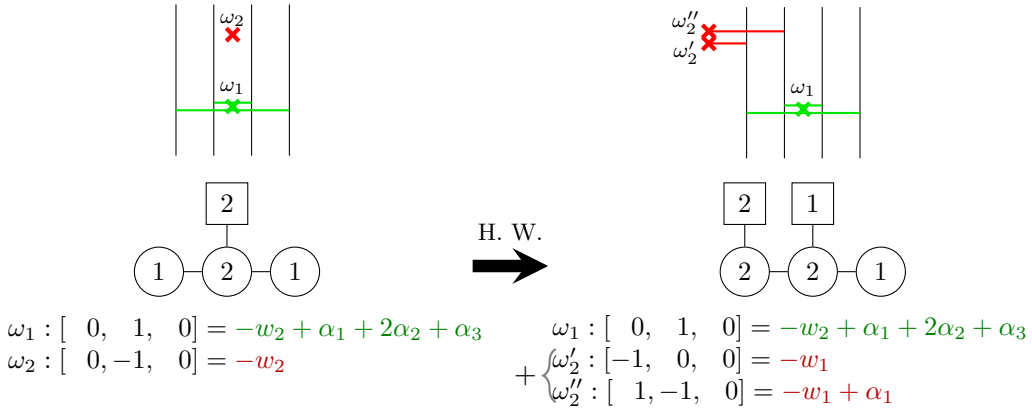

Figure C.1: Writing a weight in a fundamental representation of $\mathfrak{g}$ as a sum of several weights in (possibly different) fundamental representations results in the same theory at the root of the Higgs branch of T^{5d}. In the context of brane engineering, when $\mathfrak{g} = A_n$, this is the familiar Hanany–Witten transition [2]. In this example, we rewrite $[0, -1, 0]$ as the sum $[-1, 0, 0] + [1, -1, 0]$. As a result, the extra Coulomb parameter α_1 on the right is frozen to the value of the mass parameters denoted by ω_2' (and ω_2'').

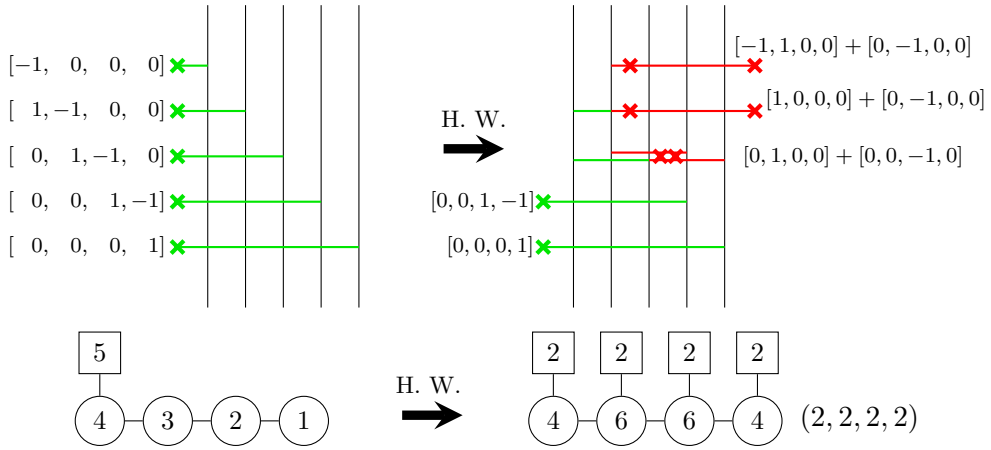

Figure C.2: An example of how one symmetrizes a little string quiver of A_n using Hanany-Witten transitions, to end up with a weighted Dynkin diagram. The Coulomb parameters in red are frozen, and therefore do not increase the Coulomb branch dimension. In this example, no matter what the details of the transition are, the resulting symmetric quiver is always (2,2,2,2), the full puncture. Note some of the masses are equal to each other in the resulting quiver, as they should after the transition.

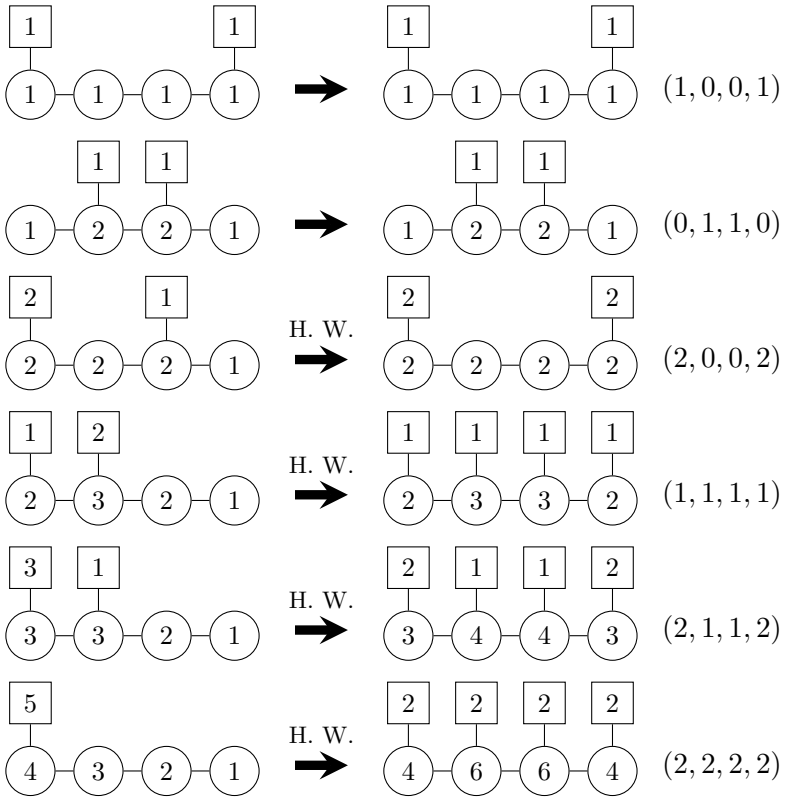

Figure C.3: Either directly, or after Hanany–Witten transitions to symmetrize the theories, the little string quivers (left) are precisely the weighted Dynkin diagrams of $\mathfrak{g}$ (right); the integers $0, 1, 2$ then get an interpretation as flavor symmetry ranks. Shown above is the case $\mathfrak{g} = A_4$.

Bibliography

[1] Sergei Gukov and Edward Witten. Gauge Theory, Ramification, And The Geometric Langlands Program. 2006.

[2] Amihay Hanany and Edward Witten. Type IIB superstrings, BPS monopoles, and three-dimensional gauge dynamics. *Nucl. Phys.*, B492:152–190, 1997.

[3] Edward Witten. Solutions of four-dimensional field theories via M theory. *Nucl.Phys.*, B500:3–42, 1997.

[4] Davide Gaiotto. N=2 dualities. *JHEP*, 08:034, 2012.

[5] Davide Gaiotto, Gregory W. Moore, and Andrew Neitzke. Wall-crossing, Hitchin Systems, and the WKB Approximation. 2009.

[6] Edward Witten. Geometric Langlands From Six Dimensions. 2009.

[7] Edward Witten. Fivebranes and Knots. 2011.

[8] Luis F. Alday, Davide Gaiotto, and Yuji Tachikawa. Liouville Correlation Functions from Four-dimensional Gauge Theories. *Lett. Math. Phys.*, 91:167–197, 2010.

[9] V.A. Fateev and A.V. Litvinov. On AGT conjecture. *JHEP*, 1002:014, 2010.

[10] Vasyl A. Alba, Vladimir A. Fateev, Alexey V. Litvinov, and Grigory M. Tarnopolskiy. On combinatorial expansion of the conformal blocks arising from AGT conjecture. *Lett.Math.Phys.*, 98:33–64, 2011.

[11] Niclas Wyllard. A(N-1) conformal Toda field theory correlation functions from conformal N = 2 SU(N) quiver gauge theories. *JHEP*, 0911:002, 2009.

[12] Shoichi Kanno, Yutaka Matsuo, Shotaro Shiba, and Yuji Tachikawa. N=2 gauge theories and degenerate fields of Toda theory. *Phys.Rev.*, D81:046004, 2010.

[13] Christoph A. Keller, Noppadol Mekareeya, Jaewon Song, and Yuji Tachikawa. The ABCDEFG of Instantons and W-algebras. *JHEP*, 03:045, 2012.

[14] Jrg Teschner. Exact results on N=2 supersymmetric gauge theories. 2014.

[15] A. Braverman, M. Finkelberg, and H. Nakajima. Instanton moduli spaces and $\mathscr W$-algebras. *ArXiv e-prints*, June 2014.

[16] W. Nahm. Supersymmetries and their Representations. *Nucl. Phys.*, B135:149, 1978. [,7(1977)].

[17] Mans Henningson. Self-dual strings in six dimensions: Anomalies, the ADE-classification, and the world-sheet WZW-model. *Commun. Math. Phys.*, 257:291–302, 2005.

[18] Nathan Seiberg. New theories in six-dimensions and Matrix description of M theory on T^5 and $T^5/\mathbb{Z}_2$. *Phys. Lett.*, B408:98–104, 1997.

[19] Edward Witten. Some comments on string dynamics. In *Future perspectives in string theory. Proceedings, Conference, Strings'95, Los Angeles, USA, March 13-18, 1995*, 1995.

[20] Andrei Losev, Gregory W. Moore, and Samson L. Shatashvili. M & m's. *Nucl. Phys.*, B522:105–124, 1998.

[21] Ofer Aharony. A Brief review of 'little string theories'. *Class. Quant. Grav.*, 17:929–938, 2000.

[22] Jungmin Kim, Seok Kim, and Kimyeong Lee. Little strings and T-duality. *JHEP*, 02:170, 2016.

[23] Lakshya Bhardwaj, Michele Del Zotto, Jonathan J. Heckman, David R. Morrison, Tom Rudelius, and Cumrun Vafa. F-theory and the Classification of Little Strings. *Phys. Rev.*, D93(8):086002, 2016.

[24] Michele Del Zotto, Cumrun Vafa, and Dan Xie. Geometric engineering, mirror symmetry and $6\mathrm{d}_{(1,0)} \to 4\mathrm{d}_{(\mathcal{N}=2)}$. *JHEP*, 11:123, 2015.

[25] Ying-Hsuan Lin, Shu-Heng Shao, Yifan Wang, and Xi Yin. Interpolating the Coulomb Phase of Little String Theory. *JHEP*, 12:022, 2015.

[26] Stefan Hohenegger, Amer Iqbal, and Soo-Jong Rey. Dual Little Strings from F-Theory and Flop Transitions. *JHEP*, 07:112, 2017.

[27] Mina Aganagic and Nathan Haouzi. ADE Little String Theory on a Riemann Surface (and Triality). 2015.

[28] Stefan Hohenegger, Amer Iqbal, and Soo-Jong Rey. Instanton-monopole correspondence from M-branes on $\mathbb{S}^1$ and little string theory. *Phys. Rev.*, D93(6):066016, 2016.

[29] Stefan Hohenegger, Amer Iqbal, and Soo-Jong Rey. Self-Duality and Self-Similarity of Little String Orbifolds. *Phys. Rev.*, D94(4):046006, 2016.

[30] Mina Aganagic and Andrei Okounkov. Elliptic stable envelope. 2016.

[31] Mina Aganagic, Edward Frenkel, and Andrei Okounkov. Quantum q-Langlands Correspondence. 2017.

[32] Brice Bastian, Stefan Hohenegger, Amer Iqbal, and Soo-Jong Rey. Dual Little Strings and their Partition Functions. 2017.

[33] Brice Bastian, Stefan Hohenegger, Amer Iqbal, and Soo-Jong Rey. Triality in Little String Theories. 2017.

[34] Babak Haghighat, Amer Iqbal, Can Kozaz, Guglielmo Lockhart, and Cumrun Vafa. M-Strings. *Commun. Math. Phys.*, 334(2):779–842, 2015.

[35] Nathan Haouzi and Christian Schmid. Little String Defects and Bala-Carter Theory. 2016.

[36] Nathan Haouzi and Can Kozaz. The ABCDEFG of Little Strings. 2017.

[37] Gregory W. Moore, Nikita Nekrasov, and Samson Shatashvili. Integrating over Higgs branches. *Commun. Math. Phys.*, 209:97–121, 2000.

[38] A. Losev, N. Nekrasov, and Samson L. Shatashvili. Testing Seiberg-Witten solution. pages 359–372, 1997.

[39] Nikita A. Nekrasov. Seiberg-Witten prepotential from instanton counting. *Adv.Theor.Math.Phys.*, 7:831–864, 2004.

[40] Nikita Nekrasov and Andrei Okounkov. Seiberg-Witten theory and random partitions. 2003.

[41] Nikita Nekrasov and Vasily Pestun. Seiberg-Witten geometry of four dimensional N=2 quiver gauge theories. 2012.

[42] Nikita Nekrasov, Vasily Pestun, and Samson Shatashvili. Quantum geometry and quiver gauge theories. 2013.

[43] E. Frenkel and N. Reshetikhin. Deformations of W-algebras associated to simple Lie algebras. In *eprint arXiv:q-alg/9708006*, page 8006, August 1997.

[44] Mina Aganagic, Nathan Haouzi, Can Kozcaz, and Shamil Shakirov. Gauge/Liouville Triality. 2013.

[45] Mina Aganagic, Nathan Haouzi, and Shamil Shakirov. A_n-Triality. 2014.

[46] Oscar Chacaltana, Jacques Distler, and Yuji Tachikawa. Nilpotent orbits and codimension-two defects of 6d $\mathcal{N} = (2, 0)$ theories. *Int. J. Mod. Phys.*, A28:1340006, 2013.

[47] Oscar Chacaltana and Jacques Distler. Tinkertoys for Gaiotto Duality. *JHEP*, 11:099, 2010.

[48] Oscar Chacaltana and Jacques Distler. Tinkertoys for the D_N series. *JHEP*, 02:110, 2013.

[49] Oscar Chacaltana, Jacques Distler, and Anderson Trimm. Tinkertoys for the Twisted D-Series. 2013.

[50] Oscar Chacaltana, Jacques Distler, and Anderson Trimm. Tinkertoys for the E_6 theory. *JHEP*, 09:007, 2015.

[51] Oscar Chacaltana, Jacques Distler, and Anderson Trimm. Tinkertoys for the Twisted E_6 Theory. *JHEP*, 04:173, 2015.

[52] Oscar Chacaltana, Jacques Distler, and Anderson Trimm. Tinkertoys for the Z3-twisted D4 Theory. 2016.

[53] Oscar Chacaltana, Jacques Distler, and Yuji Tachikawa. Gaiotto duality for the twisted A_{2N1} series. *JHEP*, 05:075, 2015.

[54] Nathan Haouzi and Christian Schmid. Little String Origin of Surface Defects. *JHEP*, 05:082, 2017.

[55] Sergei Gukov and Edward Witten. Rigid Surface Operators. *Adv. Theor. Math. Phys.*, 14(1):87–178, 2010.

[56] Cumrun Vafa. Geometric origin of Montonen-Olive duality. *Adv. Theor. Math. Phys.*, 1:158–166, 1998.

[57] T. A. Springer. The unipotent variety of a semi-simple group. In *Algebraic Geometry (Internat. Colloq., Tata Inst. Fund. Res., Bombay, 1968)*, pages 373–391. Oxford Univ. Press, London, 1969.

[58] Robert Steinberg. On the desingularization of the unipotent variety. *Invent. Math.*, 36:209–224, 1976.

[59] Baohua Fu. Symplectic resolutions for nilpotent orbits. *Invent. Math.*, 151(1):167–186, 2003.

[60] Michele Del Zotto, Jonathan J. Heckman, Daniel S. Park, and Tom Rudelius. On the Defect Group of a 6D SCFT. 2015.

[61] Michael R. Douglas and Gregory W. Moore. D-branes, quivers, and ALE instantons. 1996.

[62] Andrei S. Losev, Andrei Marshakov, and Nikita A. Nekrasov. Small instantons, little strings and free fermions. 2003.

[63] Oren Bergman and Gabi Zafrir. Lifting 4d dualities to 5d. *JHEP*, 04:141, 2015.

[64] Hirotaka Hayashi, Yuji Tachikawa, and Kazuya Yonekura. Mass-deformed T_N as a linear quiver. *JHEP*, 02:089, 2015.

[65] Albion E. Lawrence and Nikita Nekrasov. Instanton sums and five-dimensional gauge theories. *Nucl.Phys.*, B513:239–265, 1998.

[66] Dan Xie and Kazuya Yonekura. The moduli space of vacua of $\mathcal{N} = 2$ class $\mathcal{S}$ theories. *JHEP*, 1410:134, 2014.

[67] Shamit Kachru and John McGreevy. Supersymmetric three cycles and supersymmetry breaking. *Phys.Rev.*, D61:026001, 2000.

[68] Nikita A. Nekrasov. Seiberg-Witten prepotential from instanton counting. *Adv. Theor. Math. Phys.*, 7(5):831–864, 2003.

[69] Nikita Nekrasov, Vasily Pestun, and Samson Shatashvili. Quantum geometry and quiver gauge theories. 2013.

[70] Nikita Nekrasov and Vasily Pestun. Seiberg-Witten geometry of four dimensional $\mathcal{N} = 2$ quiver gauge theories. 2012.

[71] Taro Kimura and Vasily Pestun. Fractional quiver W-algebras. 2017.

[72] H. Nakajima. Handsaw quiver varieties and finite W-algebras. *ArXiv e-prints*, July 2011.

[73] Sergey Shadchin. On F-term contribution to effective action. *JHEP*, 08:052, 2007.

[74] Christopher Beem, Tudor Dimofte, and Sara Pasquetti. Holomorphic Blocks in Three Dimensions. *JHEP*, 12:177, 2014.

[75] Naofumi Hama, Kazuo Hosomichi, and Sungjay Lee. SUSY Gauge Theories on Squashed Three-Spheres. *JHEP*, 05:014, 2011.

[76] Anton Kapustin and Brian Willett. Generalized Superconformal Index for Three Dimensional Field Theories. 2011.

[77] Edward Frenkel and Nicolai Reshetikhin. Deformations of $\mathcal{W}$-algebras associated to simple Lie algebras. *Comm. Math. Phys.*, 197(1):1–32, 1998.

[78] Peter Bouwknegt and Kareljan Schoutens. W symmetry in conformal field theory. *Phys. Rept.*, 223:183–276, 1993.

[79] V. S. Dotsenko and V. A. Fateev. Conformal Algebra and Multipoint Correlation Functions in Two-Dimensional Statistical Models. *Nucl. Phys.*, B240:312, 1984.

[80] Robbert Dijkgraaf and Cumrun Vafa. Toda Theories, Matrix Models, Topological Strings, and N=2 Gauge Systems. 2009.

[81] Hiroshi Itoyama, Kazunobu Maruyoshi, and Takeshi Oota. The Quiver Matrix Model and 2d-4d Conformal Connection. *Prog. Theor. Phys.*, 123:957–987, 2010.

[82] A. Mironov, A. Morozov, and Sh. Shakirov. Conformal blocks as Dotsenko-Fateev Integral Discriminants. *Int. J. Mod. Phys.*, A25:3173–3207, 2010.

[83] A. Morozov and S. Shakirov. The matrix model version of AGT conjecture and CIV-DV prepotential. *JHEP*, 08:066, 2010.

[84] Kazunobu Maruyoshi. β-Deformed Matrix Models and 2d/4d Correspondence. pages 121–157, 2016.

[85] V. A. Fateev and A. V. Litvinov. Correlation functions in conformal Toda field theory. I. *JHEP*, 11:002, 2007.

[86] N. Dorey. The BPS spectra of two-dimensional supersymmetric gauge theories with twisted mass terms. *JHEP*, 9811:005, 1998.

[87] Heng-Yu Chen, Nick Dorey, Timothy J. Hollowood, and Sungjay Lee. A New 2d/4d Duality via Integrability. *JHEP*, 1109:040, 2011.

[88] Nick Dorey, Sungjay Lee, and Timothy J. Hollowood. Quantization of Integrable Systems and a 2d/4d Duality. *JHEP*, 1110:077, 2011.

[89] Mina Aganagic and Shamil Shakirov. Gauge/Vortex duality and AGT. 2014.

[90] Nikita A. Nekrasov and Samson L. Shatashvili. Supersymmetric vacua and Bethe ansatz. *Nucl. Phys. Proc. Suppl.*, 192-193:91–112, 2009.

[91] Nikita A. Nekrasov and Samson L. Shatashvili. Quantum integrability and supersymmetric vacua. *Prog.Theor.Phys.Suppl.*, 177:105–119, 2009.

[92] Nikita A. Nekrasov and Samson L. Shatashvili. Quantization of Integrable Systems and Four Dimensional Gauge Theories. 2009.

[93] Robbert Dijkgraaf and Cumrun Vafa. Matrix models, topological strings, and supersymmetric gauge theories. *Nucl.Phys.*, B644:3–20, 2002.

[94] Robbert Dijkgraaf and Cumrun Vafa. On geometry and matrix models. *Nucl.Phys.*, B644:21–39, 2002.

[95] Robbert Dijkgraaf and Cumrun Vafa. A Perturbative window into nonperturbative physics. 2002.

[96] F. Cachazo, S. Katz, and C. Vafa. Geometric transitions and N=1 quiver theories. 2001.

[97] Nikita Nekrasov and Edward Witten. The Omega Deformation, Branes, Integrability, and Liouville Theory. *JHEP*, 1009:092, 2010.

[98] Vyjayanthi Chari and Andrew Pressley. Quantum affine algebras and their representations. 1994.

[99] A. Malcev. On the representation of an algebra as a direct sum of the radical and a semi-simple subalgebra. *C. R. (Doklady) Acad. Sci. URSS (N.S.)*, 36:42–45, 1942.

[100] David H. Collingwood and William M. McGovern. *Nilpotent orbits in semisimple Lie algebras*. Van Nostrand Reinhold Mathematics Series. Van Nostrand Reinhold Co., New York, 1993.

[101] Nicolas Spaltenstein. *Classes unipotentes et sous-groupes de Borel*, volume 946 of *Lecture Notes in Mathematics*. Springer-Verlag, Berlin-New York, 1982.

[102] P. Bala and R. W. Carter. Classes of unipotent elements in simple algebraic groups. I. *Math. Proc. Cambridge Philos. Soc.*, 79(3):401–425, 1976.

[103] P. Bala and R. W. Carter. Classes of unipotent elements in simple algebraic groups. II. *Math. Proc. Cambridge Philos. Soc.*, 80(1):1–17, 1976.

[104] V. V. Morozov. On a nilpotent element in a semi-simple Lie algebra. *C. R. (Doklady) Acad. Sci. URSS (N.S.)*, 36:83–86, 1942.

[105] Nathan Jacobson. Completely reducible Lie algebras of linear transformations. *Proc. Amer. Math. Soc.*, 2:105–113, 1951.

[106] Amihay Hanany and Rudolph Kalveks. Quiver Theories for Moduli Spaces of Classical Group Nilpotent Orbits. *JHEP*, 06:130, 2016.

[107] Mathew Bullimore, Tudor Dimofte, and Davide Gaiotto. The Coulomb Branch of 3d $\mathcal{N} = 4$ Theories. 2015.

[108] Alexander Braverman, Michael Finkelberg, and Hiraku Nakajima. Coulomb branches of $3d$ $\mathcal{N} = 4$ quiver gauge theories and slices in the affine Grassmannian (with appendices by Alexander Braverman, Michael Finkelberg, Joel Kamnitzer, Ryosuke Kodera, Hiraku Nakajima, Ben Webster, and Alex Weekes). 2016.

[109] Gregory W. Moore, Andrew B. Royston, and Dieter Van den Bleeken. Parameter counting for singular monopoles on $\mathbb{R}^3$. *JHEP*, 10:142, 2014.

[110] Nigel J. Hitchin. The Selfduality equations on a Riemann surface. *Proc. Lond. Math. Soc.*, 55:59–131, 1987.

[111] Vasily Pestun. Quantum gauge theories and integrable systems. *IHES, France*, Oct 7-28, 2014.

[112] Sergey A. Cherkis and Anton Kapustin. Singular monopoles and supersymmetric gauge theories in three-dimensions. *Nucl.Phys.*, B525:215–234, 1998.

[113] Sergey A. Cherkis and Anton Kapustin. Singular monopoles and gravitational instantons. *Commun.Math.Phys.*, 203:713–728, 1999.

[114] Davide Gaiotto and Edward Witten. S-Duality of Boundary Conditions In $\mathcal{N} = 4$ Super Yang-Mills Theory. *Adv. Theor. Math. Phys.*, 13(3):721–896, 2009.

[115] Amihay Hanany and Noppadol Mekareeya. Complete Intersection Moduli Spaces in $\mathcal{N} = 4$ Gauge Theories in Three Dimensions. *JHEP*, 01:079, 2012.

[116] Stefano Cremonesi, Amihay Hanany, Noppadol Mekareeya, and Alberto Zaffaroni. $\mathrm{T}_\rho^\sigma(G)$ theories and their Hilbert series. *JHEP*, 01:150, 2015.

[117] Dimitri Nanopoulos and Dan Xie. Hitchin Equation, Singularity, and $\mathcal{N} = 2$ Superconformal Field Theories. *JHEP*, 1003:043, 2010.

[118] Nadav Drukker, Davide Gaiotto, and Jaume Gomis. The Virtue of Defects in 4D Gauge Theories and 2D CFTs. *JHEP*, 06:025, 2011.

[119] Peter Bouwknegt and Krzysztof Pilch. On deformed W algebras and quantum affine algebras. *Adv. Theor. Math. Phys.*, 2:357–397, 1998.

[120] Shoichi Kanno, Yutaka Matsuo, Shotaro Shiba, and Yuji Tachikawa. $\mathcal{N} = 2$ gauge theories and degenerate fields of Toda theory. *Phys. Rev.*, D81:046004, 2010.

[121] K. Thielemans. A Mathematica package for computing operator product expansions. *Int. J. Mod. Phys.*, C2:787–798, 1991.

[122] Jonathan J. Heckman, David R. Morrison, and Cumrun Vafa. On the Classification of 6D SCFTs and Generalized ADE Orbifolds. *JHEP*, 05:028, 2014. [Erratum: JHEP06,017(2015)].

[123] Michele Del Zotto, Jonathan J. Heckman, Alessandro Tomasiello, and Cumrun Vafa. 6d Conformal Matter. *JHEP*, 02:054, 2015.

[124] Jonathan J. Heckman, David R. Morrison, Tom Rudelius, and Cumrun Vafa. Atomic Classification of 6D SCFTs. *Fortsch. Phys.*, 63:468–530, 2015.

[125] Lakshya Bhardwaj. Classification of 6d $\mathcal{N} = (1, 0)$ gauge theories. *JHEP*, 11:002, 2015.

[126] Jonathan J. Heckman, Tom Rudelius, and Alessandro Tomasiello. 6D RG Flows and Nilpotent Hierarchies. *JHEP*, 07:082, 2016.

[127] Nikita Nekrasov. BPS/CFT correspondence: non-perturbative Dyson-Schwinger equations and qq-characters. *JHEP*, 03:181, 2016.

[128] Miles Reid. McKay correspondence. 1997.

[129] P.B. Kronheimer and H. Nakajima. Yang-mills instantons on ale gravitational instantons. pages 288–263, 1990.

[130] Clifford V. Johnson and Robert C. Myers. Aspects of type IIB theory on ALE spaces. *Phys. Rev.*, D55:6382–6393, 1997.